PhD Thesis

Thesis Submitted in Partial Fulfillment of the Requirements for the Degree of Doctor of Philosophy

Epithelial cell adaptation to supernumerary centrosomes

Author:

Alexander Damien Rhys

MBiochem (Hons)

Statement of originality

I, Alexander D. Rhys, confirm that the research included within this thesis is my own work or that where it has been carried out in collaboration with, or supported by others, that this is duly acknowledged below and my contribution indicated.

I attest that I have exercised reasonable care to ensure that the work is original, and does not to the best of my knowledge break any UK law, infringe any third party's copyright or other Intellectual Property Right, or contain any confidential material.

I accept that the College has the right to use plagiarism detection software to check the electronic version of the thesis. I confirm that this thesis has not been previously submitted for the award of a degree by this or any other university.

The copyright of this thesis rests with the author and no quotation from it or information derived from it may be published without the prior written consent of the author.

Signature:

Date: October 15, 2017

Acknowledgements

Firstly, I'd like to thank my supervisor Susana for giving me the opportunity to become the first member of her lab, and the chance to work on such a fascinating PhD project. Thank you too for the constant guidance and support, encouraging me to ever become a better scientist.

I owe my thanks to the members of the Godinho lab for their assistance, support and laughter which has never made the lab a dull place to be. To Teresa, Pedro and Sophie thank you for everything you have done to help me along this path. To Aman, Mohamed and Khash, the masters and undergraduate students I have supervised, thank you for putting your trust in me, and for your assistance on the project. To the extended KiSS Group, your wisdom and guidance has always been useful, and I will always have fond memories of our retreats.

My thanks go to our collaborators - in particular to Malti Vaghela and Guillaume Charras for their assistance with the atomic force microscopy experiments. Thank you to Erik Sahai, Peter Schmid, John Marshall, Priscilla Soulie and David Pellman for the donation of cell lines, and Birgit Leitinger for her DDR1 antibodies. I am also grateful to Cancer Research UK for their funding and support.

To the "Kindergarten", sharing an office with you all was fantastic fun. Who knew that 10 of us under such close quarters would all get along as well as we did. I'm glad to have made such special friends to have shared the joys of finally succeeding in CRISPR, and the downs when a western blot antibody still won't work. My special thanks go to Katy and Cathy, to the two best friends that I could ask for, thank you for always being there when a smile is needed, when I needed advice on how to reassess an experiment and all-round support.

To my family, for your patience and support I am always grateful. Thank you all for teaching me that I can do anything if I put my mind to it, and always being there for the ups and downs.

However, my biggest thanks must be paid to my husband Hefin. We embarked on our PhD journeys together, and not a day goes by where I am not thankful to have you by my side. Not only do I owe you my thanks for your constant love and support, but scientifically for your statistical assistance and generating my rosette plots. Diolch, a dw i'n caru ti.

Abstract

The centrosome is the main microtubule-organising centre in animal cells; important to assemble a bipolar mitotic spindle ensuring proper chromosome segregation and genomic stability. Whereas correct centrosome number (1-2) is tightly maintained in normal cells, cancer cells usually have an increased number of centrosomes (>2), termed centrosome amplification. Centrosome amplification has been correlated with aneuploidy, increased tumour grade, chemoresistance and overall poor prognosis.

Cancer cells primarily adapt to supernumerary centrosomes by clustering them into two poles resulting in a 'normal' pseudo-bipolar mitosis. Undermining centrosome clustering is a potential target for cancer-specific treatment. Indeed, depleting the kinesin HSET has already been shown to specifically kill cancer cells by impairing the centrosome clustering mechanism. However, it is unclear whether this process requires adaptation or it is inherent to all cell types.

Using a panel of non-transformed cell lines, we observed that cells expressing E-cadherin have inefficient clustering mechanisms compared to cell lines without E-cadherin. Loss of E-cadherin (siRNA/CRISPR) promotes centrosome clustering and survival of epithelial cells with multiple centrosomes. In addition, loss of DDR1, involved in regulating cortical contractility downstream of E-cadherin, increases centrosome clustering in epithelial cells. Using Atomic Force Microscopy we confirmed that indeed loss of E-cadherin leads to increased cortical contractility in mitotic cells. Inhibition of actomyosin contractility prevents efficient clustering in cells that do not express E-cadherin, further suggesting that it is important for this process. Loss of E-cadherin and DDR1 is strongly correlated with high levels of centrosome amplification in breast cancer cell lines suggesting that these changes are an important adaptation mechanism to centrosome amplification.

Contents

List of Figures

List of Tables

Acronyms

γ-TuRC	γ-tubulin ring complex
AFM	atomic force microscopy
APC/C	anaphase promoting complex/cyclosome
APS	ammonium persulphate
BARD1	BRCA1-associated RING Domain 1
BRIT1	BRCT-repeat inhibitor of hTERT expression
BSA	bovine serum albumin
Cas	CRISPR-associated
CDK	cyclin-dependent kinase
cDNA	complementary DNA
CIN	chromosomal instability
CPAP	centrosomal P4.1-associated protein
CPC	chromosomal passenger complex
CRISPR	Clustered Regularly Interspaced Short Palindromic Repeats
DCB	dihydrocytochalasin B
DCIS	ductal carcinoma in-situ
DDR	discoidin domain receptor
DMEM	Dulbecco's modified Eagle's medium
DMEM:F12	Dulbecco's modified Eagle's medium/nutrient mixture F-12 Ham
DMSO	dimethyl sulfoxide
DNA	deoxyribonucleic acid
Dox	doxycycline hyclate
ECL	enhanced chemiluminescence reagent
ECM	extracellular matrix
EDTA	ethylenediaminetetraacetic acid
EGF	epidermal growth factor
EMT	epithelial to mesenchymal transition
ERM	ezrin/radixin/moesin

GFP	green fluorescent protein
gRNA	guide RNA
GSC	germline stem cell
GTP	guanosine triphosphate
HDAC	histone deacetylase
HEPES	4-(2-hydroxyethyl)-1-piperazineethanesulfonic acid
HRP	horseradish peroxidase
HRV	human rhinovirus
HURP	hepatoma upregulated protein
IDC	invasive ductal carcinoma
ILK	integrin-linked kinase
InDels	small nucleotide insertions or deletions
KLD	Kinase/Ligase/Dpn1
LATS2	large tumour suppressor kinase 2
LB	Luria broth
LIMK	Lim kinase
MAPs	microtubule associated proteins
MDC1	mediator of DNA damage checkpoint protein 1
MLC	myosin light chain
mRNA	messenger RNA
MT	microtubule
MyoII	myosin II
Ncd	nonclaret disjunctional
NHEJ	non-homologous end joining
Nlp	Ninein-like protein
OD	optical density
PAM	protospacer adjacent motif
PARP	phenanthrene-derived poly-ADP-ribose polymerase
PBS	phosphate-buffered saline

PCM	pericentriolar material
PCR	polymerase chain reaction
pRB	retinoblastoma protein
PVDF	polyvinylidene fluoride
qRT-PCR	quantitivative real-time PCR
RIPA	radioimmunoprecipitation assay
RNA	ribonucleic acid
RNAi	RNA interference
rpm	revolutions per minute
RPMI	Roswell Park Memorial Institute medium
SAC	spindle assembly checkpoint
SDS	sodium dodecyl sulphate
SDS-PAGE	sodium dodecyl sulphate polyacrylamide gel electrophoresis
shRNA	short hairpin RNA
siRNA	small interfering RNA
SOC	super optimal broth with catabolite repression
SPB	spindle pole body
StDev	standard deviation
TBS	tris buffered saline
TBS-T	tris buffered saline with tween
TEMED	N,N,N',N'-Tetramethylethylenediamine
TetR	tetracycline repressor

Chapter 1

Introduction

1.1 The centrosome

The centrosome is the main microtubule (MT) organising centre in animal cells, consisting of two orthogonally positioned barrel-shaped centrioles, embedded in a proteinaceous matrix called the pericentriolar material (PCM). The pair of centrioles, which are made up of a nine-fold symmetry of microtubules, are structurally different at their distal ends, with the older mother centriole containing distal and subdistal appendages which are required for microtubule anchorage and ciliogenesis (*Reviewed in:* Bettencourt-Dias and Glover, 2007). The PCM contains hundreds of proteins, including cell cycle regulators and signalling molecules, and importantly proteins including the γ-tubulin ring complexes (γ-TuRCs) that can organise and nucleate microtubules (Andersen, Wilkinson, and Mayor, 2003; Arquint, Gabryjonczyk, and Nigg, 2014)(Figure 1.1). Until relatively recently it was thought, based on electron microscopy that the PCM was amorphous, until super-resolution microscopy has shown that the PCM is organised in concentric layers around the centriole (Fu and Glover, 2012; Lawo *et al.*, 2012; Mennella *et al.*, 2012; Sonnen, Schermelleh, *et al.*, 2012). Within proliferating cells the centrosome and its role in microtubule nucleation is important for cell shape, motility and the formation of the bipolar spindle (*Reviewed in:* Bettencourt-Dias and Glover, 2007). Additionally, within many differentiated cell types, the mother centriole acts as the basal body which is required for cilia formation (*Reviewed in:* Kim and Dynlacht, 2013).

Centrioles are present in all eukaryotic species that form cilia and flagella, but are not found in species that do not have cilia, such as higher plants and higher fungi. Interestingly, centrioles are found in the basal plant and fungal groups, suggesting that centrioles are one of the earliest features within the earlier eukaryotic ancestors (Carvalho-Santos *et al.*, 2011; Fırat-karalar and Stearns, 2014). Whilst the centrioles themselves are conserved across different species with their cylindrical structure formed of the nine-fold triplet symmetry (Figure 1.1), the microtubule arrays can

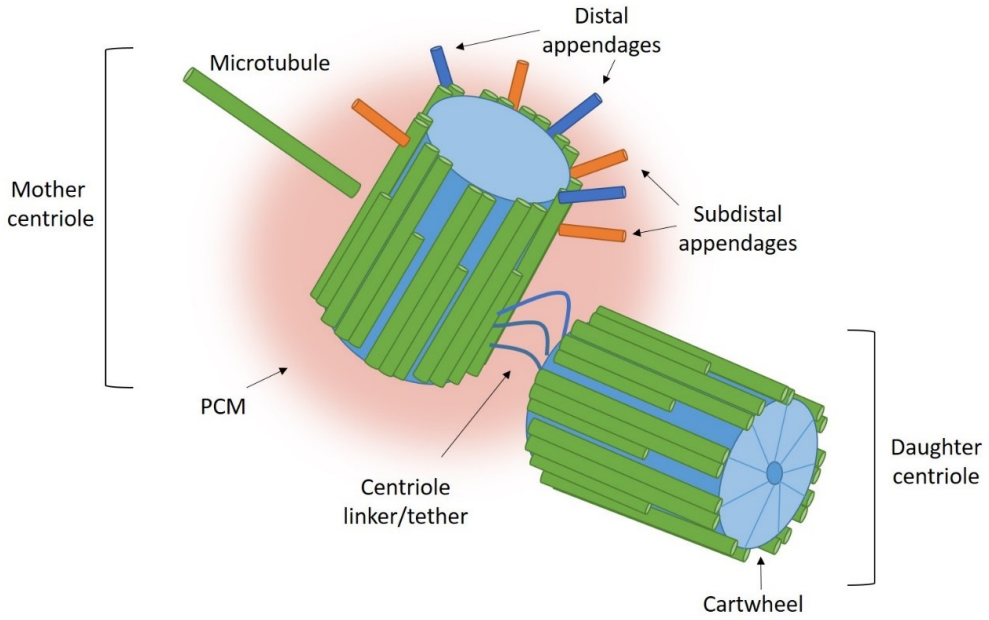

Figure 1.1: Centrosome structure.
The centrosome is composed of a pair of centrioles, each with a ninefold symmetry of triplet microtubules. The centrosome is surrounded by the pericentriolar material, the site of microtubule nucleation. The mother centriole contains distal and sub-distal appendages. The centriole linker/tether connects the two centrioles together.

vary from singlet, doublet or triplet microtubules, and centriole length ranges from 100-400nm and diameter from 100-250nm in different species (Carvalho-Santos *et al.*, 2011). A large number of centriolar proteins have been identified by both proteomic and genomic approaches (Andersen, Wilkinson, and Mayor, 2003; Dammermann *et al.*, 2004; Delattre *et al.*, 2004; Keller *et al.*, 2005; Leidel *et al.*, 2005; Fritz-Laylin *et al.*, 2010; Jakobsen *et al.*, 2011; Azimzadeh *et al.*, 2012; Hoh *et al.*, 2012). Some of these proteins are conserved among the diverse eukaryotes with centrioles, further supporting the presence of centrioles within an early eukaryotic ancestor (Hodges *et al.*, 2010; Carvalho-Santos *et al.*, 2011; Fırat-karalar and Stearns, 2014), whereas some of the proteins are specific to certain subsets of organisms, this is due to variations in centriole assembly and function (Fırat-karalar and Stearns, 2014).

Centrosomes were first described by Theodor Boveri in the 1880s as "the organ for cell division", being seen as a vital organelle required for cells to divide (Bignold, Coghlan, and Jersmann, 2006; Boveri, 2008). However, later studies started to contest this, when seed plant cells were shown to not contain centrosomes (Pickett-Heaps, 1971). Furthermore, experiments using flattened primary spermatocytes from crane flies, which lack a centrosome at one or both poles, showed that these cells could still effectively divide their chromosomes (Dietz, 1966). It is has now been established that acentrosomal cells are still capable of forming bipolar spindles

by nucleating microtubules from mitotic chromatin (Cavazza and Vernos, 2015). This mechanism, initially observed in *Xenopus* egg extracts, has been shown to be especially important for the formation of bipolar spindles in female oocytes, which lack centrosomes prior to fertilisation (Karsenti, Newport, and Kirschner, 1984; Heald *et al.*, 1996; Manandhar, Schatten, and Sutovsky, 2005).

Although centrosomes may be dispensable for cell division to occur, their loss does not come without a cost. Acentrosomal *Drosophila* mutants, lacking DSas-4, an important protein required for centriole duplication, are able to produce flies (Basto, Lau, *et al.*, 2006). Whilst these flies are able to go through development without any evident morphological abnormalities, they lack cilia and flagella, and die prematurely (Basto, Lau, *et al.*, 2006). Further examination showed defects in spindle positioning and asymmetric cell division in the neuroblasts of these flies (Basto, Lau, *et al.*, 2006). Previous work done in haploid cells which were derived from unfertilised *Drosophila* cells and therefore lack centrosomes, are inherently aneuploid, further supporting that centrosomes may play an important role in preserving genetic stability (Debec, 1978). This hypothesis was more recently explored in DT40B chicken cells, where it was shown that centrosome loss resulted in slower mitoses with higher rates of chromosomal instability – this therefore suggested that centrosomes are important for both rapid segregation of genetic material whilst also maintaining genetic integrity (Sir *et al.*, 2013).

1.1.1 Duplication cycle

In dividing cells, centrosome duplication occurs once per cell cycle, this regulation ensures that on entering mitosis cells have two centrosomes that facilitate the formation of a bipolar mitotic spindle. Defects in the regulation of centrosome duplication have been linked to a number of human diseases, including cancer and microcephaly. The morphological events that make up the centriole duplication cycle have been well characterised through the use of electron microscopy (Robbins, Jentzsch, and Micali, 1968; Allen, 1969; Cavalier-Smith, 1974; Vorobjev and Chentsov Yu., 1982). Upon exiting mitosis, the daughter centriole disengages from the older mother centriole, allowing the initiation of centrosome duplication. At the G1-S phase transition a new centriole starts to form perpendicular to each of the original centrioles, these then elongate through S and G2. In late G2 the centrosomes then recruit additional PCM proteins, and separate ready for mitosis and the formation of the spindle, where each daughter cell receives one centrosome (Figure 1.2).

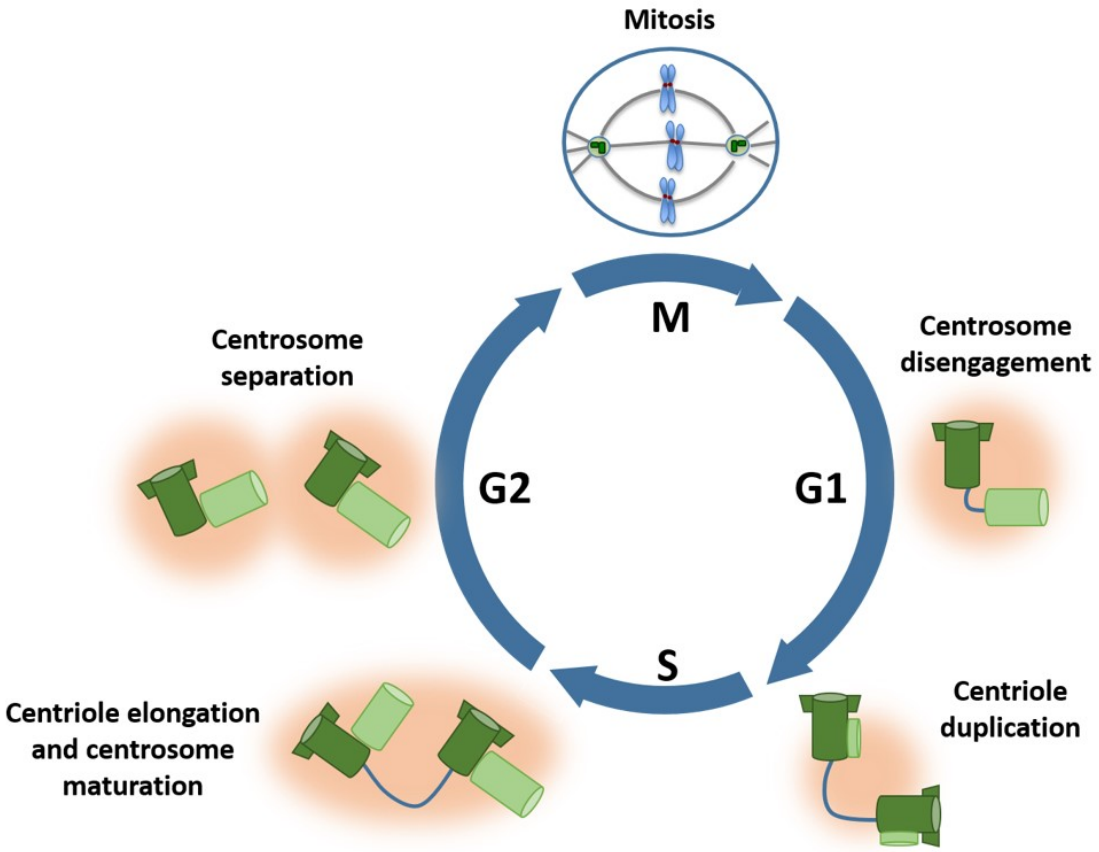

Figure 1.2: Centrosome duplication is tightly regulated in relation to the cell cycle
In dividing cells, centrosome duplication is limited to once per cell cycle. Upon exiting mitosis, the daughter centriole disengages from the older mother centriole, allowing the initiation of centrosome duplication. In S phase a new centriole forms perpendicular to each of the original centrioles. In late G2 the centrosomes then recruit additional PCM proteins, and separate ready for mitosis, enabling the formation of a bipolar spindle.

1.1.1.1 Centriole disengagement

Centriole disengagement occurs at the end of mitosis, and involves the daughter centriole separating away from the mother centriole. This process is an important regulator of the centrosome duplication cycle as it licenses the duplication to only once within the coming cell cycle (Tsou and Stearns, 2006). It is thought that the physical localisation of engaged centrioles prevents premature centriole duplication; this is supported by work done by Loncarek *et al.* which showed that if a daughter centriole is removed by laser ablation, reduplication can occur (Loncarek *et al.*, 2008). In vertebrates disengagement is controlled by the mitotic kinase PLK1 and the protease separase, which is also required for the separation of sister chromatids at

the metaphase-to-anaphase transition (Tsou, Wang, *et al.*, 2009). This link between chromatid separation and disengagement serves to link the timing of the two events together, this ensures that centriole disengagement does not occur prematurely prior to chromosome segregation in mitosis, which could otherwise result in multipolar spindles and erroneous chromosome segregation. The mechanism for the role of PLK1 and separase is not yet fully elucidated. It is suggested that there is a physical link between the mother and daughter centriole, which can be cleaved through a PLK1 driven separase mechanism (Fu, Hagan, and Glover, 2015), similar to the PLK1 separase-dependent cleaveage of chromatid linker cohesin in sister chromatid separation (Sumara *et al.*, 2002). Whilst the model that chromatid separation and centrosome disengagement having shared mechanisms may appear simple, the role of cohesin as a substrate for separase in disengagement is not clear. Work done in HeLa cells expressing a non-degradable form of the cohesin subunit SSC1 showed that sister chromatid separation was prevented, but centriole disengagement could occur, suggesting that cohesin is not the linker between the two centrioles (Tsou and Stearns, 2006). However, two years later a similar experiment was performed with the opposite results, re-implicating cohesin (Schockel *et al.*, 2011). To examine this further Schockël *et al.* engineered the SSC1 to contain cleavage sites for the human rhinovirus (HRV) protease, resulting in centriole disengagement (Schockel *et al.*, 2011). These results were compelling that cohesin plays a role in linking mother and daughter centrioles together. However, more recent work in *Drosophila* embryos using a similar model showed that cohesin cleavage was not sufficient for disengagement to occur (Oliveira and Nasmyth, 2013). Work has been done to try and identify alternative substrates for separase, including identifying pericentrin, a key component of the PCM as potentially being an important substrate for separase in centriole disengagement (Lee and Rhee, 2012; Matsuo *et al.*, 2012). Therefore whilst a physical link between the centrioles is accepted, further work needs to be done to understand the disengagement process. After disengagement a proteinaceous tether, called the centrosome cohesion (Graser, Stierhof, and Nigg, 2007) or G1-G2 tether (*Reviewed in:* Nigg and Stearns, 2011) forms between the two centrosomes, composed of C-Nap1/Cep250 and rootletin which keeps them within a localised proximity to each other until centrosome separation (*Reviewed in:* Mardin and Schiebel, 2012).

1.1.1.2 Centriole duplication

The physical duplication of centrioles begins at the G1/S transition with the formation of a procentriole perpendicular to the base of the existing centriole. This process is

coupled to the cell cycle by requiring the activity of CDK2 complexed with cyclins A or E (Hinchcliffe *et al.*, 1999; Lacey, Jackson, and Stearns, 1999; Matsumoto, Hayashi, and Nishida, 1999; Meraldi *et al.*, 1999). Two possible pathways linking CDK2 to procentriole formation have been proposed (Gönczy, 2015). The first is that CDK2 may phosphorylate substrates which then trigger procentriole formation, such as CP110, MPS1/TTK, and nucleophosmin, however it is not yet established if these three proteins are fundamentally required for the formation of procentrioles (Okuda *et al.*, 2000; Fisk and Winey, 2001; Chen, Indjeian, *et al.*, 2002; Gönczy, 2015). Another proposed model is that CDK2 inactivates the E3 ubiquitin ligase anaphase promoting complex/cyclosome (APC/C) which is complexed with CDH1. APC/CCDH1 ubiquitylates target proteins during G1, targeting them to the 26S proteasome for degradation. By inactivating APC/CCDH1, CDK2 leads to the accumulation of proteins required for S-phase entry (Peters, 2002; Peters, 2006). As well as degrading proteins required for S-phase entry, APC/CCDH1 also degrades proteins required for centriole duplication including SAS-6, STIL and CPAP, therefore CDK2 activity can couple G1/S phase transition with the increase in proteins for centriole duplication (Strnad *et al.*, 2007; Tang, Fu, *et al.*, 2009; Arquint, Sonnen, *et al.*, 2012).

It is well established that PLK4, SAS-6 and STIL, three centriolar proteins are key in initiating the centriole duplication process. It was initially thought that SAS-6 localised first for procentriole formation (Strnad *et al.*, 2007). However, more recent work has shown that PLK4 localises to a dot-like structure at this site of procentriole formation first, and recruits SAS-6 (Sonnen, Schermelleh, *et al.*, 2012; Kim, Park, *et al.*, 2013). Similar work in *Caenorhabditis elegans*, has shown that ZYG-1, the orthologue of PLK4 recruits SAS-6, suggesting this process is evolutionarily conserved (Kitagawa, Busso, *et al.*, 2009; Lettman *et al.*, 2013). This localisation of PLK4 is regulated by two scaffolds CEP152 and CEP192. PLK4 is recruited along with CEP152 to the centrioles through interaction with CEP192 (Kim, Park, *et al.*, 2013; Sonnen, Gabryjonczyk, *et al.*, 2013). CEP192 localises to the inner ring of the centriole barrel, whereas CEP152 localises to the outer ring (Lüders, 2012), where PLK4 is repositioned by competitively binding to the CEP152 from the CEP192 (Park, Park, *et al.*, 2014). PLK4 then moves from surrounding the centrioles to the sites of procentriole formation (Kim, Park, *et al.*, 2013). However, both CEP192 and CEP152 are symmetrically distributed around the centrioles (Lawo *et al.*, 2012; Sonnen, Schermelleh, *et al.*, 2012), so whilst the mechanism of recruitment of PLK4 to the centrioles is determined, how PLK4 then localises to a single point for procentriole initiation is yet to be understood. It has been suggested that STIL may play a role in this localisation and activation of PLK4.

After PLK4 localisation, the next stage in the procentriole formation is the formation of the cartwheel (Gönczy, 2012). Structural biology studies using X-ray crystallography played an important role in showing that the cartwheel is formed of a central hub surrounded by a ninefold symmetry of "spokes" made up of SAS-6 oligomers. Further work using purified SAS-6 *in vitro* showed that the SAS-6 oligomers could assemble into the ninefold cartwheel like structure. (Kitagawa, Vakonakis, *et al.*, 2011; Breugel *et al.*, 2011; Brito, Gouveia, and Bettencourt-Dias, 2012). This cartwheel provides the required ninefold symmetry of the centriole and initiates the formation of the assembly of the triplet microtubules. The positioning of the cartwheel to the luminal wall of the mother centriole is dependent on PLK4 and STIL (Fong *et al.*, 2014). In mature centrioles this cartwheel is then lost, suggesting that the cartwheel is required for centriole generation but not maintenance, although the loss of the cartwheel occurs in only some species (Tsou *et al.*, 2009; Guichard *et al.*, 2010; Gönczy, 2012).

From this cartwheel the ninefold symmetry of triplet microtubules can form (in some species it is formed of singlet or doublet microtubules). The microtubules are designated either A-, B- or C-tubules (Figure 1.1). The A-tubules are nucleated by a conical structure similar to the γ-TuRC, and are proximal to the interior of the centriole wall, whereas the B- and C-tubules each share a wall with the A- and B-tubules, respectively (Erickson, 2000; Keating and Borisy, 2000). The B- and C-tubules do not have the conical structure at their end, suggesting they are generated by a different mechanism. The A-tubule of one triplet is connected to the C-tubule of the adjoining triplet via a linker (Fujita, Yoshino and Chiba, 2016). This process requires the highly conserved centrosomal protein CEP135. The SAS-6 proteins, once formed into the cartwheel structure, are too short to bind the A-tubules, therefore CEP135 is needed to bridge this gap by binding to SAS-6 at its C-terminal region, and the tubules at its N-terminal (Lin *et al.* 2013). Depletion of CEP135 has been shown to result in abnormal centrosome structure (Lin *et al.* 2013).

1.1.1.3 Centriole elongation

After the formation of procentrioles, these start to elongate during S phase, with their distal regions elongating during G2 to a determined length, which is variable between different species (0.2–0.5µm long) (Carvalho-Santos *et al.*, 2011). The centriolar protein CPAP (centrosomal P4.1-associated protein) is fundamental for centrosome elongation, and its overexpression has been shown to generate centrioles that are longer than normal (Schmidt *et al.*, 2009; Tang *et al.*, 2009). CPAP is recruited to the cartwheel where it binds to CEP135, and stabilises the cartwheel

structure (Lin *et al.* 2013). A number of proteins have been identified which play a role co-operatively with CPAP for this elongation process including CEP120, PLK2, Spice1 and centrobin (Chang *et al.*, 2010; Gudi *et al.*, 2011, 2014, 2015; Comartin *et al.*, 2013; Y. N. Lin *et al.*, 2013). Notably centrobin is recruited to the centrosome, and upon interaction with CPAP enables the elongation of the centrioles by binding α- and β-tubulin dimers (Gudi *et al.*, 2011, 2014). After elongation, CP110 and its interacting proteins is then required to cap the distant ends of the centrioles once they reach the correct length, and prevent further elongation (Kohlmaier *et al.*, 2009; Schmidt *et al.*, 2009).

1.1.1.4 Centrosome maturation

Once centriole length has been achieved, centrosome maturation occurs towards the end of G2, which is characterised by the recruitment of PCM proteins, including γ-TuRC, which is required for MT nucleation. CPAP is further required for this process, independently of its role in centriole elongation. CPAP forms a scaffolding complex by binding to the proximal end of the centrosome, and to the PCM, tethering the two together (Gopalakrishnan *et al.*, 2011; Zheng *et al.*, 2014). Alongside this, the kinases PLK1 and Aurora A are required for centrosome maturation, and enabling the process for centrosomes to nucleate and anchor MTs. PLK1 phosphorylates a number of different PCM proteins including pericentrin, CEP215, CEP192 and NEDD1 (Santamaria *et al.*, 2011). This phosphorylation of pericentrin then enables the recruitment of a number of other key PCM components: γ-tubulin, Aurora A, CEP192, NEDD1 and PLK1 itself (Lee and Rhee, 2011). Both pericentrin and CEP192 are required for the recruitment of NEDD1 and γ-tubulin (Zhu *et al.*, 2008). CEP215 stimulates MT nucleation through interacting with γ-TuRC (Chen *et al.*, 2008). PLK1 and Aurora A work together, with PLK1 recruiting Aurora A to the centrosome, and Aurora A in initially activating PLK1 (Lens, Voest and Medema, 2010). Once PLK1 is activated, its continuous activity is then required for the retention of PCM structure, going through into mitosis (Mahen *et al.*, 2011).

1.1.1.5 Centrosome separation

At the end of G2, the centrosomes separate, this enables the formation of a bipolar spindle in mitosis, with a centrosome at each pole. This process occurs via two stages, the first is the disruption of the proteinaceous linker that connects the two mother centrioles, then the force-dependent separation of the two centrosomes by

Eg5, allowing the formation of the two separate spindle poles (Mardin and Schiebel, 2012; Fujita, Yoshino and Chiba, 2016).

The centriolar protein CEP250 localises to the tethering site at the proximal end of mother centriole, where it binds to rootletin, and LRRC45 on the proteinaceous tether (Fry *et al.*, 1998; Bahe *et al.*, 2005; He *et al.*, 2013). The NIMA-related kinase Nek2 is required for the phosphorylation-dependent dissolution of the tether by phosphorylating CEP250, rootletin and LRRC45 at the G2/M transition, as well as centlein which is also a tether protein (Fry *et al.*, 1998; Bahe *et al.*, 2005; He *et al.*, 2013). This process is temporally controlled by Aurora A. Aurora A actives PLK1, which in turn binds and phosphorylates Mst2, a Hippo pathway effector kinase (Mardin *et al.*, 2011). Mst2 directly binds to Nek2 and controls its subsequent localisation, and phosphorylation of CEP250 and rootletin (Mardin *et al.*, 2010).

After the tether is dissolved, the centrosomes are then required to move to opposite ends of the cell to form the bipolar spindle in mitosis, enabling the efficient segregation of chromosomes into the two daughter cells. This is a force-driven process, the forces are generated by the kinesin Eg5 (Mardin and Schiebel, 2012). Nek6, another NIMA-related kinase protein is required to phosphorylate Eg5, enabling Eg5 to be targeted to the centrosome by PLK1 and MTs (Bertran *et al.*, 2011; Mardin *et al.*, 2011; Smith *et al.*, 2011). Eg5 through its kinesin activity along with dynein then allows for the separation of the two centrosomes to opposite ends of the cell, cortical dynein is then important for the orientation of the subsequent mitotic spindle (Raaijmakers *et al.*, 2012; Raaijmakers and Medema, 2014; Tame *et al.*, 2014). Interestingly, Eg5 is able to separate centrosomes, by force even if the tether remains (Mardin *et al.*, 2010). The centrosome duplication cycle then occurs again in the new daughter cells.

1.2 Centrosome amplification and cancer

The first proposal that supernumerary centrosomes could be linked to tumourigenesis was made over a century ago by the German embryologist Theodor Boveri. Boveri carried out experiments using dispermic fertilised sea urchin eggs, which therefore contained extra centrosomes as the sperm provides the functioning centrosome during embryogenesis. He observed that these cells formed multipolar spindles leading to asymmetric distribution of the genetic material resulting in three or more aneuploid daughter cells. The progeny from these divisions all displayed different developmental phenotypes, and it was from this that the conclusion that chromosomes were important for cellular traits was derived (Boveri, 1887, 1888). These conclusions

were further supported by the observations of two of Boveri's contempories: Gino Galeotti and David von Hansemann, who first investigated genetic instability in cancer by examining tumour histology. They reported that abnormal mitoses, including multipolar spindles, are common features within tumours (Hansemann, 1890; Galeotti, 1893). Their observations also reinforced Boveri's suggestion that the multipolar spindles he observed resulted in unequal distribution of chromosomes, which Galeotti termed as "asymmetric karyokinesis" (Hansemann, 1890; Galeotti, 1893). Based on these observations Boveri then put forward the proposal that as extra centrosomes result in multipolar divisions, leading to genetic instability this in turn could result in tumourigenesis (Boveri, 1902, 2008) (Figure 1.3).

However, Boveri's hypothesis that extra centrosomes can lead to tumour formation contrasted with that made by Hansemann. Hansemann stated that whilst multipolar cell divisions are observed within tumours, a diagnosis of cancer should not be made based solely on these abnormal mitotic divisions, as they are also observed within benign lesions (Hansemann, 1890; *Reviewed in:* Bignold, Coghlan and Jersmann, 2006). As the cancer field progressed and focused mostly on genetics and the role of oncogenes and tumour suppressors in tumourigenesis the role of centrosomes was widely ignored until the late 1990s when it was observed that centrosome amplification was associated with loss of p53 that the field started to re-emerge (Fukasawa *et al.*, 1996).

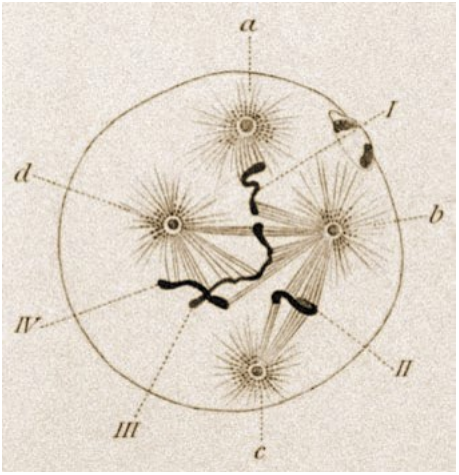

Figure 1.3: Hypothesis that supernumerary centrosomes and multipolar cell divisions may lead to tumours
Theodor Boveri stained dispermic sea urchin eggs and then made drawings based on microscopic observation. He identified the abnormal presence of multiple centrosomes (a-d) in a fertilised egg, leadings to the unequal distribution of chromosomes (I-IV) in the resultant daughter cells. Based on these observations he hypothesised that supernumerary centrosomes could lead to tumour formation (Boveri, 1888).

1.2.1 Prevalence of centrosome amplification in cancer

Since the association between centrosome amplification and loss of p53, an extensive number of studies has established that the majority of solid as well as haematological malignancies display centrosome abnormalities and, in particular, supernumerary centrosomes, see Table 1.1 (Lingle *et al.*, 1998; Pihan *et al.*, 1998; Sato *et al.*, 1999; Nigg, 2002; Giehl *et al.*, 2005; Krämer, Neben and Ho, 2005; Chan, 2011). In the majority of cases, centrosome amplification has been shown to correlate with high-grade tumours and poor prognosis. However, instances of centrosome amplification have also observed in some early low-grade malignancies, supporting the initial suggestion of Boveri that centrosome amplification could promote tumourigenesis (Lingle *et al.*, 1998; D'Assoro *et al.*, 2002; Pihan *et al.*, 2003; Yamamoto *et al.*, 2004; Giehl *et al.*, 2005; Segat *et al.*, 2010). Centrosome amplification has also been associated with tumour recurrence and increased metastasis in some cancers, therefore potentially making centrosome amplification as a biomarker for advanced disease and poor prognosis (Yamamoto *et al.*, 2004; Chan, 2011; Godinho and Pellman, 2014).

Table 1.1: Centrosome amplification in solid human tumours and haematological malignancies (part I)

Cancer	Subtype	References
Breast	AC (Adenocarcinoma)	(Lingle *et al.*, 1998; Lingle and Salisbury, 1999; D'Assoro *et al.*, 2002; Schneeweiss *et al.*, 2003; Kronenwett *et al.*, 2004; Kronenwett *et al.*, 2005; Suizu *et al.*, 2006; Guo *et al.*, 2007; Shimomura *et al.*, 2009; Bagheri-Yarmand, Biernacka, *et al.*, 2010)
	DCIS (Ductal Carcinoma in Situ)	(Lingle *et al.*, 2002; Hoque *et al.*, 2003; (Pihan *et al.*, 2003; Kronenwett *et al.*, 2005)
	IDC (Invasive Ductal Carcinoma)	(Carroll *et al.*, 1999; Lingle *et al.*, 2002; Hoque *et al.*, 2003)
	NOS (not otherwise specified)	Pihan *et al.*, 1998; Korzeniewski *et al.*, 2010; Denu *et al.*, 2016)
Lung	AC	(Koutsami *et al.*, 2006; Jung *et al.*, 2007)
	SCC (Squamous Cell Carcinoma)	(Koutsami *et al.*, 2006; Jung *et al.*, 2007)
	NOS	(Pihan *et al.*, 1998)
Prostate	AC	(Pihan *et al.*, 2001; Toma *et al.*, 2010; Li *et al.*, 2014)
	PIN (Prostate Intraepithelial Neoplasia)	(Pihan *et al.*, 1998)
Ovarian	Serous	(Hsu *et al.*, 2005; Landen *et al.*, 2007; Kuhn *et al.*, 2016)
	NOS	(Zhang *et al.*, 2013)
Anogenital	AC	(Skyldberg *et al.*, 2001)
	NOS	(Pihan *et al.*, 1998; Skyldberg *et al.*, 2001; Duensing *et al.*, 2008)
Testicular	Large number of sub-types	(Mayer *et al.*, 2003)
Adrenal	Carcinoma	(Roshani *et al.*, 2002)
	Adenoma	(Roshani *et al.*, 2002)
Renal	RCC (Renal Cell Carcinoma)	(Gisselsson *et al.*, 2004; Nakada *et al.*, 2011)
Colorectal	AC	(Pihan *et al.*, 1998; Kayser *et al.*, 2005; Gao and Zhang, 2009)
	Adenoma	(Gao and Zhang, 2009; Shinmura *et al.*, 2015)

Table 1.1: Centrosome amplification in solid human tumours and haematological malignancies (part II)

Cancer	Subtype	References
Urothelial	Bladder TCC (transitional cell carcinoma)	(Jiang *et al.*, 2003; K Kawamura *et al.*, 2004; Kenji Kawamura *et al.*, 2004; Yamamoto *et al.*, 2004, 2006, 2007, 2011; Akao *et al.*, 2006; del Rey *et al.*, 2010; Miyachika *et al.*, 2013)
Pancreatic	Adenoma	(Sato *et al.*, 1999, 2001; Shono *et al.*, 2001; Zhu *et al.*, 2005)
	Ductal	(Sato *et al.*, 1999, 2001; Shono *et al.*, 2001; Zhu *et al.*, 2005)
	Endocrine	(Sato *et al.*, 1999, 2001; Shono *et al.*, 2001; Zhu *et al.*, 2005)
Neural	DAG (Diffuse Astrocytic Glioma)	(Katsetos *et al.*, 2006)
	Glioma	(Hama *et al.*, 2003; Loh *et al.*, 2010; Telentschak *et al.*, 2015)
	Medulloblastoma	(Caracciolo *et al.*, 2010; Mikulenkova *et al.*, 2015)
	Neuroblastoma	(Carroll *et al.*, 1999; Fukushi *et al.*, 2009; Izumi and Kaneko, 2012)
	Pituitary adenoma	(Uccella *et al.*, 2005)
	NOS	(Pihan *et al.*, 1998; Weber *et al.*, 1998; Katsetos *et al.*, 2006; Caracciolo *et al.*, 2010)
Head and Neck	SCC	(Kaneko *et al.*, 1980; Carroll *et al.*, 1999; Gustafson *et al.*, 2000; Gisselsson *et al.*, 2002; Reiter *et al.*, 2006, 2009; Thirthagiri *et al.*, 2007; Syed *et al.*, 2009)
Bone and Soft Tissue	Large number of sub-types	(Seifert, 1978; Al-Romaih *et al.*, 2003; Gisselsson *et al.*, 2004; Perucca-Lostanlen *et al.*, 2004; Gong *et al.*, 2009; Moskovszky *et al.*, 2010)
Haematological	Large number of sub-types	(Neben *et al.*, 2003, 2007; Duensing *et al.*, 2003; Krämer *et al.*, 2003; Martin-Subero *et al.*, 2003; Ventura *et al.*, 2004; Kearns *et al.*, 2004; Giehl *et al.*, 2005; Maxwell *et al.*, 2005; Chng *et al.*, 2006; Nitta *et al.*, 2006; Sánchez-Aguilera *et al.*, 2006; Hensel *et al.*, 2007; Ottaggio *et al.*, 2008; Fabarius *et al.*, 2008; Patel and Gordon, 2009; Dementyeva *et al.*, 2010)

1.2.1.1 Centrosome aberrations in breast cancer

Whilst the majority of solid tumours and haematological malignancies have been shown to contain supernumerary centrosomes, breast cancer has been the most systematically studied in regards to centrosome aberrations (Chan, 2011). The first study looking at centrosome amplification in primary human cancers was done in high grade metastatic breast adenocarcinomas (Lingle *et al.*, 1998). Lingle *et al.* identified a number of centrosomal aberrations within the samples they analysed including centrosome amplification, enlarged centrosomal and PCM volume, and increased microtubule nucleation resulting from the supernumerary centrosomes (Lingle *et al.*, 1998). The same group, following this up with electron microscopy observed that within the breast tumours as well as supernumerary centrosomes, there were often irregularities in their structure – either missing triplet microtubules or variation in centriole length, and further confirming an increase in PCM (Lingle and Salisbury, 1999). They also observed that these cells with supernumerary centrosomes had higher levels of abnormal mitoses, supporting the first observations made by Boveri (Lingle and Salisbury, 1999).

Shortly after these initial studies, further work was done reporting centrosome amplification in other breast cancers including ductal carcinoma in-situ (DCIS) (Lingle *et al.*, 2002; Pihan *et al.*, 2003; Kronenwett *et al.*, 2005). These studies in early stage breast cancers supported Boveri's hypothesis that centrosome amplification may play a causal role in tumourigenesis, particularly as chromosomal instability correlated with centrosome amplification in the samples analysed (D'Assoro *et al.*, 2002). Furthermore, it was shown that the lesions with centrosomal aberrations resulted in more advanced histological grade, supporting a role of centrosome amplification in increased tumourigenesis (Pihan *et al.*, 2003).

Subsequent studies by Kronenwett *et al.* have continued to build on this link between centrosomal abnormalities and increased aggressiveness of tumours. They showed that centrosome amplification, and the resultant mitotic spindle defects correlated with higher levels of genome instability and aneuploidy, as well as increased tumour grade, compared to those with normal centrosome number which had lower levels of aneuploidy and were less invasive (Kronenwett *et al.*, 2004, 2005). This work, along with similar studies by other groups suggests that centrosome amplification could be used as a potential biomarker for aggressive disease and poor prognosis within the clinic (D'Assoro *et al.*, 2002; Schneeweiss *et al.*, 2003; Guo *et al.*, 2007; Chan, 2011; Denu *et al.*, 2016).

Interestingly, centrosome amplification has also been correlated with hormone receptor status of breast cancers by some studies, in particular with overexpression of HER2/neu, as well as negative estrogen receptor (ER), and negative progesterone receptor (PR) (Montagna *et al.*, 2002; Schneeweiss *et al.*, 2003; Guo *et al.*, 2007). Although, a contrasting study found no correlation between centrosome amplification and hormone receptor status, nor with chromosomal instability, tumour size or grade (Shimomura *et al.*, 2009).

1.2.2 Structural abnormalities of centrosomes

Centrosomal defects can be broken down into two main categories – structural and numerical abnormalities. Whilst numerical aberrations are the most widely characterised, structural abnormalities have also been observed, usually reported as alterations in centrosome size and length (Godinho and Pellman, 2014). The origin of structural centrosomal abnormalities are not yet well understood, however it has been hypothesised that they could result from genetic changes in regards to the components that control centrosome structure. One such example is CPAP which when overexpressed results in increased centriole length (Kirkham *et al.*, 2003; Kohlmaier *et al.*, 2009; Schmidt *et al.*, 2009; Tang *et al.*, 2009).

Structural abnormalities are not well characterised, primarily as they are not easy to identify. Centrioles are 0.2-0.5µM in length, which is close to the optical resolution of light microscopy, therefore for more accurate analysis specialised fluorescence microscopy must be used, or ideally electron microscopy, which is then hard to apply to a systematic study of structural aberrations. Pericentriolar markers are often used when assessing centrosomal abnormalities, however there are difficulties in interpreting changes in PCM volume/diameter as either numerical of structural centrosomal defects (D'Assoro *et al.*, 2002; Guo *et al.*, 2007). For example, if the volume of PCM is increased, this may be considered to be a structural alteration, however, this could also result from an increase in centrosome number, whereby the supernumerary centrosomes are tightly packed together, this should therefore have been classified as a numerical aberration rather than a structural one (D'Assoro *et al.*, 2002; Lingle *et al.*, 2002; Godinho *et al.*, 2014). Conversely, increased centriolar length can lead to centriole fragmentation, which may then appear as a numerical defect rather than a structural one (Kohlmaier *et al.*, 2009). A large number of studies investigating centrosomal defects within primary tumours rely on PCM staining, which then makes it systematically harder to understand the role of numerical and structural aberrations within cancer (Godinho and Pellman, 2014). This problem can

be partly overcome by the use of centriole specific markers such as centrin, whereby the number of centrioles can actually be assessed, although electron microscopy would be required to determine if centriole fragmentation had occurred.

1.2.3 Causes of centrosome amplification

The most widely studied centrosomal abnormality within cancer is centrosome amplification, however it is still not fully understood how cancer acquires these supernumerary centrosomes. There are a number of different methods which can lead to supernumerary centrosomes: centriole over duplication, mitotic slippage, cytokinesis failure, cell-cell fusion, and *de novo* centriole assembly (Godinho, Kwon and Pellman, 2009).

Centrosome over duplication can result from the deregulation of the centrosome duplication cycle described above, which is normally tightly controlled by cell cycle components. Whilst this cycle is normally robust in ensuring that centriole duplication only occurs once per cell cycle, it is only controlled by a small number of positive and negative regulatory proteins which are widely conserved between species (*Reviewed in:* Nigg and Stearns, 2011). As previously described, the master regulator of centrosome duplication is PLK4 (Holland, Lan and Cleveland, 2010). Overexpression of PLK4 has been shown to lead to supernumerary centrosomes due to centriole over duplication (Habedanck *et al.*, 2005; Kleylein-Sohn *et al.*, 2007). Conversely loss of PLK4 results in a reduction in centriole number (O'Connell *et al.*, 2001; Bettencourt-Dias *et al.*, 2005; Habedanck *et al.*, 2005). PLK4 levels are therefore regulated during the centriole duplication cycle, mostly through autophosphorylation leading to SCFβ^{TrCP}/ubiquitin-dependent proteolysis (Cunha-Ferreira *et al.*, 2009; Rogers *et al.*, 2009; Guderian *et al.*, 2010; Holland *et al.*, 2010; Sillibourne *et al.*, 2010; Brownlee *et al.*, 2011). It is possible that the supernumerary centrosomes observed in some tumours may arise from the deregulation of the ubiquitin regulators involved in targeting PLK4 for proteolysis. For example the downregulation of βTrCP has been shown to result in the stabilisation of PLK4, and subsequently centrosome amplification was observed (Wojcik, Glover and Hays, 2000; Guardavaccaro *et al.*, 2003; Cunha-Ferreira *et al.*, 2009; Rogers *et al.*, 2009). CP110, a centrosomal protein involved in controlling centriole length is also regulated by ubiquitin-dependent proteolysis by SCFcyclinF, which is itself counteracted by USP33 a deubiquitinating enzyme (Li *et al.*, 2013). Overexpression of USP33 increases CP110, also resulting in centrosome amplification (Li *et al.*, 2013).

HPV (High-risk human papillomavirus) associated tumours have also been reported to be associated with centriole over duplication. The HPV-16 E7 oncoprotein has been shown to increase PLK4 mRNA levels, resulting in centrosome amplification (Korzeniewski, Treat and Duensing, 2011). Furthermore both the E6 and E7 oncoproteins play a role in disrupting the cell cycle checkpoints, which helps facilitate the viral replication. This disruption can then result in oncogenic transformation, and may lead to centriole over duplication (Duensing *et al.*, 2009; Korzeniewski, Treat and Duensing, 2011).

As described previously, PLK4 levels are tightly regulated to ensure centriole duplication occurs once per cell cycle. p53 is able to regulate PLK4 mRNA levels by recruiting HDAC (histone deacetylases) repressors to the PLK4 promoter region (Li *et al.*, 2005). This is interesting within a cancer setting, as loss of p53 could then lead to increased levels of PLK4, in turn causing centriole over duplication. This hypothesis is supported by observations in murine fibroblasts, that centrosome amplification has been associated with loss of p53 (Fukasawa *et al.*, 1996). However, in $p53^{-/-}$ mice, when their brains were analysed, no evidence of centrosome amplification was observed (Marthiens *et al.*, 2013). Therefore it is still unclear as to whether loss of p53 may directly, or even indirectly lead to the generation of supernumerary centrosomes.

Alternatively, centrosome over duplication can occur via overexpression of some of the PCM components, such as pericentrin and γ-tubulin (Starita *et al.*, 2004; Loncarek *et al.*, 2008). For example increased γ-tubulin has been shown to result from the loss of the tumour suppressor BRCA1 (Starita *et al.*, 2004). Prolonged G2 arrest can lead to centriole over duplication, where the centrosomes mature and disengage prior to mitosis, and reduplicate due to PLK1 expression (Lončarek, Hergert and Khodjakov, 2010). Therefore it is possible that conditions such as persistent DNA damage, which result in elongated periods within G2 could result in centrosome amplification (Godinho and Pellman, 2014).

Centrosome amplification can also occur due to cytokinesis failure, cell-cell fusion or mitotic fusion, which then results in tetraploid cells containing supernumerary centrosomes that have been shown to be tumourigenic (Fujiwara *et al.*, 2005; Duelli *et al.*, 2007; Ganem, Storchova and Pellman, 2007; Davoli and de Lange, 2012). Interestingly p53-/- tetraploid tumour cells have been shown to contain high levels of supernumerary centrosomes, suggesting tetraploidy may be a route for tumours generating supernumerary centrosomes (Fujiwara *et al.*, 2005). Conversely, work done *in vitro* where transient cytokinesis failure was induced did not result in the long-

term maintenance of supernumerary centrosomes in culture, suggesting that these supernumerary centrosomes are then lost (Krzywicka-Racka and Sluder, 2011). These observations were supported by previous work showing that tetraploid cells lose their supernumerary centrosomes over time (Ganem, Godinho and Pellman, 2009). These observations would suggest that supernumerary centrosomes are deleterious, and are therefore lost by cells overtime. Therefore, whilst there are different mechanisms that may lead to the generation of supernumerary centrosomes, they do not inherently lead to the permanent maintenance of extra centrosomes over continued growth. Other conditions such as cell type or genetics must therefore play a role in the maintenance of centrosome amplification, as well as their generation (Godinho and Pellman, 2014).

Further confirming the deleterious effects of supernumerary centrosomes, centrosome amplification has been shown to result in the stabilisation of p53 and p21, leading to cell cycle arrest, which can be overcome if p53 is inhibited (Holland *et al.*, 2012). Centrosome amplification can lead to aneuploidy, which may have accounted for the p53-dependent arrest observed, however the activation of p53 upon centrosome amplification appears to be a distinct process independent of aneuploidy (Ganem, Godinho and Pellman, 2009; Thompson and Compton, 2010; Holland *et al.*, 2012). Tetraploid cells containing supernumerary centrosomes have been shown to stabilise p53 by activation of the Hippo tumour suppressor pathway (Ganem *et al.*, 2014). Therefore, cells can activate p53 and subsequently undergo cell cycle arrest by both centrosome amplification and aneuploidy. Interestingly, recent work has shown that the presence of supernumerary centrosomes can trigger activation of the PIDDosome multiprotein complex, which leads to Caspase-2 mediated MDM2 cleavage and therefore stabilisation of p53 resulting in cell cycle arrest (Fava *et al.*, 2017). As cancers have regularly been identified to contain supernumerary centrosomes there must be mechanisms that take place that allow cells to actively maintain their supernumerary centrosome population, overcoming the p53-dependent arrest observed as well as the initial process of generating them.

1.2.3.1 Causes of centrosome amplification in breast cancer

Looking particularly at breast cancer, a number of independent studies have been carried out, trying to understand the underlying mechanisms that lead to centrosome amplification. Overall the combined evidence suggests that there are different, and cooperative methods which lead to centrosome amplification within breast cancer development (Chan, 2011).

In the MCF7 cell line which has centrosome amplification, albeit at low levels of ~10% of cells containing supernumerary centrosomes, their extra centrosomes have been shown to arise due to cytokinesis failure due to the expression of a small isoform of cyclin E. The centrosome amplification was observed to increase upon the loss of p53 (Bagheri-Yarmand, Biernacka, *et al.*, 2010; Bagheri-Yarmand, Nanos-Webb, *et al.*, 2010). BRCA1 acts as a tumour suppressor within the breast and ovaries, which when associated with BARD1 (BRCA1-associated RING Domain 1), acts as an E3 ubiquitin ligase (Starita *et al.*, 2004). The BRCA1-BARD1 complex is able to help facilitate centrosome number by controlling reduplication through the ubiquitination of γ-tubulin (Starita *et al.*, 2004). Therefore, inhibition of BRCA1, which is often observed within breast tumours can result in centrosome overduplication, and negative BRCA1 expression has been correlated with centrosome amplification (Schlegel, Starita and Parvin, 2003; Starita *et al.*, 2004; Sankaran *et al.*, 2005; Ko *et al.*, 2006; Shimomura *et al.*, 2009). This phenotype is also observed within mice, where the disruption of BRCA1 has been observed to result in both centrosome amplification and subsequently aneuploidy (Xu *et al.*, 1999; Deng, 2001).

Overexpression of another BRCA1 associated protein Nlp (Ninein-like protein) has also been associated with centrosome amplification in rodent fibroblasts, and has been shown to lead to spontaneous breast tumourigenesis in mice (Shao *et al.*, 2010). Nlp is a centrosomal protein, and has been shown to be overexpressed in human breast cancers, which may then mimic BRCA1 loss, and cause centrosome amplification within these tumours (Shao *et al.*, 2010).

As described in Section 1.1.1, the kinase Aurora A is involved in the control of the centriole duplication cycle, its overexpression has been shown lead to centrosome amplification, aneuploidy and cell transformation (Zhou *et al.*, 1998). Interestingly, centrosome amplification has only been associated with Aurora A overexpression in the non-invasive DCIS (ductal carcinoma in situ) suggesting that centrosome amplification may play a role in initial tumour initiation (Hoque *et al.*, 2003; Shimomura *et al.*, 2009; Chan, 2011). In further support of this model of centrosome amplification in breast cancer initiation, supernumerary centrosomes are often found in early stages of breast cancer development within mouse models (Li *et al.*, 2004). Whilst Aurora A overexpression and centrosome amplification have been correlated, the exact mechanism linking the two is not fully understood. It has been suggested that the centrosome amplification observed may be due to cytokinesis failure, as observed by the levels of aneuploidy upon Aurora A overexpression (Katayama *et al.*, 2004; Wang *et al.*, 2006). In these cases, the AKT pathway was also activated, allowing for the continued survival and proliferation of the tetraploid cells containing

supernumerary centrosomes (Wang *et al.*, 2006). Another possibility is that Aurora A has been shown to be inhibited with the BRCA1 ubiquitin ligase by phosphorylation, so could promote centrosome phosphorylation through the impairment of BRCA1-BARD1 as described above (Sankaran *et al.*, 2007).

When examining proteins that are inversely correlated with centrosome amplification in breast cancer, both MDC1 (Mediator of DNA damage checkpoint protein 1) and BRIT1 (BRCT-repeat inhibitor of hTERT expression) were identified. Both of these proteins negatively regulate Aurora A and PLK1 which are involved in the centriole duplication pathway (Rai *et al.*, 2008). Depletion of MDC1 was directly observed to result in centrosome over-duplication, whereas BRIT1 depletion resulted in cytokinesis failure resulting in centrosome accumulation (Rai *et al.*, 2008).

Nek2, another centrosomal kinase has also been associated with cytokinesis failure in breast epithelial cells, leading to the centrosome amplification. Nek2 overexpression has been observed in both DCIS and IDC breast cancers, suggesting that Nek2 may play a role in centrosome amplification in these tumours (Hayward *et al.*, 2004). Oncogenic K-Ras has been linked to centrosome amplification within precursor legions. This can be impaired by abolishing expression of Nek2 and CDK4/cyclin D1, but not by deleting cyclin E1 or B2 suggesting that K-Ras driven centrosome amplification is an early oncogenic event, and supporting a role for K-Ras in tumour initiation (Zeng *et al.*, 2010). C-myc has been observed to induce centrosome amplification in pre-formed tumours, suggesting a role for c-myc in tumour progression (Zeng *et al.*, 2010).

Overexpression of the prolyl isomerase Pin1, which activates a number of different oncogenic pathways, has been shown to correlate with centrosome amplification in a number of human breast cancer samples (Suizu *et al.*, 2006; Chan, 2011). Pin1 has been shown to localise to the centrosome during interphase, but not during mitosis, and its overexpression results in centriole overduplication in cell lines which have been arrested during S-phase (Suizu *et al.*, 2006). Work done in mouse models has shown that the centrosome amplification resulting from Pin1 overexpression can lead to mammary hyperplasia and malignant tumour formation (Suizu *et al.*, 2006). Overexpression of YB-1, a Y-box binding protein has also been shown to lead to centrosome amplification in breast cancer, this has been suggested to be through cytokinesis failure through the mislocalistion of LIMK (Lim kinase) (Bergmann *et al.*, 2005; Davies *et al.*, 2011). YB-1 is overexpressed in ~75% of human breast carcinomas, and in mice its overexpression has been linked to the tumour initiation of a variety of different histological types (Bergmann *et al.*, 2005).

There are therefore a number of different mechanisms that have been associated with the generation of supernumerary centrosomes within cancer, however the mechanism in the majority of cancers has not yet fully been elucidated.

1.2.4 Effects of supernumerary centrosomes

Based on the detrimental effects arising from centrosome amplification, including cell cycle arrest, as well as aneuploidy, it may be considered surprising that centrosome amplification is so widely observed as a phenomenon within human tumours. It is therefore expected that centrosome amplification must confer some advantage to cancer cells that warrant tumours maintaining their population of cells with supernumerary centrosomes, despite the potentially negative consequences. As described previously, *in vitro* cell lines where supernumerary centrosomes have been generated lose them over time, suggesting that mechanisms allowing for the proliferation of cells with supernumerary centrosomes must be distinct from the mechanisms which generate them in the first place (Ganem, Godinho and Pellman, 2009; Krzywicka-Racka and Sluder, 2011; Godinho *et al.*, 2014). This effect may be influenced by the role centrosome amplification plays in promoting aneuploidy (Ganem, Godinho and Pellman, 2009; Silkworth *et al.*, 2009), affecting asymmetric cell division (Basto *et al.*, 2008), altered cilia signalling (Mahjoub and Stearns, 2012), or through developing invasive features, (Godinho *et al.*, 2014) which are described in more detail below (Figure 1.4). This may suggest that centrosome amplification could arise in later stages of tumour development, after the cancer cells have adapted to maintain their supernumerary centrosome population.

1.2.4.1 Centrosome amplification and tumourigenesis

Whilst observations within breast cancer have allowed the role of centrosome amplification in tumour initiation or development to be hypothesised, until recently Boveri's hypothesis that centrosome amplification can lead to tumourigenesis was untested.

Transgenic mouse models were used to independently access the role of centrosome amplification on tumourigenesis. Transient PLK4 overexpression, which has been well characterised as leading to centrosome amplification by centriole overduplication (Bettencourt-Dias *et al.*, 2005; Habedanck *et al.*, 2005; Kleylein-Sohn *et al.*, 2007;

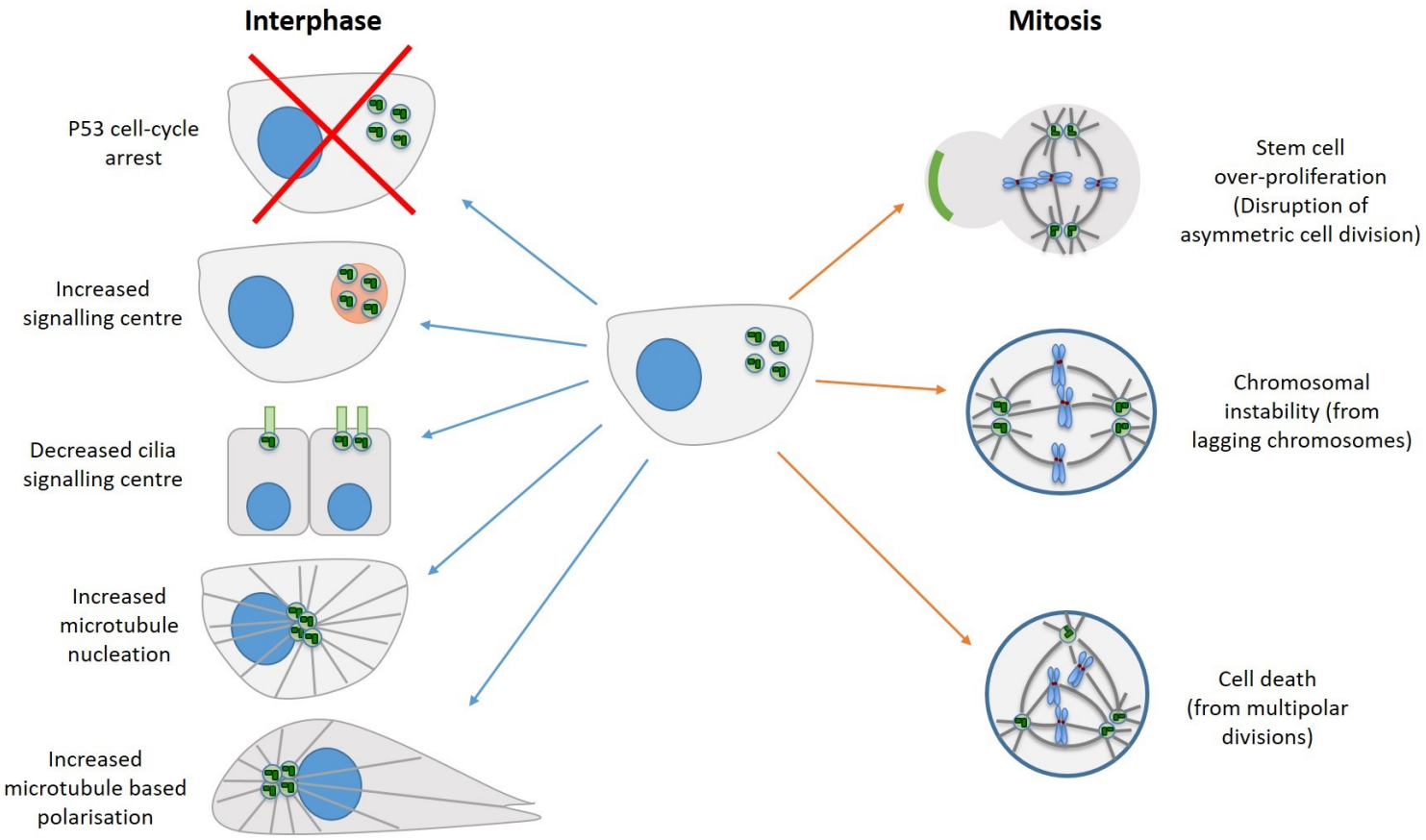

Figure 1.4: Effects of supernumerary centrosomes
Centrosome amplification can have a number of effects, both at interphase and during mitosis. During interphase centrosome amplification can result in p53-dependent cell cycle arrest, but it can also affect signalling (including cilia based signalling), increase microtubule nucleation as well as microtubule based polarisation and increased invasive properties of cells. During mitosis centrosome amplification can disrupt asymmetric cell division resulting in stem-cell over-proliferation as well as aneuploidy and chromosomal instability from lagging chromosomes or multipolar cell divisions.

Basto *et al.*, 2008), was shown to accelerate tumour development in mice which lacked p53 (Coelho *et al.*, 2015; Serçin *et al.*, 2015).

Serçin *et al.* showed that PLK4 overexpression in the absence of p53 leads to rapid skin tumour formation (Serçin *et al.*, 2015). They observed that the percentage of cells containing supernumerary centrosomes decreased along with a reduction in PLK4 mRNA levels after birth, and prior to the formation of tumours (Serçin *et al.*, 2015). Whilst centrosome amplification itself may have reduced, the aneuploidy that had resulted from this transient amplification remained and skin tumours were observed. Due to the loss of centrosome amplification over time, this further supported that there must be an independent mechanism which allows cells to adapt to maintain their supernumerary centrosome population. Conversely, another mouse model of centrosome amplification showed that it does not cause tumour formation in the brain, but instead results in microcephaly (Marthiens *et al.*, 2013). This would then suggest that centrosome amplification has different effects dependent on tissue context.

Similar work done by Coelho *et al.* using inducible PLK4 overexpression showed that centrosome amplification was able to advance lymphoma and sarcoma onset, as well as hyperplasia of the skin and pancreas, again in the absence of p53 (Coelho *et al.*, 2015). Whilst p53-/- mice do succumb to early lymphomas, this work would suggest an accelerated time course resulting from centrosome amplification (Coelho *et al.*, 2015). Taken together these studies would suggest that centrosome amplification is not sufficient on its own to enable tumour development, but instead is able to accelerate tumourigenesis upon p53 loss.

In contrast to these studies, use of a different mouse model to generate supernumerary centrosomes, using ubiquitous PLK4 overexpression did not result in accelerated tumourigenesis, even in the absence of p53 (Vitre *et al.*, 2015). The reason for the differences between the studies is not yet understood, however it is possible that the difference between transient or ubiquitous PLK4 overexpression may account for the variation. It is possible that ubiquitous PLK4 overexpression may impair accelerated tumour formation, whereas transient PLK4 overexpression can increase tumour progression (Coelho *et al.*, 2015; Serçin *et al.*, 2015; Vitre *et al.*, 2015).

In support of this, more recent work by the same group that had showed no effect of centrosome amplification on tumourigenesis, showed the reverse when supernumerary centrosomes were generated by transient PLK4 overexpression (Levine *et al.*, 2017). They showed that inducing PLK4 overexpression resulted in centrosome amplification as expected, although the higher PLK4 levels did not result in centrosome

amplification in all tissues. Where centrosome amplification was observed they then saw spontaneous tumour formation, these tumours did not expres p53 (Levine *et al.*, 2017). Whilst Boveri's hypothesis that centrosome amplification remained largely unanswered for 100 years, it is still yet to be fully understood if supernumerary centrosomes are directly oncogenic, or are limited to accelerating tumourigenesis.

1.2.4.2 p53-mediated arrest

Centrosome amplification resulting from either cytokinesis failure (Andreassen *et al.*, 2001; Fujiwara *et al.*, 2005), or from centriole over-duplication has been shown to result in the stabilisation of p53, and consequently of p21, this leads to G1 cell cycle arrest and therefore a reduction in cell proliferation (Holland *et al.*, 2012). The stabilisation of p53 was shown to be independent of the aneuploidy resulting from the extra centrosomes (Holland *et al.*, 2012). Loss of p53 was shown to rescue this cell cycle affect, allowing for the continued proliferation of cells containing supernumerary centrosomes (Holland *et al.*, 2012). More recently, a screen was used to identify the modulators involved in the p53 arrest in tetraploid cells (Ganem *et al.*, 2014). Ganem *et al.* identified LATS2 (large tumour suppressor kinase 2) as an important factor for the maintenance of tetraploid cells, containing supernumerary centrosomes during G1 (Ganem *et al.*, 2014). They identified that cells containing supernumerary centrosomes had increased levels of phosphorylated LATS2, which is involved in the activation of the Hippo pathway which limits cell proliferation (Ganem *et al.*, 2014). Furthermore, decreased RhoA activity was also observed in cells with supernumerary centrosomes, which can also lead to activation of the Hippo pathway (Ganem *et al.*, 2014; Godinho *et al.*, 2014). The lower levels of RhoA in cells with supernumerary centrosomes may arise from hyperactivation of Rac1 which has been to antagonise RhoA (Sander *et al.*, 1999), as a result of the increased microtubule nucleation arising from the increase in centrosomes (Godinho *et al.*, 2014). It is therefore possible that loss or inhibition of the Hippo pathway may enable cells to adapt to maintain cell proliferation in the presence of cells with supernumerary centrosomes, although this hypothesis has not yet been tested *in vivo*.

More recent research has also shown that in cells where supernumerary centrosomes are generated by either centrosome overduplication or cytokinesis failure can activate the PIDDosome multiprotein complex, leading to Caspase-2 mediated cleavage of MDM2, therefore resulting in p53 activation and p21-dependent cell cycle arrest (Fava *et al.*, 2017). This pathway has also been implicated in development, by controlling the polyploidisation of hepatocytes by regulating p53 levels in liver organogenesis

(Fava *et al.*, 2017). This would suggest that the PIDDosome can help protect cells against supernumerary centrosomes by activating p53 and cell cycle arrest.

1.2.4.3 Chromosomal instability

One of the most well established consequences of supernumerary centrosomes is multipolar mitoses, which can then lead to poorly tolerated levels of aneuploidy (Kwon *et al.*, 2008; Ganem, Godinho and Pellman, 2009; Krzywicka-Racka and Sluder, 2011). Whilst there is a correlation between centrosome amplification and chromosomal instability (CIN), which is the persistent rate of chromosomal alterations, in tumours, it is unlikely that this CIN arises from poorly tolerated multipolar divisions. Whilst aneuploidy and CIN can help facilitate tumourigenesis, high levels can be detrimental to tumour development (Weaver *et al.*, 2007; *Reviewed in:* Holland and Cleveland, 2012). In support of this, multipolar divisions arising from centrosome amplification in mouse neuronal cells lead to high levels of aneuploidy, and consequently undergo apoptosis. This then results in brain developmental defects, with no observed tumour formation (Marthiens *et al.*, 2013).

Studies have shown that CIN can be driven by centrosome amplification, independently of multipolar mitoses. Supernumerary centrosomes are able to form transient multipolar spindles, prior to centrosome clustering, this can lead to the formation of erroneous merotelic attachments (Figure 1.5) (Ganem, Godinho and Pellman, 2009; Silkworth *et al.*, 2009). Such erroneous attachments can comprise of microtubules from both spindle poles attaching to a single kinetochore. These attachments can then go unrepaired as the SAC (spindle assembly checkpoint) is satisfied when sister kinetochores are under tension, and cannot distinguish if the attachments are correct or not (*Reviewed in:* Wang *et al.*, 2014). These merotelic attachments can then lead to lagging chromosomes, and consequently aneuploid daughter cells (Cimini, 2008). Therefore, centrosome amplification can lead to aneuploid cells without undergoing multipolar divisions.

More recent work has implicated lagging chromosomes as having a broader role in the generation of CIN observed in cancer. Lagging chromosomes can result in DNA damage, where the chromosomes are caught at the cytokinetic furrow (Janssen *et al.*, 2011), or where they are segregated into micronuclei (Crasta *et al.*, 2012; Hatch *et al.*, 2013). Micronuclei are formed where lagging acentric chromosomes or chromatid fragments are incorporated into a smaller separate nucleus. Therefore aneuploidy, CIN, DNA damage, and "chromothripsis" where a chromosome or chromosome

arm is broken and reassembled randomly can occur as a result of supernumerary centrosomes (Stephens *et al.*, 2011; Crasta *et al.*, 2012; Zhang *et al.*, 2015). These abnormalities can then drive genetic heterogeneity within tumours, which enable tumours to evolve by gaining advantageous features (Thompson and Compton, 2011). Recent work in support of this model has shown that transient centrosome amplification can lead to low levels of aneuploidy, which results in skin carcinomas in p53 null mice (Serçin *et al.*, 2015). Therefore whilst centrosome amplification can play a role in tumourigenesis by CIN and aneuploidy, a balance has to be found where these processes do not become detrimental to the tumour.

1.2.4.4 Asymmetric cell division

Work done in *Drosophila* where neuroblasts with supernumerary centrosomes were transplanted into the abdomen of adult flies led to the formation of fast growing tumours (Basto *et al.*, 2008). What was particularly interesting was that these tumours showed low levels of aneuploidy (Basto *et al.*, 2008), and that aneuploidy was not sufficient to drive tumour formation within this model system (Castellanos, Dominguez and Gonzalez, 2008). It was observed that whilst these cells are able to cluster their supernumerary centrosomes efficiently, and divide in a bipolar manner, there were defects in asymmetric cell division (Basto *et al.*, 2008; Castellanos, Dominguez and Gonzalez, 2008). This is important in the cancer setting as defects in asymmetric cell division can lead to expansion of the stem-cell compartment and consequently promote tumour formation (Caussinus and Gonzalez, 2005).

One of the key characteristics of stem cells is their ability to "self-renew", allowing for the maintenance of the stem-cell compartment, whilst allowing for their daughter

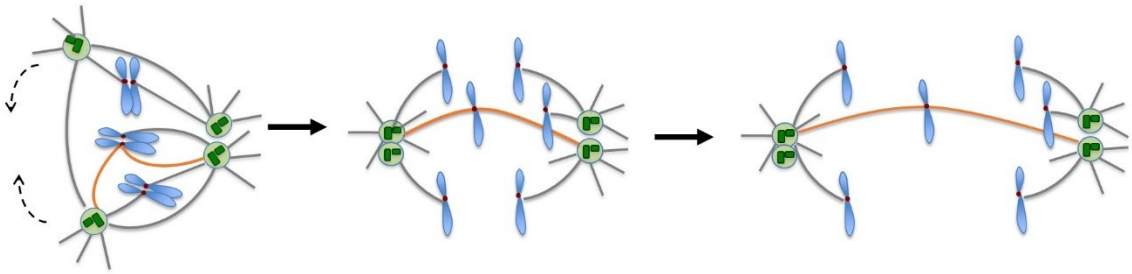

Figure 1.5: Supernumerary centrosomes can give rise to merotelic attachments and lagging chromosomes
Supernumerary centrosomes can promote merotelic attachments (when one kinetochore attaches to microtubules that emanate from opposite spindle poles) due to altered spindle geometry. This merotely can then result in lagging chromosomes and subsequently aneuploid daughter cells.

cells to differentiate. Asymmetric cell division is an important mechanism to allow stem cells to do this, with one daughter cell differentiating, whilst the other is maintained as a stem-cell (Betschinger and Knoblich, 2004; Morrison and Kimble, 2006).

The mechanism linking supernumerary centrosomes to the observed defects in asymmetric cell division are not fully understood, although different models have been proposed (Godinho and Pellman, 2014). It is possible that the presence of supernumerary centrosomes could disrupt the cues that are normally directed by the mother and daughter centrosome during mitosis, as ordinarily the mother and daughter centrosomes are differentiated into the daughter differentiating or stem cell (Reina and Gonzalez, 2014). Alternatively, the astral microtubules which link the centrosome to the cell cortex could become disorganised upon centrosome amplification which may then result in defects in spindle orientation (Siller and Doe, 2009). Defects on spindle orientation were identified in murine epidermis cells with supernumerary centrosomes which underwent asymmetric cell division; such defects in spindle orientation were not observed in symmetric cell divisions (Kulukian *et al.*, 2015). However, such spindle mis-positioning was not observed in mouse neuronal cells, suggesting that such defects may be cell type dependent (Kulukian *et al.*, 2015). Another suggestion is that supernumerary centrosomes may lead to a change in the cellular localisation of polarity determinants (Caussinus and Gonzalez, 2005).

1.2.4.5 Cell polarity, invasion and microtubules

During interphase, the centrosomes play an important role in the organisation of microtubules, which are important for cell shape, motility and polarity (Bettencourt-Dias and Glover, 2007). It is therefore a possibility that independently of their role on generating aneuploidy, supernumerary centrosomes may play a role in tumourigenesis by impacting on the microtubule array, and thus altering the cellular organisation and architecture. In support of this cells with supernumerary centrosomes and consequently increased microtubule nucleation has been positively correlated, independently of aneuploidy with high histological grade breast cancers (Salisbury, D'Assoro and Lingle, 2004).

During interphase, the supernumerary centrosomes are normally clustered together, through a yet to be fully elucidated process. Just before mitosis these centrosomes then separate allowing for the formation of the mitotic spindle. These clustered supernumerary centrosomes are then able to recruit extra PCM, resulting in increased

microtubule nucleation capacity (D'Assoro *et al.*, 2002; Lingle *et al.*, 2002).

Centrosomes play a fundamental role in directing cellular polarity, by directing the organisation of microtubules which in turn control cell shape and motility (Tang and Marshall, 2012). For instance, the centrosome localisation in neurons is important for the site of axon growth (Tang and Marshall, 2012). Similarly, the position of the centrosome has also been implicated in the formation of the immunological synapse by controlling the proper secretion of lytic granules, and for positioning the Golgi at the leading edge of cells undergoing directional migration (Tang and Marshall, 2012). Whilst the impact of these clustered supernumerary centrosomes during interphase on these processes has not been directly studied, it is possible that the increased microtubule nucleation may lead to stronger cellular polarisation (Godinho and Pellman, 2014).

There have been a number of different cellular processes that have been suggested to be affected by the increase in microtubule nucleation arising from centrosome amplification. Microtubules have been shown to regulate the disassembly of focal adhesions, a process required for cell migration (Stehbens and Wittmann, 2012). Microtubules have also been implicated in affecting Rho GTPases activity, which play key roles in controlling cellular invasion (*Reviewed in:* Lozano, Betson and Braga, 2003). Indeed, depolymerisation of microtubules is thought to lead to the release of GEF-H1 and p190RhoGEF, two guanine nucleotide exchange factors, resulting in RhoA activation (Van Horck *et al.*, 2001; Chang *et al.*, 2007). Conversely microtubule nucleation can lead to Rac1 activation, and consequently trigger Arp2/3-mediated actin polymerisation which is required for the formation for lamellipodia and for cellular migration (Waterman-Storer *et al.*, 1999). Therefore, it was hypothesised that supernumerary centrosomes and the resultant increase in microtubule nucleation could affect cellular processes, including those involved in cellular migration, playing a role in tumour formation independently of aneuploidy (Godinho and Pellman, 2014). More recent work has shown a direct link between centrosome amplification and cellular invasion in three-dimensional culture models (Godinho *et al.*, 2014). Godinho *et al.* showed that supernumerary centrosomes, and the resultant increased microtubule nucleation increased Rac1 activity which was then driving the invasive phenotype observed (Godinho *et al.*, 2014). This work further supports the link between the positive correlation between centrosome amplification and more advanced tumour grades, as well as the correlation with metastasis (Salisbury, D'Assoro and Lingle, 2004; *Reviewed in:* Chan, 2011; Godinho and Pellman, 2014).

1.2.4.6 Signalling

Alongside a role in CIN and the changes affected by increased microtubule nucleation, a role for supernumerary centrosomes in cellular signalling in tumour formation has also been identified. Many signalling pathways make use of a scaffold to help concentrate signalling molecules until the required threshold is reached to activate downstream effectors, or to localise different signalling molecules into the same localisation. The centrosome has been identified as such a signalling platform in fission and budding yeasts (*Reviewed in:* Bardin and Amon, 2001; Jaspersen and Winey, 2004).

In fission yeast, the centrosome (spindle pole body (SPB)) promotes the required signalling which enabled entry into mitosis (Hagan and Grallert, 2013). Work by Grallert *et al.* showed that the SPB is used as a platform, which through a positive feedback loop involving Plo1, the PLK1 homologue, leads to increased cyclin B/Cdk1 activity resulting in mitotic entry (Grallert *et al.*, 2013). Plo1 is recruited to the SPB during late G2, by Fin1, which normally impairs Plo1 localisation to the SPB (Grallert *et al.*, 2013). This recruitment and activation of Plo1 is thought to enhance Cdc25 and inhibit the Cdk1 inhibtor Wee1, resulting in the activation of cyclin B/Cdk1 (Hagan, 2008). This control of mitotic entry by centrosomes is thought to be widely conserved, being observed in *C. elegans*, *Xenopus* and also in humans (Perez-Mongiovi *et al.*, 2000; Jackman *et al.*, 2003; Hachet, Canard and Gönczy, 2007; Portier *et al.*, 2007).

Interestingly, use of proteomic analysis on purified centrosomes has identified a number of different signalling molecules that associate with centrosomes, however, some of these associations may only be transient (Andersen, Wilkinson and Mayor, 2003; Jakobsen *et al.*, 2011). For example, the Wnt pathway, which has been shown to contribute to tumour formation is inhibited by Diversin which has been shown to localise to the centrosome (Kfoury *et al.*, 2008; Itoh *et al.*, 2009). Use of mutant Diversin which was impaired from localising to centrosomes was no longer able to impair Wnt signalling (Itoh *et al.*, 2009).

The centrosome has also been observed to change size upon inhibition of the proteasome, or increased levels of misfolded proteins (Wigley *et al.*, 1999). It has therefore been suggested that as well as acting as a signalling platform, the centrosome may play a role in sequestering proteins from the cytoplasm, in situations such as proteasome inhibition (*Reviewed in:* Godinho and Pellman, 2014). In support of this, inhibition of the proteasome was shown to lead to increased phosphorylated Smad1,

which localised to the centrosomes, this also resulted in the hypothesis that the centrosome may play a role in proteasome-mediated degradation, although more work needs to be done to elucidate this process (Fuentealba *et al.*, 2007).

1.2.5 Coping with extra centrosomes

The ability for tumours to actively maintain their supernumerary centrosome population suggests that there must be mechanisms for cells to adapt to the detrimental effects that arise as a result. It was previously accepted, that the presence of supernumerary centrosomes would automatically result in multipolar cell divisions in mitosis. However, work done in the early 1980s in the N1E-115 mouse neuroblastoma cell line, where ~100% of cells contain supernumerary centrosomes, showed that there is the capacity for centrosomes to remain within close proximity during mitosis, in a process now referred to as "centrosome clustering" (Ring, Hubble and Kirschner, 1982). This centrosome clustering then enables the formation of a pseudo-bipolar spindle, allowing for chromosome segregation into two daughter cells, with little to no aneuploidy (Ring, Hubble and Kirschner, 1982; Brinkley, 2001; Basto *et al.*, 2008; Ganem, Godinho and Pellman, 2009).

Alternatively to centrosome clustering, other mechanisms have been identified which enable cells to survive in the presence of supernumerary centrosomes including centrosome loss, asymmetric segregation of supernumerary centrosomes during mitosis and centrosome inactivation (*Reviewed in:* Godinho, Kwon and Pellman, 2009). However, within the cancer setting, only centrosome clustering has been described so far (Figure 1.6).

1.2.5.1 Centrosome inactivation

Whilst centrosome clustering is the most widely characterised and understood process for cells to survive in the presence of supernumerary centrosomes, centrosome inactivation has also been reported as a mechanism enabling cells to form bipolar spindles and subsequently divide into two daughter cells. Work done in *Drosophila* neuroblasts, where centrosome amplification was driven by SAK/PLK4 overexpression showed that these cells were able to undergo bipolar cell divisions. Whilst centrosome clustering was observed in the majority of spindles, a number of un-clustered centrosomes were identified, which showed reduced PCM levels, and a reduction in microtubule nucleation activity (Basto *et al.*, 2008). These observations suggested that these

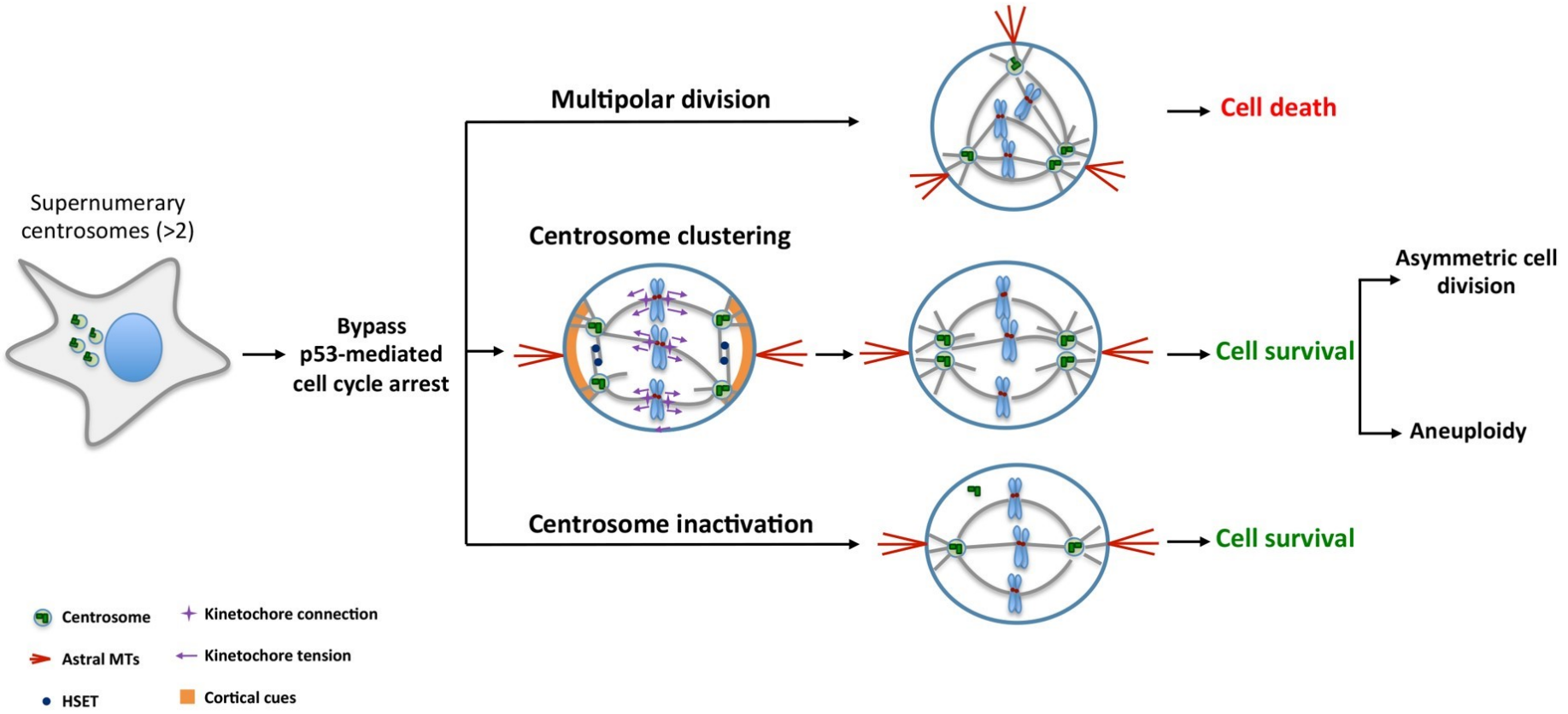

Figure 1.6: Cell survival in the presence of supernumerary centrosomes
Cells with supernumerary centrosomes (>2) can undergo different cell fates, once they have bypassed a p53-mediated cell cycle arrest. Top – cells can undergo multipolar cell division, leading to high levels of aneuploidy, which are poorly tolerated, resulting in cell death. Middle – cells can cluster their supernumerary centrosomes into two poles, this is determined by factors such as the interaction of astral microtubules with the cell cortex, minus-end directed motors such as HSET, cortical cues, SAC and kinetochore tension. Centrosome clustering results in viable daughter cells but can lead to aneuploidy and defective asymmetric cell division. Bottom – depletion of microtubule nucleating proteins results in inactivation of a centrosome, stopping the centrosome having an effect on spindle orientation, resulting in two daughter cells (not described in humans).

un-clustered centrosomes are unable to nucleate microtubules and are therefore "inactivated", so that they do not contribute to the mitotic spindle. A similar process had previously been described by Iwao *et al.* where they showed that a gradient of γ-tubulin can result in centrosome inactivation in polyspermic newt eggs, to ensure that only the centrosome that is associates with the principal sperm nucleus can facilitate the formation of mitotic spindle (Iwao *et al.*, 2002). More recent work has started to elucidate the mechanisms involved in the inactivation of centrosomes. In *Drosophila* where centrosome amplification was driven by SAK/PLK4 overexpression it was observed that moesin, a member of the ezrin/radixin/moesin (ERM) protein family was upregulated and localised to the centrosomes in the epithelial wing disks, which inhibited centrosome inactivation leading to multipolar cell divisions. However, in neuroblasts with supernumerary centrosomes, this upregulation and localisation of moesin was not observed, and centrosome inactivation occurred (Sabino *et al.*, 2015). To further test the role of moesin on impairing centrosome inactivation, a hypomorphic moesin mutant was used, resulting in a reduction in the centrosomin recruitment, a PCM protein at the centrosome (Sabino *et al.*, 2015). This evidence therefore suggests that PCM regulation by moesin impairs centrosome inactivation. Furthermore, this work suggests that different cell types can cope with centrosome amplification differently, as observed by the differences between the epithelial wing disks and the neuroblasts. Centrosome inactivation has not yet been reported within human cells.

1.2.5.2 Centrosome loss

During oogenesis, centrosome removal is used to remove/destroy the maternal centrosome, this ensures that after fertilisation there are not multiple centrosomes, with only the spermatic centrosome remaining (Manandhar, Schatten and Sutovsky, 2005). It is thought that a reduction in PCM, and the resultant decrease in microtubule nucleation could lead to the disintegration of the maternal centrosome (Mikeladze-Dvali *et al.*, 2012). This is supported by recent work in *Drosophila Melanogaster* which showed that down-regulation of PCM in the female germ line during oogenesis, results in centriole loss (Pimenta-Marques *et al.*, 2016). Whilst this exact process has not been fully understood, it has been shown that in *C. elegans*, this process requires Cki-2, a cyclin-dependent kinase inhibitor. In oocytes, depleted of Cki-2, it was observed that the maternal centriole is not destroyed, leading to multipolar zygotic cell divisions (Kim and Roy, 2006). More recent work by Mikeladze-Dvali *et al.* also in *C. elegans* showed that depletion of the helicase CHG-1 resulted in a delay in the loss of the maternal centrosome, potentially by impairing the degradation of specific

mRNAs that are involved in the centrosome removal mechanism (Mikeladze-Dvali *et al.*, 2012). Work done in *Dictyoistelium* showed that some cells are also able to directly extrude their centrosomes (Gräf *et al.*, 2003). It has also been hypothesised that cells may be able to utilise asymmetric cell division, to allow one daughter cell to have one centrosome, enabling it to successfully proliferate during future divisions, whilst the other daughter cell inherits the remaining supernumerary centrosomes (Chiba *et al.*, 2000). However, similarly to centrosome inactivation, centrosome loss has not been observed within human cells, so is unlikely to be an important process for enabling the survival of cancer cells with supernumerary centrosomes.

1.2.5.3 Centrosome clustering

Centrosome clustering is the most well-characterised mechanism of cells coping with supernumerary centrosomes. Centrosome clustering is where a cell is able to bring the supernumerary centrosomes together at each pole during mitosis, forming a pseudo-bipolar spindle that leads to two daughter cells. This process was first identified in the murine cell line N1E-115, where ~100% of cells contain extra centrosomes, since then cells containing a high proportion of cells with centrosome amplification (>30%) have been shown to be efficient at centrosome clustering (Ring, Hubble and Kirschner, 1982; Brinkley, 2001; Quintyne *et al.*, 2005; Kwon *et al.*, 2008; Ganem, Godinho and Pellman, 2009).

Two genome-wide screens were carried out, one in *Drosophila* S2 cells and the other in the human oral squamous carcinoma cell line UPCI:SCC114, to identify key proteins involved in the centrosome clustering process (Kwon *et al.*, 2008; Leber *et al.*, 2010). The screens identified four independent mechanisms as being important for centrosome clustering: the spindle assembly checkpoint (SAC) and chromosomal passenger complex CPC, kinetochore-microtubule tension, the actin cytoskeleton, and microtubule associated proteins (MAPs) (Kwon *et al.*, 2008; Leber *et al.*, 2010).

Spindle assembly checkpoint (SAC) and chromosomal passenger complex (CPC)

The SAC is important in delaying anaphase onset until each duplicated chromosome is properly attached to the mitotic spindle (Weaver and Cleveland, 2005; Nezi and Musacchio, 2009; Maresca and Salmon, 2010).

In a normal mitotic cell, containing two centrosomes, when all of the kinetochore-microtubule attachments are stabilised, this satisfies the SAC, allowing for the onset of anaphase and progression through mitosis (Lara-Gonzalez, Westhorpe and Taylor,

2012). However, in cells with supernumerary centrosomes, these attachments take longer to form and stabilise due to multipolar intermediates, leading to a SAC-dependent delay in mitosis, giving time for the centrosomes to cluster (Basto *et al.*, 2008; Kwon *et al.*, 2008; Yang *et al.*, 2008). Loss of Mad2, a component of the SAC was observed to prevent efficient centrosome clustering (Basto *et al.*, 2008; Kwon *et al.*, 2008; Yang *et al.*, 2008), resulting in multipolar spindles and decreased viability in *Drosophila* with supernumerary centrosomes (Basto *et al.*, 2008). Work done by Kwon *et al.* showed that the treatment of Mad2 depleted cells with the proteasome inhibitor MG132, which causes a delay in anaphase onset, was able to rescue the centrosome clustering phenotype (Kwon *et al.*, 2008). This would suggest that it is the delay in anaphase onset caused by the SAC, giving sufficient time for centrosome clustering that is important in centrosome clustering, rather than the SAC itself. This prolonged time in mitosis in cells with supernumerary centrosomes due to the SAC could partially explain the increased mitotic index observed in tumours (Lambert, 1913). In support of this hypothesis, it was observed that the transformed human fibroblast cell line SV40 have higher levels of tetraploidy and centrosome amplification, alongside an increased mitotic index, compared to their non-transformed equivalents (Levine *et al.*, 1991). However, this delay in mitosis in cells with extra centrosomes does not occur in all cells. The binucleated rat kangaroo kidney epithelial cell line Ptk2 which has centrosome amplification, divides without mitotic delay. However, these cell lines are also unable to cluster their centrosomes efficiently, undergoing multipolar cell divisions (Sluder *et al.*, 1997). This further supports that delaying SAC inactivation, and delaying anaphase onset might be an important process to avoid multipolarity.

A role for the CPC has also been identified in facilitating centrosome clustering, alongside the SAC (Leber *et al.*, 2010). The CPC plays a role in identifying and correcting erroneous chromosome-microtubule attachments that are not bi-orientated, these include merotely and syntely, where a chromatid may be attached to both spindle poles, or two sister chromatids attached to the same spindle pole (Nezi and Musacchio, 2009). The knockdown of the CPC components in the USCI:SCC114 cancer cell line, including AuroraB, borealin, INCENP and survivin, resulted in impaired centrosome clustering and multipolar cell divisions (Leber *et al.* 2010). It is possible that CPC components facilitate clustering through the destabilisation of syntelic and merotelic attachments that will elicit a SAC response resulting in an anaphase delay that promotes centrosome clustering.

Kinetochore/Microtubule tension

Tension produced by the kinetochore-microtubule interface has been identified to

play a role in maintaining centrosome clustering at the spindles poles. Knockdown of components of the Ndc80 complex, including SPC24, SPC25 or HEC1 which are involved in the stabilisation of kinetochore-microtubule attachments (Ciferri, Musacchio and Petrovic, 2007), were observed to result in defects in centrosome clustering (Leber *et al.*, 2010). The same effect was observed upon the depletion of proteins involved in generating kinetochore tension including SGOL1, CENPT and sororin (Leber *et al.*, 2010). Similarly, hepatoma up-regulated protein HURP was identified as being involved in centrosome clustering (Breuer *et al.*, 2010). HURP has been shown to act during mitosis as a kinetochore-microtubule stabilising factor (Silljé *et al.*, 2006; Wong and Fang, 2006). Even in the absence of centrosome amplification, forces acting on the spindle pole are required to prevent multipolarity by opposing the traction forces produced during chromosome congression in prometaphase (Logarinho *et al.* 2012). It is therefore possible that clustered supernumerary centrosomes could impact the spindle forces at the spindle poles, therefore resulting in cells with supernumerary centrosomes being more reliant on correct kinetochore-microtubule tension to maintain intact spindle poles (Figure 1.6).

Actin Cytoskeleton

The actin cytoskeleton has been shown to be integral during mitosis in translating cortical cues via the formation of retraction fibres (Mitchison 1992; Théry *et al.* 2005). Work using micro-contact printing by Théry *et al.* showed that in mitotic cell rounding, the actin-rich retraction fibres, linked to the sites of substrate adhesion, remain attached, working to translate the spatial imprint to the cell. Astral microtubule interaction with the cortical cues directed by these retraction fibres was observed to be involved in controlling spindle positioning (Théry *et al.*, 2005). These cues also dictate whether supernumerary centrosomes are able to cluster or not. Interestingly, cells where a "bipolar" distribution of retraction fibres was maintained upon cell rounding, were capable of clustering their supernumerary centrosomes efficiently, compared to those that had a more distributed pattern (Kwon *et al.*, 2008). Astral microtubules were shown to be important in translating these cues to allow centrosomes to cluster (Kwon *et al.*, 2008).

More recent work has been done to try and understand the mechanisms by which astral microtubules are able to respond to these cortical cues. Pools of subcortical actin assemble near the retraction fibres, these were then shown to be important for the pulling forces on the astral microtubules, enabling the position of the centrosomes near the retraction fibres (Fink *et al.*, 2011). Subsequently, Kwon *et al.* showed that the unconventional myosin, Myo10, which binds to actin and to microtubules, is essential for the localisation of centrosomes towards the actin pools and retraction

fibres, this process is achieved through the regulation of the microtubule dynamics and end-on cortical-microtubule interactions (Kwon *et al.* 2015). Previous work had shown the depletion of Myo10, which was observed to prevent centrosome clustering (Kwon *et al.*, 2008) made cells unresponsive to the cell adhesion footprint (Kwon *et al.*, 2015).

It is still not fully understood how this cell adhesion can then direct the cortical cues through mitosis. However, integrin-linked kinase ILK, which controls integrin-mediated cell adhesion localises to centrosomes and to focal adhesions, and has been to shown to have a role in centrosome clustering through ch-TOG and TACC3, which are two proteins involved at the spindle poles in regulating the minus end of microtubules (Fielding *et al.*, 2008). It is therefore possible, that there is a role in the control of centrosome clustering for cell adhesion proteins. However, further work is required to understand the link between adhesion proteins, the actin cytoskeleton and the cortical cues that control this process.

Work by Kwon *et al.* showed that the inhibition of cortical contractility prevents efficient centrosome clustering, suggesting that the actin cytoskeleton may be able to facilitate centrosome clustering through controlling cortical contractility (Kwon *et al.*, 2008). Both Myosin II and actin are important for the separation of centrosomes during centrosome duplication, by providing the required cortical forces (Rosenblatt *et al.*, 2004). Centrosomal separation during mitosis is aided my astral microtubules inhibiting cortical myosin II contractility, this results in asymmetrical cellular contractility, driving the centrosomes to opposing sides of the cell (Rosenblatt *et al.*, 2004). However, whilst this process explains separation of mitotic cells with two centrosomes to opposing poles, it is unclear how this would then affect cells with multiple centrosomes.

Microtubule associated proteins

Cells with supernumerary centrosomes have been shown to depend on microtubule motors and associated proteins, which are important in the organisation of the mitotic spindle, in order to cluster their extra centrosomes (Godinho, Kwon and Pellman, 2009; Krämer, Maier and Bartek, 2011; *Reviewed in:* Marthiens, Piel and Basto, 2012). The first microtubule proteins suggested to be involved in centrosome clustering were dynein, a minus-end direct motor, and NuMA, a mitotic apparatus protein involved in the mitotic spindle (Quintyne *et al.* 2005). NuMA has been shown in human cells to control the centrosomal localisation of dynein, which is then important for efficient centrosome clustering. Work done in cancer cells with supernumerary centrosomes, where the level of NuMA was increased resulted in the

dissociation of dynein from the spindle poles, this impaired centrosome clustering leading to multipolar mitoses (Quintyne *et al.* 2005). Titration of NuMA levels restored the localisation of dynein, rescuing the centrosome clustering (Quintyne *et al.* 2005). These data suggest a combined role for both NuMA and dynein in centrosome clustering.

The essential E3 ligase the anaphase-promoting complex/cyclosome (APC/C) is involved in proteasome-mediated protein degradation which is required for the regulation of mitotic progression (Pines 2011). When APC/C is bound to CDH1, its co-activator, it regulates the metaphase to anaphase transition, and has also been shown to facilitate centrosome clustering (Drosopoulos *et al.* 2014). Eg5, a microtubule motor and a substrate of APC/C-CDH1 is stabilised after APC/C-CDH1 inhibition, this results in imbalance of forces within the spindle, which impairs efficient centrosome clustering (Drosopoulos *et al.*, 2014).

Another minus-end directed motor HSET/KIFC1 (nonclaret disjunctional, Ncd, in *Drosophila*), a member of the kinesin-14 protein family has also been shown to be involved in centrosome clustering (Kwon *et al.* 2008). Depletion of HSET/KIFC1 by siRNA in cells with supernumerary centrosomes resulted in an increase in multipolar cell divisions, but not in cells with a normal complement of centrosomes, suggesting that HSET/KIFC1 has a role specific to centrosome clustering (Kwon *et al.* 2008). Similarly, in flies, the loss of Ncd decreases the survival of flies with supernumerary centrosomes, but does not adversely affect wild type flies, further supporting a specific role for HSET/KIFC1 in centrosome clustering (Endow & Komma 1998; Basto *et al.* 2008). This specificity of HSET/KIFC1 makes it a promising drug target to drive multipolarity and cell death in cancer cells with centrosome amplification.

1.2.6 Therapeutic advantage of centrosome amplification

Cells with supernumerary centrosomes have unique requirements in order to survive, such as centrosome clustering. Impairment of centrosome clustering results in multipolar mitoses, leading to high levels of aneuploidy and subsequently cell death, or cell cycle arrest (Rebacz *et al.*, 2007; Kwon *et al.*, 2008; Ganem, Godinho and Pellman, 2009; Karna *et al.*, 2011). This therefore makes the impairment of centrosome clustering an attractive therapeutic approach for treating cancer cells with centrosome amplification.

A number of drugs have been suggested to impair centrosome clustering. Griseofulvin, a nontoxic antifungal, as well as impairing mitosis has been observed to result in un-

clustered supernumerary centrosomes in a number of different human cancer cell lines, killing tumour cells at concentrations which are non-toxic to normal cells (Rebacz *et al.* 2007). Furthermore, in a range of 2'-subsituted derivatives of griseofulvin, the compound which was the most efficient at impairing centrosome clustering also had the highest potency, however further work is required to fully understand the link between the un-clustered centrosomes and the observed cell death (Raab *et al.*, 2012).

Phenanthrene-derived poly-ADP-ribose polymerase (PARP) inhibitors have also been identified as a set of compounds which have the potential as being used to impair centrosome clustering (Castiel *et al.*, 2011). The normal role of PARP-1 is to identify DNA damage and initiate base-excision repair, as well as activating DNA damage checkpoints or cell-death via apoptosis. However, a number of PARP related proteins have also been identified as being important for centrosome clustering (Tong *et al.*, 2007; Kwon *et al.*, 2008). Tumours with centrosome amplification which were treated with PJ-34, a PARP-1 inhibitor showed increased multipolar spindles, and subsequently mitotic catastrophe and cell death, supporting a role for PARP inhibitors in impairing centrosome clustering (Castiel *et al.* 2013). Non-transformed cells also treated with PJ-34 showed no defects in their spindle morphology, and cell viability was maintained, supporting a supernumerary centrosome specific mechanism for the cell death observed in the tumours (Pannu *et al.*, 2014). Furthermore, a more recent study has shown that PJ-34 can supress HSET/KIFC1 expression, this could then explain the impairment of the centrosome clustering observed in the tumour samples, as HSET/KIFC1 is required for centrosome clustering (Li *et al.*, 2015).

The identification of key proteins in the centrosome clustering process such as HSET/KIFC1, which do not appear to have essential functions in cells with normal centrosome number, make them an attractive therapeutic target. For example, recently developed HSET/KIFC1 inhibitors have been shown to lead to multipolar mitoses due to the impairment of centrosome clustering in cells with extra centrosomes, but no change on mitosis was observed in cells with normal centrosome number (Wu *et al.*, 2013). Similarly, CW069, an alternative allosteric HSET/KIFC1 inhibitor has been shown to result in multipolar cell divisions in a panel of cell lines with centrosome amplification, resulting in impaired viability. However, in the MCF-7 cell line, which has low levels of centrosome amplification, whilst the spindle formation was unimpaired as expected with CW069 treatment, there was still reported impairment in cell growth, suggesting that this drug may have some toxicity independently of its role in inhibiting centrosome clustering (Watts *et al.*, 2013; Wu *et al.*, 2013; *Reviewed in:* Bhakta-Guha *et al.*, 2015).

Therefore, whilst targeting key components of the centrosome clustering mechanisms is an attractive therapeutic strategy, more work needs to be done in developing more specific inhibitors, which are then less toxic to normal cells. The effectiveness of these drugs in impairing centrosome clustering and subsequently cell viability of cells with supernumerary centrosomes *in vivo* is still unclear, and more work is needed to properly assess the validity of this approach as a beneficial cancer treatment.

1.3 Cell-cell adhesion

Epithelial tissues play a role in separating different compartments in the body by acting as selective barriers. This compartmentalisation is required to allow distinct organs and tissues to perform their specific functions, whilst being able to receive signals from the external environment. Epithelial cells adhere to one another to form the epithelial barrier which is able to regulate the movement of different fluids, solutes and molecules (Hartsock and Nelson, 2008; Van Itallie and Anderson, 2014). This cell-cell adhesion is composed of tight junctions (TJs) and adherens junctions (AJs) (Figure 1.7). Both types of junction are connected to the actomyosin cytoskeleton, and are often impaired in cancer.

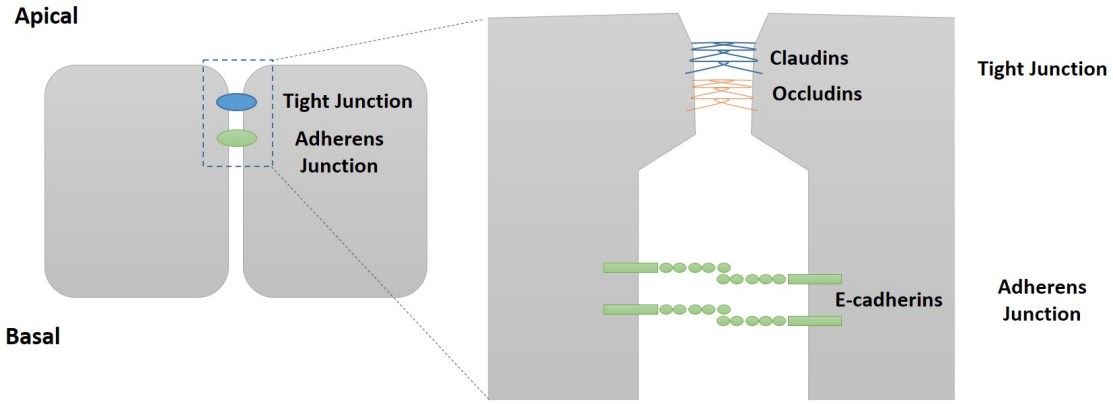

Figure 1.7: Epithelial cell-cell adhesion
Epithelial cells adhere to one another establishing an epithelial barrier through tight junctions (involving claudins and occuldins), and through adherens junctions (involving E-cadherin). The epithelial barrier allows for a regulated and selective movement of fluids, solutes and molecules.

1.3.1 E-cadherin

The organisation of cells into tissues is fundamental to the development of multicellular organisms. This organisation and maintenance of tissues is mediated by a number of cell-membrane localised receptors and ligands localised within the extracellular matrix. Cadherins are a large family of cell-membrane localised receptors, which play a key role in the adhesion of cells within tissues in a Ca^{2+}-dependent manner (Gumbiner, 2005; Halbleib and Nelson, 2006; Lien, Klezovitch and Vasioukhin, 2006). There are at least five major subfamilies of cadherins, the most prominent being the classical cadherins consisting of epithelial (E-), neuronal (N-) and vascular endothelial (VE-). All of the classical cadherins have a conserved cytoplasmic tail, which is involved in binding to the actin cytoskeleton and to catenins (Biswas and Zaidel-Bar, 2017).

E-cadherin is a multi-domain glycosylated protein of 120kDa, containing an extracellular domain including five cadherin repeats (ECs), a trans-membrane domain, and a smaller intracellular domain (Pinho *et al.*, 2011; *Reviewed in:* Brasch *et al.*, 2012). The ECs are each ~110 amino acids long and form an immunoglobulin-like structure, this structure then changes conformation after Ca^{2+} binding between each of the EC regions (Pokutta *et al.*, 1994; Nagar *et al.*, 1996; Pertz *et al.*, 1999). The transmembrane domain contains a leucine-zipper motif, which has been suggested to be involved in the oligomerisation of E-cadherin, and may facilitate interaction with other trans-membrane proteins (Bignold, Coghlan and Jersmann, 2006; Coon *et al.*, 2015; Biswas and Zaidel-Bar, 2017). The shorter and highly conserved intracellular domain is ~150 amino acids in length, and is able to bind adaptor proteins including β-catenin and p120, as well as binding to the actin cytoskeleton (McEwen, Escobar and Gottardi, 2012; Zaidel-Bar, 2013; Guo *et al.*, 2014). This ability to bind to a number of different effectors allows E-cadherin to not only have a role in cellular adhesion, but also to control a range of signalling pathways.

E-cadherin plays a fundamental role in adhering epithelial cells to each other. They are normally concentrated at adherens junctions, which are specialised structures allowing for cell-cell adhesion between adjoining cells with an intermembrane space of ~15-30nm (Meng and Takeichi, 2009; *Reviewed in:* Brasch *et al.*, 2012). At these junctions, E-cadherin forms bonds between the ectodomains of opposing E-cadherin units from the two adjoining cells, within the intermembrane space, meanwhile the cytoplasmic domain can bind to β-catenin, linking E-cadherin to the cytoskeleton, as well as to p120 which controls the cadherin turnover and facilitates actin assembly (Reynolds and Carnahan, 2004; Shapiro and Weis, 2009; Yonemura, 2011) (Figure

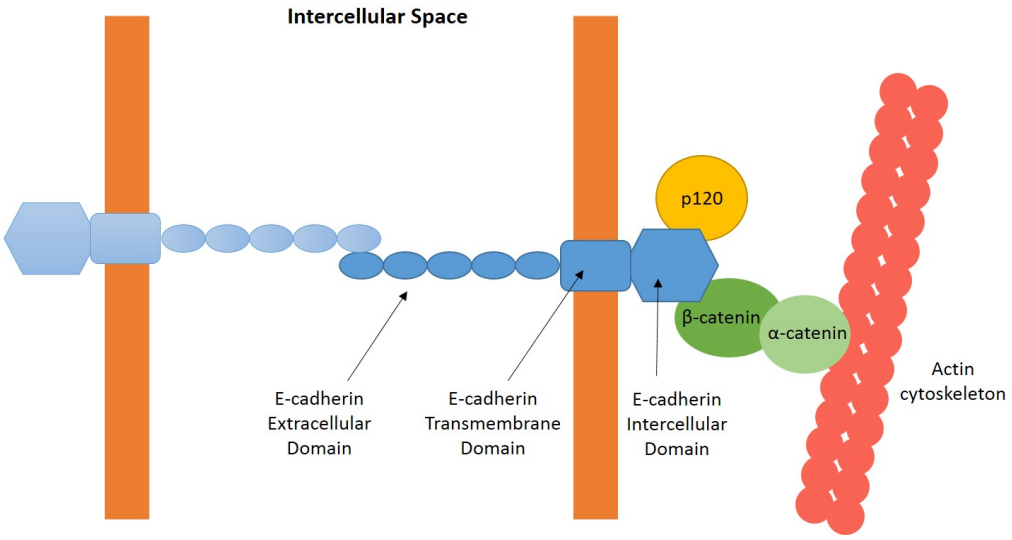

Figure 1.8: E-cadherin at the adherens junctions
E-cadherin proteins from two adjoining cells may form Ca^{2+}-dependent bonds within their extracellular domains, linking the two cells together. The intracellular domain of E-cadherin can interact with the actin cytoskeleton through β- and α-catenins, E-cadherin can also form bonds with p190. These cadherin-catenin complexes then form the adherens junctions.

1.8).

1.3.1.1 E-cadherin and centrosome positioning

Alongside a role in cell adhesion, E-cadherin has been implicated in controlling centrosome and nucleus position, as well as cellular polarisation through the regulation of cellular interactions and control of the cytoskeleton (Dupin, Camand and Etienne-Manneville, 2009; Inaba *et al.*, 2010). Work done by Dupin *et al.* in rat astrocytes plated on micropatterns showed that individual cells, or cells surrounded in a monolayer, showed a randomly localised nucleus and centrosomes (Dupin, Camand and Etienne-Manneville, 2009). In contrast to this, cells with neighbouring cells on a few sides showed polarised localisation of their nuclei and centrosomes towards the cell contacts. This then suggested a role for cell-cell adhesions in controlling nuclei and centrosome positioning. To further test this they depleted calcium, therefore impairing cadherin-dependent adhesion for 3 hours, and showed that this polarisation of nuclei position and of the centrosomes was also impaired. This data therefore suggested that cadherins, including E-cadherin are then important for controlling the cellular polarity of the nucleus and centrosomes (Dupin, Camand and Etienne-Manneville, 2009). This was supported by work done in *Drosophila* by Inaba *et al.* which showed that E-cadherin is important for mediating the maintenance of the

germline stem cell (GSC) population by controlling asymmetric cell division (Inaba *et al.*, 2010). They showed that within GSCs the centrosomes and spindle orientate to the adherens junctions, they hypothesised that these adherens junctions can then provide the required polarity cues to enable the required asymmetric cell division, maintaining the stem cell population (Inaba *et al.*, 2010).

More recent work has been undertaken to try and elucidate the role of E-cadherin on this cellular polarisation and the orientation of cellular division. Work by Gloerich *et al.* showed that the control of spindle orientation by E-cadherin is mediated by the evolutionarily conserved LGN/NuMA complex, which is involved in the regulation of cortical attachments of astral microtubules (Gloerich *et al.*, 2017). They showed that LGN can directly bind to the cytosolic tail of E-cadherin. Upon mitotic entry, NuMA is released from the nucleus and displaces LGN from E-cadherin forming the LGN/NuMA complex. This complex can then facilitate the stabilisation of astral microtubules associations at the cell cortex, which in turn orientates the mitotic spindle. Therefore E-cadherin is important in mediating the localisation of the LGN/NuMA complex at the cell-cell contacts which in turn dictates spindle orientation (Gloerich *et al.*, 2017).

1.3.1.2 E-cadherin in cancer

It has been well established that epithelial tumours lose E-cadherin either partially or completely as they become more malignant (Strumane, Berx and Van Roy, 2004; Van Roy and Berx, 2008). There is also evidence that E-cadherin plays a role in being anti-invasive and anti-metastatic (Frixen *et al.*, 1991; Vleminckx *et al.*, 1991; Perl *et al.*, 1998). A number of different mechanisms have been identified for the loss of E-cadherin in tumours including mutations, epigenetic silencing, and cadherin switching (Van Roy and Berx, 2008).

The first evidence that loss of E-cadherin may play a role in tumour development came from studies that showed regular loss of heterozygosity of chromosome 16q21-22 in a number of different cancer types (*Reviewed in:* Strumane, Berx and Van Roy, 2004). The 16q22.1 region was identified as being the site of the CDH1 gene, which encodes for E-cadherin (Berx *et al.*, 1995). Further work identified that this loss of heterozygosity of 16q is frequently observed in breast cancer, occurring in ~50% of ductal carcinomas (Cleton-Jansen *et al.*, 2001) and more so in lobular breast carcinomas (Berx *et al.*, 1996).

The first described E-cadherin inactivating mutations were observed in diffuse gastric

cancer, where somatic mutations were regularly observed to result in a skipping of exons 7 and 9, resulting in in-frame deletions (Becker *et al.*, 1993). Comparatively, such observations have not been seen in lobular breast carcinomas where inactivating mutations are found more broadly across the gene rather than at a particular localisation (Machado *et al.*, 2001). These mutations then result in out-of-frame mutations which are suggested to lead to truncated E-cadherin fragments, or no expression of the protein at all (Machado *et al.*, 2001). It was also reported that alongside these mutations promoter methylation of the CDH1 gene was also increased, further resulting in loss of E-cadherin (Berx *et al.*, 1996, 1998). In some cases of lobular breast carcinomas, germline mutations have been observed across the CDH1 gene (Caldas *et al.*, 1999; Pharoah, Guilford and Caldas, 2001; Brooks-Wilson *et al.*, 2004; Suriano *et al.*, 2005; Hansford *et al.*, 2015). In such cases the lifetime risk of those with such mutations of getting breast cancer is 39% (Carneiro *et al.*, 2008).

Hypermethylation of the CDH1 promoter has also been implicated in the loss of E-cadherin expression during tumour progression. Within the 5' proximal promoter region of CDH1 a large CpG island has been identified as being regularly hypermethylated in a number of different cancers, leading to a loss of E-cadherin protein expression (Berx *et al.*, 1995; Graff *et al.*, 1995; Yoshiura *et al.*, 1995; Chang *et al.*, 2002; Kanazawa *et al.*, 2002). Similarly, CDH1 CpG island methylation is observed to increase during tumour progression within both breast and hepatocellular carcinomas (Kanai *et al.*, 2000; Nass *et al.*, 2000). Other repressors of E-cadherin transcription have also been associated with tumour progression. Increased Snail expression is strongly associated with loss of E-cadherin in ductal breast carcinomas, high-grade breast carcinomas and lymph node tumours (Cheng *et al.*, 2001; Blanco *et al.*, 2002). A number of transcription factors have also been identified such as Twist, and deltaEF1/ZEB1 as resulting in loss of E-cadherin (Guaita *et al.*, 2002; Yang *et al.*, 2004; Eger *et al.*, 2005; Martin *et al.*, 2005; Spaderna *et al.*, 2008; Yu *et al.*, 2010).

Whilst genetic mutations, and epigenetic silencing are the most well established mechanisms for E-cadherin silencing in tumour development, other mechanisms have been identified which may play a role in impairing the normal function of E-cadherin (*Reviewed in:* Van Roy and Berx, 2008). During the normal life-cycle of E-cadherin it is recycled to new sites of cell-cell adhesion by endocytosis, it has been hypothesised that impairment of this process could then lead to its premature degradation (*Reviewed in:* Van Roy and Berx, 2008). Activation of oncogenes including c-Met, Src and EGFR have been shown to result in the increased phosphorylation of the tyrosine residues in the cytoplasmic tail of E-cadherin, this results in the recruitment

of Hakai, an E3-ubiquitin ligase, leading to ubiquitin-dependent degradation of E-cadherin (Fujita *et al.*, 2002; Shen *et al.*, 2008). A similar role in inducing E-cadherin degradation has also been implicated for MDM2, another E3-ubiquitin ligase (Yang *et al.*, 2006). Upregulation of enzymes which can directly cleave E-cadherin have also been suggested to potentially play a role in E-cadherin silencing in cancer progression such as some of the matrix metalloproteases as well as calpain (Steinhusen *et al.*, 2001; Rios-Doria *et al.*, 2003; De Wever *et al.*, 2007; *Reviewed in:* Van Roy and Berx, 2008).

Loss of E-cadherin expression can also be induced by expression of mesenchymal cadherins, such as N-cadherin during processes such as epithelial to mesenchymal transition (EMT). This process of change of cadherin expression is termed "cadherin switching" (Hazan *et al.*, 2004; Wheelock *et al.*, 2008). Overexpression of N-cadherin can also result in increased invasion and metastatic potential of cells when injected into nude mice, even in the presence of E-cadherin (Hazan *et al.*, 2004; Wheelock *et al.*, 2008).

1.4 Discoidin Domain Receptor 1

One of the proteins that E-cadherin can signal downstream through is DDR1 (Discoidin Domain Receptor 1). There are two discoidin domain receptor DDR proteins, DDR1 and DDR2 which are part of a larger family of tyrosine kinase receptors. DDR1 was first described in *Dictyostelium discoideum* and was shown to mediate cell aggregation (Breuer and Siu, 1981; Springer, Cooper and Barondes, 1984). DDR2 was then identified by homology cloning based on their catalytic kinase domains (Shrivastava *et al.*, 1997). Both DDR1 and DDR2 were then classified as orphan receptors, until further work then identified that they were actually activated by collagen (Shrivastava *et al.*, 1997; Vogel *et al.*, 1997). DDR1 is activated by collagen types I, IV, V, VI and VII, whereas DDR2 is only activated by fibrillary collagens such as collagen types I, III and X (Shrivastava *et al.*, 1997; Vogel *et al.*, 1997; Leitinger and Kwan, 2006).

Structurally, both receptors are comprised of four different regions. An extracellular region containing both a discoidin domain, and a discoidin-like domain which are then able to bind to collagen (Rammal *et al.*, 2016). The juxta-membrane region in DDR1 has an extracellular region of ~50 amino acids, followed by a larger cytosolic juxta-membrane region of ~170 amino acids (Leitinger, 2011; Carafoli and Hohenester, 2013). The cytosolic region is then much larger of ~300 amino acids and is the site

of the catalytic tyrosine kinase domain which after phosphorylation then activates downstream signalling (Leitinger, 2011; Carafoli and Hohenester, 2013).

There are five different isoforms of DDR1 in humans – DDR1a, b, c, d and e, which have been described based on differences in their phosphorylation, glycosylation, function, expression patterns and their protein interactions (Vogel, 1999; Carafoli and Hohenester, 2013). DDR1a, b and c are all kinase active, whereas DDR1d and e due to frame shift truncations are kinase deficient (Alves *et al.*, 2001). DDR1a and b are the most abundant isoforms, however it can be hard to distinguish isoforms by normal protein analysis as they are all of a similar size, with the exception of DDR1d which is much smaller (DDR1a – 97kDa, b – 101kDa, c – 102kDa, d – 56kDa, and e – 86 kDa) (Alves *et al.*, 1995, 2001; Rammal *et al.*, 2016).

The DDR dimerization, phosphorylation and activation upon binding to collagen are then important in several different cellular processes, including proliferation, migration and adhesion (Rammal *et al.*, 2016). The phosphorylation of the tyrosine residues upon collagen activation has been shown to recruit different Src homology 2 (SH2) and phosphotyrosine binding domain containing proteins, and is thought to autophosphorylate other tyrosines in the juxta-membrane region allowing for downstream signalling (Ikeda *et al.*, 2002; Carafoli and Hohenester, 2013). Whilst work has been done to try and understand the role of the different DDRs and isoforms, due to the range of expression, and the activation by different collagen types more work is needed to fully understand these processes and the role of DDRs in cellular behaviour.

1.4.1 DDR1 and E-cadherin

Alongside DDR1's role upon activation by collagen, it has also been implicated in regulating cortical contractility at adherens junctions, in a mechanism independent of collagen activation, and of its tyrosine kinase activity (Hidalgo-Carcedo *et al.*, 2011).

Work by Hidalgo-Carcedo *et al.* showed that E-cadherin is able to recruit DDR1 to the cell membrane, where through a signalling cascade DDR1 leads to an impairment of the phosphorylation of myosin light chain (p-MLC), resulting in a reduction in cortical contractility at the adherens junctions. This work was done in interphase cells, in a model for collective cell migration. They hypothesised that this reduction in cortical contractility at the adherens junctions was required for the maintenance of adherens junctions, enabling cells to remain together during migration rather

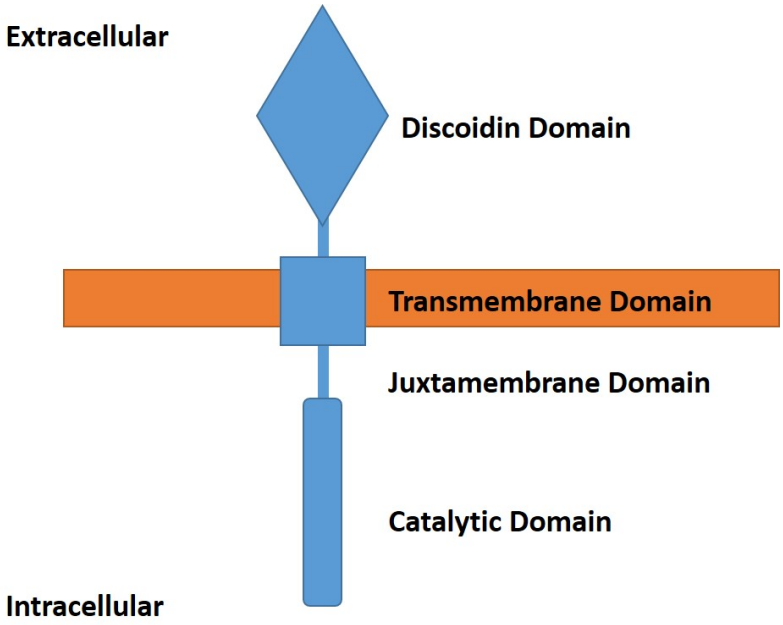

Figure 1.9: DDR1 structure
Schematic diagram of the DDR1 protein including the extracellular discoiding domain, transmembrane domain, and intracellular juxtamembrane and catalytic domains.

than moving off as individual cells. They suggested a mechanism where E-cadherin recruits DDR1 to the membrane at the adherens junctions, then subsequently DDR1, through an unknown mechanism recruits Par3 and Par6. This recruitment of the Par proteins then controls the localisation of RhoE/p190RhoGAP which subsequently antagonises RhoA/ROCK-1. RhoA/ROCK-1 normally lead to the phosphorylation of MLC, therefore by activating RhoE/p190RhoGAP this phosphorylation process is inhibited (Figure 1.10) (Hidalgo-Carcedo *et al.*, 2011). The full mechanism of this control was not fully elucidated, and the mechanism that leads DDR1 to be recruited to the membrane by E-cadherin is unclear.

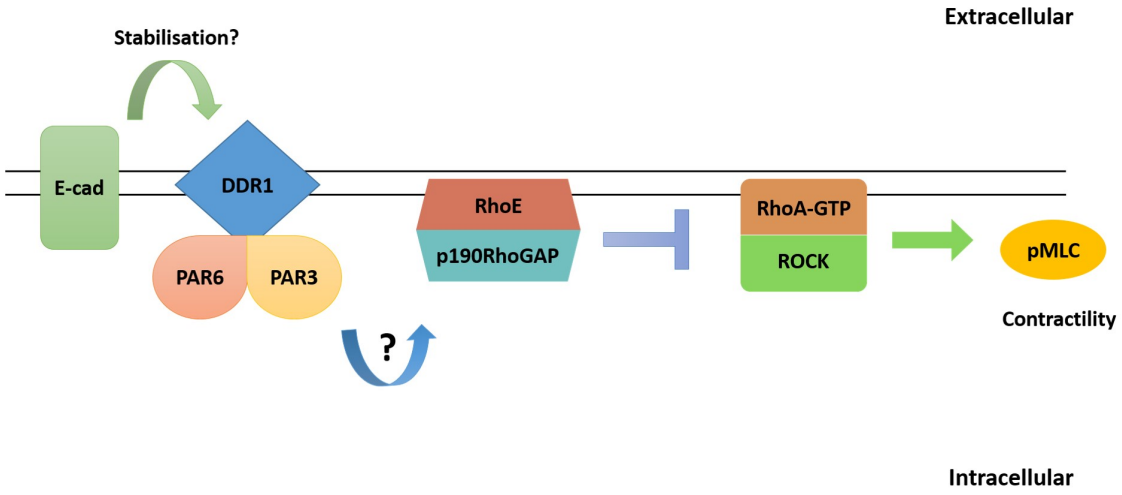

Figure 1.10: Regulation of cortical contractility at adherens junctions E-cadherin has been shown to localise DDR1 to the cell membrane, where through Par3 and Par6 it can then activate, through a yet to be elucidated mechanism, RhoE and p190RhoGap. RhoE/p190RhoGAP antagonise RhoA-GTP/ROCK, resulting in a loss of p-MLC and therefore reduction in cortical contractility at the adherens junctions.

1.4.2 DDR1 in cancer

Both of the DDRs have been linked to tumour progression in a number of human cancers, and studies have shown that their activation and expression can be dysregulated within tumours, including the identification of somatic mutations in various cancers (Ford *et al.*, 2007; Valiathan *et al.*, 2012). Dependent on the type of cancer the expression of DDR1 has been reported as both pro- and anti-tumourigenic (Tables 1.2 and 1.3).

The silencing of DDR1 by siRNA in both pancreatic adenocarcinoma and glioma cell lines inhibited cell proliferation and impaired tumour growth in xenograft mice models (Yamanaka *et al.*, 2006; Rudra-Ganguly *et al.*, 2014). Similarly, the inhibition of DDR1 in breast cancer, colon, and Hodgkin lymphoma cell lines after DNA damage resulted in increased cell death, suggesting that DDR1 may confer a chemotherapeutic resistance effect to cancer cell lines, potentially through NfκB or notch signalling (Cao and Prescott, 2002; Ongusaha *et al.*, 2003; Das *et al.*, 2006; Cader *et al.*, 2013). Conversely, in luminal breast cancer cells, DDR1 has been reported to induce the pro-apoptotic Bcl-2 interacting killer protein (BIK) which can trigger apoptosis, and therefore in this capacity DDR1 is anti-proliferative (Maquoi *et al.*, 2012; Assent *et al.*, 2015).

During the process of EMT, where cells become more invasive and motile, and can promote tumour progression (Thiery *et al.*, 2009), there is a reported switch from DDR1 (epithelial) to DDR2 (mesenchymal) (Maeyama *et al.*, 2008; Toy *et al.*, 2015). Therefore, suggesting that in some cancers DDR1 may need to be silenced to allow for EMT to occur and DDR2 expression, which can then drive further pro-tumourigenic factors (Rammal *et al.*, 2016).

Whilst DDR1 has been shown to be beneficial for the regulation of cell migration in breast, colorectal, pancreatic, lung, glioma and hepatocarcinomas (Ram *et al.*, 2006; Park *et al.*, 2007; Huang *et al.*, 2009; Castro-Sanchez *et al.*, 2010; Yang *et al.*, 2010; Neuhaus *et al.*, 2011; Hu *et al.*, 2014; Rudra-Ganguly *et al.*, 2014), other reports have also suggested an inhibitory effect on cell migration (Hansen *et al.*, 2006; Koh *et al.*, 2015).

As well as a potential role in the regulation of cell migration, DDR1 has also been implicated in cell invasion (Valiathan *et al.*, 2012). DDR1 has been observed to be highly expressed in invasive tumours. Evidence that collagen type I can act as a barrier within the ECM, suggests a role for DDR1 in inducing the metalloproteases, MMP-2 and MMP-9, that can then assist in degrading the ECM in a variety of different cancers (Ram *et al.*, 2006; Park *et al.*, 2007; Yoshida and Teramoto, 2007; Shimada *et al.*, 2008; Castro-Sanchez *et al.*, 2010; Yang *et al.*, 2010; Hidalgo-Carcedo *et al.*, 2011; Miao *et al.*, 2013; Hu *et al.*, 2014; Juin *et al.*, 2014).

Therefore, whilst there is accumulating evidence that DDR1 activity can be pro-tumourigenic, there is also evidence that in certain tumour types DDR1 can also be inhibitory towards tumour progression. Further work needs to be done to more fully understand the role of DDR1, including its different isoforms in tumour development.

Table 1.2: Putatative roles of DDR1 in promoting tumour progression.

Function	Cancer Type	References
Proliferation/survival	Glioma	(Yamanaka *et al.*, 2006)
	Pancreatic adenocarcinoma	(Rudra-Ganguly *et al.*, 2014)
	Colon carcinoma	(Ongusaha *et al.*, 2003; Kim *et al.*, 2011)
	Osteosarcoma	(Ongusaha *et al.*, 2003)
	Breast cancer	(Ongusaha *et al.*, 2003; Das *et al.*, 2006)
	Hodgkin lymphoma	(Cader *et al.*, 2013)
EMT	Hepatoma	(Maeyama *et al.*, 2008)
	Non-small lung carcinoma	(Walsh, Nawshad and Medici, 2011)
	Colorectal cancer	(Hu *et al.*, 2014)
	Pancreatic adenocarcinoma	(Shintani *et al.*, 2008)
Migration	Glioma	(Ram *et al.*, 2006)
	Hepatocellular carcinoma	(Park *et al.*, 2007)
	Oral squamous cell carcinoma	(Yang *et al.*, 2010)
	Pancreatic cancer	(Rudra-Ganguly *et al.*, 2014)
	Colorectal cancer	(Hu *et al.*, 2014)
	Breast cancer	(Huang *et al.*, 2009; Castro-Sanchez *et al.*, 2010; Neuhaus *et al.*, 2011)
Invasion	Glioma	(Ram *et al.*, 2006)
	Hepatocellular carcinoma	(Park *et al.*, 2007)
	Oral squamous cell carcinoma	(Hidalgo-Carcedo *et al.*, 2011)
	Colorectal cancer	(Tang, Hu and Tang, 2004)
	Non-small lung carcinoma	(Yang *et al.*, 2010; Miao *et al.*, 2013; Juin *et al.*, 2014)
	Hepatoblastoma	(Juin *et al.*, 2014)
	Breast cancer	(Castro-Sanchez *et al.*, 2010; Juin *et al.*, 2014)
	Prostate cancer	(Shimada *et al.*, 2008)
	Pituitary adenoma	(Yoshida and Teramoto, 2007)

Table 1.3: Putatative roles of DDR1 in blocking tumour progression.

Function	Cancer Type	References
Proliferation/survival	Breast cancer	(Maquoi *et al.*, 2012; Assent *et al.*, 2015)
EMT	Breast cancer	(Koh *et al.*, 2015)
Migration	Breast cancer	(Hansen *et al.*, 2006; Koh *et al.*, 2015)

1.5 Project aims

Whilst centrosome clustering has been characterised as a mechanism for cell survival in the presence of supernumerary centrosomes, it is not currently known whether all cell types are inherently able to cluster, or if this is limited to certain cell types.

Work is currently being undertaken to identify drugs which can impair centrosome clustering. However, current technology to identify patients with tumours with centrosome amplification requires the use of fluorescent microscopy techniques by a trained microscopist, making this too expensive and difficult to regularly use as a diagnostic tool. Furthermore, more research is needed to better understand why some tumours support centrosome amplification at high levels, and other tumours do not. This can then potentially be used to help identify patients who would then benefit from this anti-centrosome clustering treatment. The aims of the project were to:

- Determine the mechanisms of adaptation to extra centrosomes, in particular those that promote centrosome clustering.
  - Investigate centrosome clustering in a panel of cell lines, using multiple mechanisms of generating supernumerary centrosomes to identify if all cell lines are inherently able to cluster supernumerary centrosomes efficently.
- Identify key molecules that affect centrosome clustering.
  - Use siRNA, shRNA and CRISPR-Cas9 to knockdown/knockout genes of interest to identify if the proteins affect efficient centrosome clustering.
- Determine if adaptation to centrosome amplification is required for cell survival.
  - Use colony formation assays, and cell growth assays to assess if increased centrosome clustering allows for increased cell survivial in the presence of supernumerary centrosomes.

- Characterise if the mechanisms of adaptation to centrosome amplification correlate within human tumours.
  - Use a panel of cancer cell lines to identify if the mechanisms of adaptation identified correlate with high levels of centrosome amplification within human tumours.

Chapter 2

Materials and Methods

2.1 Cell culture

2.1.1 Media reagents

Dulbecco's modified Eagle's medium (DMEM): 4.5g/L glucose, 2mM L-glutamine and 100mg/L sodium pyruvate (D6429, Sigma-Aldrich, MO, USA). Media was stored at 4°C.

Roswell Park Memorial Institute medium (RPMI): 2.0g/L glucose, 2.1mM L-glutamine and 2g/L sodium bicarbonate (R8758, Sigma-Aldrich, MO, USA). Media was stored at 4°C.

Dulbecco's modified Eagle's medium/nutrient mixture F-12 Ham (DMEM:F12): 3.15g/L glucose, with 2.5mM L-glutamine, 15mM HEPES, and 14.2mM sodium bicarbonate (D847, Sigma-Aldrich, MO, USA). Media was stored at 4°C.

McCoy's 5A (modified), GlutaMAX®: 3.0g/L glucose, 1.5mM L-Alanyl-L-Glutamine (36600, Thermo Scientific, MA, USA). Media was stored at 4°C.

Opti-MEM® reduced serum medium: L-glutamine, no Phenol Red, was used for nucleic acid transfection. (31985062, Gibco, NY, USA). Media was stored at 4°C.

Serum: 50ml aliquots were stored at -20°C. Prior to use aliquots were thawed in a 37°C water bath. Aliquots were added to the appropriate media and concentration (see Table 2.1) (Foetal Bovine Serum: 10500064, Gibco, NY, USA. Horse Serum: H1138, Sigma-Aldrich, MO, USA. HyClone Fetal Bovine Serum (U.S.), Tetracycline Screened: SH30070.03T, GE Healthcare, OH, USA. Donor Calf Serum: Donor Calf Serum Heat Inactivated, PAA Laboratories Ltd, UK).

Cholera toxin: Stock solution of 1mg/ml cholera toxin was prepared in autoclaved distilled water was stored at 4°C. Final concentration used was 100ng/ml (C8052-2MG, Sigma-Aldrich, MO, USA).

Epidermal growth factor (EGF): Stock solution of 25µg/ml of EGF was prepared in 1% v/v Horse Serum in DMEM:F12 and stored at -20°C. Final concentration used was 20ng/ml (E4127, Sigma-Aldrich, MO, USA).

Hydrocortisone: Stock solution of 1mg/ml of hydrocortisone was prepared in absolute ethanol, and stored at -20°C. Final concentration used was 0.5µg/ml (H0881, Sigma-Aldrich, MO, USA).

Insulin: Stock solution of 4mg/ml of human recombinant insulin was stored at -20°C. Final concentration used was 10µg/ml (12585014, Invitrogen, ON, Canada).

2.1.2 Antibiotics

Penicillin/Streptomycin: 100U/ml penicillin and streptomycin, was used in growth media. Storage was at -20°C for long term and 4°C whilst in use (P4333, Sigma-Aldrich, MO, USA).

Puromycin: Stock solution of 10mg/ml was stored at -20°C. Final concentration used was 1 – 5µg/ml (ant-pr, Invivogen, CA, USA).

Blasticidin hydrochloride: A sterile-filtered aqueous solution of 10mg/ml blasticidin hydrochloride in 20mM HEPES was stored at -20°C. Final concentration used was 2.5 – 20µg/ml. (EZSolution® 2805, Biovision, USA).

Geneticin® (G418) Sulphate: Stock solution of 50mg/ml was stored at -20°C. The final concentration used was 0.5 – 1mg/ml (108321-42-2, Santa Cruz, CA, USA).

2.1.3 Maintenance of a monolayer culture

Adherent cell lines were maintained at 37°C with 5% CO_2 atmosphere, primarily in 25cm^2 flasks in a monolayer culture. Cells were cultured in their respective media as per Table 2.1.

Cells were examined using an inverted light microscope at 400X magnification, and were passaged when they reached 80% confluency. To passage cells, medium was aspirated from cells, cells were then washed in 5 ml of autoclaved phosphate-buffered saline (PBS) and incubated with 1 ml 0.05% v/v Trypsin-ethylenediaminetetraacetic acid (EDTA) with phenol red (25300-054, Thermo Scientific, MA, USA) or for MCF10A with 0.25% v/v Trypsin-EDTA with phenol red (25300-056, Thermo Scientific, MA, USA) for approximately 5 minutes at 37°C. Flasks were then tapped to remove any remaining cells adhering to the surface. 5ml of growth medium was then added to neutralise the enzymatic activity of the Trypsin-EDTA. For MCF10A cells, resuspension medium was used consisting of DMEM:F12 with 10% v/v horse serum and 100 U/ml Penicillin/Streptomycin, as the normal growth medium had a lower volume of serum (5% v/v) which would not inactivate the Trypsin-EDTA as effectively. The cell suspension was then pipetted up and down to ensure that any cell clumps were dissociated and that the Trypsin-EDTA was fully neutralised. The cell suspension was then transferred to a 15ml centrifuge tube and cells were pelleted by centrifugation at 1200rpm for 3 minutes. The supernatant was then discarded, and the cell pellet was resuspended in 5ml of medium (MCF10A cells were resuspended in Resuspension Medium). 0.5-1ml was then plated into a new flask, according to cell line doubling time and experimental requirements. Growth medium was added to the flask to make a total volume of 7ml, and the flask was gently rocked to evenly distribute cells and placed in an incubator.

Table 2.1: Cell lines

Cell line	Cell type	Growth medium	Source
MCF10A	Mammary epithelial	DMEM:F12 + 5% v/v Horse Serum, 20ng/mL EGF, 0.5µg/mL hydrocortisone, 100ng/mL Cholera Toxin, 10ug/mL Insulin	ATCC
HaCaT	Skin keratinocyte	DMEM + 10% FBS	John Marshall (BCI)
EpH4-J3B1A	Mammary epithelial	DMEM + 10% Donor Calf Serum	Priscilla Soulie (Université de Genève)
RPE-1	Retinal epithelial	DMEM:F12 + 10% FBS	David Pellman (Harvard)
BJ	Foreskin fibroblast	DMEM + 10% FBS	David Pellman (Harvard)
NIH-3T3	Murine embryonic fibroblast	DMEM + 10% FBS	David Pellman (Harvard)
HEK-293M	Embryonic kidney cells	DMEM + 10% FBS	David Pellman (Harvard)
A431	Epidermoid carcinoma	DMEM + 10% FBS	Erik Sahai (Francis Crick)
MCF-7	Breast cancer, luminal	RPMI + 10% FBS	Peter Schmid (BCI)
BT-474	Breast cancer, luminal	DMEM + 10% FBS	Peter Schmid (BCI)
SKBR-3	Breast cancer, luminal	McCoy's 5A + 10% FBS	Peter Schmid (BCI)
JIMT-1	Breast cancer, luminal	DMEM + 10% FBS	Peter Schmid (BCI)
MDA-453	Breast cancer, luminal	DMEM + 10% FBS	Peter Schmid (BCI)
HCC1954	Breast cancer, basal	RPMI + 10% FBS	Peter Schmid (BCI)
BT20	Breast cancer, basal	DMEM + 10% FBS	Peter Schmid (BCI)
MDA-468	Breast cancer, basal	DMEM + 10% FBS	Peter Schmid (BCI)
HCC-38	Breast cancer, basal	RPMI + 10% FBS	Peter Schmid (BCI)
HCC-1143	Breast cancer, basal	RPMI + 10% FBS	Peter Schmid (BCI)
BT-549	Breast cancer, basal	RPMI + 10% FBS	Peter Schmid (BCI)
CAL-120	Breast cancer, basal	DMEM + 10% FBS	Peter Schmid (BCI)
HCC1937	Breast cancer, basal	RPMI + 10% FBS	Peter Schmid (BCI)
HS578T	Breast cancer, basal	DMEM + 10% FBS	Peter Schmid (BCI)
MDA-231	Breast cancer, basal	DMEM + 10% FBS	Peter Schmid (BCI)

2.1.4 Freezing

The same process of passaging cells was applied as in Section 2.1.3, although cells were typically grown in 175cm^2 flasks to allow enough cells to freeze down. After centrifugation of the cell suspension (see Section 2.1.3), the supernatant was removed and the cell pellet was resuspended in 5ml of 10% v/v dimethyl sulfoxide (DMSO) in Growth Medium (MCF10A cells were resuspended in 5ml of 10% v/v DMSO in Resuspension Medium). The cell suspension was then aliquoted at 1ml per cryovial and frozen at -80°C in a Nalgene® Mr. Frosty freezing container, allowing for an optimal cooling rate of -1°C/minute. For long term storage, the cryovials were transferred to liquid nitrogen stores and kept at -196°C.

2.1.5 Thawing

Cells removed from liquid nitrogen were transported on dry ice at -78.5°C to prevent premature defrosting of the cell suspensions. The cryovials were then placed in a 37°C water bath until defrosted. The cell suspension was then added to 5ml of growth medium in a 15ml centrifuge tube and centrifuged at 1200rpm for 3 minutes. The supernatant was then removed and the cell pellet was resuspended in 5ml of growth medium and placed into a 25cm^2 flask. Six hours later the medium was changed to remove any dead cells that did not survive the DMSO and freeze-thaw process.

2.1.6 Cell counting

When a specific number of cells were required for experimentation, such as measuring cell viability, cells in suspension were counted using a TC20® Automated Cell Counter (Bio-Rad Laboratories, CA, USA). The suspension was evenly mixed by pipetting up and down with a p1000 pipette, and 10µl of suspension was added to the chamber in a counting slide (1450011, Bio-Rad Laboratories, CA, USA), which was inserted into the instrument, and the cell number quantified. Readings were done in triplicate per slide and an average taken.

2.1.7 Drug treatments

Dihydrocytochalasin B (DCB)
DCB is an actin-depolymerising agent, resulting in cytokinesis failure and tetraploid cells. To generate tetraploid cells, therefore containing supernumerary centrosomes, cells were treated with 4µM DCB for 20 hours. Cell medium was then removed and replaced with Growth Medium containing 10µM of p38 inhibitor (SB203580, New England Biolabs, MA, USA) to ensure cells re-entered the cell cycle, for 24 hours. Stock solution of 10mM DCB was prepared in DMSO and stored at -20°C (D1641, Sigma-Aldrich, MO, USA).

Blebbistatin
Blebbistatin is an inhibitor of non-muscle Myosin II, resulting in cytokinesis failure. To generate tetraploid cells, cells were treated with 50µM blebbistatin for 20 hours. Cell medium was then removed and replaced with Growth Medium containing 10µM of the p38 inhibitor SB203580 (New England Biolabs, MA, USA) for 24 hours. To analyse the effects of cortical contractility on centrosome clustering, cells were treated with 50µM blebbistatin for 4 hours prior to fixation. Stock solution of 50mM blebbistatin was prepared in DMSO and stored at -20°C (B0560, Sigma-Aldrich, MO, USA).

RO-3306 (CDK1 inhibitor)
RO-3306 is a selective ATP-competitive inhibitor of CDK1, causing cell cycle arrest at G2. Prolonged arrest at this stage causes centrosome overduplication. Cells were treated with 5µM RO-3306 for 40 hours. Cell medium was then removed and washed twice with 37°C Growth Medium to ensure full washout of the drug, and replaced with Growth Medium containing 10µM of the p38 inhibitor SB203580 (New England Biolabs, MA, USA) for 24 hours. Stock solution of 10mM RO-3306 was prepared in DMSO and stored at -20°C (SML0569, Sigma-Aldrich, MO, USA).

Doxycycline hyclate (Dox)
Dox was used to induce PLK4 overexpression in the TetR PLK4 and pInducer PLK4 cell lines, 2µg/ml Dox was added for 48 hours. Stock solution of 2mg/ml Dox was prepared in autoclaved, deionised water and stored at -20°C (D9891, Sigma-Aldrich, MO, USA).

MG132

MG132 is a proteasome inhibitor which can be used to arrest cells during metaphase in mitosis. Cells were treated with 10µM MG132 for 4 hours. Cell medium was then removed and cells were washed twice with 37°C Growth Medium to ensure full washout of the inhibitor. Cells were then incubated for an hour to allow release from metaphase. Stock solution of 10mM MG132 was prepared in DMSO and stored at -20°C (1748, Tocris Bioscience, UK).

Nocodazole

Nocodazole is a microtubule-depolymerising drug. In order to deplete cells of astral microtubules during mitosis, 5nM nocodazole was added for 3 hours. Stock solution of 10mM Nocodazole (methyl (5-(2-thienylcarbonyl)-1H-benzimidazol-2-yl) carbamate) was prepared in DMSO and stored at -20°C (M1404, Sigma-Aldrich, MO, USA). Working stocks were then prepared when required of 10µM in DMSO and stored at -20°C for up 4 weeks.

Calyculin-A

Calyculin-A is a protein phosphatase inhibitor. In order to increase the levels of phosphorylated myosin II, 1µM Calyculin-A was added to cells for 2 hours. Stock solution of 1mM Calyculin-A was prepared in DMSO and stored at -20°C (CAY19246, Cambridge Bioscience, UK).

Y-27632 dihydrochloride (ROCK1 inhibitor)

Y-27632 dihydrochloride is a ROCK1 inhibitor. Cells were treated with 10µM for 4 hours to perturb ROCK1 driven contractility. Stock solution of 10mM Y-27632 dihydrochloride was prepared in autoclaved, deionised water and stored at -20°C (1254, Tocris Bioscience, UK).

DDR1-IN-1 (DDR1 kinase inhibitor)

DDR1-IN-1 is a selective DDR1 kinase inhibitor. For quantification of DDR1 activation in the presence of collagen - cells were plated in 6cm diameter tissue culture dishes, and were pre-treated with 0 – 15mM DDR1-IN-1 for 1 hour. The medium was then removed and replaced with medium containing 10µg/ml of collagen (Collagen I, Rat tail, 354236, Corning, NY, USA) and DDR1-IN-1 for 2 hours. Stock solution of 10mM DDR1-IN-1 was prepared in autoclaved, deionised water in a 60°C water bath for full solubility before storing at -20°C (5077, Tocris Bioscience, UK).

2.1.8 SiRNA transfection

Cells were plated in a 6-well tissue culture plate in 2ml of Growth Medium per well which did not contain Penicillin/Streptomycin. For the transfection, Lipofectamine® RNAiMAX (Thermo Scientific, MA, USA) was used to form liposomes around the siRNA which could then be internalised by the cells. If antibiotics were present in the medium then they would be encapsulated by the liposome and kill the cells after uptake. Cells were transfected at 50% confluency. 10µl lipofectamine® RNAiMAX was diluted in 250µl Opti-MEM® per well in a microcentrifuge tube, whilst 5µl of siRNA (Stocks were made at 20µM, diluted in RNase-free water and stored at -20°C) was diluted in 250µl Opti-MEM® per well in a separate microcentrifuge tube. Solutions were incubated at room temperature for 5 minutes to allow equilibration. The siRNA solution was then added dropwise onto the Lipofectamine® RNAiMAX solution and incubated at room temperature for 20 minutes, allowing the formation of liposomes. The solution was then added onto the cells. The medium was replaced 6 hours later with normal Growth Medium. Cells were analysed 72 hours post transfection. siNegative (1027310, Qiagen, MD, USA) was used as a control. Details of specific siRNAs used can be found in Table 2.2.

Table 2.2: siRNA sequences from Dharmacon, CO, USA

siRNA Name	Product Code	Sequence Number	Target Sequence	Antisense Sequence
siCDH1 on-TARGET smart pool	L-003877-00	1	GGCCUGAAGUGACUCGUAA	UUACGAGUCACUUCAGGCC
		2	GAGAACGCAUUGCCACAUA	UAUGUGGCAAUGCGUUCUC
		3	GGGACAACGUUUAUUACUA	UAGUAAUAAACGUUGUCCC
		4	GACAAUGGUUCUCCAGUUG	CAACUGGAGAACCAUUGUC
siDDR1 on-TARGET smart pool	L-003111-00	1	GGGACACCCUUUGCUGGUA	UACCAGCAAAGGGUGUCCC
		2	GAAUGUCGCUUCCGGCGUG	CACGCCGGAAGCGACAUUC
		3	GAGCGUCUGUCUGCGGGUA	UACCCGCAGACAGACGCUC
		4	AAGAGGAGCUGACGGUUCA	UGAACCGUCAGCUCCUCUU
siSAS6 on-TARGET smart pool	M-004158-02	1	GGACAGUCUCUUCGAAUUA	UAAUUCGAAGAGACUGUCC
		2	UGUUGAAUGCCACGAGAAA	UUUCUCGUGGCAUUCAACA
		3	CAACUGGACUUUACACGAA	UUCGUGUAAAGUCCAGUUG
		4	GAGAGUAAGUAUAAGAAUG	CAUUCUUAUACUUACUCUC
siRnd3 on-TARGET smart pool	M-007794-02	1	GAACGUGAAAUGCAAGAUA	UAUCUUGCAUUUCACGUUC
		2	GAAAUUAUCCAGCAAAUCU	AGAUUUGCUGGAUAAUUUC
		3	UAGUAGAGCUCUCCAAUCA	UGAUUGGAGAGCUCUACUA
		4	AGAAUUACACGGCCAGUUU	AAACUGGCCGUGUAAUUCU
siRnd3 on-TARGET siRNA Plus	J-007794-09	–	GCGGACAGAUGUUAGUACA	UGUACUAACAUCUGUCCGC
sip190RhoGAP on-TARGET smart pool	M-004158-02	1	GGAGGAAUCUGUAUACAUG	CAUGUAUACAGAUUCCUCC
		2	GAACAGCGAUUUAAAGCAU	AUGCUUUAAAUCGCUGUUC
		3	GAUGGGCUGUCUUUCAUUA	UAAUGAAAGACAGCCCAUC
		4	UCAGCGAGAUCCAAUGUAA	UUACAUUGGAUCUCGCUGA
siSTARD8 on-TARGET smart pool	M-010254-00	1	GAAGAAGGACACUCCAUUU	AAAUGGAGUGUCCUUCUUC
		2	CGACGUGGCUGACCUGCUA	UAGCAGGUCAGCCACGUCG
		3	GAACCUGCGUCAAAUGAAU	AUUCAUUUGACGCAGGUUC
		4	GAACCCACCUUUGCCUCUA	UAGAGGCAAAGGUGGGUUC
siKIFC1 on-TARGET smart pool	L-004958-00	1	GGACUUAAAGGGUCAGUUA	UAACUGACCCUUUAAGUCC
		2	GGACAGAGCGCACAACACU	AGUGUUGUGCGCUCUGUCC
		3	GAACUUGCGUGCUUGUGUC	GACACAAGCACGCAAGUUC
		4	GGACUCAAACGUUGGACCA	UGGUCCAACGUUUGAGUCC

2.2 Bacterial Culture Methods

2.2.1 Media and Antibiotics

Luria broth (LB): 2% w/v LB (L3022, Sigma-Aldrich, MO, USA) was dissolved in deionised water and autoclaved for 20 minutes at 125°C. Once cooled, antibiotics were added (see below) and LB was stored at 4°C.

LB-Agar: 3.5% w/v LB-agar (L2897, Sigma-Aldrich, MO, USA) was dissolved in deionised water and autoclaved for 20 minutes at 125°C. Once cooled enough to hold, antibiotics were added and the solution was mixed by swirling. The LB-agar was poured into sterile 10cm diameter circular plates and were left to set at room temperature. LB-agar plates were stored at 4°C.

Kanamycin: 50mg/ml Kanamycin solution was stored at 4°C (K0254, Sigma-Aldrich, MO, USA). Kanamycin was diluted in the LB and LB-Agar to a working concentration of 50µg/ml.

Ampicillin: 100mg/ml Ampicillin solution was stored at 4°C (A5354, Sigma-Aldrich, MO, USA). Ampicillin was diluted in the LB and LB-Agar to a working concentration of 100µg/ml.

2.2.2 Transformation of chemically competent cells

One Shot® Stbl3™ Chemically Competent *E. coli* were stored at -80°C (C737303, Thermo Scientific, MA, USA). Prior to transformation, one vial of Stbl3™ cells was allowed to thaw on ice. Once thawed, 1µl of plasmid was added to the bacterial cells and mixed by pipetting. The mixture was then incubated for 30 minutes on ice to allow the plasmid to fuse to the bacterial cell membrane. The cells were then heat shocked at 42°C in a water bath for 45 seconds. The heat shock causes the bacterial cells to release lipids, forming pores in the cell wall, which allow the plasmid DNA to enter. Cells were then placed back on ice for 2 minutes, causing the pores to close, and the DNA to be contained within the bacterial cells. 500µl of super optimal broth with catabolite repression (SOC) medium was then added, and the mixture was incubated at 37°C whilst shaking at 200rpm for 1 hour. 100µl of cell suspension was then plated onto an LB-agar plate with plasmid-selective antibiotic and incubated overnight at 37°C. Colonies were then selected using a pipette tip and inoculated

into 5ml of LB containing antibiotic which was then placed at 37°C at 200rpm for 8 hours. To make bacterial stocks, a 1:1 dilution was made of bacterial suspension and 30% v/v glycerol in water, 1ml was placed into a cryovial and stored at -80°C.

2.2.3 Propagation of chemically competent cells

A 5ml starter culture of LB with the appropriate antibiotic was inoculated by scraping a pipette tip against the frozen transformed bacterial cells and placing it into the broth. The starter culture was then placed at 37°C whilst shaking at 200rpm for 8 hours. The starter culture was then added to 50ml of LB with appropriate antibiotic in a conical flask and placed at 37°C whilst shaking at 200rpm overnight.

2.2.4 Plasmid DNA extraction from bacteria

To extract plasmid DNA from bacterial cultures, a Genopure Plasmid Midi Kit (Roche, Germany) was used. Bacterial cells were pelleted by centrifugation at 3000g at 4°C for 10 minutes. The supernatant was removed and the cell pellet was resuspended in 4ml Suspension Buffer with added RNase. 4ml of Lysis Buffer was added, and the mix was inverted 7 times to ensure it was evenly mixed before incubating at room temperature for 3 minutes. 4ml of chilled Neutralisation Buffer was added to counteract the Lysis Buffer, forming a cloudy suspension of cell debris, and inverted until a homogenous mixture had formed. The suspension was then incubated on ice for 5 minutes. Whilst the mixture was incubating, a glass funnel was placed into a 50ml centrifuge tube, and filter paper was placed into the funnel, which was moistened with a few drops of Equilibration Buffer. The mixture was then poured into the funnel and the flow through, containing the plasmid DNA was collected. A Midi Prep column was then placed into a 50ml centrifuge tube and 2.5ml of Equilibration Buffer was added to the column and allowed to pass through by gravity flow. The collected lysate from the bacterial culture was then added to the column, and passed through by gravity flow, allowing the DNA to bind to the anion exchange resin under low salt and pH conditions. The column was then washed twice with 5ml of Wash Buffer to remove any remaining contaminants. The column was then placed into a collection tube capable of undergoing high speed centrifugation and the DNA was eluted using the prewarmed 50°C high salt concentration Elution Buffer. The DNA was precipitated by the addition of 3.6ml of isopropanol. The suspension was then centrifuged immediately at 15,000g at 4°C for 30 minutes to pellet the DNA. The supernatant was carefully discarded so as to not dislodge the

pellet. 3ml of 4°C 70% v/v ethanol in distilled water was then carefully added to remove precipitated salt, and to displace the isopropanol, making the DNA more soluble. The tube was then centrifuged at 15,000g at 4°C for 10 minutes before removing the ethanol. The pellet was then allowed to air dry at room temperature before dissolving the pellet in 50µl of sterile DNase free water.

2.2.5 Determination of DNA concentration

DNA concentration was determined using a Nanodrop-1000 spectrophotometer (Thermo-Scientific, MA, USA). Prior to quantification, a blank measurement was taken using 1µl of sterile DNase free water. Quantification of DNA concentration was then taken by adding 1µl of the DNA solution. The Nanodrop-1000 measured absorbance at 260nm, the wavelength at which nucleic acids absorb light. The absorbance was then converted into a concentration in ng/µl using a derivative of the Beer-Lambert equation. The Nanodrop-1000 also measured absorbance at 280nm, the wavelength where proteins absorb light. The purity of the DNA could then be determined by dividing the OD_{260} (Optical Density) by the OD_{280} value. An OD_{260}/OD_{280} of less than 1.8 indicated that there was protein contamination within the sample and could not be used for future applications.

2.3 Lentivirus and Generation of Cells

As a sub-class of retroviruses, lentiviruses were used to create genetically modified cell lines by making use of their ability to integrate into the genome in both dividing and non-dividing cells.

2.3.1 Lentivirus preparation

HEK 293M cells were used for lentiviral production due to their transfectability. HEK 293M were plated in 6-well plates in Growth Medium without Penicillin/Streptomycin. Cells were transfected 24 hours post seeding, when plates were 50% confluent. The transfection reagent used was Lipofectamine® 2000 (Thermo Scientific, MA, USA). 10µl Lipofectamine® 2000 was added to 250µl Opti-MEM® per well in a microcentrifuge tube, whilst 2µg of plasmid DNA, 1µg Gag-Pol DNA and 0.5µg VSV-G DNA were added to 250µl Opti-MEM® in a separate microcentrifuge tube

(Gag-Pol: psPAX2 plasmid, 12260, Addgene, MA, USA; VSV-G: pMD2.G plasmid, 12259, Addgene, MA, USA). Gag is a structural precursor protein, Pol is a polymerase, and VSV-G is an envelope gene required for the formation of the lentivirus, which then encapsulates the plasmid of interest. The mixtures were incubated at room temperature for 5 minutes before pipetting the plasmid mixture dropwise onto the Lipofectamine® 2000 mixture to allow the formation of liposomes, and incubated at room temperature for 20 minutes. The mixture was then added to the HEK 293M. 6 hours later the medium was replaced with 1.5ml Growth Medium. Twenty-four hours later, virus was harvested by removing the medium with a pipette and passing it through a 10ml syringe attached to a 0.45µM Millex-HP Syringe Filter Unit (SLHP033RS, Merck Millipore, Germany), into a 15ml centrifuge tube. By filtering the medium, any dislodged or dead cells in the medium were removed, whilst the virus was small enough to pass through. The virus collected was then aliquoted into cryovials at 1.5ml and stored at -80°C. 1.5ml pre-warmed 37°C Growth Medium was then carefully added to the transfected HEK 293M so as to not dislodge them. A second viral collection was then taken 48 hours post initial transfection. All pipette tips, syringes and plates that were used for lentiviral preparation were decontaminated in 1% w/v Virkon S, a virucidal disinfectant for 15 hours.

2.3.2 Lentivirus infection

Cells were plated in 6cm diameter cell culture plates in 3ml of Growth Medium. Twenty-four hours post seeding, the first collection from the lentiviral harvest was thawed at 37°C in a water bath. The Growth Medium was removed from the cells and replaced with 1ml of Growth Medium without Penicillin/Streptomycin. The lentivirus was added on top of the cells with 8µg/ml polybrene (Hexadimethrine bromide: H9268, Sigma-Aldrich, MO, USA). Polybrene is a cationic polymer which increases the transduction efficiency by neutralising the charge between sialic acid on the cell surface and the lentiviral virions. A stock solution of polybrene was prepared at 8mg/ml in autoclaved deionised water and stored at -20°C. Six hours later, the medium was removed and replaced with 3ml of Growth Medium. Forty-eight hours post seeding, the infection was repeated using the second lentiviral collection. Twenty-four hours post final infection, antibiotic selection was started, or cells were amplified for cell sorting. To sort cells based on fluorescence, cells were passaged as previously described from a 175cm^2 flask. Cells were resuspended in 1ml of serum-free medium to prevent aggregation of cells. Cells were then passed through a cell strainer cap (352235, BD Bioscience, CA, USA) and collected. The cell suspension was sorted on a BD FACSAria II (BD Bioscience, CA, USA). For a

full list of cell lines generated by lentiviral infection, refer to Table 2.3.

Table 2.3: Generated cell lines from lentiviral infection and their selection

Cell line	Generated by	Selection	Antibiotic concentration
MCF10A.H2B-GFP	Susana Godinho	Cell sorting for GFP	-
HaCaT.H2B-GFP	Alexander Rhys	Cell sorting for GFP	-
RPE-1.H2B-GFP	Alexander Rhys	Cell sorting for GFP	-
BJ.H2B-GFP	Susana Godinho	Cell sorting for GFP	-
MCF10A.TetR	Susana Godinho	Blasticidin	5µg/ml
HaCaT.TetR	Alexander Rhys	Blasticidin	10µg/ml
RPE-1.TetR	Alexander Rhys	Blasticidin	10µg/ml
NIH-3T3.TetR	Alexander Rhys	Blasticidin	5µg/ml
BJ.TetR	Alexander Rhys	Blasticidin	5µg/ml
MCF10A.TetR.PLK4	Susana Godinho	Geneticin	1mg/ml
HaCaT.TetR.PLK4	Alexander Rhys	Geneticin	0.5mg/ml
RPE-1.TetR.PLK4	Alexander Rhys	Geneticin	0.5mg/ml
NIH-3T3.TetR.PLK4	Alexander Rhys	Geneticin	0.5mg/ml
BJ.TetR.PLK4	Alexander Rhys	Geneticin	0.5mg/ml
MCF10A.TetR.PLK4.shCDH1 #8	Alexander Rhys	Puromycin	10µg/ml
MCF10A.TetR.PLK4.shCDH1 #9	Alexander Rhys	Puromycin	10µg/ml
MCF10A.TetR.PLK4.shCDH1 #10	Alexander Rhys	Puromycin	10µg/ml
MCF10A.TetR.PLK4.shCDH1 #11	Alexander Rhys	Puromycin	10µg/ml
MCF10A.CDH1-/-	Alexander Rhys	Puromycin	10µg/ml
HaCaT.CDH1-/-	Alexander Rhys	Puromycin	10µg/ml
MCF10A.CDH1-/-.TetR	Alexander Rhys	Blasticidin	5µg/ml
HaCaT.CDH1-/-.TetR	Alexander Rhys	Blasticidin	10µg/ml
MCF10A.CDH1-/-.TetR.PLK4	Alexander Rhys	Geneticin	1mg/ml
HaCaT.CDH1-/-.TetR.PLK4	Alexander Rhys	Geneticin	0.5mg/ml
MCF10A.TetR.PLK4.H2B-GFP	Alexander Rhys	Cell sorting for GFP	-
HaCaT.TetR.PLK4.H2B-GFP	Alexander Rhys	Cell sorting for GFP	-
MCF10A.CDH1-/-.TetR.PLK4.H2B-GFP	Alexander Rhys	Cell sorting for GFP	-
HaCaT.CDH1-/-.TetR.PLK4.H2B-GFP	Alexander Rhys	Cell sorting for GFP	-
MCF10A.Centrin-GFP	Alexander Rhys	Cell sorting for GFP	-
MCF10A.CDH1-/-.Centrin-GFP	Alexander Rhys	Cell sorting for GFP	-
MCF10A.pInducer.PLK4	Alexander Rhys	Cell sorting for GFP	-

2.3.3 Inducible PLK4 overexpression vectors

To generate cell lines transiently overexpressing PLK4, cell lines were initially infected with lentivirus containing the tetracycline repressor (TetR), pLenti-CMV-TetR-Blast (17492, Addgene, MA, USA) and selected using Blasticidin (2.5 - 20µg/ml), or pInducer and selected via cell sorting for green fluorescent protein (GFP), pInducer21 ORF-EG (46948, Addgene, MA, USA)(Meerbrey *et al.* 2011). These enabled the expression of PLK4 to be inducible. PLK4 cDNA was previously cloned using the Gateway system into the pLenti-CMV/TO-Neo-Dest vector by Susana Godinho (Godinho *et al.* 2014). After selection, cells were then secondarily infected with the PLK4-containing lentivirus and selected with Geneticin (0.5 - 1mg/ml). Due to the TetR and pInducer overexpression of PLK4 could not occur until the addition of Dox.

2.3.4 shCDH1

To generate cell lines expressing shCDH1, MCF10A.TetR.PLK4 cell lines were infected with lentivirus containing pLKO.1 lentiviral vectors expressing 4 different CDH1 short hairpin RNA (shRNA; #8, #9, #10 and #11) which were obtained from Dana-Farber Cancer Institute and Broad Institute, Boston, USA. Cell lines were then selected using 10µg/mL puromycin.

2.3.5 CRISPR-Cas9 Gene Knockout

To generate cell lines with stable gene knockout, CRISPR-Cas9 lentiviral gene editing was used (Cong *et al.* 2013).

2.3.5.1 Principle of CRISPR-Cas9 Gene Knockout

The Clustered Regularly Interspaced Short Palindromic Repeats (CRISPR) and CRISPR-associated (Cas) genes were first discovered in bacteria, and act as a mechanism of defence against foreign DNA, either viral or plasmid (Mali *et al.* 2013; Jinek *et al.* 2012; Hwang *et al.* 2013; Cong *et al.* 2013). Since 2013, this technology has been used to perform gene editing. The CRISPR-Cas9 system is made up of two components: the guide RNA and the Cas9 enzyme (CRISPR-associated

protein-9 nuclease). The guide RNA (gRNA) consists of a 20-base pair length of RNA which is designed to be complementary to the targeted region of DNA for the gene of interest. The 20-base pair region of DNA is immediately followed by a protospacer adjacent motif (PAM), which is an essential targeting component for the CRISPR-Cas9 system. This gRNA is then located within a longer RNA scaffold. The Cas9 enzyme can then localise to the targeted region and make a double strand incision, which is then repaired using non-homologous end joining (NHEJ). NHEJ is a rapid process of repairing double strand breaks, but often results in small nucleotide insertions or deletions (InDels). These InDels can result in in-frame amino acid deletions/insertions, or frameshift mutations, leading to premature stop codons in the targeted gene. Therefore, the protein may be prematurely truncated if there is a stop codon, or a loss of function if incorrect amino acids are now incorporated due to frame shifts. The knock-out phenotype is then determined by residual gene function (Figure 2.1).

2.3.5.2 Site-Directed Mutagenesis

The LentiCRISPRv2 plasmid was used, as it contains two expression cassettes, hSpCas9, and one for the guide RNA which localises the nuclease to the exact location on the DNA for the gene editing event to occur (52961, Addgene, MA, USA)(Shalem *et al.* 2014). Using site directed mutagenesis, the LentiCRISPRv2 could be edited to substitute the 20 base pair target sequence for a different targeting sequence. For primers and primer design see Page 69.

The Q5® Site-Directed Mutagenesis Kit (E0554S, New England Biolabs, MA, USA) was prepared in a thin-walled PCR tube as per the dilutions in Table 2.4.

Table 2.4: Reagent dilutions for site-directed mutagenesis

Reagent	Per 25µl reaction mix	Final concentration
Q5 Hot Start High-Fidelity 2X Master Mix	12.5µl	1X
10µM Forward primer	1.25µl	0.5µM
10µM Reverse primer	1.25µl	0.5µM
Template DNA (10ng/µl)	1µl	10ng
Nuclease-free water	8.3µl	-
DMSO	0.7µl	2.8% v/v

The addition of DMSO was to reduce secondary structures in the DNA which can then

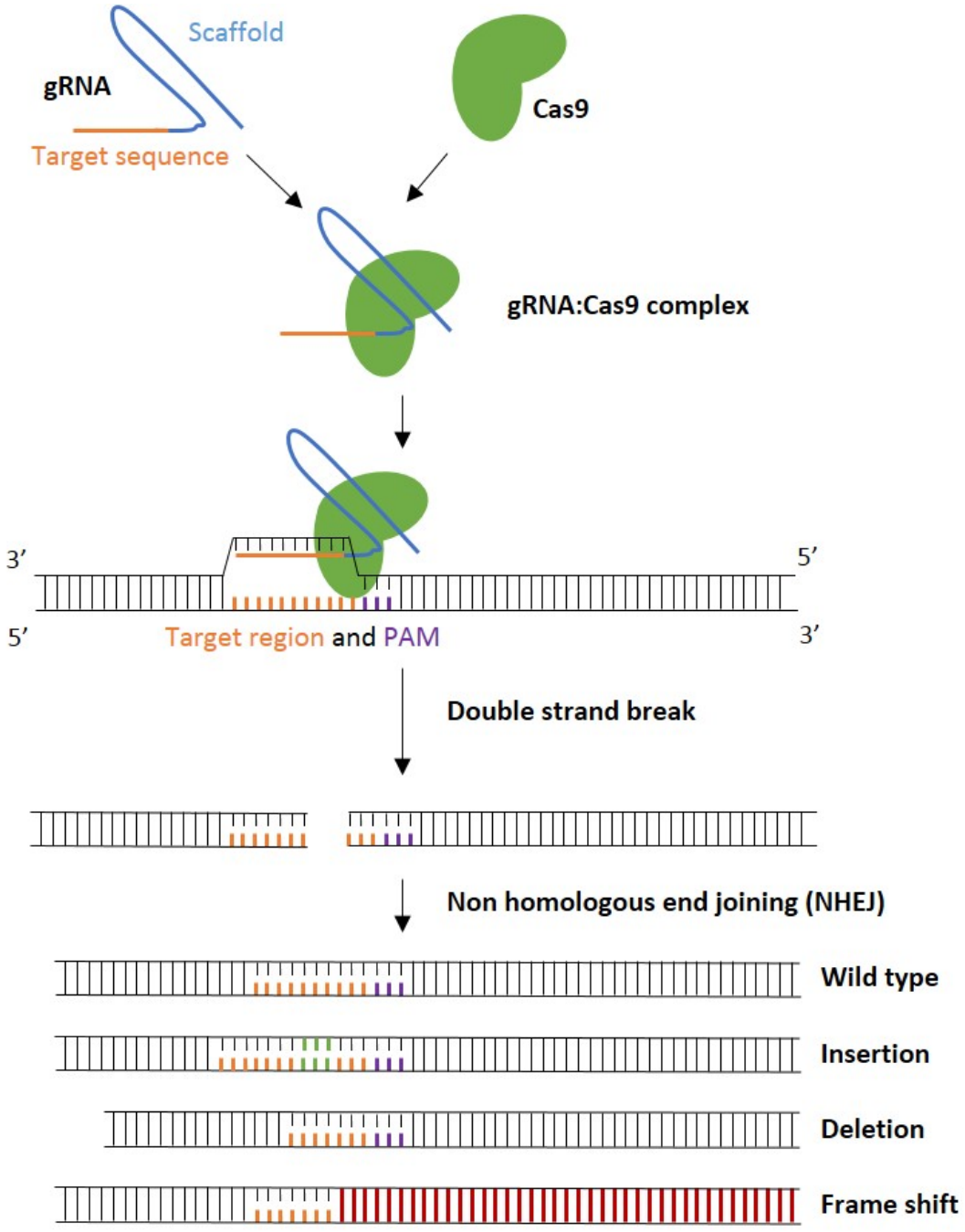

Figure 2.1: CRISPR-Cas9 gene editing
CRISPR-Cas9 gene editing. Schematic of CRISPR-Cas9 gene editing. gRNA with the target sequence localises to the Cas9 enzyme forming a complex. The gRNA then targets the complex to the correct location within the DNA, where the Cas9 enzyme forms a double strand break. This is repaired using non homologous end joining (NHEJ). NHEJ is error prone so can result in either a repaired wild type gene, or where gene editing has occurred insertion/deletion of base pairs or a mutation resulting in frame shift.

inhibit polymerase progress. The PCR tubes were then centrifuged on a benchtop PCR centrifuge for 5 seconds to ensure the mixture was collected at the bottom of the tube, and transferred to a C1000 Touch™ Thermal Cycler (Bio-Rad Laboratories, CA, USA). The lid of the Thermal Cycler was set to 100°C to stop condensation within the lid, which would reduce the concentration within the mixture. The PCR was then run under the conditions in Table 2.5.

Table 2.5: PCR conditions for site-directed mutagenesis

Step	Temp	Time
Initial denaturation	98°C	30s
25 cycles	98°C	10s
	50-72°C (primer specific)	30s
	72°C	30s
Final Extension	72°C	10min
Hold	4°C	-

During the PCR process, the specifically-designed primers substituted the previous target sequence, generating a new plasmid with the new target sequence incorporated. At the completion of the PCR, a KLD enzyme reaction mix was prepared as per Table 2.6.

Table 2.6: Conditions for KLD enzyme reaction

Reagent	Volume	Final Concentration
PCR product	1µl	-
2X KLD reaction buffer	5µl	1X
10X KLD enzyme mix	1µl	1X
Nuclease-free water	3µl	-

The kinase and ligase respectively allow for the phosphorylation and circularisation of the plasmid whilst the Dpn1 removes any residual template DNA. The reaction was incubated at room temperature for 5 minutes. One Shot® Stbl3™ Chemically Competent *E. coli* were then transformed as per Section 2.2.2.

2.3.5.3 Sequence design

Guide RNAs were designed using the ATUM CRISPR gRNA design tool (ATUM, CA, USA). They were designed for use with the wild-type Cas9, and within the first exon of the gene. By targeting the first exon this minimises the risk of truncated protein

expression, which may still be active, instead of full protein loss. The top guide RNAs were selected based on their predicted likelihood of being specific to the target gene, therefore reducing the risk of off-target effects. Primers were then designed to enable the guide RNAs to be incorporated into the LentiCRISPRv2 plasmid by site directed mutagenesis. Primers were designed using the NEBaseChanger® (New England Biolabs, MA, USA). Primers were purchased from Sigma-Aldrich (Sigma-Aldrich, MO, USA) and resuspended to a stock concentration of 100µM in nuclease free water and stored at -20°C; working stocks were made at 10µM (R0582, Invitrogen, ON, Canada). For details of primers please see Table 2.7 for E-cadherin and Table 2.8 for DDR1.

Table 2.7: Mutagenesis primers for CDH1

Lowercase letters identify guide RNA to be inserted, uppercase identify alignment to the plasmid

gDNA	Target sequence	Mutagenesis primers
1	CCCTTGGAGCCGCAGCCTCT	FW - cgcagcctctGTTTTAGAGCTAGAAATAGCAAG RV - gctccaagggTTTCGTCCTTTCCACAAG
2	GCCGAGAGGCTGCGGCTCCA	FW - tgcggctccaGTTTTAGAGCTAGAAATAGCAAG RV - gcctctcggcTTTCGTCCTTTCCACAAG
3	CCGAGAGGCTGCGGCTCCAA	FW - gcggctccaaGTTTTAGAGCTAGAAATAGCAAG RV - agcctctcggTTTCGTCCTTTCCACAAG
4	CCCGGCCAGCCATGGGCCCT	FW - catgggccctGTTTTAGAGCTAGAAATAGCAAG RV - gctggccgggTTTCGTCCTTTCCACAAG
5	GCAGCAGCAGCAGCGCCGAG	FW - cagcgccgagGTTTTAGAGCTAGAAATAGCAAG RV - ctgctgctgcTTTCGTCCTTTCCACAAG
6	CGGCTCCAAGGGCCCATGGC	FW - ggcccatggcGTTTTAGAGCTAGAAATAGCAAG RV - cttggagccgTTTCGTCCTTTCCACAAG

Table 2.8: Mutagenesis primers for DDR1

Lowercase letters identify guide RNA to be inserted, uppercase identify alignment to the plasmid

gDNA	Target sequence	Mutagenesis primers
1	GTGGAATGTCGCTTCCGGCG	FW - gcttccggcgGTTTTAGAGCTAGAAATAGCAAG RV - gacattccacTTTCGTCCTTTCCACAAG
2	CCCCCTAGGTTGTGGCGCAT	FW - tgtggcgcatGTTTTAGAGCTAGAAATAGCAAG RV - acctaggggTTTCGTCCTTTCCACAAG
3	CACGGTATGTCCGTCATAGG	FW - ccgtcataggGTTTTAGAGCTAGAAATAGCAAG RV - acataccgtgTTTCGTCCTTTCCACAAG

2.3.5.4 Selection

Following lentiviral production and infection as described above, cells were treated with puromycin at 1 – 5µg/ml to select for cells that had been infected with the lentivirus. Cells were then seeded at 100 cells per 10cm diameter cell culture plates and incubated for 7 days to allow colonies to form from single cells. Growth Medium was changed every 2 days. Colonies to be selected were identified by using an inverted light microscope using a 40X objective, and marked on the bottom of the plate. Growth medium was removed and the cells were washed in autoclaved PBS. Autoclaved 8mm glass cloning cylinders had one end dipped in autoclaved Vaseline, this end was then placed onto the plate forming a well around the colony to be selected, this was repeated for all the colonies (c1059, Sigma-Aldrich, MO, USA). 20µl of Trypsin-EDTA was then added to the cylinder and incubated for 10 minutes, the Vaseline formed a hydrophobic seal with the plate keeping the Trypsin-EDTA within the cylinder, coating the cells to be selected. 200ul of Growth Medium was then added to the cylinder and pipetted up and down to ensure the cells were in suspension. The cell suspension was then transferred to a well in a 96-well plate; this was repeated for each clone. The clonal cylinders were washed in 1% w/v Virkon followed by 70% v/v ethanol, before being autoclaved for future use. The cells were grown until 80% confluency, where they were then amplified into a 24-well plate and subsequently further amplified into 12-well, 6-well and 25cm^2 plates until they could be analysed by western blot for protein loss.

2.3.6 E-cadherin

To overexpress E-cadherin, pWZL-blast-DN-E-cadherin (18800, Addgene, MA, USA) and pWZL-blast-E-cadherin (18804, Addgene, MA, USA) were used (Onder *et al.* 2008). Cells were selected with 2.5 – 20µg/ml blasticidin.

2.3.7 H2B GFP and H2B RFP

The LV-GFP plasmid (25999, Addgene, MA, USA) was used to express H2B-GFP, and LV-RFP (26001, Addgene, MA, USA) for H2B RFP (Beronja *et al.* 2010).

2.3.8 Centrin GFP

Lentilox Centrin1-eGFP construct was a gift from J. Loncarek (National Cancer Institute, USA). Cells were sorted as per Section 2.3.2.

2.4 Protein analysis

2.4.1 Reagents

Radioimmunoprecipitation assay (RIPA) buffer: Pre-mixed 25mM Tris-HCl pH 7.6, 150mM NaCl, 1% v/v NP-40, 1% w/v sodium deoxycholate, 0.1% v/v sodium dodecyl sulphate (SDS) diluted in distilled water was stored at 4°C (89901, Thermo Scientific, MA, USA).

Protease Inhibitor: 1 tablet of cOmplete™ Mini Protease Inhibitor Cocktail was dissolved in 10ml RIPA buffer in a 15ml centrifuge tube using a vortex (11836153001, Roche, Germany). 1ml aliquots were prepared in microcentrifuge tubes and stored at -20°C. Aliquots were thawed on ice prior to use.

Phosphatase Inhibitor: For experiments looking at phosphorylated proteins, a 1:100 dilution of Phosphatase Inhibitor Cocktail was made with RIPA buffer containing protease inhibitor and used immediately (5870, New England Biolabs, MA, USA). Phosphatase Inhibitor Cocktail was stored at 4°C.

Bovine serum albumin (BSA): A stock of 10mg/ml BSA in deionised water was stored at -20°C (A2153, Sigma-Aldrich, MO, USA). Protein standards were made to 0 – 6mg/ml in microcentrifuge tubes and stored at 4°C.

Laemmli SDS sample buffer 4x: Premixed 250mM Tris-HCl pH 6.8, 8% v/v SDS, 40% v/v glycerol, 8% v/v beta-mercaptoethanol, and 0.02% w/v bromophenol blue was stored at room temperature (J60015, Alfa Aesar, UK).

N,N,N',N'-Tetramethylethylenediamine (TEMED): TEMED was stored at room temperature (T9281, Sigma-Aldrich, MO, USA).

Ammonium persulphate (APS): A solution of 10% w/v APS was made in deionised water (A3678, Sigma-Aldrich, MO, USA). 1ml aliquots were made in microcentrigufe tubes and stored at -20°C.

ProtoFLOWGel: ProtoFLOWGel is a pre-mixed 30% w/v acrylamide/methylene bisacrylamide solution in a 37.5:1 ratio in distilled water (H16996, Scientific Laboratory Supplies, UK).

Resolving gel buffer: 4X Resolving Buffer was diluted when required in deionised water forming a solution of 0.375M Tris-HCl and 0.1% v/v SDS, pH 8.8 (EC-892, Scientific Laboratory Supplies, UK).

Stacking gel buffer: 4X Stacking Buffer was diluted when required in deionised water forming a solution of 0.125M Tris-HCl and 0.1% v/v SDS, pH 6.8. (EC-893, Scientific Laboratory Supplies, UK).

Running buffer: 10X Tris Glycine SDS (250mM Tris, 2M Glycine and 1% w/v SDS) was diluted to 1X when required in deionised water. (20640050, Severn Biotech, UK). The buffer was used immediately.

Transfer Buffer: 10X Tris Glycine (250mM Tris and 2M Glycine) was diluted to 1X when required in deionised water (20630050, Severn Biotech, UK). A solution of 20% v/v methanol was then made in the 1X Tris Glycine. The buffer was used immediately.

TWEEN® 20: TWEEN® 20 was stored at room temperature (P9416, Sigma-Aldrich, MO, USA).

Tris buffered saline (TBS)-T: TBS was diluted to 1X in deionised water as required (20730110, Severn Biotech, UK). The 1X TBS solution consisted of 137mM Sodium Chloride and 20mM Tris. 0.1% v/v Tween-20 was added to create TBS-T. The buffer was used immediately.

Blocking solution: 5% w/v skimmed milk powder (70166, Sigma-Aldrich, MO, USA) was dissolved in TBS-T. Blocking solution was stored at 4°C for a maximum of 48 hours.

Phospho-blocking solution: 5% w/v BSA was dissolved in TBS-T. Phospho-blocking solution was stored at 4°C for a maximum of 48 hours.

2.4.2 Protein harvesting

Cells to be processed for protein analysis were plated on 6-well plates or 6cm diameter cell culture dishes. At 80% confluency, Growth Medium was removed and cells were

washed in 5ml of autoclaved PBS. After PBS was removed, 150µl of RIPA buffer with protease inhibitors was added. For analysis of phosphorylated proteins, phosphatase inhibitors were also used. The plates were then stored at -80°C for 24 hours to prevent protein degradation. Cells were thawed on ice and using a cell scraper the lysed cell mix was pippeted into a microcentrifuge tube. The suspension was centrifuged at 10,000g for 15 minutes to pellet cell debris. The supernatant containing the protein was then pipetted into a new microcentrifuge tube and the pellet discarded.

2.4.3 Bradford assay

A Bradford assay was used to determine the protein concentration of each sample. In a 96-well plate, 1µl of BSA protein standards (1-6µg/ml) and protein sample was loaded in triplicate. 200µl of Bradford Protein Assay Dye Reagent was added to each well (5000006, Bio-Rad Laboratories, CA, USA). The dye contains Coomassie brilliant blue G-250 dye which, on binding to protein, changes colour. The absorbance of each well was quantified using a Victor^3 Multilabel Counter plate reader (Perkin Elmer, MA, USA) at an excitation of 595nm. Using the BSA standards, a standard curve was generated using concentration plotted against absorbance in Microsoft Excel. Microsoft Excel generated an equation for the standard curve using a linear regression. The protein concentrations for the samples could then be calculated by substituting the average absorbance from the triplicates into the equation. To ensure equal protein loading between samples, the samples were diluted to a final concentration of 1µg/µl in the RIPA buffer with protease inhibitor. Laemmli Buffer was then added to a final concentration of 1X. To denature the proteins, the samples were placed in a heat block at 98°C for 5 minutes. The samples were then placed in a benchtop centrifuge for 5 seconds to collect any condensation that occurred. Samples were stored at -80°C until required.

2.4.4 SDS-PAGE

Depending on the size of the protein of interest, protein samples were resolved on 10% or 12% acrylamide sodium dodecyl sulphate polyacrylamide gel electrophoresis (SDS-PAGE) using the Mini-PROTEAN® system (Bio-Rad Laboratories, CA, USA). Glass plates were prepared for the gels, a glass front plate was placed over a 1mm back plate and held within a green casting cassette. Resolving gels were prepared by adding 5ml of the required percentage of ProtoFLOWGel to each cassette as per the recipe in Table 2.9 (10ml was made for 2 gels).

Table 2.9: Protocol for resolving gel preparation

Reagent	Volume for 10% v/v gel	Volume for 12% v/v gel
ProtoFLOWGel	3.3ml	4.0ml
4% ProtoGel Resolving Buffer	2.5ml	2.5ml
Deionised water	4.1ml	3.4ml
10% APS	100µl	100µl
TEMED	10µl	10µl

The mixture was immediately added between the glass plates, leaving space for the stacking gel. 500µl isopropanol was pipetted onto the solution to ensure the gel set evenly. The gel was left to solidify at room temperature for 10 minutes and the isopropanol was removed with blotting paper. 5ml of stacking gel solution was prepared as per the recipe in Table 2.10 for 2 gels.

Table 2.10: Protocol for resolving gel preparation

Reagent	Volume
ProtoFLOWGel	650µl
4% ProtoGel Stacking Buffer	1.25ml
Deionised water	3.05ml
10% APS	50µl
TEMED	5µl

The Stacking Gel solution was pipetted on top of the set resolving gel, and a 10-well or 15-well comb inserted. The gel was incubated at room temperature for 20 minutes to solidify. The gels were inserted into the clamped electrode apparatus and placed within the electrophoresis tank. The tank was then filled with running buffer and the combs carefully removed. The wells were loaded with 15µl (15µg) of protein sample, leaving at least one well to be loaded with 5µl PageRuler™ Plus Prestained Protein Ladder (26619, Thermo Scientific, MA, USA) as a marker for protein size. 80V was applied to the gels for 15 minutes to allow the proteins to enter the resolving gel, and 120V then applied for 1.5 hours, or until the proteins had resolved to a sufficient degree based on the protein ladder.

2.4.5 Western blot transfer

Resolved proteins were then transferred onto polyvinylidene fluoride (PVDF) membranes (03010040001, Roche, Germany) via the Mini Trans-Blot® wet transfer

system (Bio-Rad Laboratories, CA, USA). PVDF membranes were equilibrated in methanol for 5 minutes. Cassettes were prepared in a plastic tray filled with 1L of Transfer Buffer. 3 pieces of chromatography paper were placed on the negative side of the cassette (11567393, Fisher Scientific, UK). The gels were removed from the electrophoresis tank, and carefully removed from the glass plates. The stacking gel was removed from the gel, and the resolving gel placed onto the chromatography paper. The PVDF membrane was then placed onto the gel, and 3 pieces of chromatography paper placed on top, ensuring no air bubbles remained within the stack. The cassette was then closed and placed within the transfer tank. An ice block was placed with the tank, to prevent overheating during the transfer process. The transfer buffer was then poured from the plastic tray into the tank. 100V was then applied to the tank for 1.25 hours, enabling the negatively charged protein to transfer onto the membrane.

2.4.6 Immunoblot detection

After transfer, membranes were removed from the cassettes and immediately placed in 10ml of blocking solution (for phosphorylated proteins, phospho-blocking solution was used) for 1 hour at room temperature with gentle rocking. Membranes were then cut to size for the specific proteins of interest with a scalpel and ruler based on the protein ladder, and placed in a 30ml universal container. Membranes were incubated in 2ml of diluted primary antibody in the appropriate blocking buffer overnight at 4°C with gentle rolling (see Table 2.11 for antibody dilutions). Membranes were washed 3 times for 5 minutes each at room temperature with gentle rolling in TBS-T. Membranes were then incubated in 2ml of diluted secondary, species-specific, horseradish peroxidase (HRP)-conjugated antibody in the appropriate blocking buffer for 1 hour at room temperature with gentle rolling (see Table 2.11 for antibody dilutions). Membranes were washed 3 times for 5 minutes each at room temperature in TBS-T. Membranes were then placed protein side up on clear plastic film. A 1:1 mixture of Peroxide Solution and Luminol Enhancer in the Pierce™ enhanced chemiluminescence reagent (ECL) Western Blotting Substrate (32106, Thermo Scientific, MA, USA) was made in a centrifuge tube. 1ml of ECL was then added to each membrane and incubated at room temperature for 5 minutes. Excess ECL was then removed and the membranes were placed protein side up between clear plastic sheets in an autoradiography cassette, which was taped down to prevent movement. In a dark room, under red light, X-ray film (MOL7016, Scientific Laboratory Supplies, UK) was placed onto the membrane and exposed for an appropriate time depending on signal strength, between 5 second – 5 minutes. Films were developed using a

SRX-101A table top film processor (Konica Minolta, NJ, USA). Developed films were then scanned onto a computer and saved.

Table 2.11: Antibody list with dilutions

Antibody	Clone	Product number	Manufacturer	Species raised	Dilution
β-actin	13E5	4970	Cell Signalling	Rabbit	1:5000
E-cadherin	HECD1	ab1416	Abcam	Mouse	1:200
DDR1	C-20	sc-532	Santa Cruz	Rabbit	1:200
KIFC1/HSET	1-50	A300-951A-T	Bethy Laboratories	Rabbit	1:500
Mad2	100-150	A300-300A-T	Bethy Laboratories	Rabbit	1:500
Rnd3/RhoE	4	R6153	Sigma-Aldrich	Mouse	1:100
P190	30	610149	BD Bioscience	Mouse	1:250
STARD8/ DLC3	731-830	sc-166725	Santa Cruz	Mouse	1:100
N-cadherin	32	610920	BD Bioscience	Mouse	1:500
Vimentin	RV202	550513	BD Pharmingen	Mouse	1:500
ERM	567	3142	Cell Signalling	Rabbit	1:500
p-MLC	T18/S19	3674	Cell Signalling	Rabbit	1:500
pDDR1	T513	TA311934	Origene	Rabbit	1:100
p-HH3	S11	9764	Cell Signalling	Rabbit	1:1000
HRP- anti rabbit secondary	Polyclonal	NA934V	GE Healthcare	Donkey	1:5000
HRP- anti mouse secondary	Polyclonal	NA931V	GE Healthcare	Sheep	1:5000

2.4.7 Antibody stripping and re-probing

When required, membranes were stripped of primary and secondary antibodies using 5ml of Restore™ Western Blot Stripping Buffer for 10 minutes at room temperature with gentle rocking (21059, Thermo Scientific, MA, USA). Membranes were then washed in TBS-T for 5 minutes at room temperature with gentle rocking. Membranes were then re-blocked and probed as per Section 2.4.6.

2.5 Microscopy

2.5.1 2D indirect immunofluorescence microscopy

2.5.1.1 Reagents

Formaldehyde: 16% v/v formaldehyde (28906, Thermo Scientific, MA, USA) was stored at room temperature in the dark for up to 1 month. 4% v/v formaldehyde was prepared in PBS when required and used immediately.

Methanol: ≥99.9% methanol was stored at -20°C (154903, Sigma-Aldrich, MO, USA).

Acetone:Methanol: A 50:50 v/v solution of methanol and acetone was prepared and stored at -20°C.

Permeabilisation buffer: A solution of 0.2% v/v Triton X-100 in PBS was prepared and stored at room temperature.

Blocking solution: 5% w/v BSA and 0.1% v/v Triton X-100 were dissolved in PBS. The solution was filtered through a 0.2µM 500ml Rapid Flow Filter Unit (156-4020, Thermo Scientific, MA, USA). Blocking solution was stored at 4°C for up to two months.

2.5.1.2 Immunofluorescence Microscopy

Cells were split as per Section 2.1 and resuspended in serum-free medium. 100 - 200µl of cell suspension (dependent on cell number) was carefully plated on 18mm uncoated glass coverslips (CS-18R15, Warner Instruments, CT, USA) in 12-well dishes. Plates were incubated for 1 hour. Serum-free medium was used to prevent cell aggregates forming, allowing cells to adhere as a monolayer onto the coverslips. 1ml of growth medium was then carefully pipetted into each well so as not to disturb cell adhesion. Prior to fixation, Growth Medium was removed and cells were washed in autoclaved PBS. Cells were then fixed dependent on the antibodies to be used, either in 4% v/v formaldehyde at room temperature for 15 minutes, ice-cold methanol at -20°C or ice-cold 1:1 methanol/acetone at -20°C for 10 minutes. For a list of antibodies and fixation method see Table 2.12. Cells were washed twice in autoclaved PBS, before being permeabilised at room temperature for 5 minutes in 1ml permeabilization buffer. Cells were then blocked in 1ml blocking solution per well for 30 minutes. The blocking solution was then removed and primary antibodies were diluted in 50µl per coverslip in blocking solution. 25µl of diluted primary antibodies was added onto each coverslip and incubated at room temperature for 30 minutes, onto which another 25µl was added for a further 30 minutes. Cells were then washed twice for 5 minutes at room temperature in PBS. The remaining steps were done in the dark. Secondary antibodies were diluted in 50µl per coverslip in blocking solution. 25µl of diluted secondary antibodies was added onto each coverslip and incubated at room temperature for 25 minutes, onto which 25µl was added for a further 25 minutes. For details of secondary antibodies see Table 2.13. For F-actin staining, Phalloidin conjugated with Alexa Fluor 568 (A12380, Life Technology) was used at 1:250 dilution and incubated for 1 hour at room temp in combination with the secondary antibodies. Cells were then washed twice for 5 minutes at room temperature in PBS. Hoechst 33342 was diluted at 1:5000 in PBS (H3570, Thermo Scientific, MA, USA). 1ml of diluted Hoechst 33342 was added per well and incubated at room temperature for 5 minutes. Coverslips were then washed in PBS for 10 minutes. Coverslips were inverted onto glass slides with a drop of ProLong® Gold Antifade Reagent (P36934, Thermo Scientific, MA, USA). Excess mounting reagent was removed with tissue paper. Slides were stored in slide boxes at -4°C. Cells were imaged on an Olympus DeltaVision microscope (GE Healthcare, OH, USA) equipped with a coolsnap HQ camera. Details of the DelataVision optical filters can be found in Table 2.14.

Table 2.12: Primary antibodies for immunofluorescence and fixation

Antibody (clone)	Species raised	Product number	Manufacturer	Dilution	Fixation
α-tubulin (DM1α)	Mouse	T9026	Sigma Aldrich	1:1000	Methanol or formaldehyde
Centrin-2 (N-17-R)	Rabbit	sc-27793-R	Santa Cruz	1:100	Methanol
γ-tubulin (GTU88)	Mouse	T5326	Sigma Aldrich	1:500	Formaldehyde
E-cadherin (HECD-1)	Mouse	ab1416	Abcam	1:500	Formaldehyde
DDR1 (IF10)	Mouse	-	Birgit Leitinger (Imperial, UK)	1:500	Formaldehyde
DDR1 (7A9)	Mouse	-	Birgit Leitinger (Imperial, UK)	1:500	Formaldehyde
Pericentrin	Rabbit	ab4448	Abcam	1:1500	Formaldehyde
EB1 (5/EB1)	Mouse	610535	BD Bioscience	1:500	Methanol followed by formaldehyde
α-tubulin FITC-conjugated (DM1α)	Mouse	F2168	Sigma Aldrich	1:500	Methanol or Formaldehyde

Table 2.13: Secondary antibodies for immunofluorescence

Antibody	Species raised	Product number	Manufacturer	Dilution
Anti-Rabbit Alexa Fluor 488	Goat	A11008	Life Technologies	1:1000
Anti-Rabbit Alexa Fluor 568	Goat	A11011	Life Technologies	1:1000
Anti-Mouse Alexa Fluor 488	Goat	A11001	Life Technologies	1:1000
Anti-Mouse Alexa Fluor 568	Goat	A11004	Life Technologies	1:1000

Table 2.14: DeltaVision Microscope optical filters used

Channel	Band (nm)	Center Wavelength (nm)	Bandwidth (nm)
DAPI	411–459	435	48
FITC/GFP	501—549	525	48
TRITC	574.5—619.5	597	45

2.5.2 Live cell imaging

H2B-GFP expressing cells were seeded onto glass-bottom dishes with 2ml of Growth Medium (P35G-0-10-C, MatTek, MA, USA). Cells were imaged on an Olympus DeltaVision microscope (GE Healthcare, OH, USA) equipped with a coolsnap HQ camera. The microscope was enclosed within temperature and CO_2-controlled environments that maintained an atmosphere at 37°C and 3-5% humidified CO_2. GFP and brightfield images were captured at multiple points for 16 hours at 40X (1.3 NA) objective. Captured images from each experiment were analysed using the softWoRx Explorer software (GE Healthcare, OH, USA)

2.6 Cell viability

2.6.1 Colony formation assay

Using serial dilution, 100 cells were plated on 6cm diameter cell culture dishes in triplicate per each condition. Cells were incubated for 10 days, with Growth Medium being replaced every 48 hours. Growth Medium was removed and cells were washed in 5ml of PBS. Cells were fixed in v/v 1% glutaraldehyde in PBS for 15 minutes at room temperature (G6257, Sigma-Aldrich, MO, USA). Cells were washed in PBS before incubating in 3ml of 0.5% w/v Crystal Violet (C6158, Sigma-Aldrich, MO, USA) and 20% v/v methanol in deionised water for 30 minutes at room temperature. Cells were washed 3 times in PBS for 5 minutes each at room temperature with gentle rocking before being air dried overnight. Images of the plates were taken on an Amersham Imager 600 (GE Healthcare, OH, USA). Crystal violet was then dissolved in 3ml of 0.05% Triton-X 100 in PBS overnight with gentle rocking. 200µl of the dissolved crystal violet was pippeted into a 96-well plate in triplicate for each plate. The absorbance of crystal violet was analysed at 560nm and 405nm on the Victor^3 Multilabel Counter plate reader (Perkin Elmer, MA, USA).

2.6.2 IncuCyte

H2B-GFP-expressing cells were passaged and counted as described in Section 2.1. Using serial dilution, 3×10^3 cells were plated per well in a 12-well plate in triplicate with 1ml of Growth Medium. Plates were incubated for 24 hours to allow cells to

adhere, and were then placed into an IncuCyte Zoom (Essen Bioscience, MI, USA) for 7 days within an incubator at 37°C and 5% CO_2. Brightfield and GFP images were acquired at 100X magnification every hour, at 4 locations per well. Images were then quantified using a "top-hat" mask based upon GFP using the IncuCyte Zoom software to identify the number of individual nuclei based on the H2B-GFP and thus cell number.

2.7 qRT-PCR

RNA was prepared using the Qiagen RNAeasy kit (Qiagen, MD, USA). Cells grown in 6cm diameter dishes were passaged as previously described and resuspended in 1ml of Growth Medium. The cell suspension was placed in a 1.5ml autoclaved microcentrifuge tube and centrifuged at 300g for 5 minutes. The medium was removed and the cell pellet resuspended in 350µl RLT buffer to lyse the cells, the suspension was then passed through a sterile 20-gauge needle to aid lysis. 350µl of 70% v/v ethanol in autoclaved deionised water was added and mixed by pipetting to precipitate the RNA. The sample was then transferred to a RNeasy spin column placed in a 2ml collection tube. The column was then centrifuged for 15 seconds at 8000g and the flow through discarded, allowing the RNA to bind to the membrane in the column. 700µl of RW1 Buffer was added to the column and centrifuged at 8000g for 15 seconds and the flow through discarded. The column was then further washed twice with 500µl RPE Buffer and centrifuged at 8000g, the first time for 15 seconds, and the second time for 2 minutes. The column was then transferred to a new microcentrifuge tube and centrifuged for 1 minute to ensure no residual buffer remained. The column was placed into a sterile microcentrifuge tube and 50µl RNase-free water was carefully pipetted directly onto the spin column membrane and incubated for 1 minute at room temperature. The column was then centrifuged at 8000g for 1 minute and the flow through was quantified using the Nanodrop-1000 for RNA concentration as described in Section 2.2.5. RNA was stored at -20°C.

RNA was diluted in RNase-free water to 200ng/µl. Using the High-Capacity RNA-to-cDNA™ Kit (4387406, Thermo Scientific, MA, USA) RNA was reverse transcribed into cDNA. Per reaction, 5µl of RNA was added to 10µl 2X Reaction Mix, 1µl Enzyme Mix and 4µl RNase-free water in a PCR tube. The tubes were then placed in a C1000 Touch™ Thermal Cycler (Bio-Rad Laboratories, CA, USA). The lid of the Thermal Cycler was set to 100°C to stop condensation within the lid, which would reduce the concentration within the mixture. The PCR was then run under

the following conditions:

Reverse transcription	37°C	60 minutes
Reverse Transcription inactivation	95°C	5 minutes
Hold	4°C	-

cDNA generated from the reverse transcription was then analysed by qRT-PCR in triplicate using the Power SYBR® Green PCR Master Mix (4367659, Thermo Scientific, MA, USA). A PCR cocktail was made for each gene being analysed made up of 12.5µl 2X Power SYBR® Green PCR Master Mix, 3.75µl of both the gene specific forward and reverse primers at 10µM, and 4µl nuclease free water per well. 24µl of PCR cocktail was added to each well of a 96-well PCR plate, with 1µl of cDNA, for a final volume of 25µl. The 96-well plate was then sealed and centrifuged in a plate centrifuge for 5 seconds to collect samples at the bottom of the wells. The plate was then placed in a 7500 Real Time PCR machine (Thermo Scientific, MA, USA) and the following programme was run:

Enzyme activation	95°C	10 minutes	
PCR cycle	95°C	15 seconds	40 cycles
Primer annealing and amplification	6°C	1 minute	
Dissociation curve	Default settings		

The Ct (Cycle threshold) values (the number of cycles required for the fluorescent signal to cross the threshold) generated from qRT-PCR were analysed using the comparative Ct method ($2^{-\Delta\Delta Ct}$). GAPDH was used as a housekeeping gene for normalisation. The primers used for qRT-PCR are shown in Table 2.15.

Table 2.15: Primers for qRT-PCR

Target	Primer	Sequence
DDR1	Forward	5'-CTGGTTAGTCTTGATTTCCC-3'
	Reverse	5'-GGAAATCATTCCTGGCATTC-3'
GAPDH	Forward	5'-TTAAAAGCAGCCCTGGTGAC-3'
	Reverse	5'-CTCTGCTCCTCCTGTTCGAC-3'

2.8 Atomic force microscopy

Cells were plated onto glass bottom MatTek dishes. When cells reached 70% confluency they were arrested at metaphase for 2 hours using 10µM MG132 in Leibovitz L15 medium (11415064, Life Technologies, CA, USA) supplemented with serum and cell specific additives. Leibovitz L15 medium is designed for cell growth in environments without CO_2 equilibration, allowing cells to survive within the Atomic Force Microscope environment. Atomic Force Microscopy experiments were kindly performed by Malti Vaghela in Dr. Guillaume Charras's lab at UCL. Indentations of cells by AFM were performed using a JPK NanoWizard-1 AFM (JPK, Berlin, Germany) mounted on an inverted microscope (IX-81, Olympus, Berlin, Germany). For measurements, soft cantilevers with V-shaped tips were used (BioLever (OBL-10), Bruker; nominal spring constant of 0.006 N m-1). The actual spring constant of the cantilever was calibrated using the thermal noise method implemented in the AFM software (JPK SPM). Before each experiment, the sensitivity of the cantilever was measured from the slope of force-distance curves that were acquired on glass. For each measurement, the cantilever was first aligned above a metaphase cell using the optical microscope. Then, force-distance curves were acquired over the centre of the cell at the 4 vertices of a square with a 2µm side length. At each of these four positions, up to 10 curves were acquired with an approach speed of 2.5 µm/s and a target force of 2.5nN. Experimental force-distance curves were post-processed to compute an apparent elastic modulus. The contact point between the cantilever tip and the cell was determined using the method outlined by Crick and Yin implemented in MATLAB (MathWorks, Natick,MA, USA)(Crick & Yin 2007). The indentation depth was then calculated by subtracting the cantilever deflection d from the piezo displacement beyond the contact point z (δ=z-d). The resultant force-indentation curves were then averaged over each position and fitted with the Sneddon model in order to calculate the apparent elasticity of each location probed in the cell (Sneddon 1965). Curve fitting was restricted to indentation depths shallower than 800nm to maximise contributions of the cortex to restoring force and minimise contributions from the cytoplasm.

2.9 Statistics

Appropriate statistics were carried out using GraphPad Prism version 5.0 for Windows (GraphPad Software, CA, USA). For each experiment see specific figure legends. Rosette plots were created by Hefin Rhys (Queen Mary, University of London, UK) in R 3.3.1 (R Development Core Team 2016) using packages ggplot2 2.1.0, and dplyr 0.5.0 (Wickham & Francois 2015).

Chapter 3

Results:

Centrosome clustering efficiency varies in different cell types

3.1 Models for generating supernumerary centrosomes

To understand if cells have the same capacity to efficiently cluster supernumerary centrosomes, centrosome amplification was induced in a panel of 6 non-cancer-derived cell lines: MCF10A (human mammary epithelium), HaCaT (human keratinocyte), J3B1A (murine mammary epithelium), RPE-1 (human retina pigmented epithelium), NIH-3T3 (murine fibroblast) and BJ (human fibroblast). Supernumerary centrosomes were initially generated using three different methods. DCB is an actin depolymerising drug resulting in cytokinesis failure whereby the subsequent tetraploid cells contain supernumerary centrosomes. Blebbistatin was also used to generate tetraploid cells with supernumerary centrosomes by inhibiting myosin II (MyoII), which is required for the formation of the cytokinetic furrow, also resulting in cytokinesis failure by an independent mechanism to that of DCB. The CDK1 inhibitor R0-3306 (CDK1 inhibitor) was used to arrest cells at the end of G2 in the cell cycle, which results in centrosome overduplication without DNA endoreplication (Steere *et al.* 2011).

Centrosome amplification was induced by either treating cells plated on glass coverslips with 4µM DCB, or 50µM blebbistatin for 20 hours, or 5µM R0-3306 for 40 hours. The drugs were then washed off, and after 24 hours the cells were fixed for analysis (Figure 3.1).

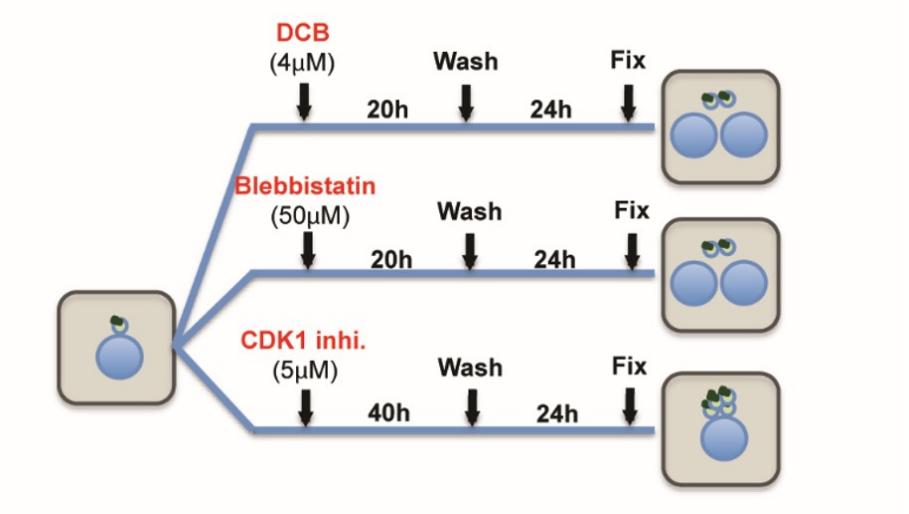

Figure 3.1: Inducing centrosome amplification
Schematic of the 3 initial methods for generating supernumerary centrosomes. Centrosome amplification was induced by either treating cells plated on glass coverslips with 4μM DCB, or 50μM blebbistatin for 20 hours, or 5μM of the CDK1 inhibitor R0-3306 for 40 hours. The drugs were then washed off, and after 24 hours the cells were fixed for analysis. Both DCB and blebbistatin lead to cytokinesis failure, and the resultant tetraploid cells have supernumerary centrosomes. The CDK1 inhibitor arrests cells in G2 and leads to centrosome overduplication.

Cells were then antibody labelled for α-tubulin and centrin whilst DNA was stained with Hoechst dye. Centrosome number per cell was quantified at metaphase using 2D immunofluorescence microscopy (identified by the mitotic spindle labelled by α-tubulin), where cells with >4 centrioles (centrin labels individual centrioles, with 2 centrioles per centrosome) were identified as containing supernumerary centrosomes (Figure 3.2). Centrosome number was quantified during mitosis to ensure that the centrosome duplication had occurred, whereas if cells were quantified during interphase centrosome duplication may not have occurred and the quantification of centrosome number would have been inaccurate.

Generation of cells containing extra centrosomes can lead to cell cycle arrest in normal cell lines (Holland *et al.* 2012). To overcome this, cells were released for 24 hours after each treatment into p38 inhibitor. p38 inhibition has been shown to allow cells to overcome cell cycle arrest. Work by Zarubin and Han showed that the stress of tetraploidy can lead to a p38 dependent cell cycle arrest (Zarubin & Han 2005). They showed that p38 is able to stabilise, phosphorylate and activate p53 which in turn drives cell cycle arrest. MCF10A seems to be the exception as it does not arrest upon induction of extra centrosomes. Whilst MCF10A express both p38 and p53, they do not express p16 which is an inhibitor of cyclin dependent kinases such as CDK4 and CDK6 which phosphorylate the retinoblastoma protein (pRB)

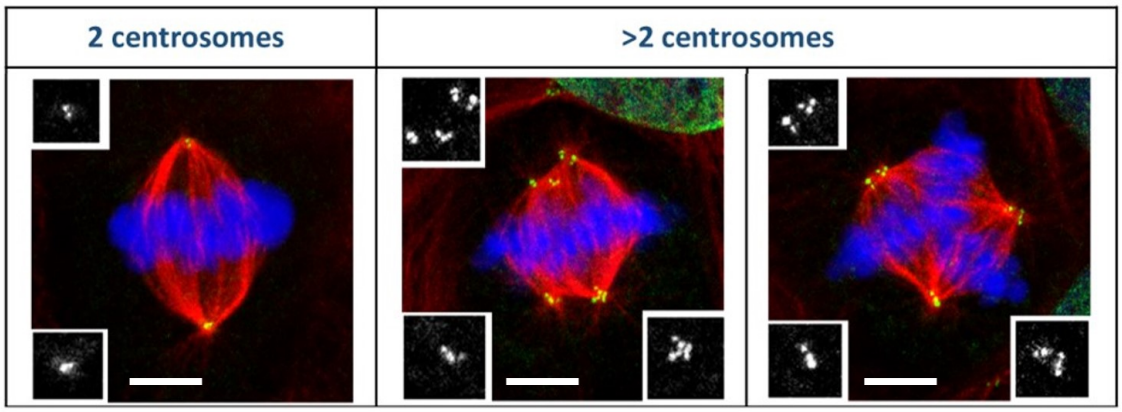

Figure 3.2: Representation of mitotic cells with normal and supernumerary centrosomes
Representative images of RPE-1 cells with normal centrosome number (left, identified by 2 centrin foci at each pole) and supernumerary centrosomes (middle and right) where the cell contains >4 centrin foci. Cells were stained for centrioles (centrin, green), microtubules (α-tubulin, red) and DNA (Hoescht, blue). Inset are the centriole foci for each cell. Scale bars: 10µM

resulting in progression from G1 phase to S phase, which could be why they do not arrest.

Centrosome amplification was quantified in all 6 cell lines with the different drug treatments with the use of the p38 inhibitor. Centrosome amplification in control cells was low at 8-20% of the cell population containing supernumerary centrosomes (Figure 3.3). DCB treatment increased centrosome amplification to 40-75% of cells containing supernumerary centrosomes. Blebbistatin resulted in 42-50% of cells with supernumerary centrosomes. The CDK1 inhibitor had the highest levels of centrosome amplification with 65-90% of cells with supernumerary centrosomes, however, the CDK1 inhibitor in the RPE-1 cells resulted in the formation of micronuclei and cell cycle arrest at G2, even with the addition of the p38 inhibitor, therefore as cells did not enter mitosis centrosome amplification could not be quantified (Figure 3.3). Therefore, all the conditions for generating supernumerary centrosomes resulted in significantly higher levels of centrosome amplification in all cell lines, with the exception of the RPE-1 with the CDK1 inhibitor which could not be quantified.

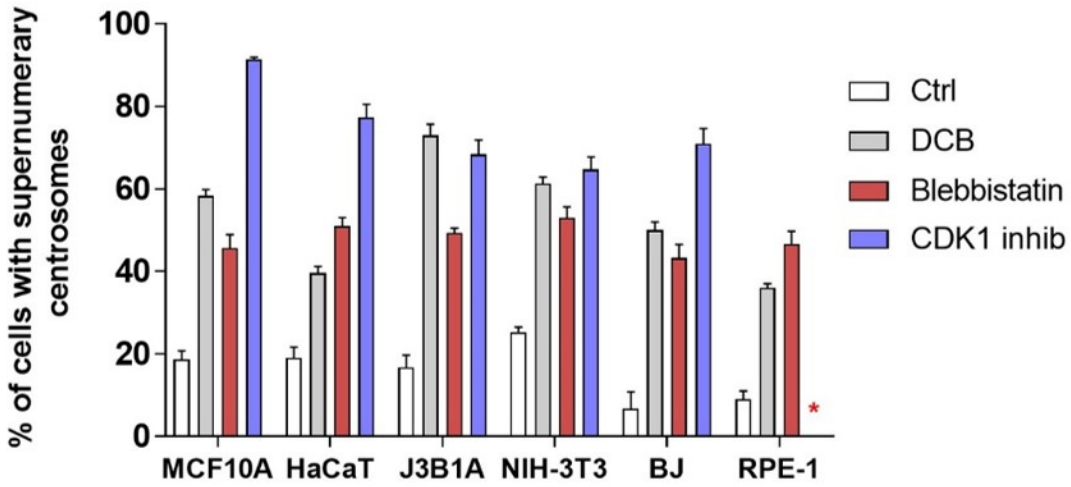

Figure 3.3: Quantification of centrosome amplification
Quantification of centrosome amplification for the different methods utilised to generate supernumerary centrosomes. Cells were treated with either 4µM DCB, or 50µM Blebbistatin for 20 hours before being washed with fresh growth medium and incubated with 10µM p38 inhibitor for 24 hours. For CDK1i treatment, 5µM inhibitor was added for 40 hours, cells were then washed and incubated with 10µM p38 inhibitor. ∗RPE-1 cells treated with CDK1 inhibitor for 40hrs arrested in interphase with fragmented nuclei and could not be analysed. Data are mean ± SD (standard deviation), n = 300 individual cells, 100 per experiment at metaphase.

3.2 Clustering efficiency varies with cell type

Centrosome clustering was quantified in cells containing supernumerary centrosomes (>4 centrioles) at both metaphase and cytokinesis. Multipolar cells were identified at metaphase as having three or more poles, and at cytokinesis as dividing into three or more daughter cells (Figure 3.4 A and C). Clustered cells were identified at metaphase and cytokinesis as the cell dividing in a pseudo-bipolar manner, whereby supernumerary centrosomes were clustered at one or both poles.

When comparing centrosome clustering between the different cell lines there was no significant trend at metaphase, except for the BJ which were able to cluster very efficiently compared to the other cells lines (~80% of cells with supernumerary centrosomes) with both the DCB and Blebbistatin treatment, although this difference was not seen with the CDK1 inhibitor (Figure 3.4 B). The remaining cell lines only clustered in 20-40% of their cells with supernumerary centrosomes, with J3B1A having particularly low efficiency of ~10% with the DCB and Blebbistatin treatment. At cytokinesis, however, there was a clear trend, with the NIH-3T3, BJ and RPE-1 cell lines all being able to cluster efficiently (~80%) for all of the methods of inducing supernumerary centrosomes, whilst the MCF10A, HaCaT and J3B1A were less efficient with centrosome clustering only occurring in 10-40% of cells with supernumerary centrosomes, showing little variation from metaphase in these three lines (Figure 3.4 D).

These data suggest that centrosome clustering efficiency is cell line dependent, with not all cell lines having the same efficiency to cluster their supernumerary centrosomes. The level of centrosome clustering was lower at metaphase than at cytokinesis, suggesting that at metaphase they are a mixed population of cells that have clustered and those that are still in a multipolar configuration, and as a consequence centrosome clustering is higher in cytokinesis For future experiments, as metaphase was not a clear indicator of clustering efficiency cytokinesis was used.

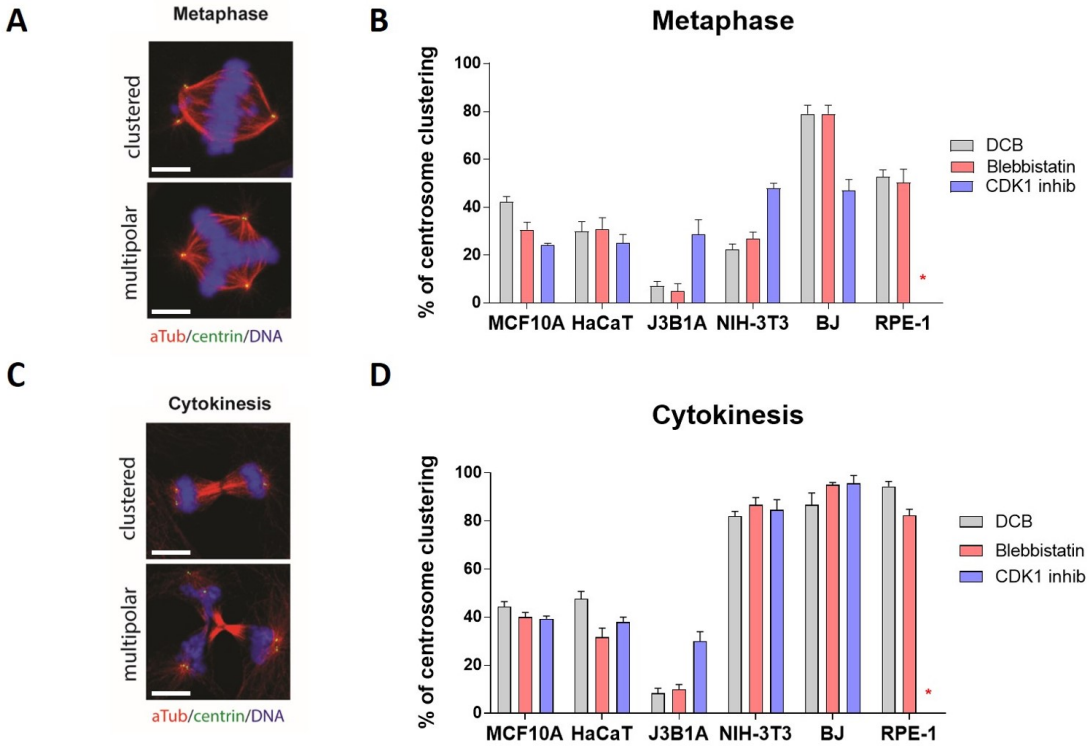

Figure 3.4: Centrosome clustering efficiency is cell type dependent
A Representative images of HaCaT cells with supernumerary centrosomes, generated by DCB treatment with p38 inhibitor, undergoing multipolar and clustered metaphases. **B** Quantification of centrosome clustering in metaphase. Data are mean ± SD, n = 300 individual cells, 100 per experiment. **C** Representative images of HaCaT cells with supernumerary centrosomes, generated by DCB treatment with p38 inhibitor, undergoing multipolar and clustered cytokinesis. **D** Quantification of centrosome clustering in cytokinesis. Data are mean ± SD, n = 150 individual cells, 50 per experiment. *RPE-1 cells treated with CDK1 inhibitor for 40hrs arrested in interphase with fragmented nuclei and could not be analysed. Scale bar = 10µM.

3.3 p38 inhibitor does not affect centrosome number or centrosome clustering

Because the cell lines were treated with p38 inhibitor, to assess whether this could impact centrosome number and centrosome clustering MCF10A cells had supernumerary centrosomes induced by DCB treatment with and without the addition of the p38 inhibitor. Centrosome amplification was then quantified (Figure 3.5 A). No significant effect was observed in centrosome amplification upon the addition of the p38 inhibitor, suggesting the hypothesis that the use of the p38 inhibitor in the remaining cell lines would not affect centrosome amplification. Similarly, no significant difference was observed in centrosome clustering with and without the inhibitor, suggesting that the p38 inhibitor does not affect clustering efficiency (Figure 3.5 B).

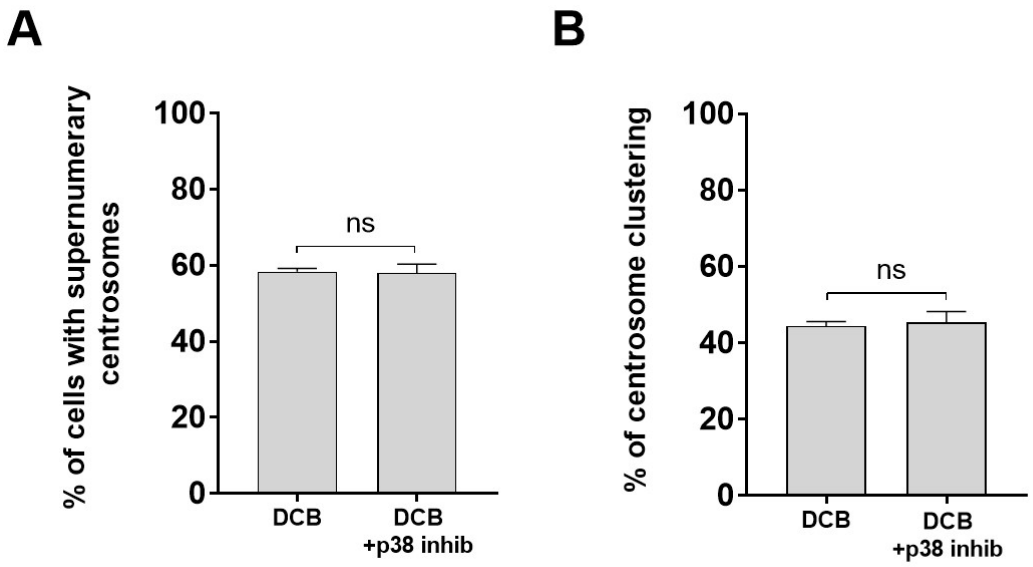

Figure 3.5: p38 inhibitor does not affect centrosome clustering
A Quantification of centrosome amplification in MCF10A cells with supernumerary centrosomes induced by DCB treatment, with and without the addition of p38 inhibitor. No significant difference in centrosome amplification was observed upon p38 treatment. **B** Quantification of centrosome clustering in MCF10A cells with supernumerary centrosomes induced by DCB treatment, with and without the addition of p38 inhibitor. No significant difference in centrosome clustering was observed upon p38 treatment. Data are mean ± SD, n = 150 individual cells, 50 per experiment at cytokinesis. Data analysed using Student's t-test.

3.4 Live cell imaging

To further confirm these results live cell imaging of tetraploid cells was performed. MCF10A, HaCaT, RPE-1 and BJ cell lines expressing H2B-GFP (Histone 2B Green Fluorescent Protein tagged) were generated via lentivirus infection. The H2B-GFP construct allows DNA to be followed. The cell lines were then plated on glass bottom microscopy dishes and supernumerary centrosomes were induced by DCB treatment. Cells that failed cytokinesis, and therefore contained supernumerary centrosomes, were easily identified by containing 2 nuclei (binucleated) (Figure 3.6 B, time 0). These cells were then tracked through mitosis by live cell imaging and were quantified as either undergoing a bipolar (as a proxy for clustered centrosomes) or multipolar division (Figure 3.6 A). The results supported the observations observed at cytokinesis in the fixed cell lines with the MCF10A and HaCaT not clustering very efficiently (33 and 44%) whereas the RPE-1 and BJ cells cluster more efficiency (>70%). These results support the observations made in the fixed cells and indicate that quantification of clustering at cytokinesis is a better readout of clustering efficiency.

A

Cell line	n	% bipolar divisions
MCF10A	90	33%
HaCaT	118	42%
RPE-1	72	71%
BJ	68	93%

B

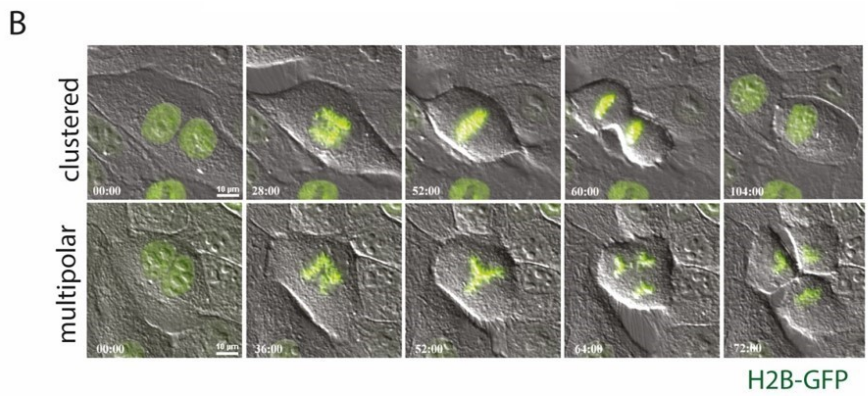

Figure 3.6: Quantification of centrosome clustering by live cell imaging **A** Quantification of centrosome clustering via live cell imaging in H2B-GFP expressing cells where supernumerary centrosomes were generated by DCB treatment. **B** Representative images of MCF10A H2B GFP tetraploid cells undergoing clustered and multipolar cell divisions over time. Scale bar = 10µM.

3.5 Centrosome amplification by PLK4 overexpression

In addition to drug treatments to induce supernumerary centrosomes, transient overexpression of PLK4, the master regulator of centrosome duplication was also used. PLK4 overexpression is an established method for generating supernumerary centrosomes (Bettencourt-Dias *et al.*, 2005; Habedanck *et al.*, 2005; Kleylein-Sohn *et al.*, 2007; Basto *et al.*, 2008). To ensure that PLK4 overexpression was transient, it was controlled by a tetracycline repressor (TetR), this was necessary as it has previously been shown that constitutive overexpression of PLK4 results in centrosome amplification, which is then lost over time, whereas using a transient system allows the analysis of supernumerary centrosomes when required. Cell lines expressing the tetracycline repressor were generated by lentivirus, and subsequently infected with lentivirus containing inducible PLK4. The tetracycline repressor binds to the CMV/TO promoter, thereby inhibiting the expression of PLK4. Upon the addition of Doxycycline hyclate (Dox) the repressor is suppressed and PLK4 overexpressed enabling centrosome overduplication.

Centrosome amplification was quantified in the panel of cell lines upon the addition of Dox in the PLK4 cell lines (Figure 3.7). Centrosome amplification went from ~20% to ~80% in the MCF10A, HaCaT, BJ and RPE-1 treated with doxycycline hyclate. Centrosome amplification was not as efficient in the NIH-3T3 where 40% of cells contained supernumerary centrosomes after Dox treatment (Figure 3.7).

Upon PLK4 overexpression there was little variation in centrosome clustering between cell lines at metaphase, except for the NIH-3T3 which was more efficient at 60% compared to ~30% in the other cell lines (Figure 3.8 A). At cytokinesis, the BJ and NIH-3T3 cluster more efficiently at ~80% compared to the MCF10A, HaCaT and RPE-1 which cluster ~60% of their cells with supernumerary centrosomes (Figure 3.8 B). This data is in contrast to the other methods of generating supernumerary centrosomes, as both the MCF10A and HaCaT cell lines are more efficient (by ~20%) at clustering their supernumerary centrosomes with PLK4 overexpression, whereas the NIH-3T3, BJ and RPE-1 have impaired centrosome clustering of ~15%. Therefore, there was no specific trend observed.

To evaluate if Dox affects centrosome number, independently of PLK4 overexpression, centrosome number in MCF10A cells with and without Dox was quantified. No significant difference in centrosome amplification was observed between control MCF10A

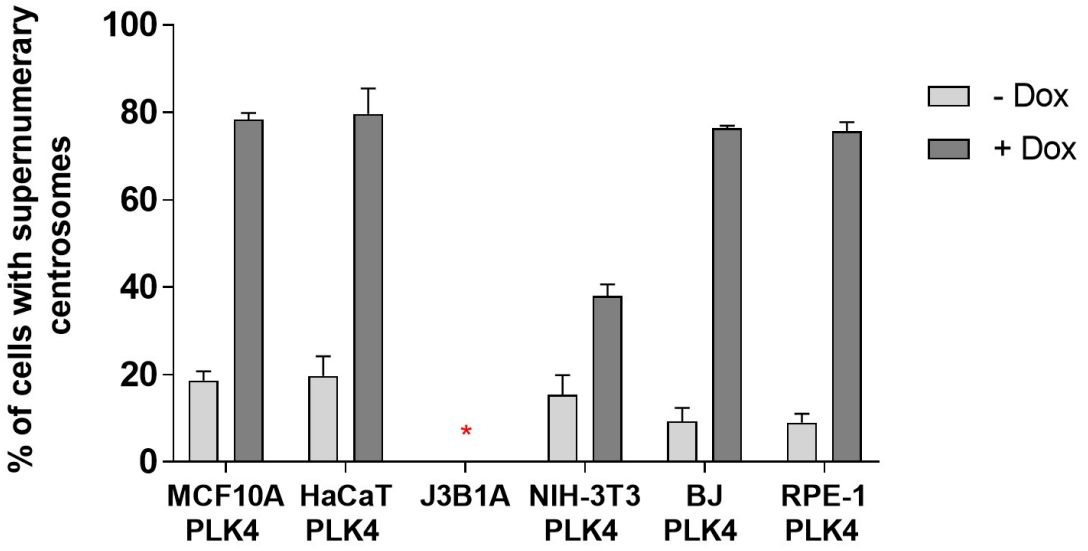

Figure 3.7: Centrosome amplification by PLK4 overexpression
Quantification of centrosome amplification in the panel of cells lines expressing TetR PLK4 with and without the addition of 2mg/ml doxycycline hyclate for 48 hours. Centrosome amplification is significantly increased upon PLK4 overexpression. Data are mean ± SD, n = 150 individual cells, 50 per experiment at metaphase. *J3B1A.TetR.PLK4 cells were not generated.

and those treated with Dox, this indicated that Dox does not affect centrosome number directly, and any increase observed with the PLK4 cell lines is due to PLK4 overexpression (Figure 3.9 A). Similarly, to determine if Dox affects, or could explain the variation between centrosome clustering observed with PLK4 overexpression compared to the other methods of inducing supernumerary centrosomes, MCF10A cells were treated with DCB to induce supernumerary centrosomes with and without Dox for 48 hours. No significant change in centrosome clustering at cytokinesis was observed, suggesting that Dox does not affect centrosome clustering, and therefore does not explain the discrepancies observed in centrosome clustering between PLK4 overexpression and the other methods for generating supernumerary centrosomes (Figure 3.9 B).

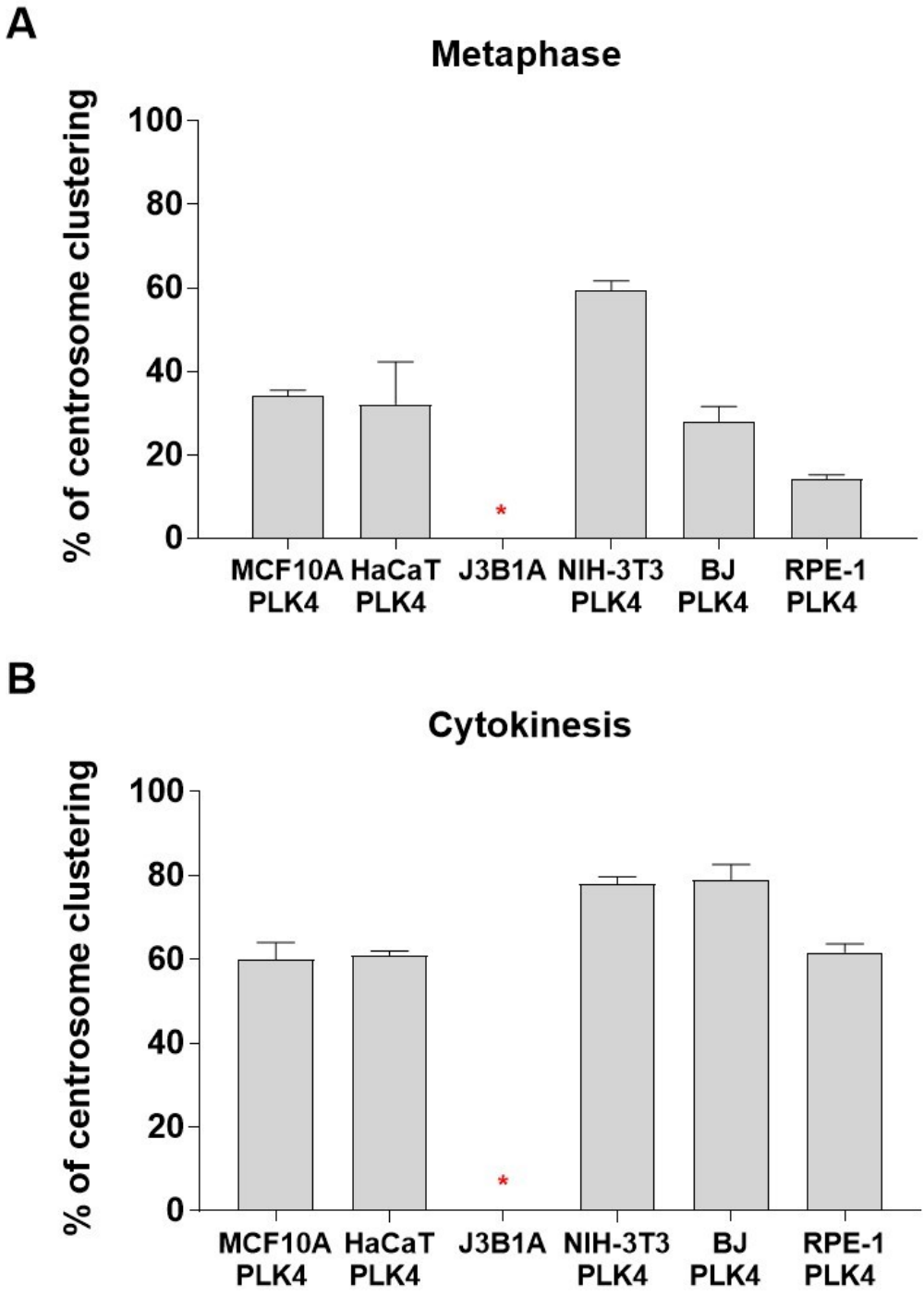

Figure 3.8: Centrosome clustering in cell lines where supernumerary centrosomes are generated by PLK4 overexpression
A Quantification of centrosome clustering in cell lines expressing TetR PLK4 with supernumerary centrosomes induced upon PLK4 overexpression after the addition of 2mg/ml doxycycline hyclate at metaphase. **B** Quantification of centrosome clustering at cytokinesis. Data are mean ± SD, n = 150 individual cells, 50 per experiment at cytokinesis.

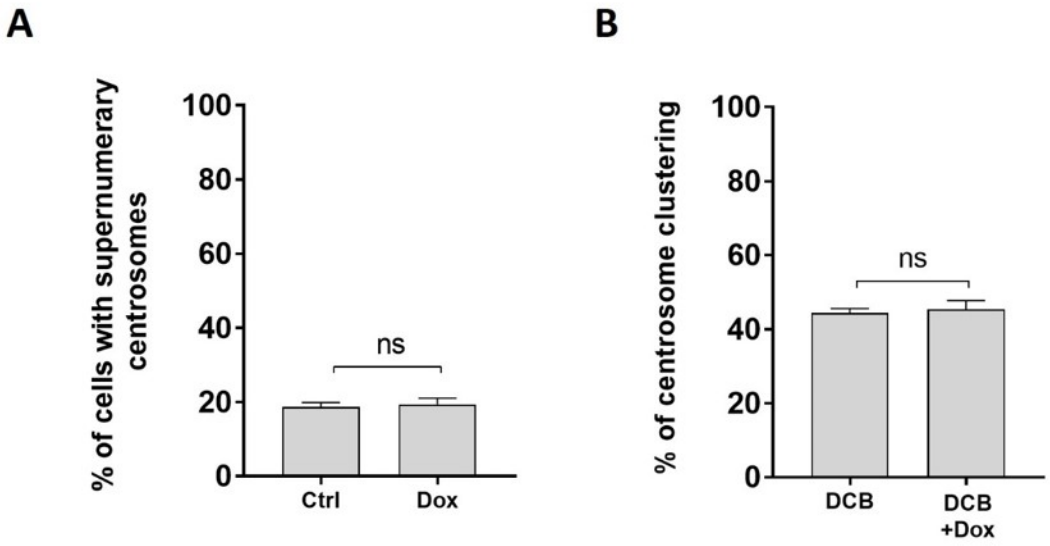

Figure 3.9: Doxycycline hyclate does not affect centrosome amplification or centrosome clustering

A Quantification of centrosome amplification in MCF10A with and without the addition of 2mg/ml doxycycline hyclate for 48 hours. No significant difference was observed in centrosome amplification with doxycycline hyclate. **B** Quantification of centrosome clustering in MCF10A cells with supernumerary centrosomes induced by DCB treatment, with and without the addition of 2mg/ml doxycycline hyclate. No significant difference in centrosome clustering was observed upon doxycycline hyclate treatment. Data are mean ± SD, n = 150 individual cells, 50 per experiment at cytokinesis. Data analysed using Student's t-test.

3.5.1 TetR affects centrosome clustering

To understand if PLK4 overexpression was influencing centrosome clustering or if it was the expression of the tetracycline repressor that was having an impact, MCF10A overexpressing TetR alone, or in combination with PLK4, in the absence of Dox, were treated with DCB to induce centrosome amplification. It was observed that TetR overexpression alone, or in combination with PLK4, increased clustering efficiency in tetraploid cells (Figure 3.10). These results suggest that the tetracycline repressor itself is having an effect on centrosome clustering, independently of PLK4 overexpression, although it is unclear why the tetracycline repressor is affecting clustering. Because of this effect the preferred method for most of the remaining experiments was DCB treatment.

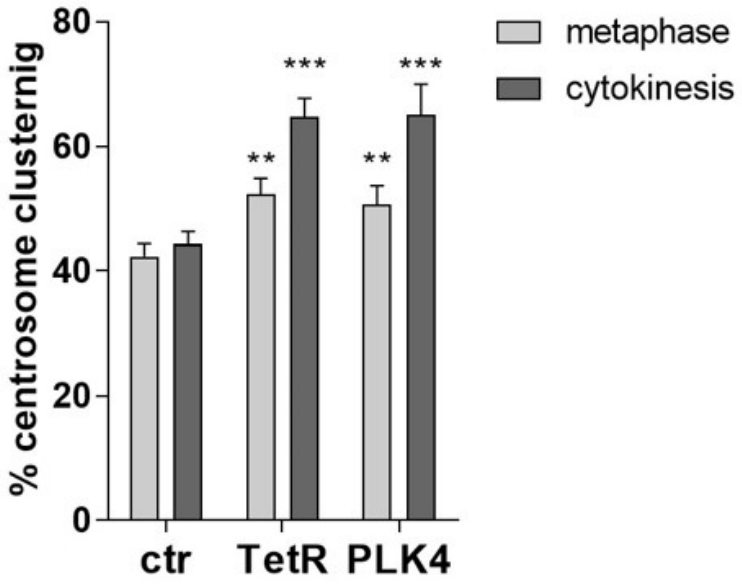

Figure 3.10: The tetracycline repressor affects centrosome clustering
Percentage of centrosome clustering at cytokinesis in MCF10A, MCF10A.TetR and MCF10A.TetR.PLK4 in cells with supernumerary centrosomes which were generated by DCB treatment. TetR expressing cells cluster more efficiently than control cells, suggesting that TetR is having an effect on centrosome clustering. Data are mean ± SD, n = 150 individual cells, 50 per experiment. Data analysed using two-way ANOVA with Šidák post hoc test, $^{**}p<0.01$, $^{***}p<0.001$.

3.6 Discussion

Previous work suggests that cells have intrinsic mechanisms that facilitate centrosome clustering, such as the spindle assembly checkpoint and the kinesin HSET, and thus are unlikely to require adaptation to centrosome amplification (*Reviewed in:* Godinho and Pellman, 2014). This was further supported by the fact that most cancer cell lines with extra centrosomes seem to be able to cluster centrosomes efficiently (Ring, Hubble and Kirschner, 1982; Quintyne *et al.*, 2005; Kwon *et al.*, 2008; Ganem, Godinho and Pellman, 2009). However, a systematic analysis of clustering efficiency in different cell types has never been performed.

Using three different and independent methods to generate supernumerary centrosomes in a panel of six non-cancerous cell lines, it was interesting to observe that not all cell lines had the same ability to efficiently cluster their supernumerary centrosomes by cytokinesis. Cytokinesis was found to be a more reliable stage to quantify centrosome clustering, as during metaphase cells may still be within a multipolar configuration, which may ultimately cluster before the end of cell division. These results were also confirmed by live cell imaging of tetraploid cells with supernumerary centrosomes, supporting that fixed cell analysis was a sufficient method for reliably analysing efficiency.

Interestingly, whilst PLK4 overexpression using a Tet-inducible system is widely used within the field to generate supernumerary centrosomes, it was observed that overexpression of the TetR alone or in combination with PLK4 increased clustering efficiency in epithelial cells upon DCB treatment suggesting that TetR overexpression is unexpectedly affecting this process. As a large amount of the research within the field is done with PLK4 overexpression to generate supernumerary centrosomes, the observation that the TetR may itself affect centrosome clustering efficiency may then skew reported results of centrosome clustering. The mechanism through which the TetR may be affecting centrosome clustering is unclear.

Because of the effect of the TetR on clustering efficiency, DCB treatment was used for the majority of the remaining experiments for generating supernumerary centrosomes. DCB results in cytokinesis failure through actin depolymerisation, with the resultant tetraploid cells containing supernumerary centrosomes. Tetraploidy is often reported in cancer, and may therefore be a mechanism for centrosome amplification. Therefore, DCB treatment could be a representative model of centrosome amplification within a tumour.

The observation that not all cell types have the same ability to cluster their supernumerary centrosomes raises the question that some cells might need to adapt for centrosome clustering. Potential adaptation mechanisms include increased time in mitosis or increased levels of the kinesin HSET allowing for centrosome clustering.

Chapter 4

Results II: Cell-cell adhesion in centrosome clustering

4.1 Time in metaphase does not increase centrosome clustering

The spindle assembly checkpoint has been shown to be important in centrosome clustering, allowing cells time to cluster their supernumerary centrosomes prior to anaphase onset (Basto *et al.*, 2008; Yang *et al.*, 2008). In support of this, cancer cells with supernumerary centrosomes have been shown to have an increase in mitotic index, the proportion of cells undergoing mitosis, which would suggest that cells with supernumerary centrosomes take longer to go through mitosis, potentially giving them time to cluster their centrosomes (Chan, 2011). To evaluate whether cells that do not efficiently cluster supernumerary centrosomes, if given more time in mitosis were then able to cluster more efficiently, MCF10A and HaCaT cells were treated with 10µM of the proteasome inhibitor MG132 to block cells in metaphase (Kwon *et al.*, 2008). After 4 hours, the inhibitor was washed out, and the cells were allowed to progress through mitosis for 1 hour (Figure 4.1 A). Under these conditions, no significant difference in centrosome clustering was observed either at metaphase or cytokinesis, suggesting that the low efficiency of centrosome clustering in the MCF10A and HaCaT cell lines is not due to an insufficient time in metaphase, and that there must be intrinsic differences that cannot be overcome by increasing time in mitosis (Figure 4.1 B).

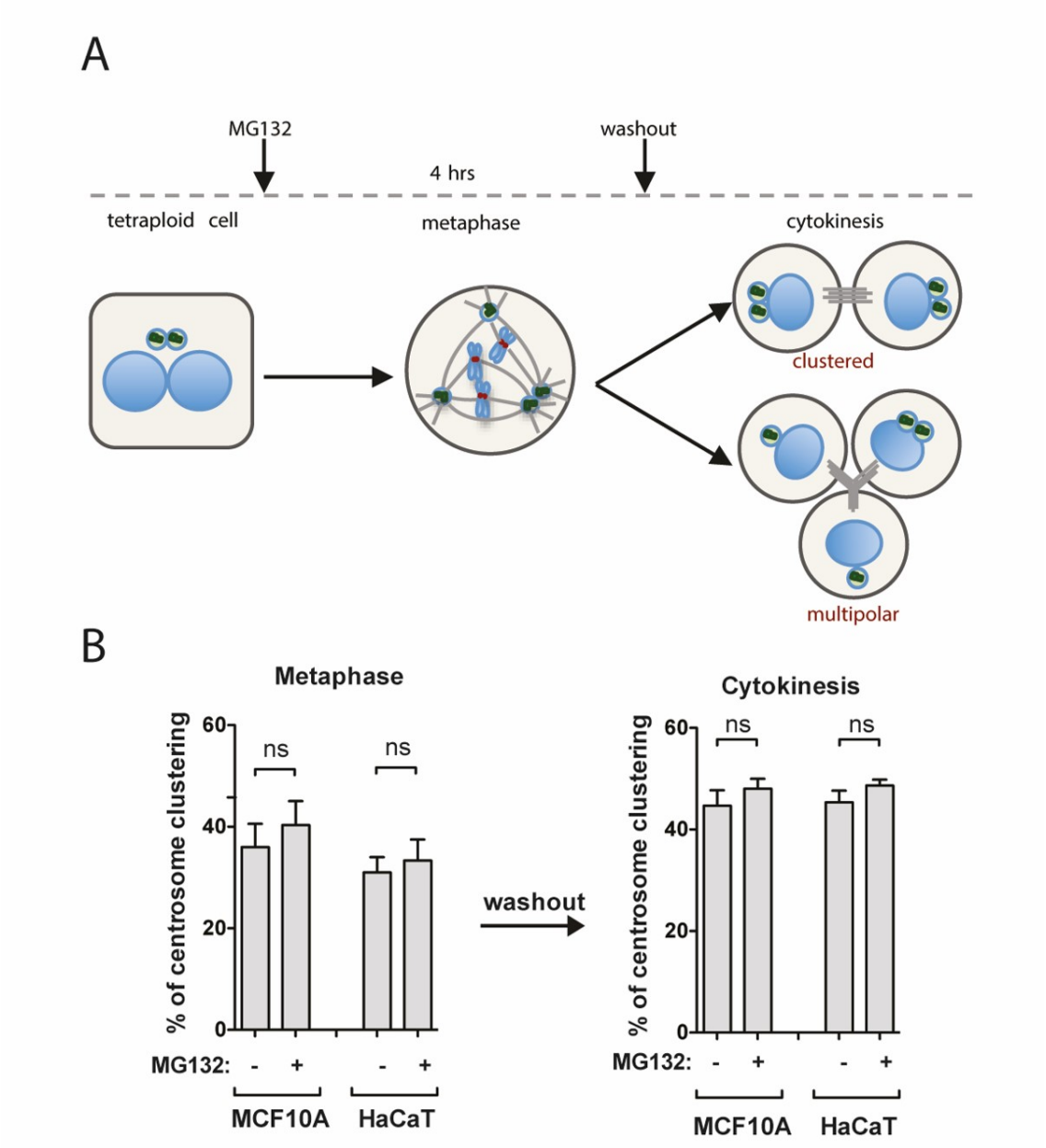

Figure 4.1: Time in mitosis does not affect centrosome clustering
A) Schematic of the treatment of MCF10A and HaCaT cells using 10µM of the proteasome inhibitor MG132 for 4 hours before washout and incubation at 37C for 1 hour. **B)** Quantification of MCF10A and HaCaT after MG132 treatment, showing no significant difference between vehicle and MG132 treated. Data are mean ± SD, n = 300 individual cells. Data analysed using two-way ANOVA with Šidák post-hoc test.

4.2 Levels of HSET do not correlate with centrosome clustering

The kinesin HSET (KIFC1) is well established as an essential factor in centrosome clustering (Basto *et al.*, 2008; Kwon *et al.*, 2008). To determine if there was a correlation between HSET levels and clustering efficiency, the protein levels of HSET were analysed using western blotting. HSET levels were consistent between the panel of cell lines, suggesting that the differences in efficiency of centrosome clustering are not due to HSET protein level variation (Figure 4.2).

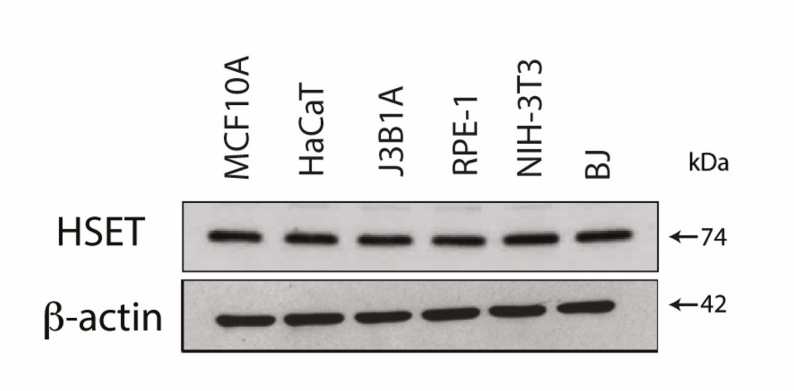

Figure 4.2: HSET presence does not independently allow for efficient centrosome clustering
Western blot analysis of HSET levels between the panel of 6 cell lines, showing little variation in HSET abundance between cell lines. β-actin was used as a loading control. Representative blot of 3 independent experiments.

4.3 Cells expressing E-cadherin have an impaired ability to cluster supernumerary centrosomes

The RPE-1, BJ and 3T3 cell lines cluster supernumerary centrosomes considerably more efficiently (~80% with DCB treatment) compared to the MCF10A, HaCaT and J3B1A cell lines (~40% with DCB treatment). In trying to account for this difference, it was noted that both the BJ and 3T3 cell lines were fibroblasts, and therefore do not express E-cadherin. Similarly, whilst the RPE-1 cell line was originally derived from epithelia, RPE-1 cells no longer express E-cadherin (Figure 4.3). This led to the hypothesis that E-cadherin expression may be impairing centrosome clustering.

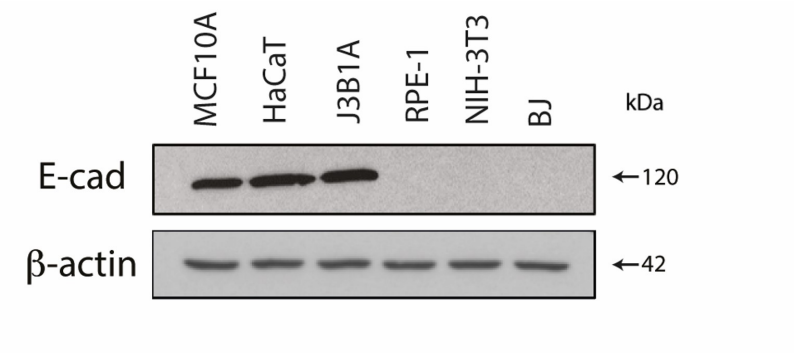

Figure 4.3: E-cadherin expression in the cell line panel
Western blot analysis of E-cadherin in the panel of 6 cell lines, showing that the epithelial cells MCF10A, HaCaT and J3B1A express E-cadherin, whereas the 2 fibroblast cell lines BJ and NIH-3T3 do not express E-cadherin. RPE-1 cells, whilst originally epithelial by origin, no longer express E-cadherin. β-actin was used as a loading control. Representative of 3 independent experiments.

4.3.1 siRNA knockdown of E-cadherin increases centrosome clustering

To test the hypothesis that E-cadherin impairs centrosome clustering, small interfering RNA (siRNA) was used to deplete E-cadherin protein levels. siRNA allows for the short term (2-4 days) silencing of a particular protein of interest. The synthetic double stranded RNA targets the mRNA of the protein of interest for degradation, resulting in a loss of protein translation. MCF10A and HaCaT cells were transfected either with siNegative, a non-targeting siRNA which controls for effects based on transfection (but is designed not to target any mRNA), or on-target SMARTpool for E-cadherin (gene name *CDH1*). The SMARTpool siRNAs are composed of 4 different siRNAs targeting the same gene, these sequences are designed to minimise off-target effects. In addition, the sequences were designed to target different regions within the gene transcript to maximise efficiency of protein knockdown. Cells were analysed 72 hours post transfection. Knockdown with the SMARTpool siRNA was highly efficient, as analysed by western blot (Figure 4.4 A). Centrosome clustering in MCF10A and HaCaT cells, where supernumerary centrosomes were induced by DCB treatment, increased with the knockdown of E-cadherin from ~40 to ~70% (Figure 4.4 B). This supported the hypothesis that E-cadherin impairs centrosome clustering.

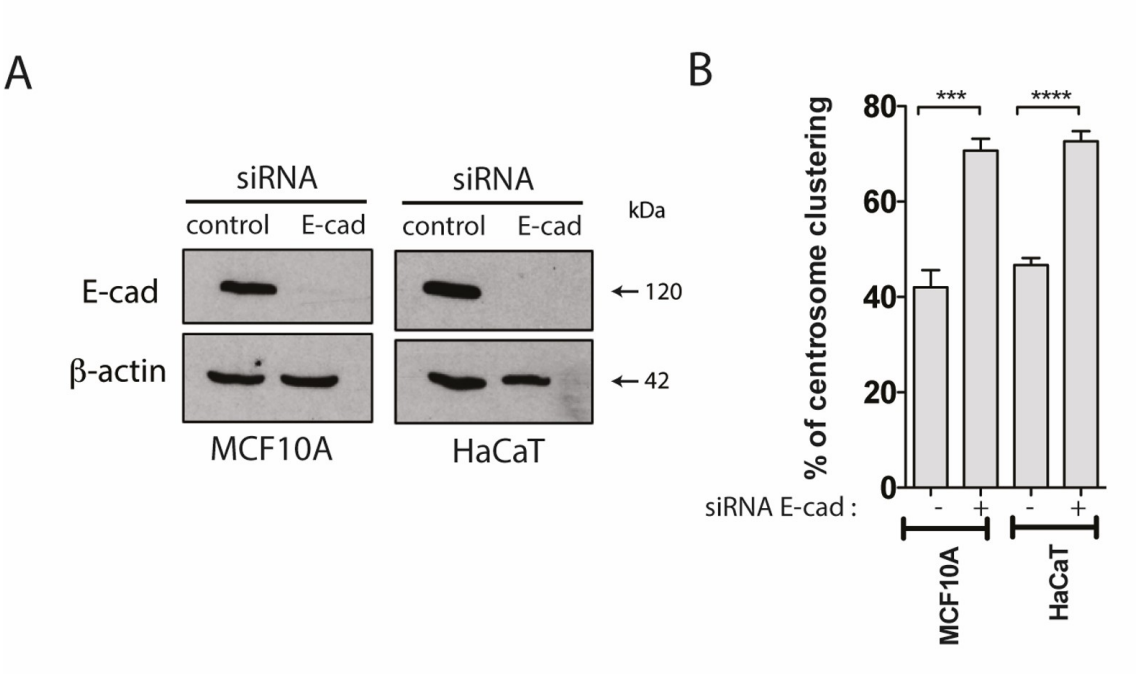

Figure 4.4: Knockdown of E-cadherin by siRNA increases centrosome clustering
A) Western blot analysis of E-cadherin in MCF10A and HaCaT cells treated with siNegative (control) and on-TARGET SMARTpool siRNA against E-cadherin (E-cad). Cells were analysed at 72 hours post transfection. β-actin was used as a loading control. Representative blot of 3 independent experiments. **B)** Centrosome clustering increases upon knockdown of E-cadherin by siRNA. Data are mean ± SD, n = 150 individual cells, 50 per experiment. Data analysed using two-way ANOVA with Šidák post-hoc test, *** $p<0.001$, **** $p<0.0001$.

4.3.2 shRNA silencing of E-cadherin increases centrosome clustering

In order to be able to examine the role of E-cadherin silencing for periods longer than 72 hours, short hairpin RNA (shRNA) was used. shRNA differs from siRNA in that instead of the RNA being directly transfected into the cells, they are encoded in a DNA vector which is transfected via plasmid or viral transduction, enabling them to silence proteins for the longer time period. Once inside the cell, the shRNA is transcribed under the control of an RNA polymerase. The shRNA transcript consists of a stem-loop structure, this is then transcribed in the nucleus and enters the RNA interference (RNAi) pathway resulting in reduction in the translation of the protein of interest. MCF10A.TetR.PLK4 cells expressing four different shRNA against E-cadherin were generated by lentiviral transduction and selected using 10µg/ml puromycin. To examine the silencing efficiency of the different shRNA, protein levels

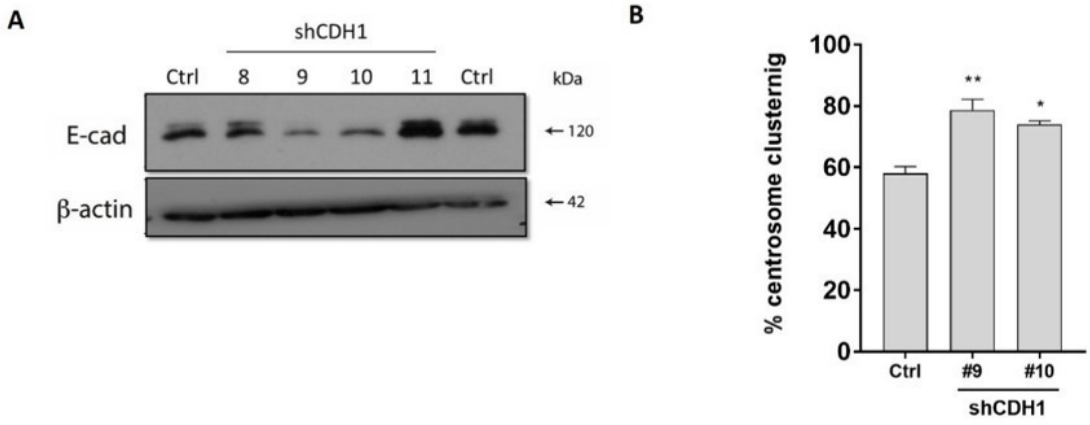

Figure 4.5: shRNA silencing of E-cadherin increases centrosome clustering
A) Western blot analysis of E-cadherin levels in MCF10A TetR PLK4 with 4 different shRNA against CDH1. Silencing was most efficient with shRNAs 9 and 10, whereas sequences 8 and 11 did not alter E-cadherin protein levels. β-actin was used as a loading control. Representative blot of 3 independent experiments **B)** Centrosome clustering increases upon silencing of E-cadherin by shRNA. Data are mean ± SD, n = 150 quantified at cytokinesis. Data analysed using one-way ANOVA with Tukey post-hoc test, * $p<0.05$, ** $p<0.01$.

were analysed by western blotting (Figure 4.5 A). Sequences 9 and 10 were the most efficient at silencing E-cadherin, whereas sequences 8 and 11 did not affect E-cadherin levels. Therefore, shRNA number 9 and 10 were used for the remaining analysis. Although TetR.PLK4 cells have already improved clustering efficiency due to the TetR expression (see Section 3.5.1), it was still possible to observe that when E-cadherin was silenced by shRNA, centrosome clustering increased by ~20% (Figure 4.5 B). This supports the data observed with siRNA that loss of E-cadherin can improve centrosome clustering in epithelial cells.

4.3.3 CRISPR-Cas9 knockout of E-cadherin increases centrosome clustering

To further evaluate the role of E-cadherin in impairing efficient clustering, knockout of E-cadherin by CRISPR-Cas9 technology was performed.

To maximise the effect of each CRISPR-Cas9 reaction, all sequences were designed to target within the first exon of E-cadherin. This ensures that if a truncation occurs, that the protein expressed should have the least likelihood of being active. Lentiviral vectors were generated as described in Section 2.3.5. To further increase

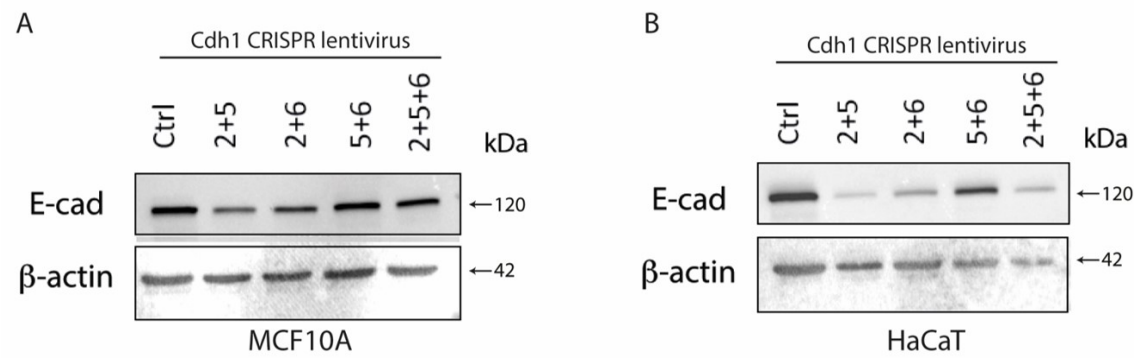

Figure 4.6: CRISPR-Cas9 efficiency in MCF10A and HaCaT
Western blots of CRISPR-Ca9 efficiency in **A)** MCF10A and **B)** HaCaT cell lines co-infected with multiple guide RNAs against E-cadherin. In both cell lines gRNAs 2 and 5 when co-infected had the greatest loss of E-cadherin in the mixed populations, suggesting the greatest percentage of knockout. β-actin was used as a loading control.

the likelihood of successful gene knockout, multiple lentiviruses using two or more gRNA were co-infected into the MCF10A and HaCaT cell lines. After two weeks of selection using 1-5µg/ml puromycin, E-cadherin levels in the mixed cell populations were analysed by western blot analysis (Figure 4.6). In both the MCF10A and HaCaT cell lines, co-infection with lentivirus with gRNA sequences 2 and 5 showed the lowest levels of E-cadherin, suggesting the highest percentage of gene knockout occurred in these populations.

Having identified the polyclonal populations with the highest levels of E-cadherin knockout, these cell lines were then used for clonal selection. 100 cells were plated in a 15cm dish and incubated for 10 days to allow colonies to form from single cells. Colonies were then selected using a clonal selection column and trypsinisation. The individual colonies were then amplified, and once expanded to a large enough population, the protein expression of E-cadherin was analysed. For both the MCF10A and HaCaT cell lines, multiple clones of E-cadherin knockout were identified (Figure 4.7 A and C). In both cell lines, where supernumerary centrosomes were generated by DCB treatment, loss of E-cadherin resulted in increased centrosome clustering, whereas the control clones where the gene knockout was unsuccessful had no significant effect on centrosome clustering (Figure 4.7 B and D). Therefore, supporting the results observed with both siRNA and shRNA.

To mitigate any effect due to clonality of the knockout cell lines, an equal mix of the knockout clones were made for both the MCF10A and HaCaT, generating a polyclonal population of E-cadherin cell lines, referred to as MCF10A *CDH1-/-* and HaCaT *CDH1-/-* respectively. E-cadherin knockout in the polyclonal populations was re-confirmed by both western blot and 2D immunofluorescence microscopy (Figure

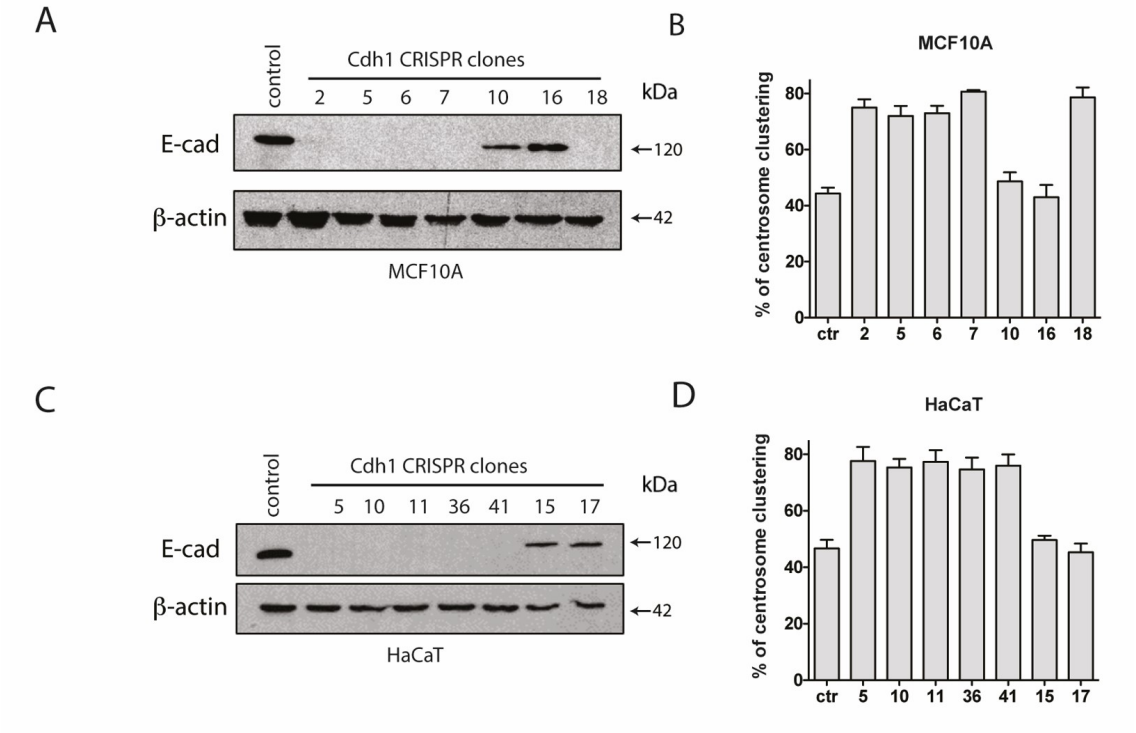

Figure 4.7: Loss of E-cadherin in clonal populations increases centrosome clustering
Western blot analysis of MCF10A and HaCaT cell lines showing E-cadherin levels in individual clonal populations (**A** and **C**) where β-actin is used as a loading control. Representative blot of 3 independent experiments. Centrosome clustering increases in the clones where E-cadherin has been successfully knocked out, but remains unchanged in the control clones (**B** and **D**). Supernumerary centrosomes were generated by DCB treatment. Data are mean ± SD, n = 150 individual cells, 50 per experiment, quantified at cytokinesis.

4.8 A and B) These polyclonal populations of *CDH1-/-* cells were able to cluster their supernumerary centrosomes significantly more efficiently than control E-cadherin expressing cells from ~40 to ~80% (Figure 4.8 C).

As well as examining the effect of loss of E-cadherin on non-cancerous cell lines, comparison of the A431 human epidermoid carcinoma cell lines was also performed. A431 *CDH1-/-* cells were generated by Takuya Kato in the lab of Erik Sahai at the Francis Crick Institute. A431 normally express E-cadherin, and have a ~15% population of cells containing supernumerary centrosomes (Supplementary Table 7.1). After treatment with DCB, A431 cells behave similarly to other epithelial cell lines, with only ~30% of cells clustering at cytokinesis (Figure 4.9 C). Upon loss of E-cadherin by CRISPR-Cas9, as confirmed by western blot analysis and 2D immunofluorescence microscopy (Figure 4.9 A and B), ~55% of A431 *CDH1-/-* cells can cluster their supernumerary centrosomes at cytokinesis (Figure 4.9 C). No

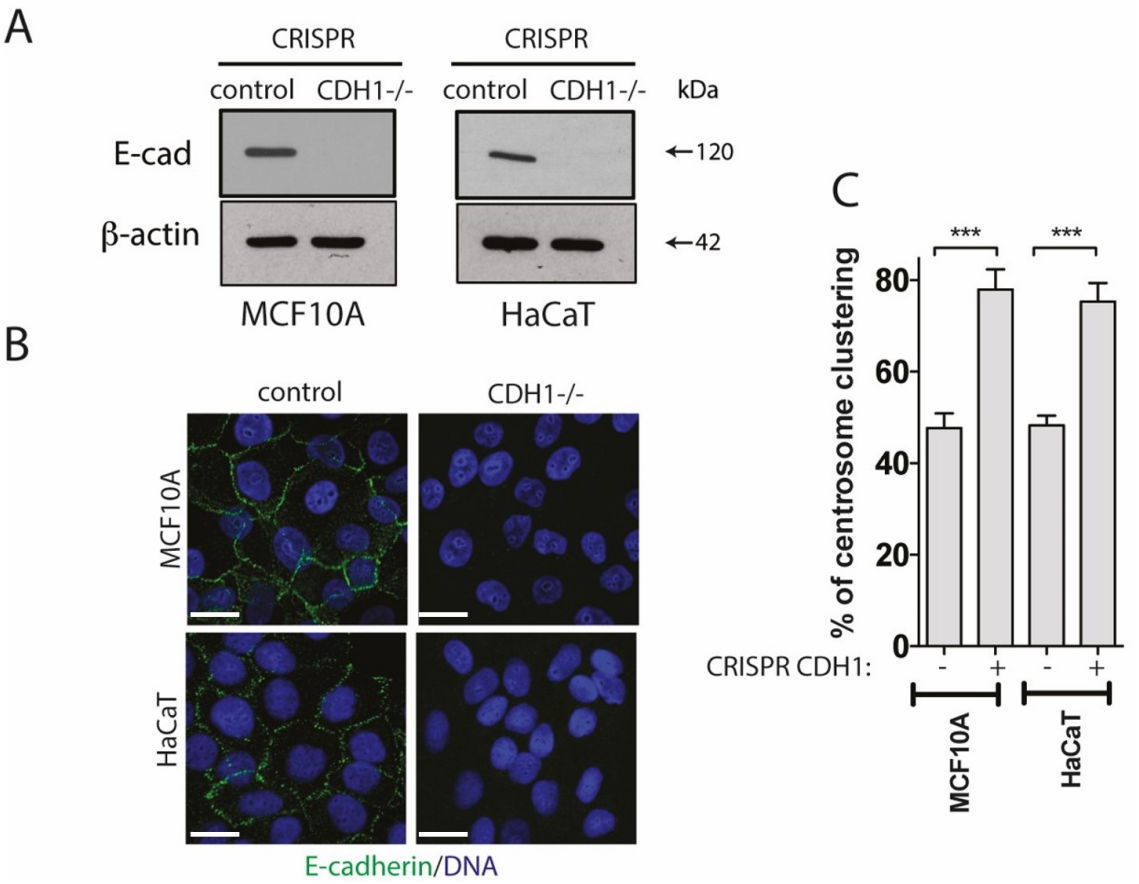

Figure 4.8: Gene knockout of E-cadherin increases centrosome clustering **A)** Western blot analysis of E-cadherin levels after an equal combination of E-cadherin knockout clones were mixed for the MCF10A and HaCaT cell lines, generating polyclonal populations. **B)** 2D immunofluorescence microscopy images of both WT and *CDH1-/-* MCF10A and HaCaT cell lines, confirming E-cadherin loss. **C)** Centrosome clustering increases with loss of E-cadherin in cells where supernumerary centrosomes are generated by DCB. Data are mean ± SD, n = 150 individual cells, 50 per experiment, quantified at cytokinesis. Data analysed using a two-way ANOVA with Šidák post-hoc test, *** $p<0.001$. Scale bar = 10µM.

significant difference was observed at metaphase, supporting the previous results, that metaphase is not an adequate measure of clustering efficiency (Figure 4.9 C). In turn, this supports the conclusion that in cancer cells, as well as in non-cancer cell lines, loss of E-cadherin is sufficient to improve centrosome clustering efficiency.

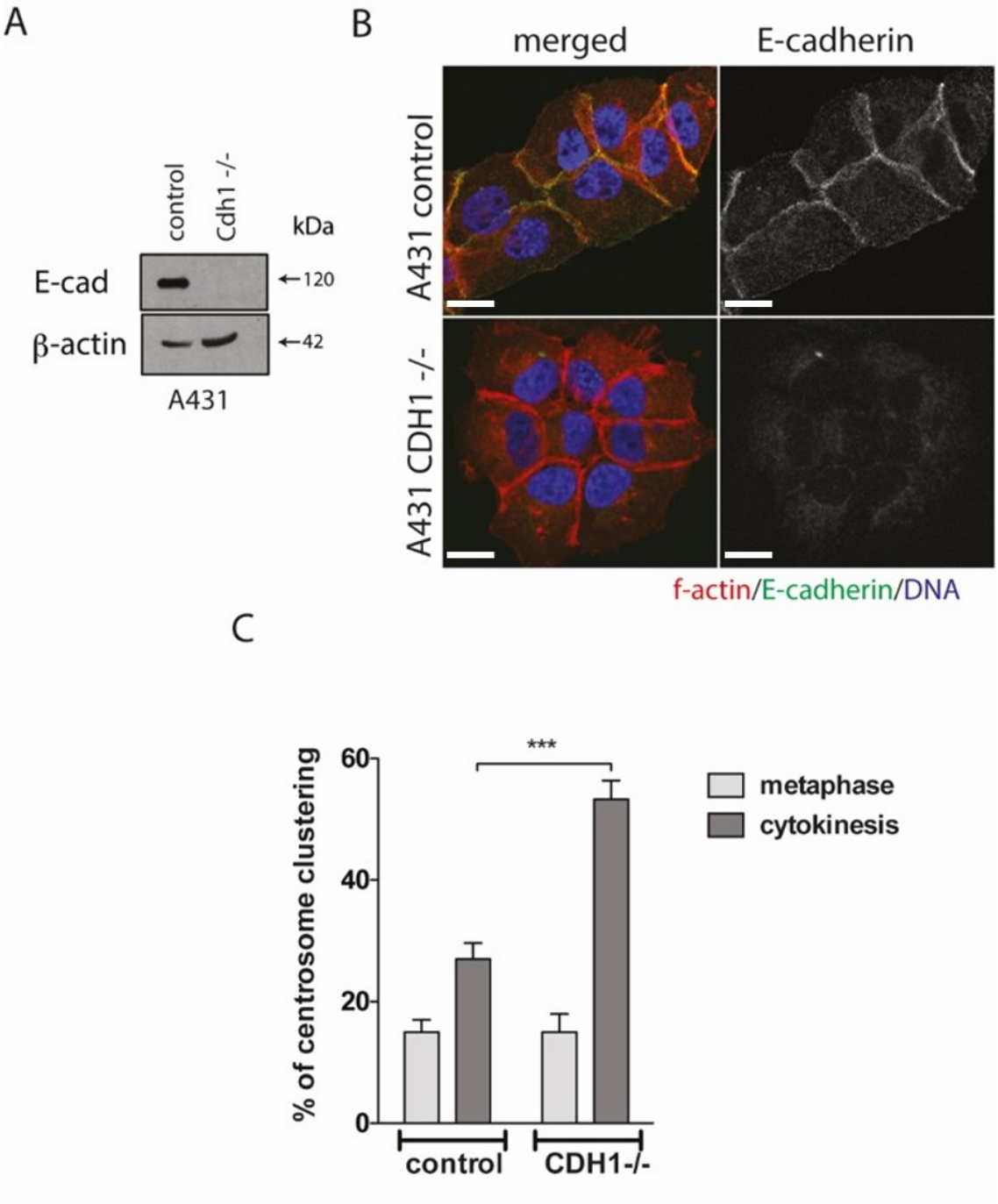

Figure 4.9: Loss of E-cadherin in A431 human epidermoid carcinoma cells increases centrosome clustering
A) Western blot analysis in the A431 human epidermoid carcinoma cell line, and A431 *CDH1-/-* given by Erik Sahai. **B)** 2D Immunofluorescence images of A431 and A431 *CDH1-/-* confirming loss of E-cadherin. **C)** Centrosome clustering increases with loss of E-cadherin in cells where supernumerary centrosomes are generated by DCB, quantified at cytokinesis. No significant change was observed at metaphase. Data are mean ± SD, n = 150 individual cells, 50 per experiment. Data analysed using two-way ANOVA with Šidák post-hoc test. ***p<0.001. Scale bar = 10µM.

4.3.4 Expressing E-cadherin in RPE-1 impairs centrosome clustering

To explore if expression of E-cadherin affects centrosome clustering in a cell line that does not normally express it, RPE-1 cells that expressed full length E-cadherin were generated. To control for a lentiviral infection RPE-1 cells expressing a truncated form that only contained the intracellular domains (E-cadDN) were also generated. Western blot analysis was performed confirming both E-cadherin and E-cadDN protein expression at the correct sizes 120 and ~50kDa respectively (Figure 4.10 A). 2D immunofluorescence microscopy was used to determine that the localisation of the two constructs was correct, with the full-length E-cadherin being membrane bound, whereas the truncated form localised to the cytoplasm (Figure 4.10 B). RPE-1 cells in which supernumerary centrosomes are induced by DCB treatment cluster supernumerary centrosomes efficiently (~90%), however after expressing full length E-cadherin, centrosome clustering was impaired to a level that is comparable to the centrosome clustering efficiency in the MCF10A, HaCaT and J3B1A epithelial cell lines at ~40% (Figure 4.10 C). Expression of the truncated E-cadDN had no significant effect on centrosome clustering (Figure 4.10 C). These data further support the hypothesis that E-cadherin loss is both required and sufficient to enable efficient clustering supernumerary centrosomes in epithelial cells.

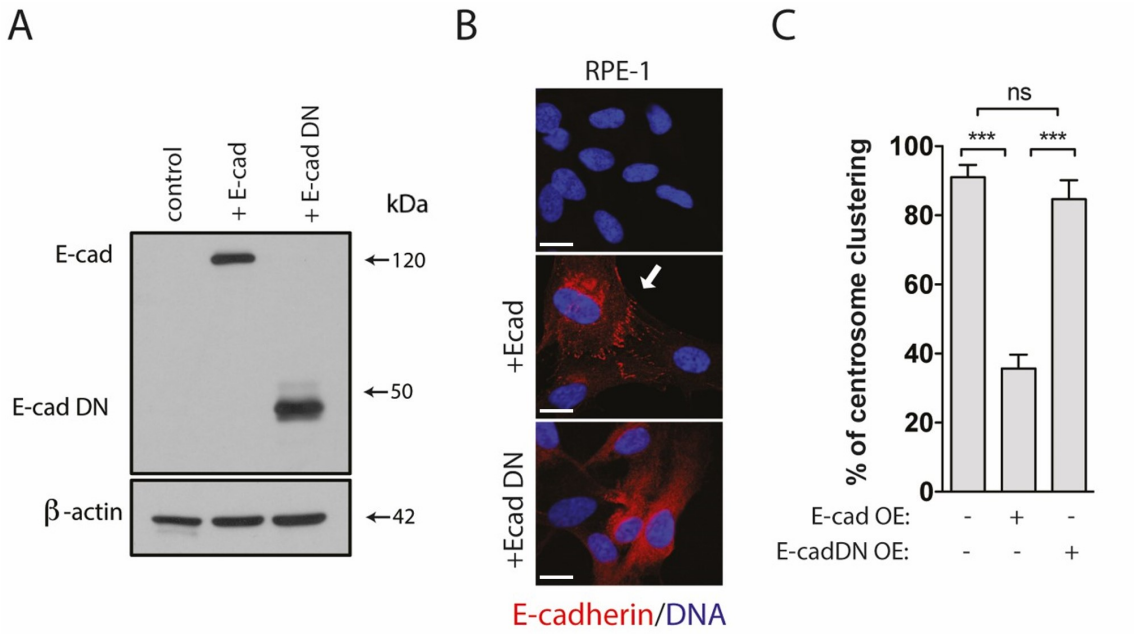

Figure 4.10: Expression of full length E-cadherin in RPE-1 cells impairs centrosome clustering

A) Western blot analysis of E-cadherin protein levels in RPE-1 control cells, RPE-1 cells expressing full length E-cadherin (+E-cad), and a truncated form of E-cadherin which only contains the intracellular domain (+E-cad DN). **B)** 2D immunofluorescence microscopy images to show localisation of E-cadherin in RPE-1 cells, and the full and truncated forms of E-cadherin. Scale bar = 10µM. **C)** Centrosome clustering decreases with full length expression of E-cadherin in cells where supernumerary centrosomes are generated by DCB. No significant effect on centrosome clustering was observed with the truncated form of E-cadherin. Data are mean ± SD, n = 150 individual cells, 50 per experiment, at cytokinesis. Data analysed using one-way ANOVA with Tukey post-hoc test. *** $p<0.001$.

4.4 Change in centrosome clustering is not due to epithelial to mesenchymal transition

Loss of E-cadherin is associated with epithelial to mesenchymal transition (EMT). However, previous work by Chen *et al.* has stated that loss of E-cadherin in MCF10A is not sufficient to drive this transition (Chen *et al.*, 2014). To test if EMT had occurred in the *CDH1-/-* cell lines, N-cadherin and vimentin protein levels were analysed. If EMT had occurred N-cadherin and vimentin levels would increase. In both the MCF10A *CDH1-/-* and HaCaT *CDH1-/-* cell lines, no increase in N-cadherin or vimentin levels were observed, suggesting that EMT had not occurred (Figure 4.11). Therefore, changes in centrosome clustering are not due to effects of EMT, but rather the loss of E-cadherin itself.

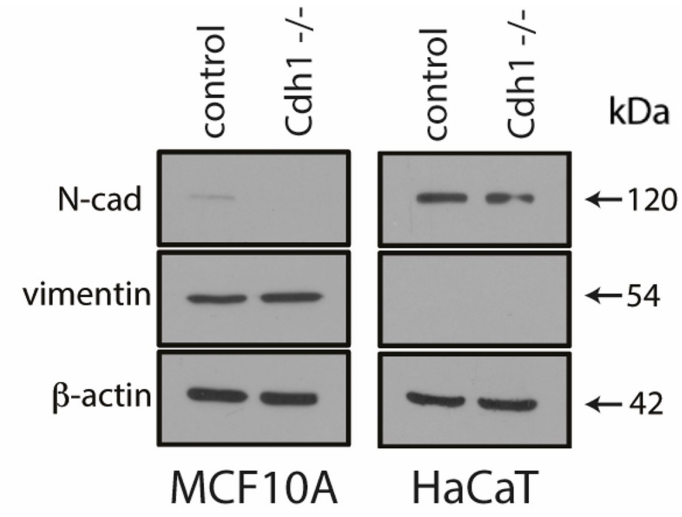

Figure 4.11: Knockout of E-cadherin in MCF10A and HaCaT cell lines is not sufficient to drive epithelial to mesenchymal transition
Western blot analysis of the protein level of two EMT markers – N-cadherin (N-cad) and vimentin in MCF10A and HaCaT cell lines. No change in protein expression is observed after knockout of E-cadherin, suggesting EMT has not occurred. β-actin was used as a loading control.

4.5 Change in centrosome clustering is not due to centrosome inactivation

The efficiency of different cells to divide in a bipolar fashion with supernumerary centrosomes has previously been observed in *Drosophila* (Sabino *et al.*, 2015). Neuroblasts were observed to undergo bipolar divisions compared to epithelial cells within the developing wing disks when centrosome amplification was generated by SAK/PLK4 overexpression (Basto *et al.*, 2008; Sabino *et al.*, 2015). These increases in bipolar divisions were not due to increased centrosome clustering, but due to centrosome inactivation which is characterised by low centrosomal levels of γ-tubulin and pericentrin, see Section 1.2.4 (Basto *et al.*, 2008; Sabino *et al.*, 2015). Sabino *et al.* reported that overexpression of moesin, the sole member of the conserved ezrin-radixin-moesin (ERM) family of proteins found in *Drosophila*, compromised centrosome inactivation within the wing disks, resulting in increased multipolar cell divisions (Sabino *et al.*, 2015). To confirm that centrosome inactivation was not occurring in the cell lines observed centrosomal localisation of γ-tubulin and pericentrin was analysed (Figure 4.12 A and B). No evidence of centrosome inactivation was observed, all extra centrosomes in both multipolar and clustered spindles showed similar levels of both γ-tubulin and pericentrin (Figure 4.12 A and B). In addition, no change was observed in the levels of ERM proteins in the epithelial cells with and without E-cadherin (Figure 4.12 C).

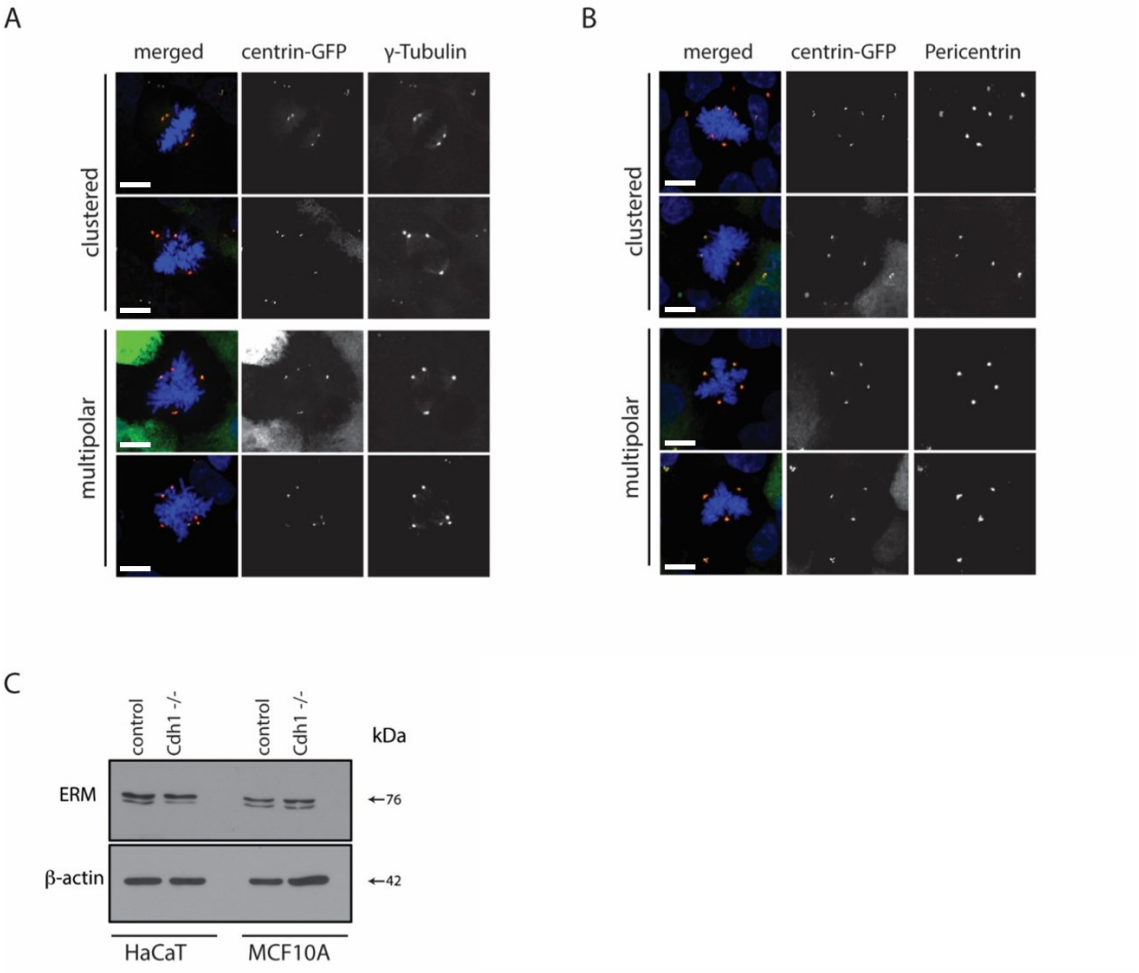

Figure 4.12: E-cadherin loss does not lead to centrosome inactivation **A** and **B)** Representative 2D immunofluorescence microscopy images of MCF10A.*CDH1-/-*.centrin-GFP cell lines, co-stained with γ-tubulin (A) and pericentrin (B). All supernumerary centrosomes showed similar levels of γ-tubulin and pericentrin, suggesting that centrosome inactivation does not occur within these cells. 150 individual cells were analysed for each condition. Scale bar = 10μM. **C)** Western blot analysis of ERM levels in MCF10A and HaCaT cell lines with and without E-cadherin. No change in ERM protein level was observed. β-actin was used as a loading control. Representative image of 3 independent experiments.

4.6 Loss of E-cadherin leads to increased cell viability in the presence of supernumerary centrosomes

To determine if the increase in centrosome clustering as a result of loss of E-cadherin provided a survival benefit in the presence of supernumerary centrosomes cell viability assays were carried out.

4.6.1 Colony formation assay

Colony formation assays were used for MCF10A.TetR.PLK4 cells expressing shCDH1, as described in Section 2.6. Supernumerary centrosomes were induced by PLK4 overexpression, by the addition of Dox for 48 hours; after which 100 cells were plated per 6cm dish and incubated for 7 days. Colonies were fixed and stained using crystal violet, images were taken and the number of colonies was counted and analysed. Alongside this, to control for colony size, colonies were dissolved in 0.05% v/v Triton-X 100 in PBS overnight and absorbance read on a plate photospectrometer at 560nm and 405nm and normalised to the control for each cell line where Dox had not been added. Both colony number, and absorbance methods gave similar results (Figure 4.13). For MCF10A.TetR.PLK4 cells expressing E-cadherin, addition of doxycycline and the resultant centrosome amplification resulted in a loss of ~40% viability (Figure 4.13). Cells expressing shCDH1 #9, which had the lowest protein expression of E-cadherin, had no significant difference between the control cells, and those containing supernumerary centrosomes, and the shCDH1 #10 expressing cells had a loss of ~20% viability compared to controls (Figure 4.13). Therefore, loss of E-cadherin and the subsequent increase in centrosome clustering, enables cells to survive better in the presence of supernumerary centrosomes.

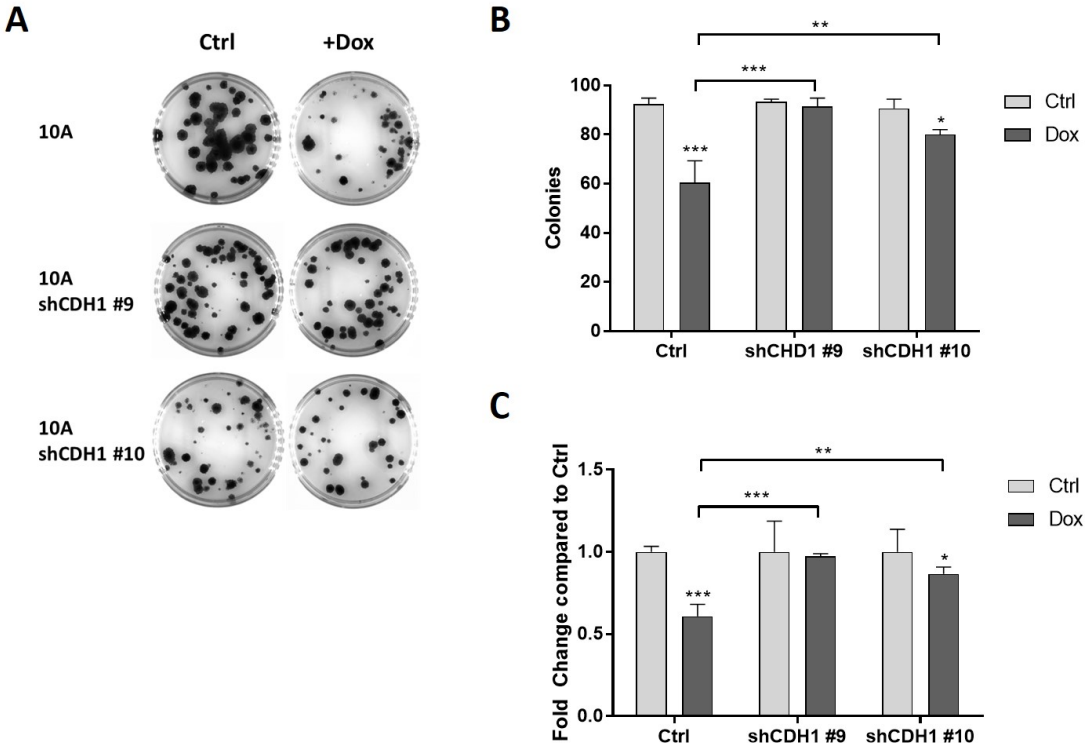

Figure 4.13: Knockdown of E-cadherin by shRNA increases cell viability in MCF10A.TetR.PLK4 cells with supernumerary centrosomes
A) Representative images of 3 independent experiments (3 plates per condition, per experiment) of MCF10A TetR PLK4, and shCDH1 treated colonies where supernumerary centrosomes were induced by the addition of doxycycline (+Dox). Cells were incubated for 7 days to allow for colony growth. **B)** Quantification of number of colonies after 7 days incubation. **C)** Quantification after colonies were dissolved in 0.05% Triton-X 100 in PBS overnight. Knockdown of E-cadherin increases colony number in the presence of supernumerary centrosomes. Absorbance was measured at 560nm and a background absorbance of 405nm was deducted. Data was normalised to the control for cell line. Data are mean ± SD, n = 3. Data analysed using two-way ANOVA with Šidák post-hoc test. * p<0.05, ** p <0.01, *** p<0.001.

4.6.2 IncuCyte

To investigate cell viability in the E-cadherin CRISPR knockout cells, the IncuCyte system was used. The IncuCyte is a live cell imaging system built within a cell culture incubator, allowing for long term live cell imaging. By generating cells expressing histone H2B-GFP which enables the tracking of DNA, a mask could be applied to accurately count cell number. This system meant that DCB treatment could not be used, as the resultant tetraploid cells would show two nuclei per cell, giving incorrect measurements of cell number. Therefore *CDH1-/-* cells expressing TetR.PLK4.H2B-GFP were generated. To quantify if the E-cadherin knockout cell lines clustered efficiently upon PLK4 overexpression and with H2B-GFP expression, centrosome clustering was analysed. Both the MCF10A and HaCaT cell lines had ~80% of their cells containing supernumerary centrosomes after PLK4 overexpression (+Dox) (Figure 4.14 A). The *CDH1-/-* cells could cluster these supernumerary centrosomes more efficiently at both metaphase and cytokinesis (Figure 4.14 B), supporting the previous data shown using DCB treatment in the CDH1 -/- cell lines.

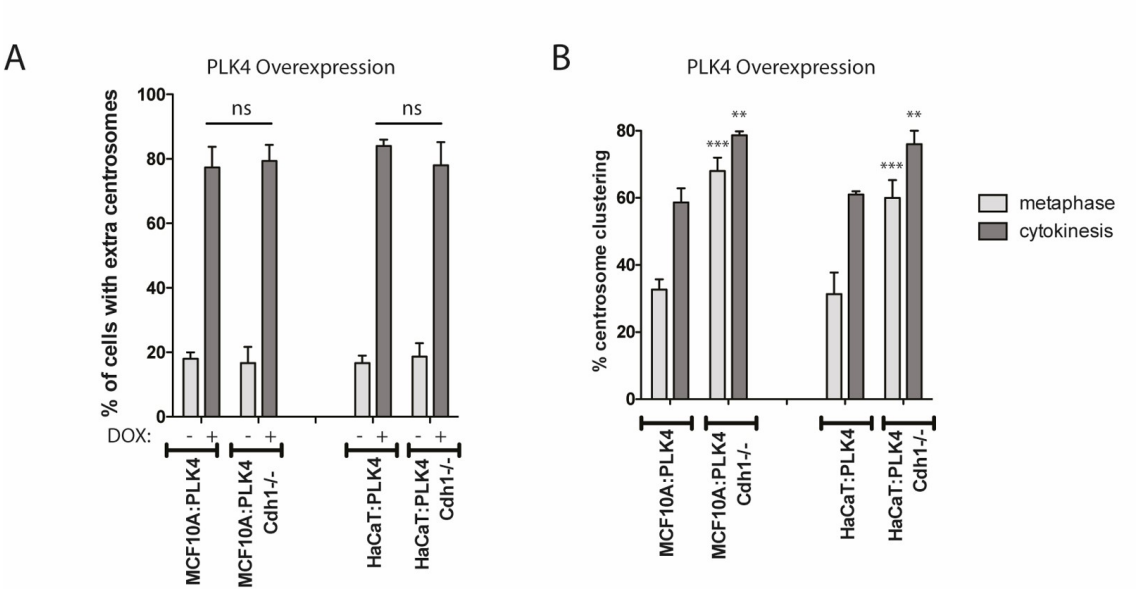

Figure 4.14: Generation of cell lines for IncuCyte viability
A) MCF10A and HaCaT cell lines expressing TetR PLK4 H2B-GFP had ~80% of their cells containing supernumerary centrosomes after induction of PLK4 overexpression by doxycycline. **B)** Centrosome clustering was more efficient in the *CDH1-/-* cells at both metaphase and cytokinesis. Data are mean ± SD, n = 150. Data analysed using two-way ANOVA with Šidák post-hoc test compared to WT cells ** $p<0.01$, *** $p<0.001$.

After 48 hours of PLK4 overexpression, cells were plated in 12 well plates and placed into the IncuCyte. Images were recorded every hour at 4 locations per well. After 7 days, the images were analysed using the IncuCyte software. Masks were created for each experiment using the "top-hat" mask, ensuring that the thresholds were appropriate for the H2B-GFP to be identified, and that no background was included within the cell count (Figure 4.15).

Cell counts were then calculated using the mask, with an average of the four images per well being used to generate an average cell count for each condition. In both the MCF10A and HaCaT samples there was significantly impaired cell growth between the control cells (-Dox), and those with supernumerary centrosomes (+Dox) (Figure 4.16). In the E-cadherin knockout cells, there was a smaller reduction in cell viability between the cells with and without supernumerary centrosomes (Figure 4.16). Suggesting that loss of E-cadherin enables cells to survive in the presence of extra centrosomes.

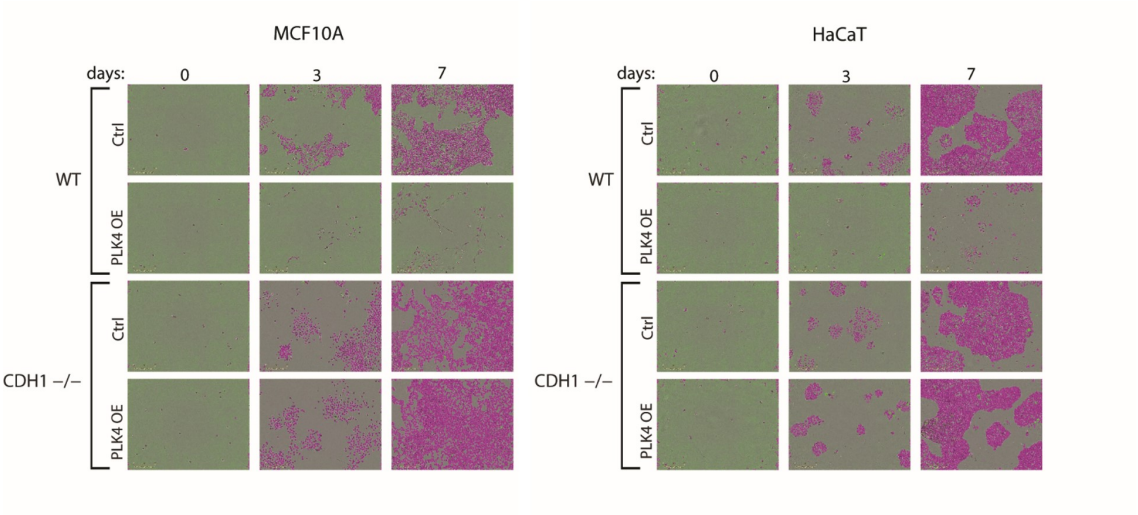

Figure 4.15: IncuCyte masks for H2B-GFP
Cell counts were calculated based on masks for individual H2B-GFP labelled nuclei within the cells. These were re-calculated for each experiment and thresholds set to ensure each nuclei was included with no background. These are representative images of 3 independent experiments for the MCF10 and HaCaT cells expressing TetR.PLK4.H2B-GFP with and without doxycycline overexpression. Control = -Dox, PLK4 OE = +Dox. Purple represents masked H2B-GFP.

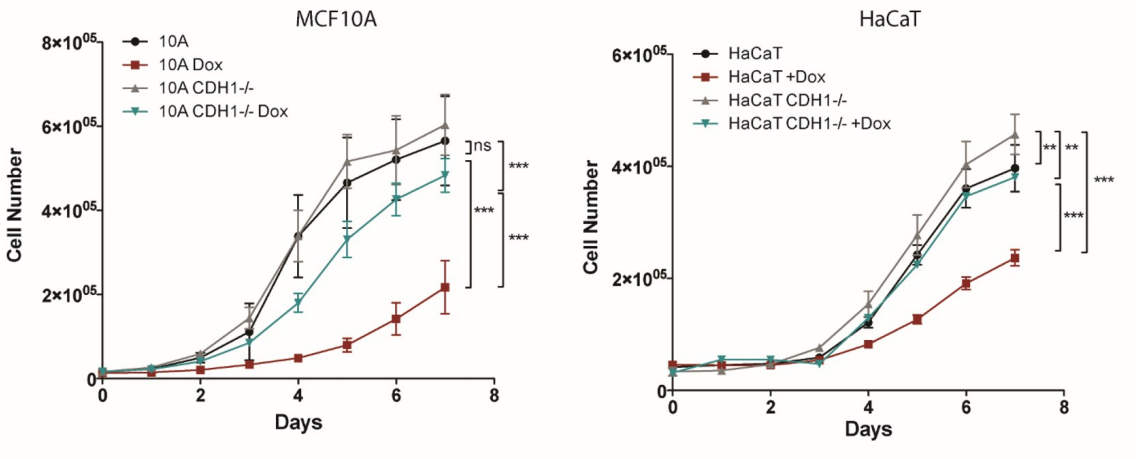

Figure 4.16: E-cadherin knockout increases cell viability in the presence of supernumerary centrosomes
Analysis of survival curves in control and *CDH1-/-* cells upon induction of centrosome amplification. Data are mean ± SD of repeated measurements, n = 3. Data analysed using two-way ANOVA with Šidák post-hoc test based on area under the curve. ** p $p<0.01$, *** $p<0.001$.

4.7 DDR1 localises to adherens junctions

E-cadherin has previously been shown to play a role in inhibiting cortical contractility at the adherens junctions. Research by Hidalgo-Carcedo *et al.* in interphase cells showed that E-cadherin can recruit DDR1 to the adherens junctions, through a not fully elucidated mechanism (Hidalgo-Carcedo *et al.*, 2011). They reported that DDR1 through Par3 and Par6 controls the localisation of RhoE to cell-cell contacts, where it antagonises ROCK-driven actomyosin contractility. Cortical contractility had previously been shown to play a role in centrosome clustering (Kwon *et al.*, 2008). It was hypothesised that the low levels of clustering efficiency in epithelial cells may result from the lower levels of contractility. To test if E-cadherin's recruitment of DDR1 was preventing efficient clustering of supernumerary centrosomes, DDR1 localisation at cell-cell contacts was first confirmed using 2D immunofluorescence microscopy (Figure 4.17).

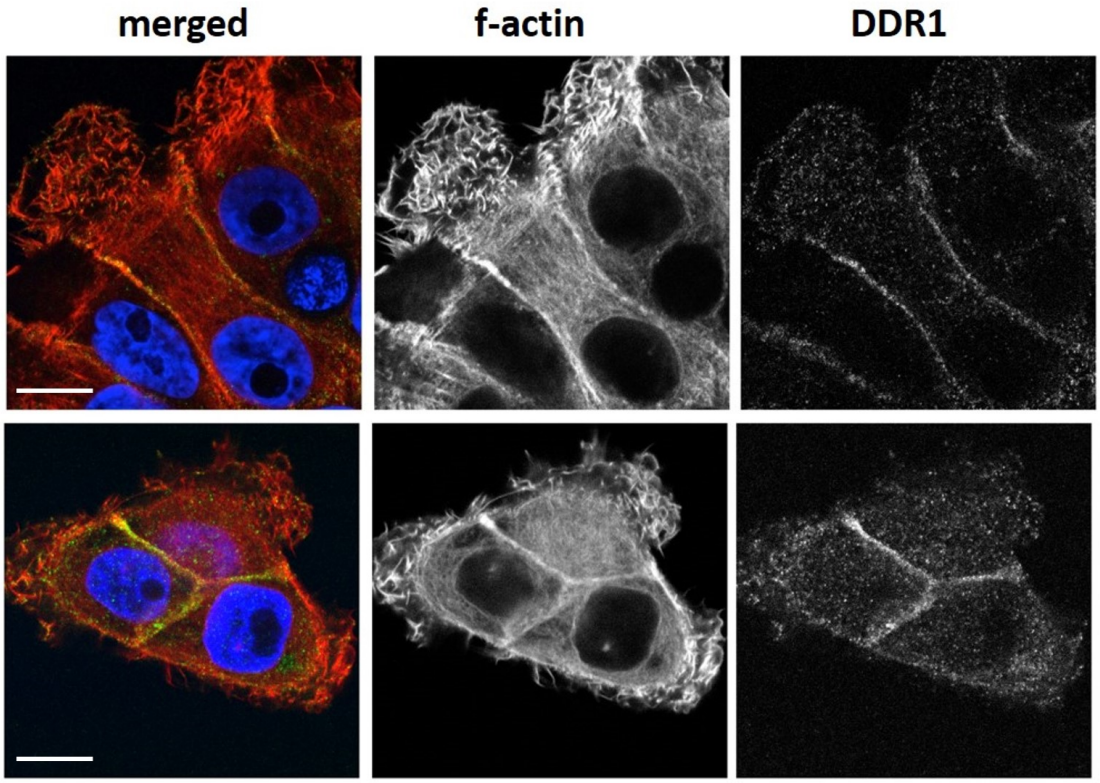

Figure 4.17: DDR1 localises to cell-cell contacts
2D immunofluorescence confirming that DDR1 localises to cell-cell contacts in MCF10A, but does not localise where cells are not in contact. DDR1 shown in green, f-actin in red (Phalloidin Alex Fluor 568), DNA in blue. Scale bar = 10µM.

4.7.1 DDR1 localisation is maintained during mitotic rounding

If DDR1 was playing a role in impairing centrosome clustering, it was hypothesised that its localisation must be maintained during mitosis. DDR1 localisation was analysed by 2D immunofluorescence microscopy, which showed that its localisation is maintained to cell-cell contacts during mitosis, including through to telophase (Figure 4.18). This suggested that DDR1 could regulate cortical contractility in mitosis.

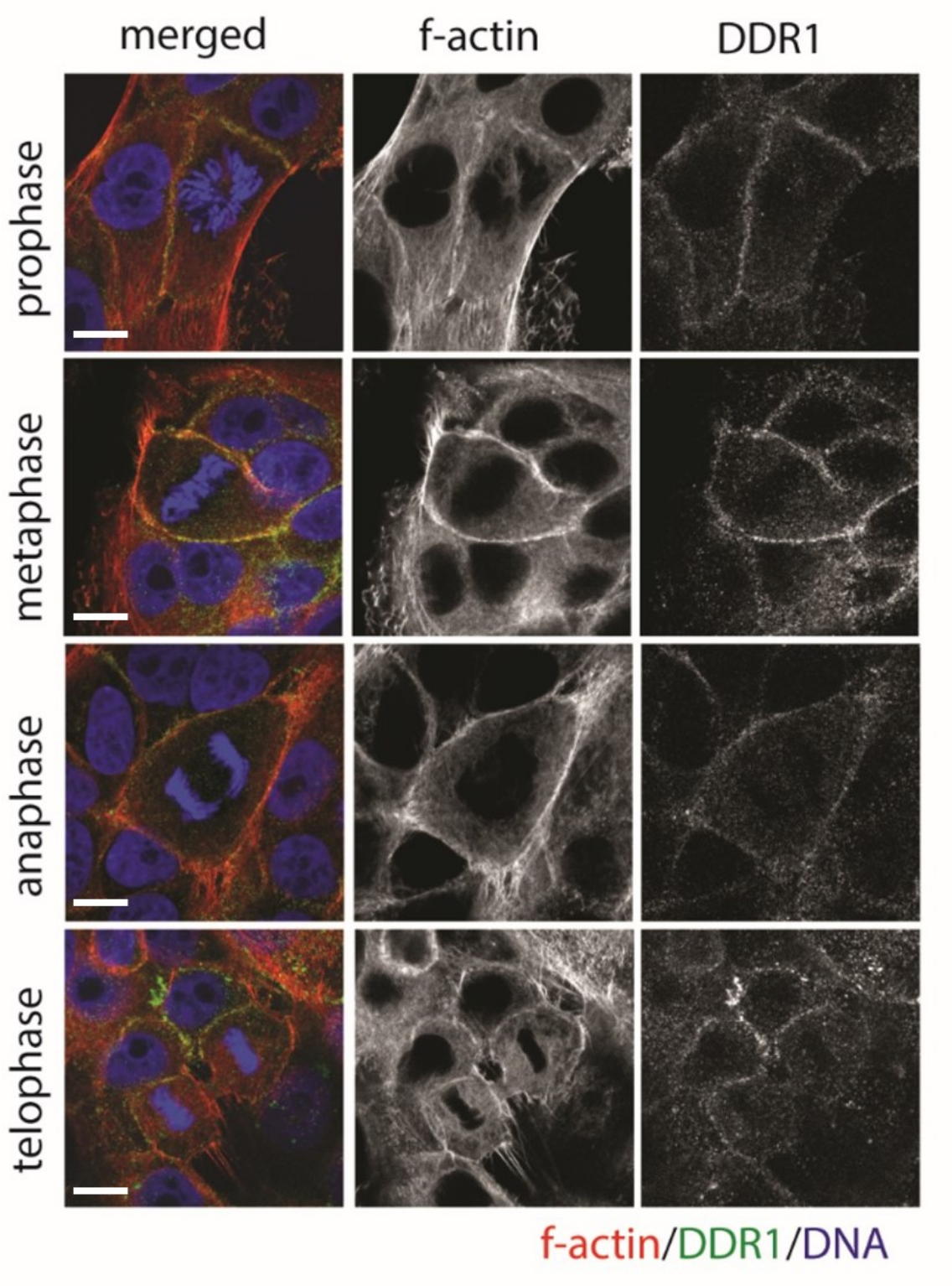

Figure 4.18: DDR1 localisation to cell-cell contacts is maintained during mitosis
2D immunofluorescence confirming that DDR1 localises to cell-cell contacts in MCF10A during the different stages of mitosis. DDR1 shown in green, f-actin in red, DNA in blue. Scale bar = 10µM.

4.8 Loss of DDR1 correlates with increased centrosome clustering efficiency

When examining DDR1 protein expression in the panel of cell-lines, none of the cell lines that were efficient at clustering their supernumerary centrosomes (RPE-1, NIH-3T3 and BJ) expressed DDR1 as seen by western blot, whereas the cell lines that did not cluster efficiently (MC10A, HaCaT and J3B1A) did (Figure 4.19). The lower band is a high-mannose immature form of DDR1 (Noordeen *et al.*, 2006).

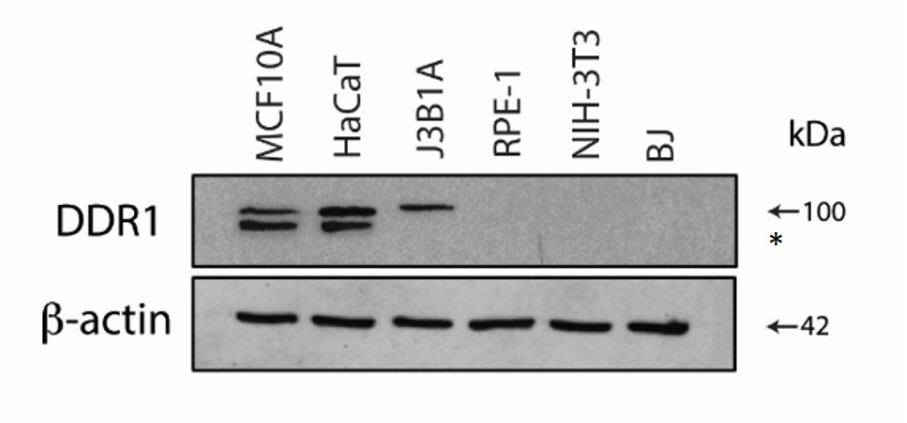

Figure 4.19: Expression of DDR1 correlates with impaired centrosome clustering efficiency
Western blot analysis of DDR1 protein level in a panel of cell lines. The cell lines expressing DDR1 - MCF10A, HaCaT and J3B1A cluster ~40% in cells with supernumerary centrosomes generated by DCB, whereas those not expressing DDR1, the RPE-1, NIH-3T3 and BJ all cluster ~80%. β-actin was used as a loading control. * refers to a high-mannose immature form of DDR1.

4.8.1 Knockdown of DDR1 by siRNA increases centrosome clustering

To investigate if loss of DDR1 increased clustering efficiency in the MCF10A and HaCaT cell lines, cells were treated with on-target SMART-pool siRNA against DDR1, as described for E-cadherin in Section 4.3.1. Knockdown efficiency of DDR1 was analysed by western blot (Figure 4.20 A and B). In both the MCF10A and HaCaT cells DDR1 was efficiently depleted and this resulted in a significant improvement in centrosome clustering (Figure 4.20 A and B). To ensure that siRNA treatment against DDR1 did not result in loss of E-cadherin which could explain

the improved clustering phenotype, E-cadherin levels were also assessed. E-cadherin levels remained unchanged with loss of DDR1 as shown by western blot analysis, and 2D immunofluorescence microscopy (Figure 4.20). These data therefore support the hypothesis that DDR1 impairs centrosome clustering, downstream of E-cadherin.

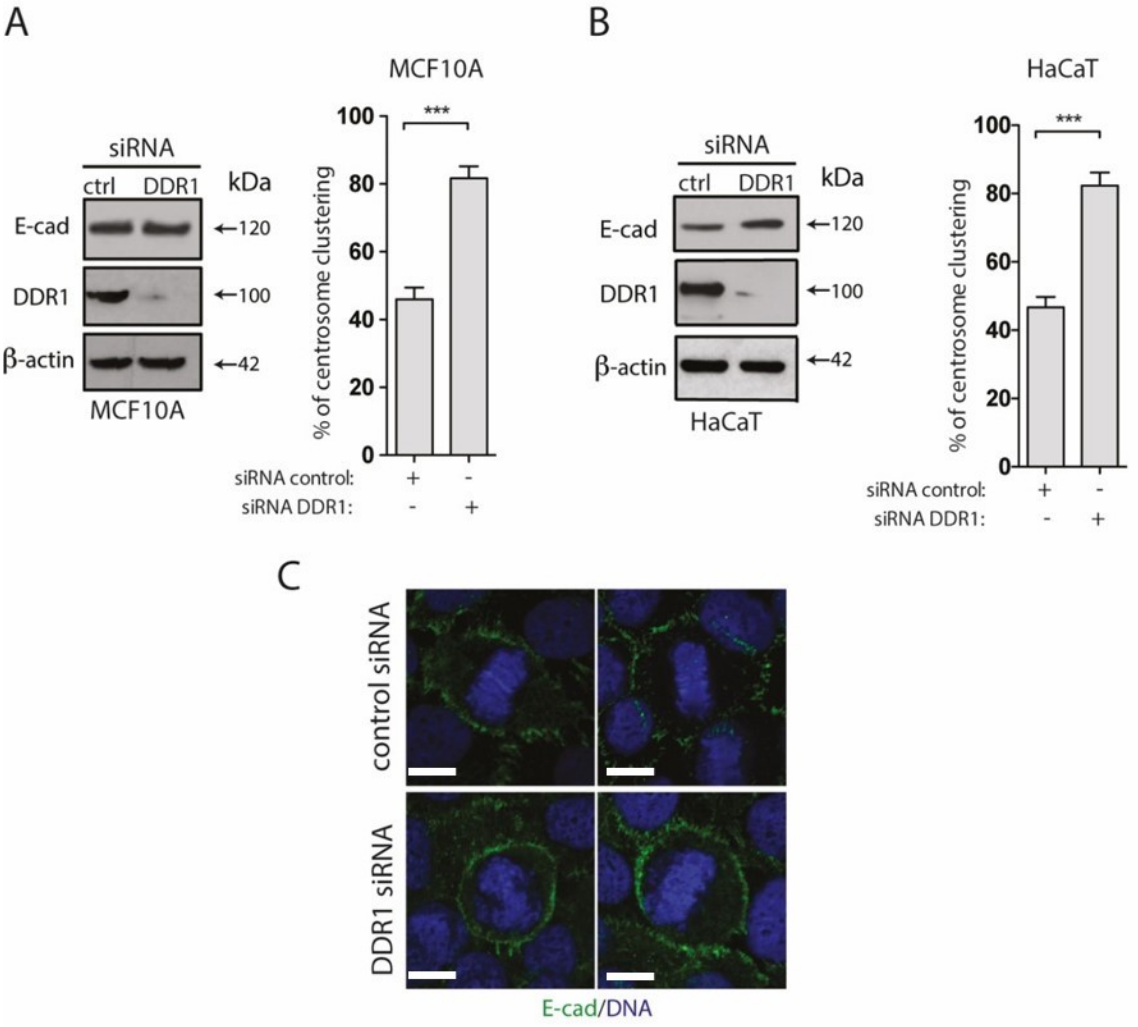

Figure 4.20: Knockdown of DDR1 by siRNA increases centrosome clustering
Aand **B)** Western blot analysis of DDR1 and E-cadherin in siRNA against DDR1 treated cells in MCF10A (A) and HaCaT (B). β-actin was used as a loading control. Representative blot of 3 independent experiments. Alongside each is quantification of centrosome clustering in the control and DDR1 treated cells, where knockdown of DDR1 increases centrosome clustering. Data are mean ± SD, n = 150 individual cells, 50 per experiment at cytokinesis. Data analysed using Student's t-test. *** $p<0.001$. **C)** 2D immunofluorescence of E-cadherin in control and DDR1 siRNA treated MCF10A mitotic cells at metaphase, showing that E-cadherin level and localisation is maintained upon knockdown of DDR1. Scale bar = 10µM.

4.8.2 Unsuccessful attempt to CRISPR knockout DDR1

To further confirm the siRNA results and examine cell lines with knockout of DDR1, CRISPR-Cas9 was used as described in Section 2.3.5 in HaCaT cells. Three different gRNA were co-infected via lentivirus into HaCaT cells, however despite selecting 100 clones, no full knockout clone was identified, although some clones displayed partial knockout (Figure 4.21). Due to time restrictions, further work to generate a successful oomplete DDR1 knockout clone was not carried out.

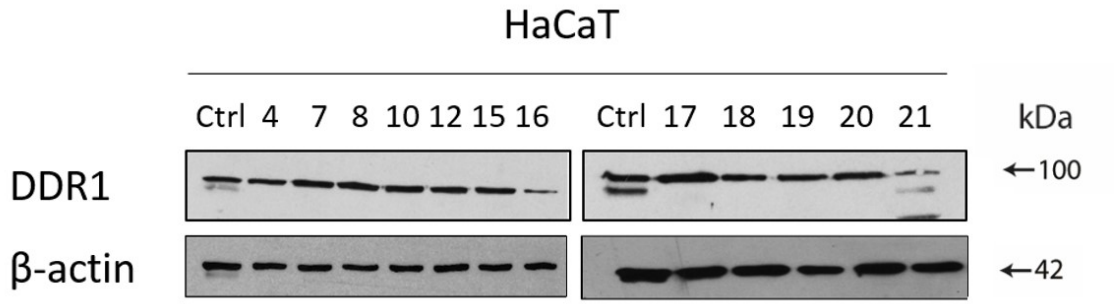

Figure 4.21: Unsuccessfully attempted to gene knockout DDR1 in HaCaT cells
Representative western blot of 12 out of 100 clones analysed showing no positive gene knockout for DDR1 in HaCaT cell lines. β-actin is used as a loading control.

4.9 DDR1 levels are regulated by E-cadherin expression

The work of Hidalgo-Carcedo *et al.* reported that E-cadherin localises DDR1 to the adherens junctions (Hidalgo-Carcedo *et al.*, 2011). However, having observed that DDR1 is only present in epithelial cells, it was hypothesised that E-cadherin may play a role in DDR1 stabilisation and not just localisation. Western blot analysis of DDR1 levels showed that DDR1 was lost in the E-cadherin *CDH1-/-* cell lines (Figure 4.22 A). Analysis of mRNA for DDR1 was also performed, and no significant difference was observed between the control and *CDH1-/-* cell lines, suggesting that E-cadherin regulates DDR1 protein levels but not mRNA expression (Figure 4.22 B). Similar results were observed in the A431 *CDH1-/-* cell line, where DDR1 is not observed after loss of E-cadherin, as seen by 2D immunofluorescence microscopy (Figure 4.22 C).

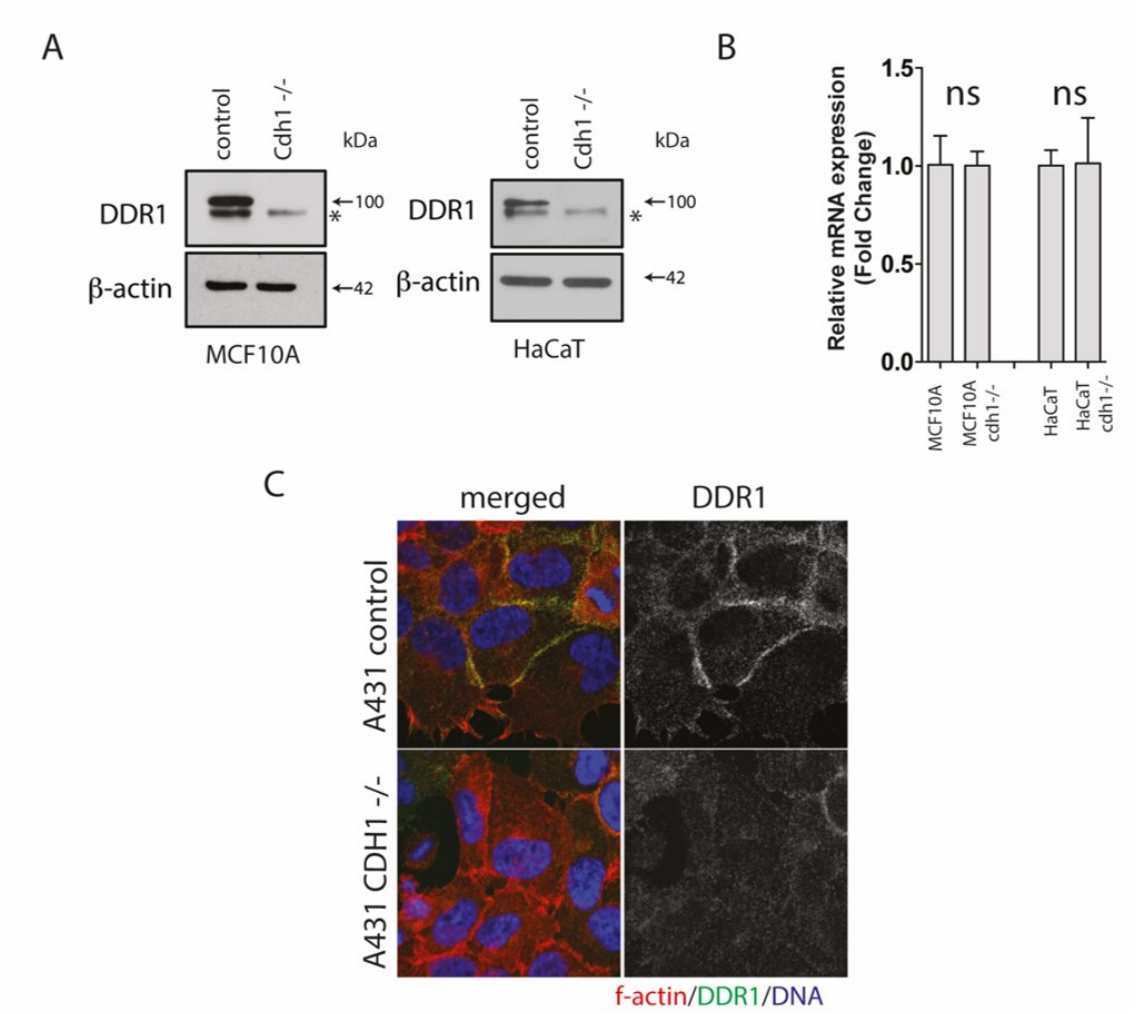

Figure 4.22: E-cadherin stabilises DDR1 at protein level
A) Western blot analysis of DDR1 in MCF10A *CDH1-/-* and HaCaT *CDH1-/-* cell lines. DDR1 is lost in the cell lines where E-cadherin has been knocked out. * refers to a high-mannose immature form of DDR1. β-actin is used as a loading control. Representative of 3 independent experiments **B)** qRT-PCR analysis of DDR1 mRNA levels in MCF10A *CDH1-/-* and HaCaT *CDH1-/-* cell lines compared to controls. Data has been normalised to GAPDH. Data are mean ± SD, n = 3. Data analysed using two-way ANOVA with Šidák post-hoc test. No significant difference was observed between control and knockout cells. **C)** 2D immunofluorescence microscopy of A431 and A431 *CDH1-/-* cells with f-actin stained in red, DDR1 in green and DNA in blue. The *CDH1-/-* cells do not express DDR1, supporting that E-cadherin stabilises DDR1 levels. Scale bar = 10µM.

4.9.1 RPE-1 cells expressing E-cadherin express DDR1

Conversely, when examining DDR1 levels by western blot in the RPE-1 cell line expressing E-cadherin, DDR1 protein was observed, whilst it was not seen in the EcadDN line. (Figure 4.23 A). This therefore supported that E-cadherin may play a role in stabilising DDR1, and not just localisation of the protein. Furthermore, when the RPE-1 E-cadherin expressing cells were treated with siRNA against DDR1, centrosome clustering significantly increased (Figure 4.23 B). This suggests that DDR1 impairs centrosome clustering, and requires E-cadherin to be stabilised.

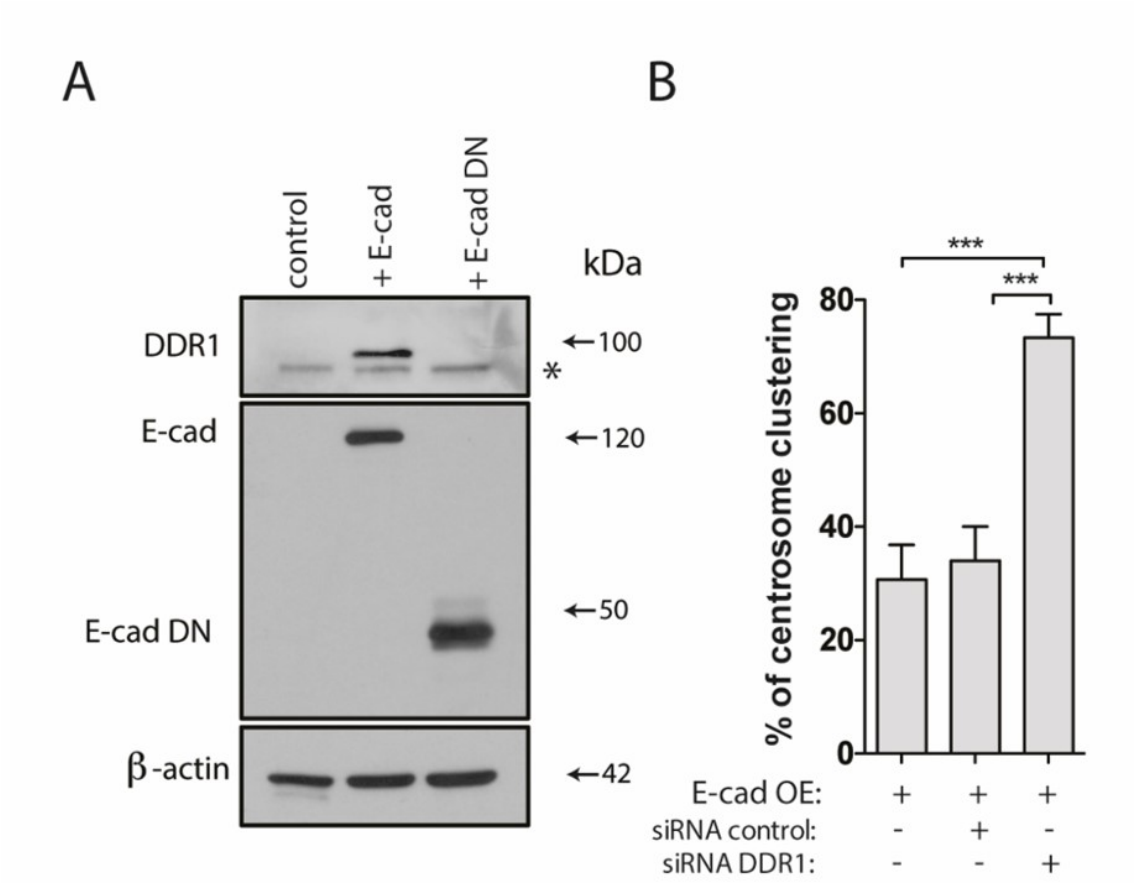

Figure 4.23: Knockdown of DDR1 in RPE-1 E-cadherin cells increases centrosome clustering
A) Western blot analysis of DDR1 levels in RPE-1 cells expressing E-cadherin and truncated E-cadherin compared to controls. Expression of full length E-cadherin results in DDR1 protein expression, suggesting E-cadherin stabilises DDR1. β-actin is used as a loading control. Representative blot of 3 independent experiments. * refers to a high-mannose immature form of DDR1. **B)** Quantification of RPE-1 E-cadherin expressing cells treated with DDR1 siRNA, showing an increase in centrosome clustering upon knockdown of DDR1. Data are mean ± SD, n = 150 individual cells, 50 per experiment at cytokinesis. Data analysed using one way ANOVA with Tukey post-hoc test. *** $p<0.001$.

4.10 Increased centrosome clustering upon depletion of DDR1 is not due to loss of kinase function

The primary function of DDR1 within a cell is as a collagen activated tyrosine kinase, that has a number of downstream functions including cell proliferation, survival, adhesion and migration. DDR1 is activated upon binding to collagen where it is then autophosphorylated, through a mechanism that has yet to be fully elucidated (*Reviewed in:* Leitinger, 2011) (Figure 4.24 A). However, DDR1 localisation to adherens junctions and the signalling cascade which leads to antagonism of ROCK1 mediated actoymyosin contractility is reported to be independent of the collagen activated tyrosine kinase function (Hidalgo-Carcedo *et al.*, 2011). To determine if the resultant increase in clustering was due to a loss of DDR1, or the loss of the tyrosine kinase signalling, the DDR1 tyrosine kinase inhibitor DDR1-IN-1 was used. MCF10A cells were pre-treated with 0 – 15mM DDR1-IN-1 for 1 hour. The medium was then removed and replaced with medium containing 10µg/ml of collagen and DDR1-IN-1 for 2 hours. Western blot analysis showed that upon addition of collagen DDR1 was phosphorylated, as observed by a phospho-shift in the protein size (Figure 4.24 B, lane 1). After addition of inhibitor the phospho-shift was no longer observed at 10 and 15mM concentration of inhibitor (Figure 4.24 B). As the growth medium does not contain collagen in normal tissue culture conditions, DDR1 is not phosphorylated under normal growth conditions (Figure 4.24 B, lane 5). Quantification of centrosome clustering at both metaphase and cytokinesis in the presence of 15mM DDR1-IN-1 shows no significant difference in centrosome clustering (Figure 4.24 C). These data confirm that the increase in centrosome clustering observed upon loss of DDR1 is not due to the loss of the tyrosine kinase function.

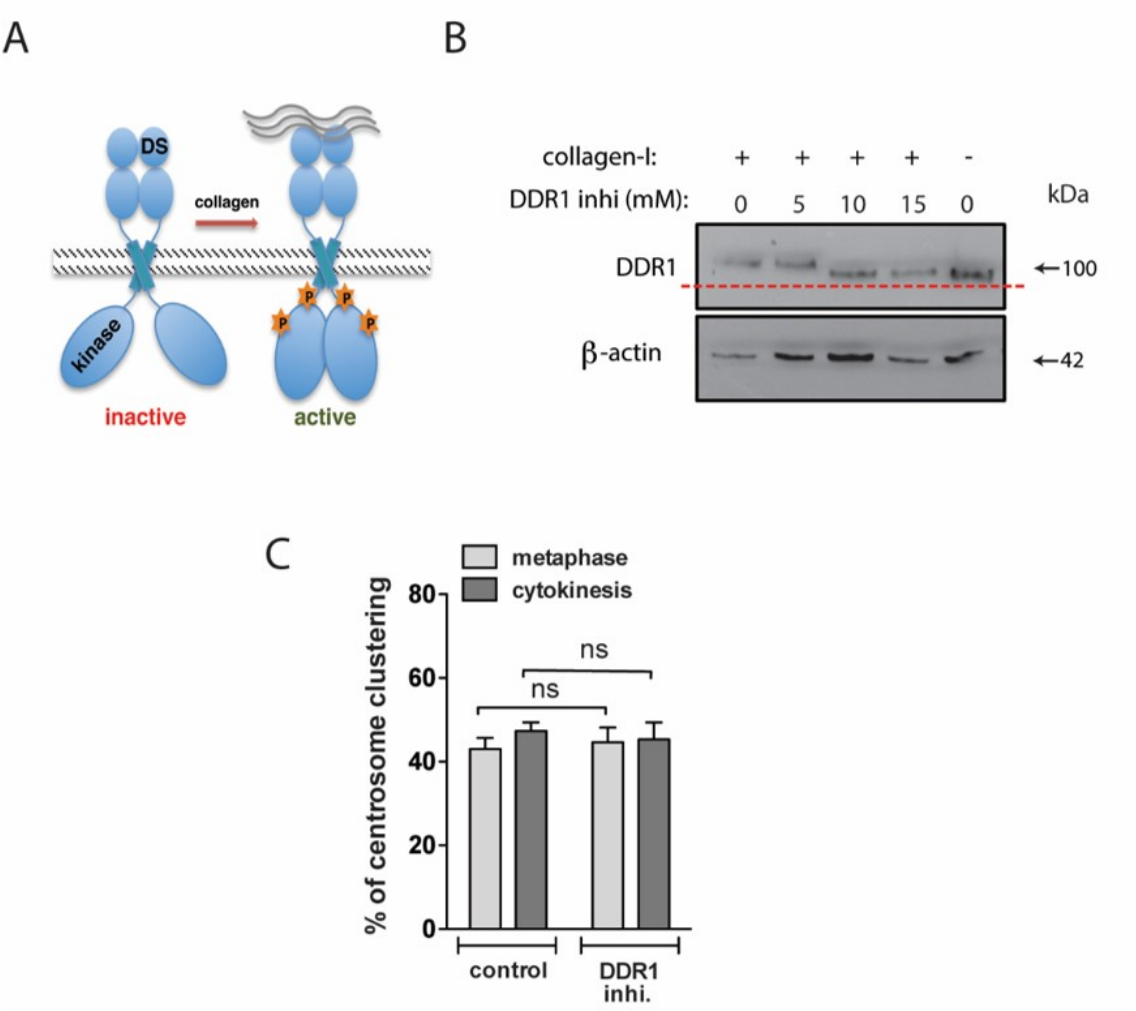

Figure 4.24: Increased centrosome clustering upon knockdown of DDR1 is not due to loss of tyrosine kinase function
A) Schematic of DDR1 which upon binding to collagen, autophosphorylates and becomes activated. DS represents Discoidin domain. **B)** Western blot analysis of MCF10A cells treated with 0-15mM of the DDR1 inhibitor DDR1-IN-1, with and without addition of 10µM collagen. Addition of collagen results in activation of DDR1 as seen by a phospho-shift in size (where the red line is placed to show normal DDR1 size), which is lost upon addition of 10-15mM DDR1-IN-1. **C)** Quantification of centrosome amplification in MCF10A cells with 10µM collagen, with and without 15mM DDR1-IN-1, showing no significant effect on centrosome clustering. Data are mean ± SD, n = 150 individual cells, 50 per experiment. Data analysed using two-way ANOVA with Šidák post-hoc test. *** $p<0.001$.

4.11 RhoA negative regulators do not affect centrosome clustering

During interphase, it has been shown that DDR1 regulation of contractility is mediated by recruitment of p190RhoGAP, which inhibits RhoA activity (Hidalgo-Carcedo *et al.*, 2011). Therefore, to test if p190RhoGAP was affecting centrosome clustering, p190RhoGAP was depleted by siRNA. The knockdown of p190RhoGAP was very efficient as analysed by western blot, but no significant effect on centrosome clustering were observed (Figure 4.25). This suggests that p190RhoGAP is not involved in the E-cadherin/DDR1 signalling cascade that impairs centrosome clustering.

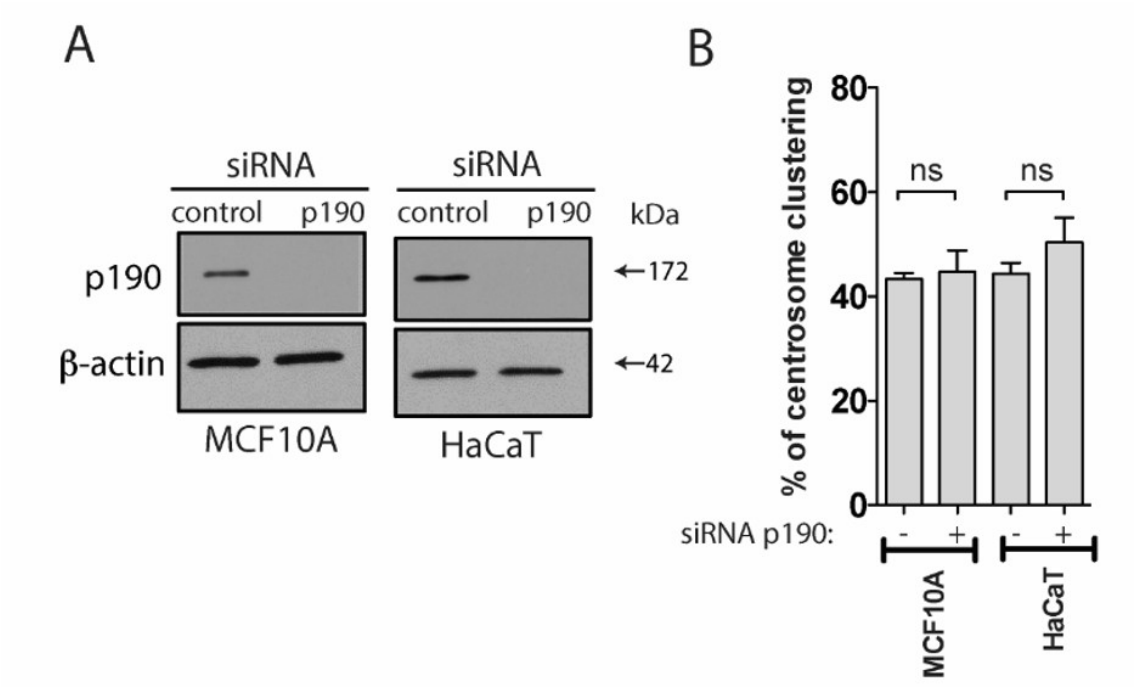

Figure 4.25: Loss of p190RhoGAP does not affect centrosome clustering **A)** Western blot analysis of p190RhoGAP in MCF10A and HaCaT cells treated with siNegative (control) and on-TARGET SMARTpool siRNA against p190RhoGAP (p190). Cells were analysed at 72 hours post transfection. β-actin was used as a loading control. Representative blot of 3 independent experiments **B)** Centrosome clustering is not significantly affected upon knockdown of p190RhoGAP by siRNA. Data are mean ± SD, n = 150. Data analysed using two-way ANOVA with Šidák post-hoc test.

DLC3, another regulator of RhoA at adherens junctions, was also depleted by siRNA (Hendrick *et al.*, 2016). Similarly to p190RhoGAP, no effect was observed with knockdown of DLC3, suggesting that the regulation of cortical contractility in epithelial mitotic cells may not mediated through RhoA (Figure 4.26).

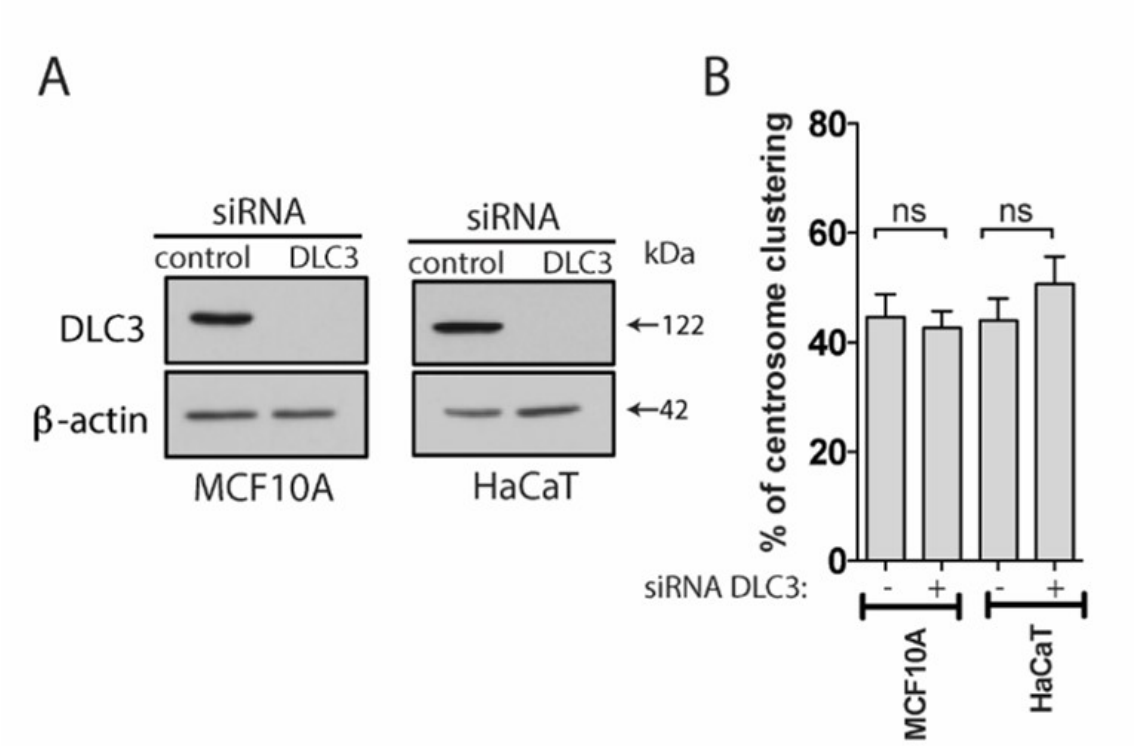

Figure 4.26: Loss of DLC3 does not affect centrosome clustering
A) Western blot analysis of DLC3 in MCF10A and HaCaT cells treated with siNegative (control) and on-TARGET SMARTpool siRNA against DLC3. Cells were analysed at 72 hours post transfection. β-actin was used as a loading control. Representative blot of 3 independent experiments. **B)** Centrosome clustering is not significantly affected upon knockdown of DLC3 by siRNA. Data are mean ± SD, n = 150 individual cells, 50 per experiment at cytokinesis. Data analysed using two-way ANOVA with with Šidák post-hoc test.

4.12 Loss of RhoE increases centrosome clustering

4.12.1 RhoE siRNA

It is known that RhoE, a small GTPase, which is recruited to the adherens junctions in a DDR1-dependent manner, can negatively regulate actomyosin contractility by directly inhibiting ROCK1 activity, downstream of RhoA (Riento *et al.*, 2003; Hidalgo-Carcedo *et al.*, 2011). To test whether downregulation of contractility by RhoE was affecting centrosome clustering, RhoE was depleted by siRNA. Unexpectedly, depletion of RhoE decreased centrosome clustering efficiency in HaCaT cell lines (Figure 4.27). The siRNA for RhoE used did not result in RhoE depletion in MCF10A (Figure 4.27 C).

4.12.1.1 RhoE siRNA affects Mad2 levels

During quantification of the RhoE depleted HaCaT cells, it was observed that the increase in multipolar mitosis was accompanied by an increase in lagging chromosomes, identified during anaphase (Figure 4.28).

This suggested that RhoE depletion may also have been affecting the spindle assembly checkpoint (SAC), which prevents efficient clustering, as described in Section 1.2.5. This would have been a novel role for RhoE as a regulator of the SAC. However, work by Sigoillot *et al.* using a bioinformatics approach suggested that Mad2, a known regulator of the SAC can be prominently affected as an off target effect by other siRNA (Sigoillot *et al.*, 2012). To test whether Mad2 levels were being affected by the RhoE siRNA, Mad2 protein levels were analysed by western blotting. The western blot showed that Mad2 was being depleted upon treatment of RhoE siRNA (Figure 4.29). These data therefore suggested that the effect observed on the decrease in centrosome clustering, and increase in lagging chromosomes is due to decreased levels of Mad2, which in turn leads to premature anaphase onset from an absence of the SAC.

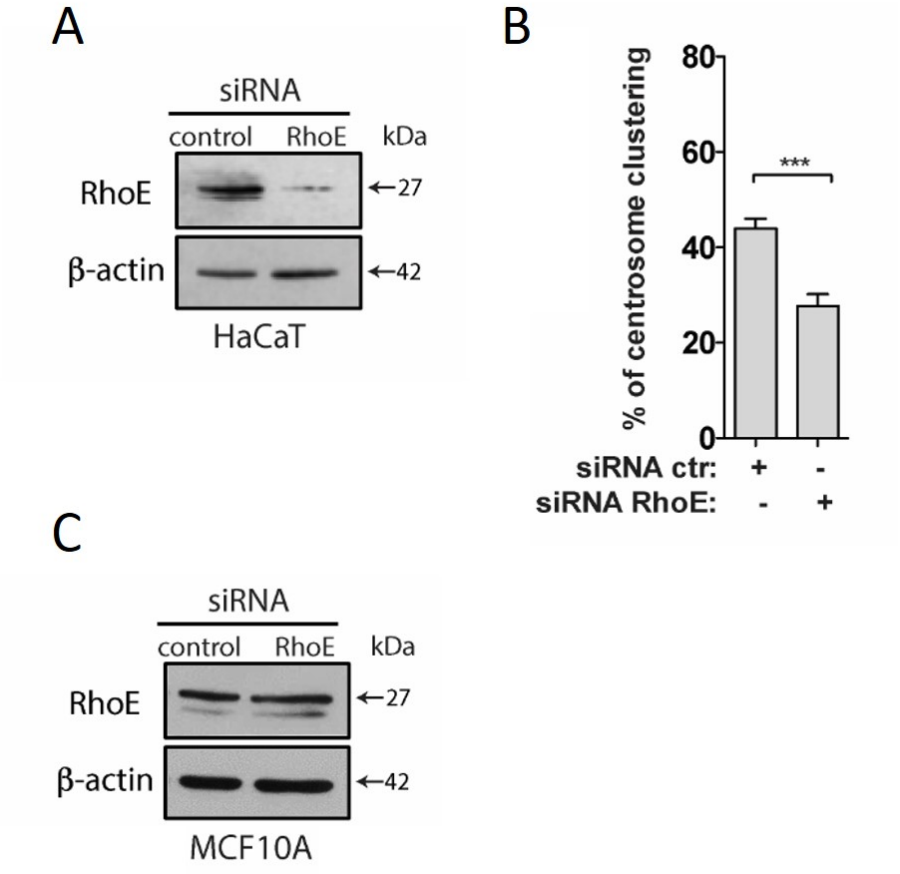

Figure 4.27: RhoE depletion by siRNA results in an increase of multipolar divisions
A) Western blot analysis of RhoE in HaCaT cells treated with siNegative (control) and on-TARGET SMARTpool siRNA against RhoE. Cells were analysed at 72 hours post transfection. β-actin was used as a loading control. Representative blot of 3 independent experiments. **B)** Centrosome clustering is impaired upon knockdown of RhoE by siRNA. Data are mean ± SD, n = 150 individual cells, 50 per experiment at cytokinesis. Data analysed using Student's t-tests. *** $p<0.001$. **C)** Western blot analysis of RhoE in MCF10A cells treated with siNegative (control) and on-TARGET SMARTpool siRNA against RhoE. Cells were analysed at 72 hours post transfection. β-actin was used as a loading control. Representative blot of 3 independent experiments.

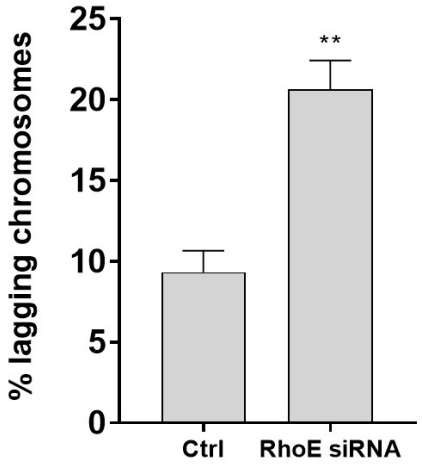

Figure 4.28: RhoE depletion by siRNA results in an increased number of lagging chromosomes
Quantification of percentage of cells with lagging chromosomes in HaCaT cells upon depletion of RhoE by siRNA. Data are mean ± SD, n = 150 individual cells, 50 per experiment at anaphase. Data analysed using Student's t-test. ** $p<0.01$.

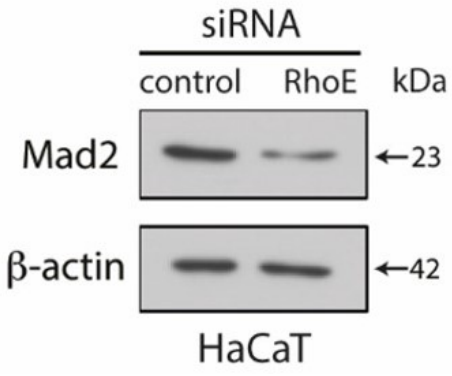

Figure 4.29: RhoE siRNA results in a decrease in Mad2 protein levels
Western blot analysis of Mad2 protein levels in HaCaT cells with RhoE siRNA, showing a depletion of Mad2. β-actin was used as a loading control. Representative blot of 3 independent experiments.

4.12.1.2 MG132 enables increased centrosome clustering in the absence of RhoE

Mad2 depletion prevents efficient centrosome clustering by affecting the SAC resulting in too short a time in mitosis to enable clustering. To overcome the effect of Mad2 knockdown on the SAC, MG132 was used to prolong metaphase in RhoE depleted cells. In this condition centrosome clustering improved upon RhoE depletion with MG132 treatment (Figure 4.30). Taken together, these results suggest that downregulation of RhoE prevents efficient centrosome clustering in epithelial cells. This data also supports previously published data that cells require sufficient time in mitosis to cluster efficiently, and that reduced time in mitosis can impair efficient centrosome clustering (Basto *et al.*, 2008; Kwon *et al.*, 2008; Yang *et al.*, 2008).

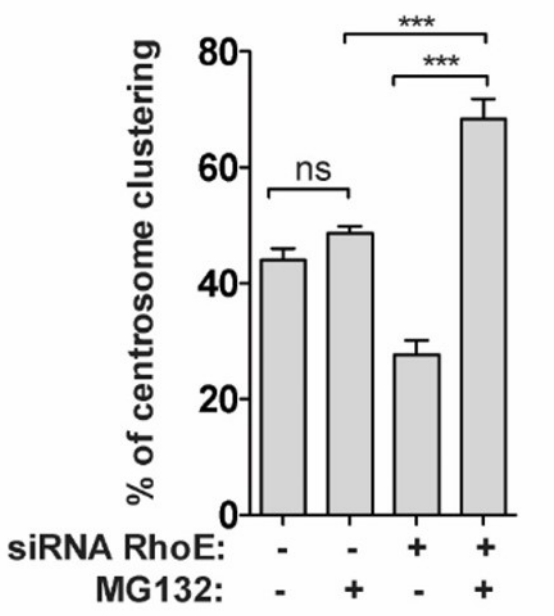

Figure 4.30: MG132 treatment in RhoE siRNA treated cells increases centrosome clustering
Quantification of centrosome clustering in HaCaT cells treated with siRNA targeting RhoE. Cells were treated with 10µM MG132 to prolong metaphase for 4 hours, and released for 1 hour. RhoE cells with MG132 treatment clustered their supernumerary centrosomes significantly more efficiently than control cells. Data are mean ± SD, n = 150 individual cells, 50 per experiment at cytokinesis. Data analysed using two-way ANOVA with Šidák post-hoc test. *** $p<0.001$.

4.12.2 Single target siRNA against RhoE increases centrosome clustering

Having identified that the initial siRNA targeting RhoE was also decreasing Mad2, which was in turn affecting centrosome clustering, a different single siRNA targeting RhoE was used. Depletion of RhoE by this single siRNA did not affect Mad2 levels, whilst remaining efficient at depleting RhoE levels, as shown by western blot (Figure 4.31 A). Quantification of centrosome clustering showed that depletion of RhoE increases centrosome clustering, as initially expected (Figure 4.31 B). This suggests that the downregulation of contractility by RhoE impairs centrosome clustering.

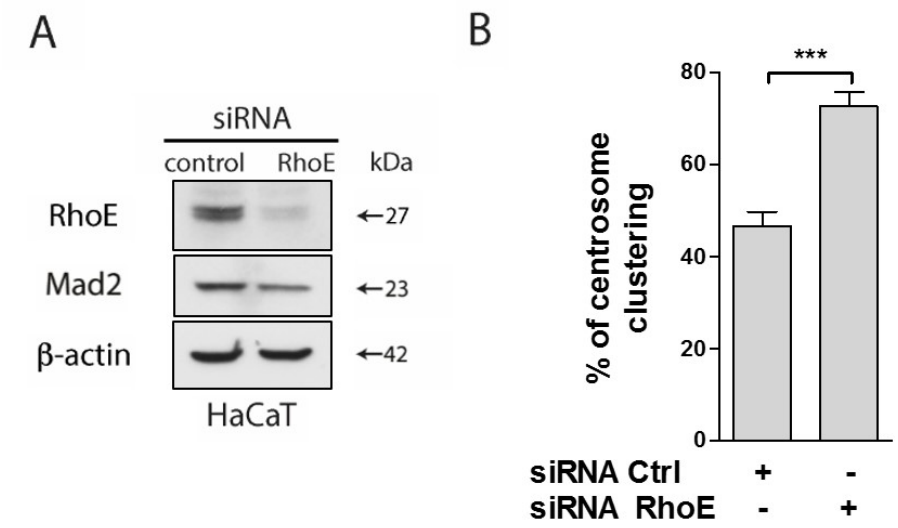

Figure 4.31: Single target siRNA against RhoE increases centrosome clustering
A) Western blot analysis of RhoE in HaCaT cells treated with siNegative (control) and on-TARGET plus single siRNA against RhoE. Cells were analysed at 72 hours post transfection. β-actin was used as a loading control. Representative blot of 3 independent experiments. Mad2 levels were unaffected with this siRNA. **B)** Centrosome clustering is improved upon knockdown of RhoE by siRNA. Data are mean ± SD, n = 150 individual cells, 50 per experiment at cytokinesis. Data analysed using Student's t-tests. *** $p<0.001$.

4.13 Loss of E-cadherin and DDR1 correlates with centrosome amplification in a panel of breast cancer cell lines

Many solid tumours of an epithelial origin have been shown to contain supernumerary centrosomes (*Reviewed in:*Zyss and Gergely, 2009; Chan, 2011). However, the previous data suggest that epithelial cells have a low efficiency of clustering supernumerary centrosomes, resulting in poor survival. Therefore, it is possible that cancer cells from an epithelial origin need to adapt in order to survive in the presence of extra centrosomes, and loss of E-cadherin and DDR1 may be part of this adaptation mechanism. To test this, centrosome amplification was analysed in a panel of 15 breast cancer cell lines along with E-cadherin and DDR1 protein levels (Figure 4.32 A and B). Six cell lines were identified which had high levels of centrosome amplification (>30% of cells contain supernumerary centrosomes). When E-cadherin protein levels were examined in these cell lines, all 6 did not express E-cadherin (Figure 4.32 B). In support of the data suggesting that E-cadherin is important for the stabilisation of DDR1, all 6 cell lines did also not express DDR1 (Figure 4.32 B). When looking at HSET protein expression, all cell lines expressed HSET, and there was no observable trend with HSET level and clustering efficiency, supporting the hypothesis that HSET alone is not sufficient to enable centrosome clustering. As expected, all of the cell lines with high levels of centrosome amplification were able to cluster their supernumerary centrosomes effectively (>80%) by cytokinesis (Figure 4.32 C), independently of breast cancer subtype, although higher levels of centrosome amplification have been reported in basal cell lines (D'Assoro *et al.*, 2002; Denu *et al.*, 2016).

Similarly to the *CDH1-/-* cell lines, ERM protein expression was analysed by western blot, and no correlation between ERM protein level and centrosome amplification was observed (Figure 4.33). This supported that centrosome inactivation does not occur within these cell lines.

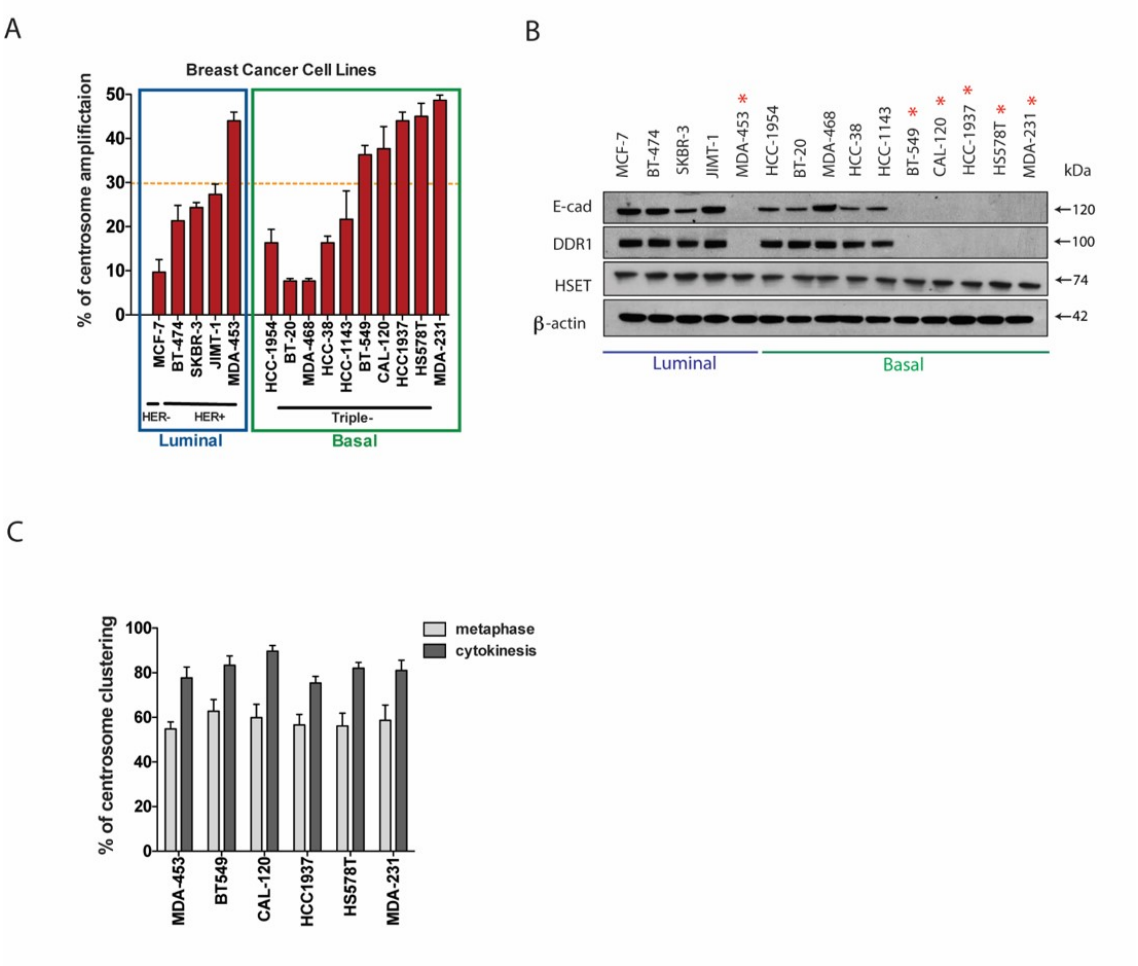

Figure 4.32: Loss of E-cadherin and DDR1 correlates with high levels of centrosome amplification in breast cancer
A) Quantification of centrosome amplification in a panel of 15 breast cancer cell lines. Cell lines with >30% of their cells containing supernumerary centrosomes are classed as having high levels of centrosome amplification. Data are mean ± SD, n = 150 at metaphase. **B)** Western blot analysis of E-cadherin and DDR1 in the breast cancer panel. * denotes cell lines with high levels of centrosome amplification, which correlates with loss of E-cadherin and DDR1. **C)** Quantification of centrosome amplification in the 6 cell lines with high levels of centrosome amplification. All cell lines are efficient are clustering their supernumerary centrosomes (>80%). Data are mean ± SD, n = 150 individual cells, 50 per experiment at cytokinesis.

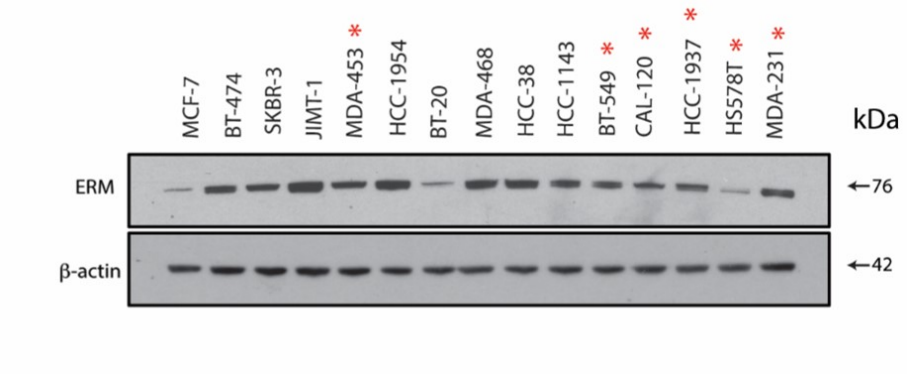

Figure 4.33: Centrosome amplification in a panel of breast cancer cell lines does not correlate with ERM protein expression
Western blot analysis of ERM levels in the panel of 15 breast cancer cell lines. No correlation between ERM protein level and level of centrosome amplification was observed. β-actin was used as a loading control. * represents high levels of centrosome amplification (>30% of cells). Representative image of 3 independent experiments.

4.14 Discussion

Having shown that not all cell types are inherently able to cluster their supernumerary centrosomes efficiently, it was important to try and understand the intrinsic mechanisms which enabled the NIH-3T3, BJ and RPE-1 to cluster their centrosomes efficiently, which was not occurring in the remaining cell lines.

Previous work showed that time spent in metaphase as well as the kinesin HSET are important for centrosome clustering. However, when given more time in metaphase using the proteasome inhibitor MG132, centrosome clustering was not improved in the MCF10A and HaCaT cell lines. In addition, the levels of HSET were consistent in all six cell lines analysed, suggesting that HSET is not a limiting factor for centrosome clustering efficiency, although the localisation of HSET was not explored.

Having ruled out two potential mechanisms which might have accounted for the variation in centrosome clustering efficiency between the two groups of cells, the background of the cell lines in the panel was explored more deeply to try and identify a potential cause for the differences observed. It was noted that the MCF10A, HaCaT and J3B1A were all of epithelial origin and expressed E-cadherin, the BJ and NIH-3T3 were both fibroblasts, and interestingly the RPE-1 cell lines whilst of epithelial origin has subsequently lost E-cadherin expression. Based on this it was hypothesised that the presence of E-cadherin may impair centrosome clustering.

Using siRNA, shRNA and CRISPR-Cas9 in the MCF10A and HaCaT cell lines, it was found that depletion of E-cadherin significantly increased centrosome clustering efficiency from ~40% to ~80%. These results strongly support a role for E-cadherin in preventing efficient clustering in epithelial cell lines. Comparable results were observed in cell lines where supernumerary centrosomes were generated by PLK4 overexpression. Increased centrosome clustering was also observed in the A431 skin cancer cell line upon knockout of E-cadherin, suggesting that loss of E-cadherin could be a mechanism of adaptation for cancers with supernumerary centrosomes. It is unclear however if E-cadherin loss may facilitate the preservation of centrosome amplification, or if centrosome amplification may drive the loss of E-cadherin for cell survival.

Conversely, overexpression of E-cadherin in the E-cadherin deficient cell line RPE-1 impaired centrosome clustering efficiency, comparable to the MCF10A, HaCaT and J3B1A. These data further support that the expression of E-cadherin impairs centrosome clustering, and that loss of E-cadherin may be a mechanism of adaptation for cells with supernumerary centrosomes.

Adaptation to centrosome clustering has always been assumed to be important for cell survival, with multipolar cell divisions leading to severe levels of aneuploidy which are poorly tolerated leading to cell death. Loss of E-cadherin was shown to increase cell survival/viability in both colony formation and cell growth assays. These data confirm that adaptation to centrosome amplification by centrosome clustering enables cells to adapt to, and maintain prolonged survival.

It was found that DDR1 depletion, which controls cortical contractility downstream of E-cadherin was able to increase centrosome clustering in epithelial cells, therefore suggesting that DDR1 can impair centrosome clustering. Use of a DDR1 tyrosine kinase inhibitor did not affect centrosome clustering, therefore supporting that the observed change in centrosome clustering is due to the loss of the E-cadherin-DDR1 pathway, which is independent of DDR1's tyrosine kinase function rather than through DDR1 tyrosine kinase receptor signalling.

Regulation of cortical contractility by DDR1 has been reported to involve the RhoA negative regulator p190RhoGAP, which acts downstream of DDR1 to prevent cortical contractility (Hidalgo-Carcedo *et al.*, 2011). However, p190RhoGAP depletion has no role on centrosome clustering suggesting that RhoA activity might be dispensable. Similarly, depletion of DLC3, another negative of RhoA had no effect on centrosome clustering. In contrast, depletion of RhoE, which can directly bind and inhibit ROCK to prevent cortical contractility, led to efficient clustering. These data therefore

suggest that RhoE may directly impair centrosome clustering rather than through RhoA signalling, although depletion of RhoA was not tested.

Taken together, these results suggest that loss of E-cadherin and/or DDR1 could play a role in the adaptation to supernumerary centrosomes in cancer. The findings in the panel of 16 breast cancer cell lines further supports the idea that loss of E-cadherin/DDR1 could be part of an adaptation mechanism to centrosome amplification in cancer. This mechanism is suggested to be through control of cortical contractility as no observed changes in centrosome inactivation, HSET levels or cell rounding were observed.

Chapter 5

Results III: Elucidating the role of cortical contractility in centrosome clustering

5.1 E-cadherin knockout cells have increased cortical tension

Having identified that loss of E-cadherin and DDR1 results in increased centrosome clustering, it was hypothesised that this may be due to increased cortical contractility. To test the hypothesis that loss of E-cadherin could result in increased cortical contractility, atomic force microscopy (AFM) was used to measure cortical tension (Figure 5.1). Cortical tension has been shown to be dependent upon actomyosin contractility, and therefore can be regarded as a surrogate measure of cortical contractility (Harris, Daeden and Charras, 2014). AFM works by a cantilever being lowered with a known force onto a cell, and a laser beam is aimed down the cantilever which then measures the deflection of the cantilever upon contact with the cell. Based on the recorded changes of the cantilever, the cortical tension can be calculated based on the Sneddon model of elasticity (Sneddon, 1965).

Cells were plated on glass-bottom tissue culture dishes, when they reached 70% confluency they were treated with 10µM MG132 to increase the number of mitotic cells for analysis. The AFM experiments were kindly performed and analysed by Malti Vaghela in the laboratory of Guillaume Charras at University College London. Measurement of cortical tension/elasticity was recorded in mitotic cells in a monolayer (Figure 5.2 B). Measurement of cortical tension/elasticity in both the MCF10A and HaCaT cell lines increased significantly in the E-cadherin knockout cell lines (Figure 5.2 A). This confirmed that loss of E-cadherin was sufficient to increase cortical contractility as expected.

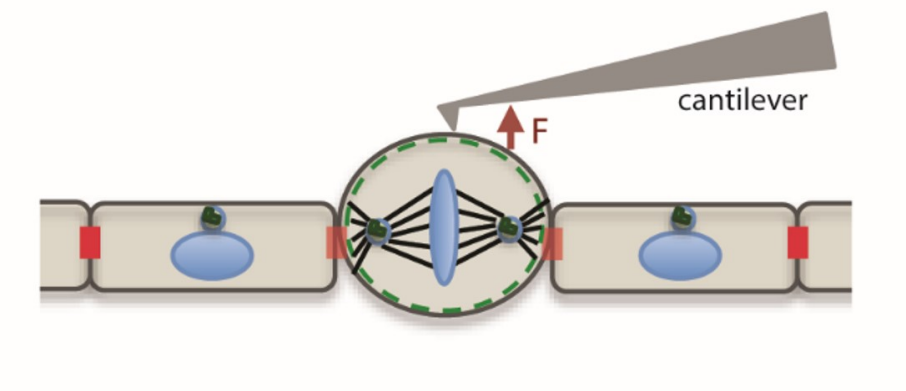

Figure 5.1: Atomic force microscopy
Schematic of atomic force microscopy. A cantilever is lowered with a known force onto a mitotic cell. A laser aimed down the cantilever then detects deflection of the cantilever upon contact with the cell. From the deflection, the cortical tension can be calculated based upon the Sneddon model of elasticity.

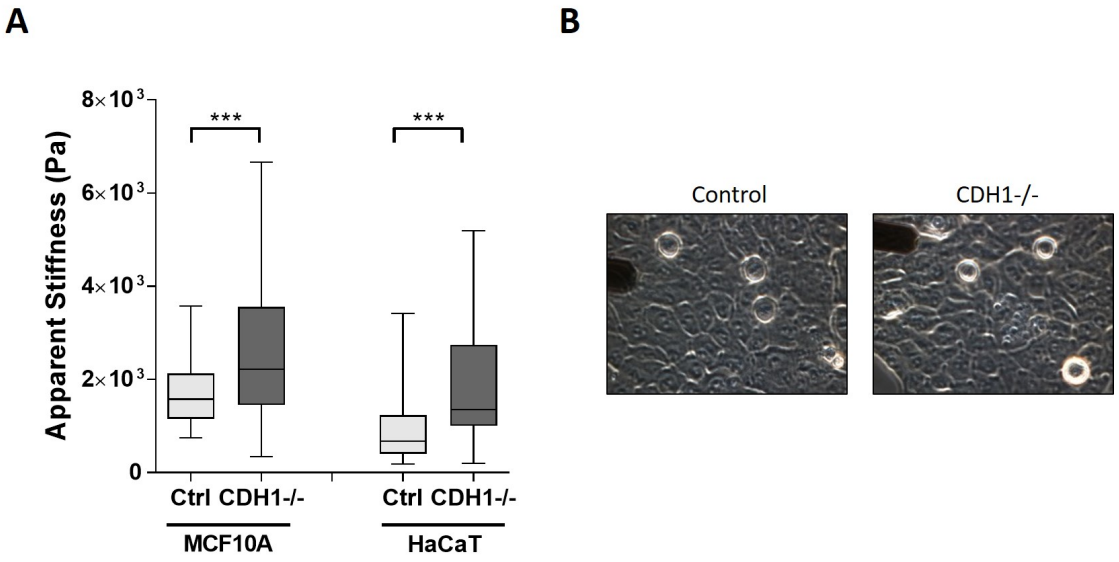

Figure 5.2: Loss of E-cadherin increases cortical tension/stiffness in a monolayer
A) Quantification of cortical elasticity/tension based on the Sneddon model in MCF10A and HaCaT control and *CDH1-/-* cell lines in a 70% confluency monolayer. Cells were treated with 10µM MG132 for 2 hours prior to analysis. Loss of E-cadherin increases cortical stiffness/tension. Data are 25-75th percentile with the median, where the whiskers represent minimum and maximum measurements. N = 14 individual cells, with 4 measurements per cell. Data analysed using two-way ANOVA with Šidák post-hoc test. *** $p<0.001$. **B)** Representative images of MCF10A and MCF10A *CDH1-/-* cell lines within the AFM. Measurements were taken of mitotic cells. The cantilever can be observed on the left-hand side of each image, this was then located over the cell to be quantified.

As the proposed hypothesis relies on E-cadherin at cell-cell junctions, it was therefore predicted that in single cells where E-cadherin does not localise, the tension/elasticity would not vary between the control and *CDH1-/-* cell lines. To test this, AFM was performed on single cells. As expected, no significant difference was observed between the two conditions (Figure 5.3). This supported that there is an increase in cortical tension due to a loss of E-cadherin at the cell cortex.

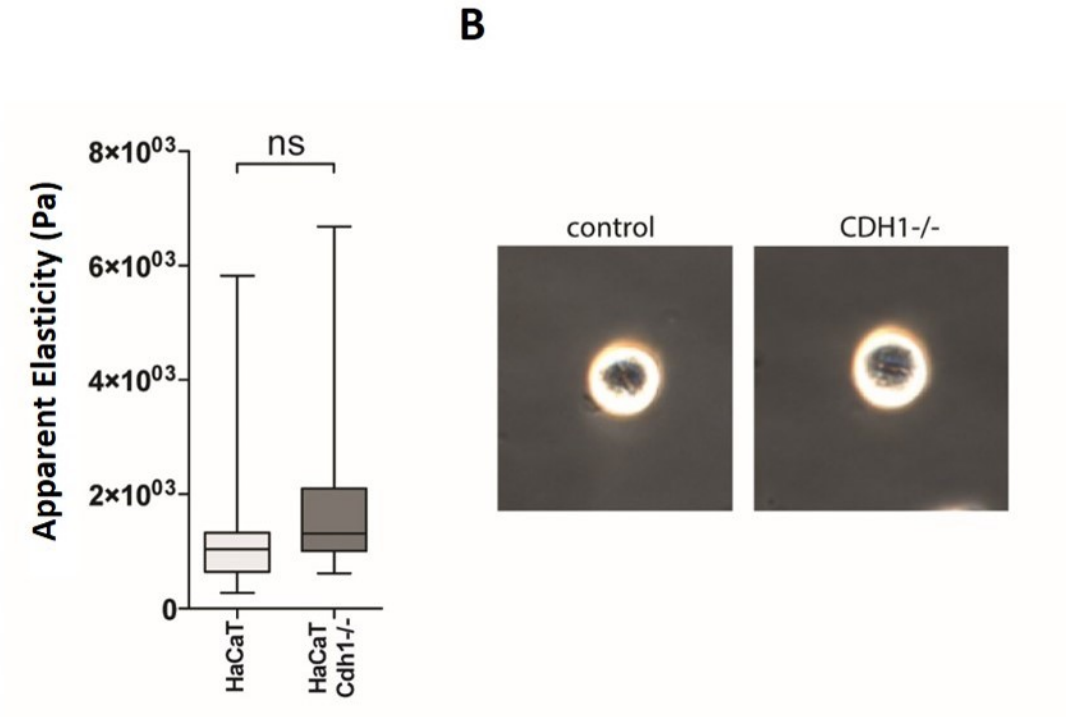

Figure 5.3: Loss of E-cadherin does not increase cortical tension/stiffness in single cells
A) Quantification of cortical tension/elasticity based on the Sneddon model in HaCaT control and *CDH1-/-* cell lines single mitotic cells. Cells were treated with 10µM MG132 for 2 hours prior to analysis. No significant difference is observed between E-cadherin proficient and knockout cell lines. Data are 25-75th percentile with the median, where the whiskers represent minimum and maximum measurements. N = 14 individual cells, with 4 measurements per cell. Data analysed using Student's t-test. **B)** Representative images of HaCaT and HaCaT *CDH1-/-* cells within the AFM. Single cells during metaphase, as identified by the metaphase plate were measured.

5.2 Change in centrosome clustering is not due to change in cell rounding

Having identified that E-cadherin loss increases cortical tension/contractility, to test that these changes did not affect cell rounding, which may have played a role on the centrosome clustering efficiency, the ratio of length vs width was measured in mitotic cells (Figure 5.4). No change in mitotic rounding was identified upon loss of E-cadherin in both the MCF10A and HaCaT cell lines, suggesting that the increase in centrosome clustering efficiency is not due to cell rounding changes (Figure 5.4).

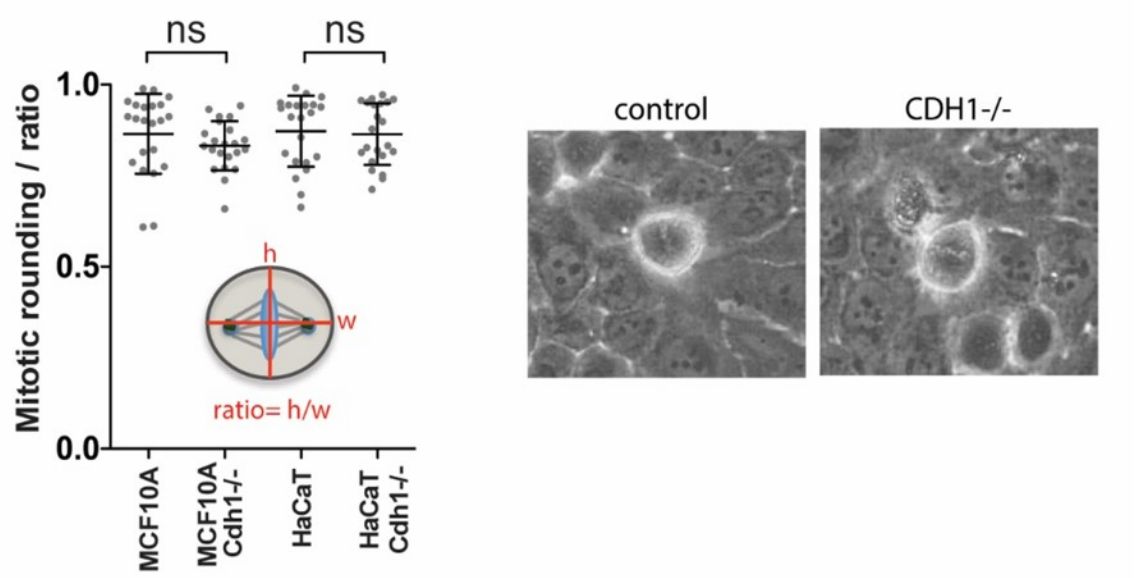

Figure 5.4: Knockout of E-cadherin does not affect cell rounding in mitosis
Cell rounding was quantified by measuring the ratio of the length (h) over width (w) in mitotic cells, identified by a metaphase plate by brightfield microscopy. No significant differences were identified after E-cadherin knockout in MCF10A and HaCaT cell lines. Data are mean ± SD, n = 30 individual cells. Data analysed using two-way ANOVA with Šidák post-hoc test.

5.3 Perturbing cortical contractility impairs centrosome clustering

To test if efficient centrosome clustering requires cortical contractility, a number of different drug treatments were used to alter contractility.

5.3.1 Blebbistatin inhibition of cortical contractility impairs centrosome clustering

Blebbistatin is a MyoII inhibitor resulting in decreased cortical contractility. Cells were treated with 50µM blebbistatin for 4 hours prior to fixation. As blebbistatin inhibits MyoII, which is required for the formation of the cytokinetic furrow, cells were unable to enter cytokinesis and were therefore analysed at telophase (Figure 5.5 A). In all of the cell lines treated with blebbistatin, centrosome clustering was impaired, resulting in ~30% of cells being able to cluster (Figure 5.5 B). Any advantage that loss of E-cadherin gave to MCF10A and HaCaT cells in clustering supernumerary centrosomes was lost upon inhibition of cortical contractility, supporting that this additional contractility is a key driver in centrosome clustering.

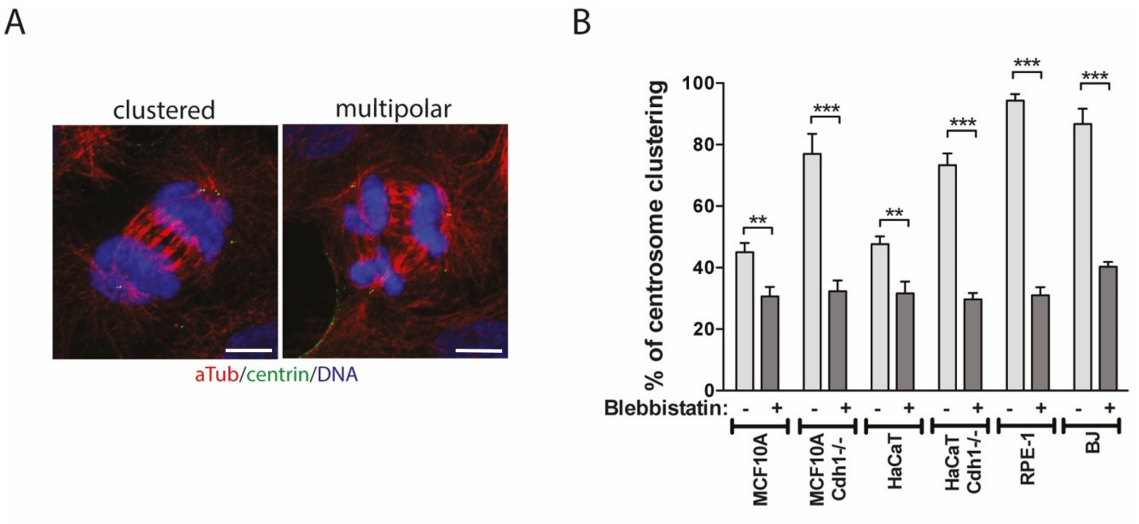

Figure 5.5: Blebbistatin inhibition of cortical contractility impairs centrosome clustering
A) 2D immunofluorescence microscopy images of MCF10A cells treated with 50µM blebbistatin for 4 hours. Cells were quantified at telophase as blebbistatin impairs the formation of the cytokinetic furrow. **B)** Quantification of centrosome clustering in cells treated with 50µM blebbistatin for 4 hours pre-fixation in cells where supernumerary centrosomes were generated by DCB treatment. Blebbistatin resulted in significant decrease of centrosome clustering to a basal level of ~30%. Data are mean ± SD, n = 150 individual cells, 50 per experiment at telophase. Data analysed using two way ANOVA with Šidák post-hoc test.. ** p<0.01, *** p<0.001. Scale bar = 10µM.

5.3.2 ROCK1 inhibition impairs centrosome clustering

To further confirm the importance of cortical contractility on centrosome clustering, the ROCK1 inhibitor Y-27632 dihydrochloride was used. Cells were treated with 10µM Y-27632 dihydrochloride for 4 hours before fixation and quantified at telophase as per the blebbistatin treated cells. Supporting the blebbistatin results, there was a significant reduction of centrosome clustering to the basal level of ~30% in all cell lines tested (Figure 5.6). This basal level of centrosome clustering suggested that there are other mechanisms independent of cortical contractility that enable cells to cluster, however cortical contractility is important in enabling a large proportion of cells to cluster efficiently.

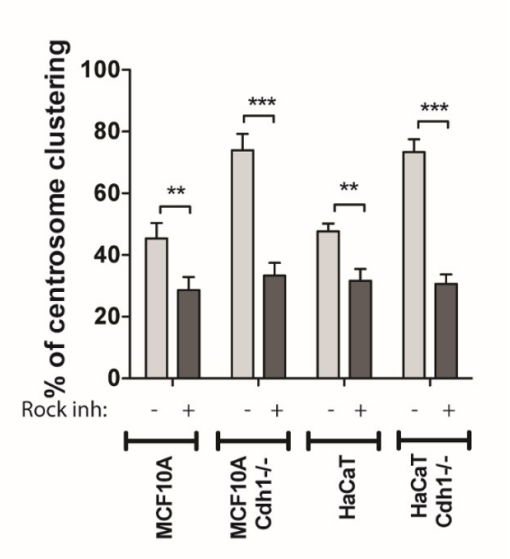

Figure 5.6: ROCK1 inhibition impairs centrosome clustering
Quantification of centrosome clustering in cells treated with 10µM Y-27632 dihydrochloride for 4 hours pre-fixation in cells where supernumerary centrosomes were generated by DCB treatment. Y-27632 dihydrochloride resulted in a significant decrease of centrosome clustering to a basal level of ~30%. Data are mean ± SD, n = 150 individual cells, 50 per experiment at telophase. Data analysed using two way ANOVA with Šidák post-hoc test. ** $p<0.01$, *** $p<0.001$.

5.3.3 Calyculin-A treatment increases centrosome clustering in epithelial cells

In contrast to the blebbistatin and Y-27632 dihydrochloride treatment, which impairs cortical contractility, Calyculin-A was used to determine if increasing cortical contractility in epithelial cells would enable them to cluster supernumerary centrosomes more efficiently. Calyculin-A is a natural product which was originally isolated from the marine sponge *Discodermia calyx* (Ishihara *et al.*, 1989). Calyculin-A is a potent phosphatase inhibitor and therefore increases the levels of phosphorylated proteins, including the accumulation of p-MLC (phosphorylated myosin light chain) which is involved in increasing cortical contractility. MCF10A and HaCaT cells were treated with 1µM Calyculin-A for 2 hours. Both cell lines showed significantly increased centrosome clustering after Calyculin-A treatment (Figure 5.7). This data combined with the blebbistatin and Y-27632 dihydrochloride data suggests that an increase in cortical contractility is sufficient to increase centrosome clustering efficiency within epithelial cells. This observation that increased corticial contracility improves centrosome clustering supports the hypothesis that that low cortical contractility observed in epithelial cells compromises efficient clustering.

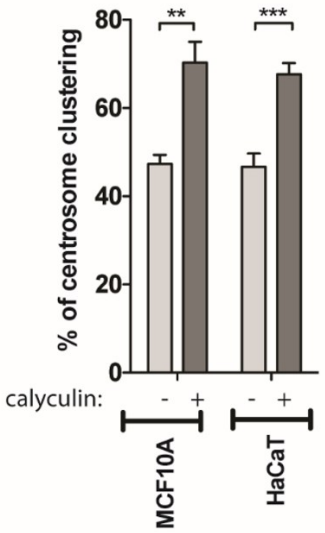

Figure 5.7: Calyculin-A treatment increases centrosome clustering in epithelial cells
Quantification of centrosome clustering in cells treated with 1µM Calyculin-A for 2 hours pre-fixation in epithelial cells where supernumerary centrosomes were generated by DCB treatment. Calyculin-A treatment results in an increase in centrosome clustering. Data are mean ± SD, n = 150 individual cells, 50 per experiment at telophase. Data analysed using two-way ANOVA with Šidák post-hoc test. ** $p<0.01$, *** $p<0.001$.

5.4 Increased cortical contractility results in closer centrosomes at metaphase

After demonstrating that cortical contractility is important for centrosome clustering, it was hypothesised that increased cortical contractility brings centrosomes in closer proximity, which then enables clustering. To test this hypothesis, the angle between the closest centrosomes in tripolar metaphase spindles were measured in MCF10A and HaCaT cells, with and without E-cadherin (Figure 5.8 A). The rosette plots are a graphical representation of the number of cells with a certain angle from 0-120° (Figure 5.8 B and C). In epithelial cells without E-cadherin the centrosomes are closer together than in E-cadherin expressing cells (Figure 5.8 B and C, top). This difference in proximity is lost upon the addition of blebbistatin which perturbs MyoII contractility, supporting the hypothesis that contractility is required for centrosomes to be within closer proximity and that this proximity allows them to be clustered (Figure 5.8 B and C).

To further test the importance of cortical contractility on the proximity of supernumerary centrosomes in tripolar metaphase spindles, the ROCK1 inhibitor, Y-27632 dihydrochloride (ROCKi) was used. Similarly to blebbistatin treatment, perturbing ROCK1-mediated contractility resulted in centrosomes being further apart, in both the MCF10A *CDH1-/-* and HaCaT *CDH1-/-* cell lines (Figure 5.9 A). Conversely, to test if increased cortical contractility could bring centrosomes together in epithelial cells, Calyculin A treatment was used. Increased cortical contractility resulted in the centrosomes being in closer proximity, as analysed by the angles between extra centrosomes in both the MCF10A and HaCaT cell lines (Figure 5.9 B). Altogether these data suggest that cortical contractility is required to bring centrosomes into closer proximity, and it is the increased cortical contractility which enables to centrosomes to cluster in the absence of E-cadherin.

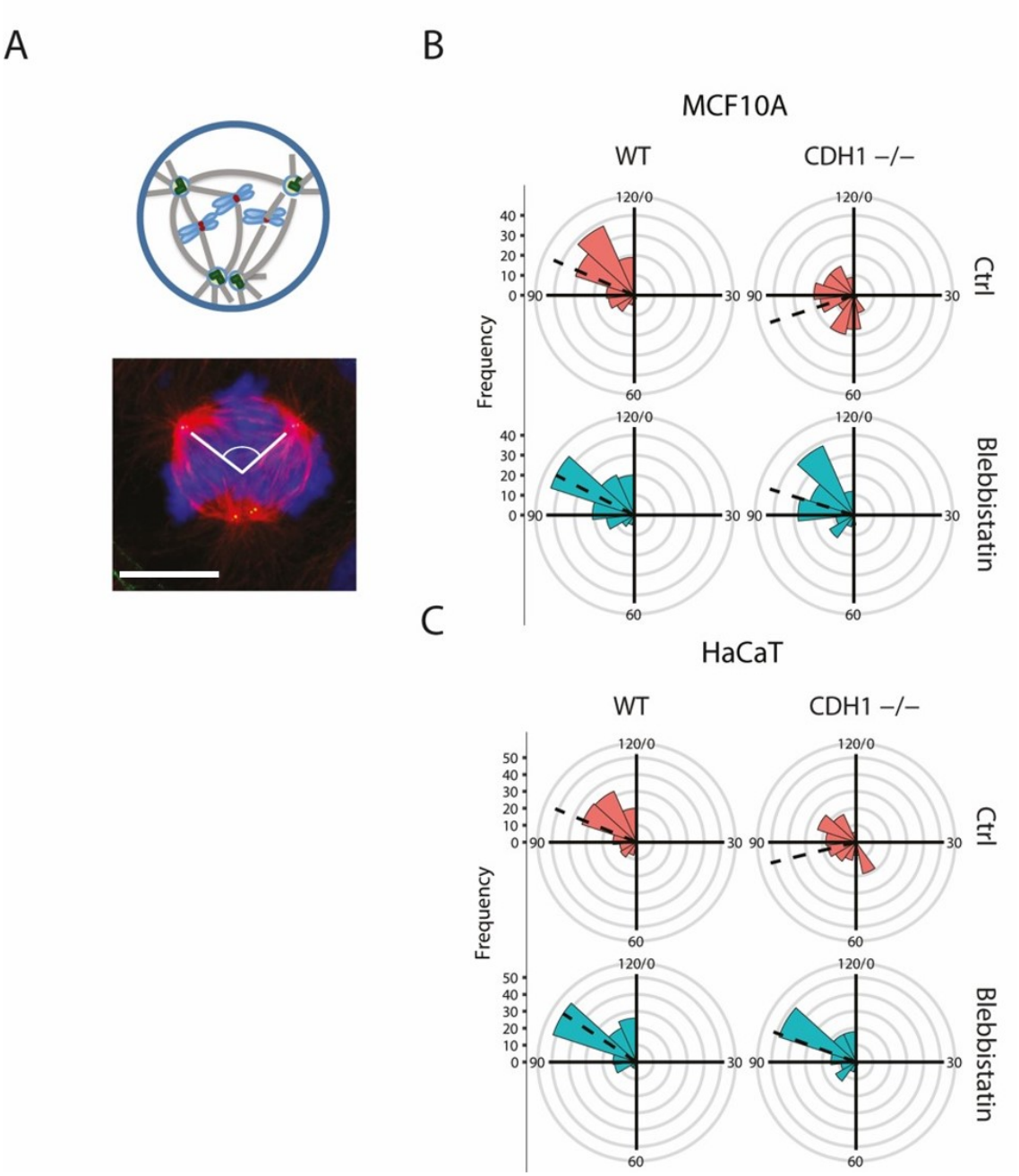

Figure 5.8: E-cadherin loss in epithelial cells results in closer proximity centrosomes, which requires cortical contractility
A) Representative 2D immunofluorescence microscopy image of a MCF10A cell undergoing a tripolar division with supernumerary centrosomes induced by DCB treatment. Overlaid is a representation of how angles were measured between the closest centrosomes. Scale bar = 10µM. **B)** and **C)** Quantification of the number of cells in MCF10A (B) and HaCaT (C) with angles measured between the closest centrosomes in tripolar metaphases from 0-120°, each bar represents a division of 5°. n = 150 individual cells, 50 per experiment, overlaid black bar = mean. Supernumerary centrosomes were induced by DCB treatment. Red bars represent control cells, green bars represent 4 hours 50µM blebbistatin treatment pre-fixation. *CDH1-/-* cells have closer proximity centrosomes than E-cadherin expressing cells, this observation is lost upon the perturbation of MyoII contractility by blebbistatin.

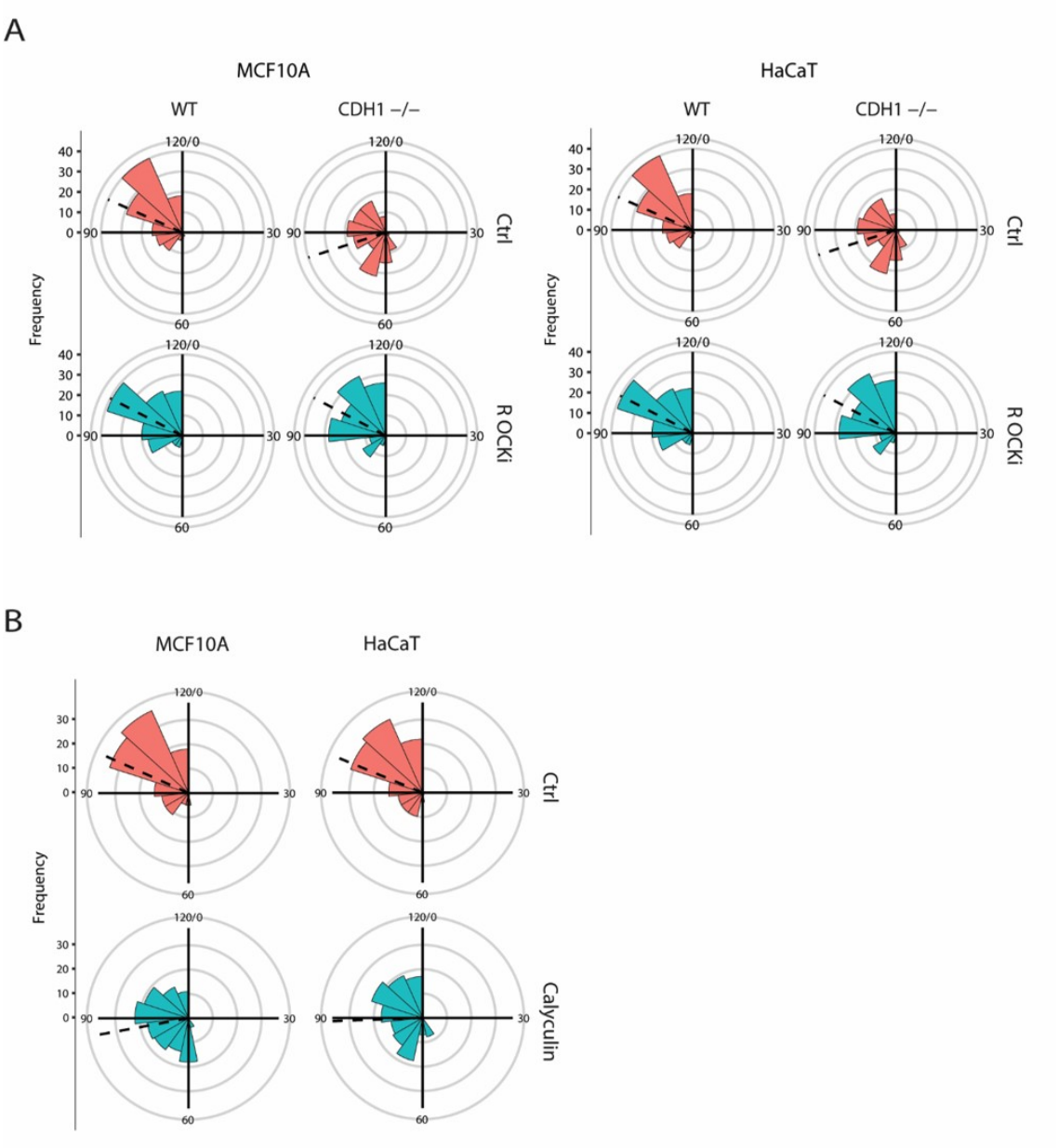

Figure 5.9: Cortical contractility is required to bring centrosomes into closer proximity

A) Quantification of the number of cells in MCF10A and HaCaT cell lines with angles measured between the closest centrosomes in tripolar metaphases from 0-120°, each bar represents a division of 5°. Supernumerary centrosomes were induced by DCB treatment. Red bars represent control cells, green bars represent 4 hours treatment with 10µM ROCK1 inhibitor (ROCKi) pre-fixation. *CDH1-/-* cells have closer proximity centrosomes than E-cadherin expressing cells, this observation is lost upon the perturbation of contractility by ROCKi. **B)** Quantification of angles in tripolar metaphases in MCF10A and HaCaT cells treated with 1µM Calyculin-A. Increase of contractility by the addition of Calyculin-A leads to closer proximity supernumerary centrosomes. n = 150 individual cells, 50 per experiment, overlaid black bar = mean.

5.5 Astral microtubules are important for centrosome clustering

It has previously been shown that cortical forces are transmitted to the centrosomes via astral microtubules (Rosenblatt *et al.*, 2004; Théry *et al.*, 2005). Alongside this astral microtubules have previously been implicated in centrosome clustering, but the mechanism has not been explored (Kwon *et al.*, 2008). It was therefore hypothesised that astral microtubules play a role in translating the cortical contractility in *CDH1-/-* cells to facilitate centrosome clustering. To test this low doses of nocodazole (5nM), which depolymerise astral microtubules whilst allowing for the formation of the mitotic spindle, were used for 3 hours prior to fixation. EB1 staining which identifies the ends of growing microtubules, suggests a depletion in astral microtubules upon nocodazole treatment (Figure 5.10 A). Upon addition of nocodazole and the disruption of astral microtubules, centrosome clustering was significantly impaired in the MCF10A and HaCaT cells lines, both with and without E-cadherin (Figure 5.10 B). The cells clustered to the basal level of ~30%, similar to the results observed upon addition of blebbistatin or the ROCK1 inhibitor. When examining the distance of the closest centrosomes in tripolar metaphases, depletion of the astral microtubules impaired centrosomes moving closer in the *CDH1-/-* cell lines (Figure 5.10 C). These data suggest that astral microtubules play a role in translating the cortical forces to the centrosomes, allowing them to move in closer proximity.

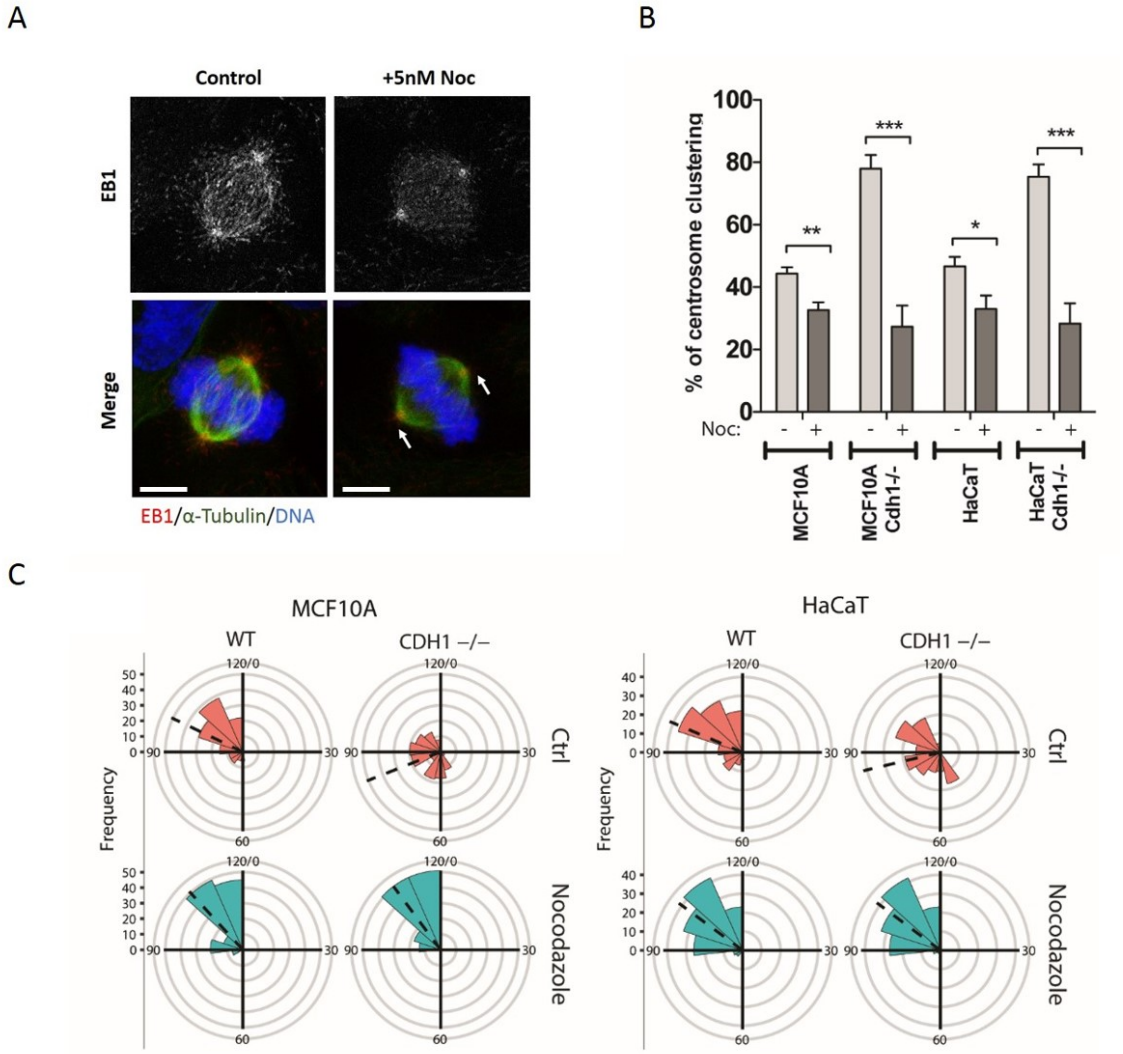

Figure 5.10: Astral microtubules transmit cortical forces to the centrosomes

A) 2D immunofluorescence microscopy in HaCaT cells. Left panel shows growing astral microtubules as visualised by EB1 staining. Right panel shows cells after 3 hours treatment with 5nM nocodazole, resulting in a loss of astral microtubules, shown by a depletion of EB1 at the spindle poles (identified by the arrows) Scale bar = 10µM. **B)** Quantification of centrosome clustering, which decreases upon loss of astral microtubules in nocodazole treated cells. Supernumerary centrosomes were generated by DCB treatment. Data are mean ± SD, n = 150 individual cells, 50 per experiment. Data analysed using two way ANOVA with Šidák post-hoc test., * $p<0.05$, ** $p<0.01$, ** $p<0.001$. **C)** Quantification of angles in tripolar metaphase spindles in MCF10A and HaCaT cells treated with 5nM nocodazole. Loss of astral microtubules results in a reduction in closer proximity supernumerary centrosomes. n = 150 individual cells, 50 per experiment, overlaid black bar = mean smallest angle in tripolar metaphases.

5.6 HSET is important for centrosome clustering independently of E-cadherin loss

As the kinesin HSET, a minus-end directed microtubule motor has already been identified as a requirement for centrosome clustering (Basto *et al.*, 2008; Kwon *et al.*, 2008), it was hypothesised that the closer proximity of centrosomes, facilitated by the increase in cortical contractility, could then allow for HSET to be able to cluster them. To confirm that HSET was required for centrosome clustering, HSET was knocked down by siRNA in control and *CDH1-/-* MCF10A and HaCaT cell lines (Figure 5.11 B). The analysis of centrosome clustering showed that depletion of HSET prevented centrosome clustering in all cell lines, independently of E-cadherin expression, leading to a basal level of ~10%, the lowest level of centrosome clustering observed (Figure 5.11 A).

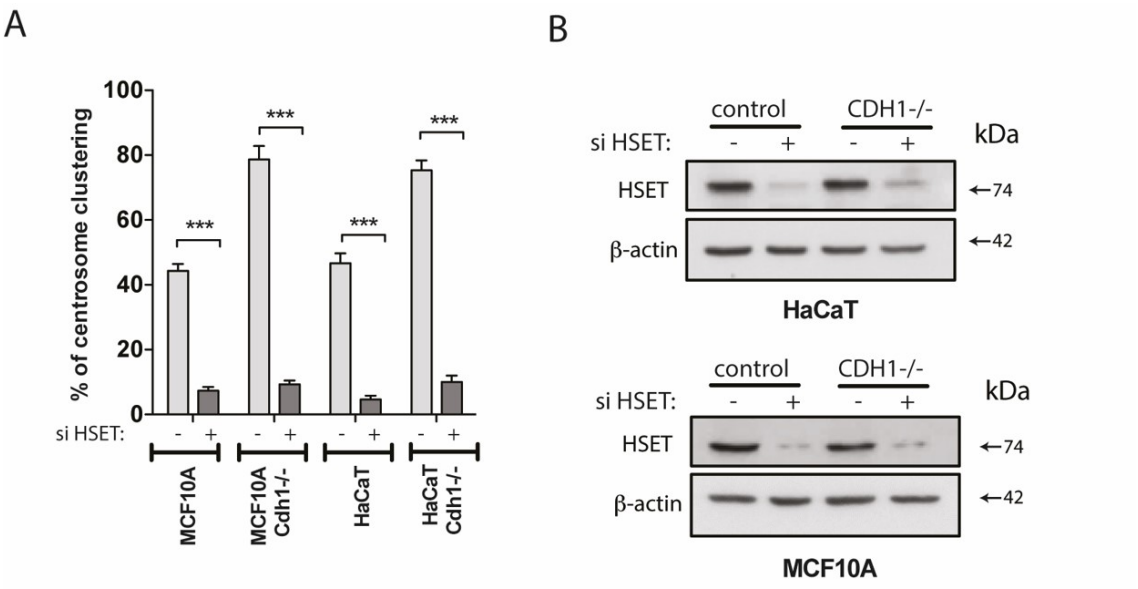

Figure 5.11: The kinesin is required for centrosome clustering, independently of E-cadherin expression
A) Centrosome clustering is impaired upon depletion of HSET by siRNA, independently of E-cadherin levels. Supernumerary centrosomes were induced by DCB treatment. Data are mean ± SD, n = 150 individual cells, 50 per experiment at cytokinesis. Data analysed using two way ANOVA with Šidák post-hoc test, *** $p<0.001$. **B)** Western blot analysis of cells treated with siNegative (control) and on-TARGET SMARTpool siRNA against HSET. Cells were analysed at 72 hours post transfection. β-actin was used as a loading control.

When examining the effect of knockdown of HSET by siRNA on the proximity of supernumerary centrosomes, no change on the smallest angle distribution in tripolar metaphases was observed, unlike with changes in contractility (Figure 5.12). This suggests that through the increased cortical contractility centrosomes are still able to move closer to each other, but due to the lack of HSET, these centrosomes cannot be clustered. This could explain why the presence of HSET is not by itself enough to enable supernumerary centrosomes to cluster efficiently.

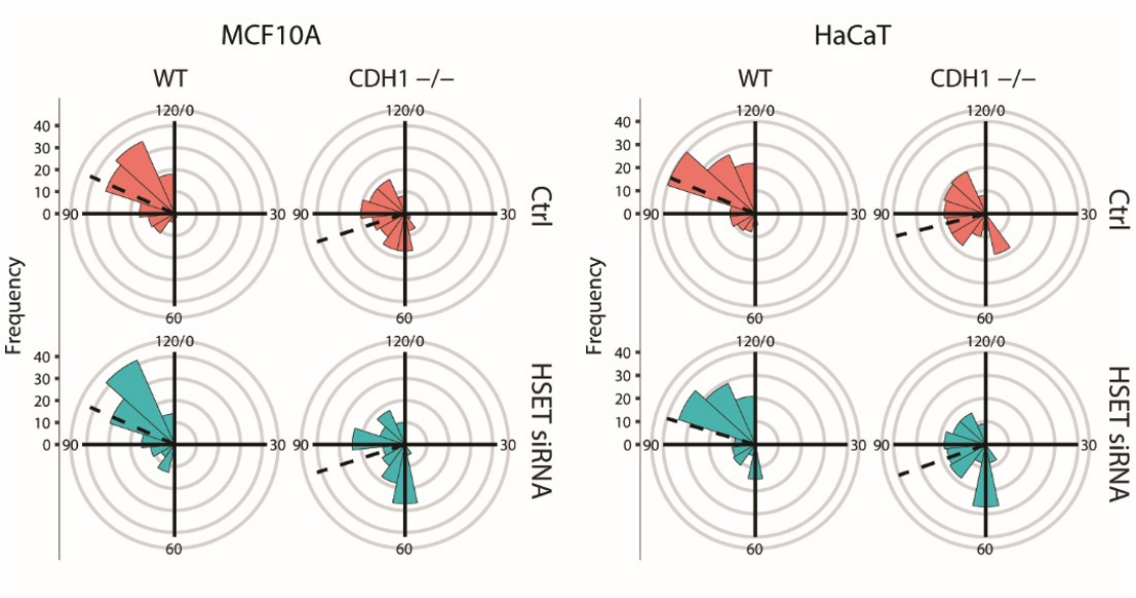

Figure 5.12: Knockdown of HSET does not affect centrosome proximity in tripolar metaphases
Quantification of the number of cells in MCF10A and HaCaT cell lines with angles measured between the closest centrosomes in tripolar metaphases from 0-120°, each bar represents a division of 5°. n = 150, overlaid black bar = mean. Supernumerary centrosomes were induced by DCB treatment. Red bars represent control cells, green bars represent HSET knockdown by siRNA. HSET deletion does not affect the smallest angle distribution in tripolar metaphases.

5.7 High centrosome number per cell increases centrosome clustering efficiency

Based on these observations, it was proposed that the cortical contractility is required for bringing centrosomes close enough together for HSET to then enable the clustering. From this model, it was then suggested that if there was a large number of supernumerary centrosomes, which were then in close proximity, centrosome clustering would be efficient, independent of cortical contractility. In order to

investigate this hypothesis, supernumerary centrosomes were generated by PLK4 overexpression controlled by the pInducer vector, which generates a larger number of supernumerary centrosomes per cell. pInducer is a tetracycline-inducible system similar to that of the tetracycline repressor (Meerbrey *et al.*, 2011). MCF10A cells were transfected with lentivirus expressing pInducer.PLK4. Positively transfected cells were identified by cell sorting for GFP, expressed as part of the pInducer vector. To determine if the pInducer may be altering centrosome clustering efficiency, centrosome clustering was measured after generation of supernumerary centrosomes by DCB treatment in MCF10A, MCF10A.TetR.PLK4 and MCF10A.pInducer.PLK4 in the absence of Dox. Unlike the TetR cell line, the pInducer cell line behaved as per the control, suggesting that the pInducer does not affect centrosome clustering (Figure 5.13).

Having identified that the pInducer expression does not affect centrosome clustering in the same way as the tetracycline repressor (Section 3.5.1, Figure 3.10), centrosome clustering was quantified after PLK4 overexpression. MCF10A.pInducer.PLK4 cells were treated with 2µg/ml Dox for 48 hours. As hypothesised, these cells were able to cluster their supernumerary centrosomes with high efficiency (~90%), compared to ~40% with DCB treatment, and ~60% with TetR.PLK4 (Figure 5.14 A). This correlated with the large level of centrosome amplification per cell (Figure 5.14 B). Quantification of centriole number per cell showed that in DCB treated cells the mean number of centrioles measured at metaphase was ~6, whereas this increased to ~18 in the pInducer.PLK4 cells, with the TetR.PLK4 having ~12 (Figure 5.14 B).

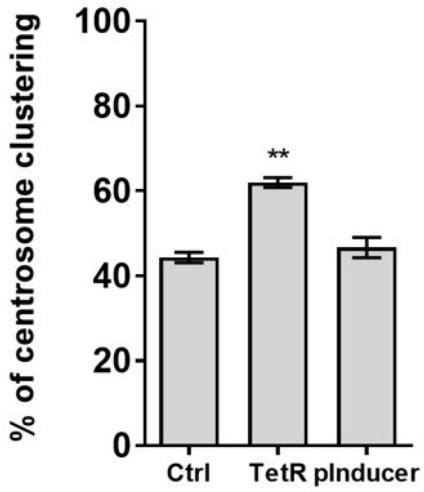

Figure 5.13: pInducer expression does not affect centrosome clustering Quantification of centrosome clustering measured after generation of supernumerary centrosomes by DCB treatment in MCF10A, MCF10A.TetR.PLK4 (TetR) and MCF10A.pInducer.PLK4 (pInducer) in the absence of doxycycline. Without doxycycline, the TetR expressing cells are more efficient at clustering their supernumerary centrosomes compared to controls, there is no significant difference observed between pInducer PLK4 cells and controls. Data are mean ± SD, n = 150 individual cells, 50 per experiment at cytokinesis. Data analysed using one way ANOVA with Tukey post-hoc test, ** $p<0.01$.

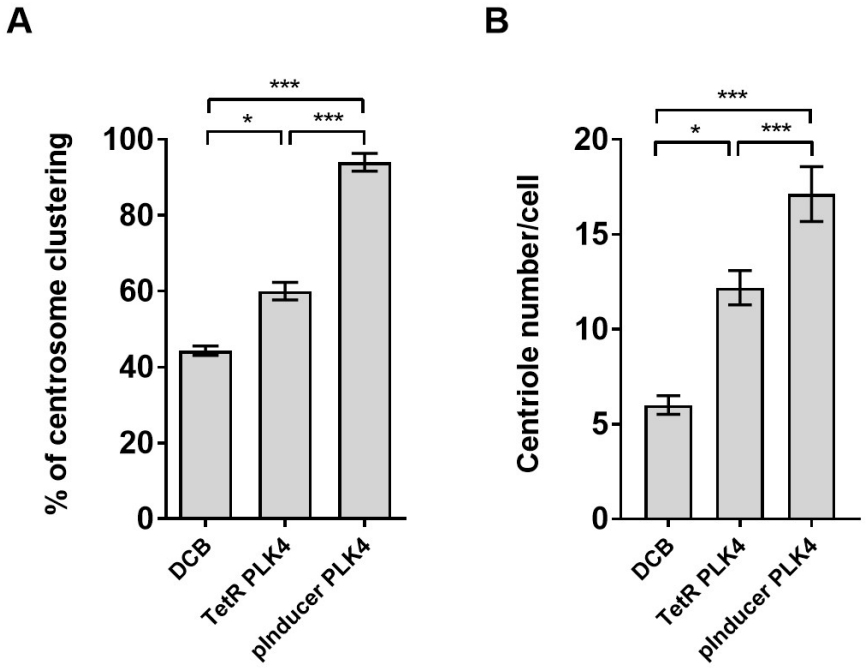

Figure 5.14: Centrosome clustering and centrosome number increase in pInducer.PLK4 cells
A) Quantification of centrosome clustering in MCF10A after DCB treatment, and MCF10A.TetR.PLK4 and MCF10A.pInducer.PLK4 are treatment with 2µg/ml Dox for 48 hours. Data are mean ± SD, n = 150 individual cells, 50 per experiment at cytokinesis. **B)** Centriole number quantified in MCF10A after DCB treatment, and MCF10A.TetR.PLK4 and MCF10A.pInducer.PLK4 are treatment with 2µg/ml doxycycline for 48 hours. Data are mean ± SD, n = 150 individual cells, 50 per experiment at metaphase. Data analysed using one way ANOVA with Tukey post-hoc test, * $p<0.05$, ** $p<0.01$, *** $p<0.001$.

To try and reduce the efficiency of generating supernumerary centrosomes, the level of Dox was titrated. MCF10A.pInducer.PLK4 cells were treated with 0.5-2µg/ml Dox for 48 hours, the Dox was then washed out for 24-72 hours and centriole number quantified. Even at the lowest dosage of Dox (0.5µg/ml) and 72 hours post washout the high level of centrosome number was still observed, therefore variation of Dox was not sufficient to control the level of centrosome number (Figure 5.15).

Whilst the attempted titration of Dox did not significantly reduce centrosome number, an alternative method of using SAS-6 siRNA to reduce centrosome number was used. SAS-6 is required for centrosome duplication, and has previously been described to abrogate centrosome overduplication (Leidel *et al.*, 2005). Supernumerary centrosomes were generated in MCF10A.pInducer.PLK4 cells upon treatment with 2µg/ml of Dox for 48 hours, cells were then treated with SAS-6 siRNA for 72 hours. Quantification of centrosome number showed that under these conditions

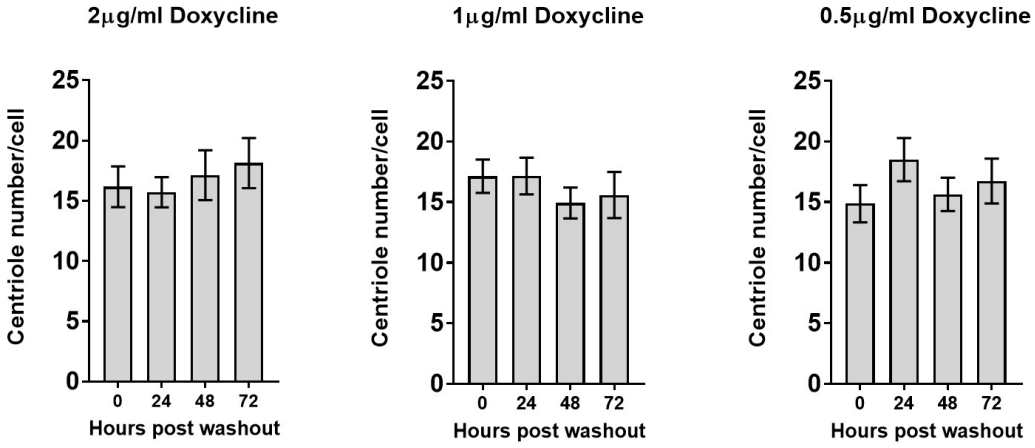

Figure 5.15: Titration of doxycycline does not significantly affect centrosome number in pInducer.PLK4 cells
Centriole number quantified in MCF10A.pInducer.PLK4 after treatment with 0.5-2μg/ml doxycycline for 48 hours. Doxycycline was washed out, and cells were incubated for 24-72 hours. Data are mean ± SD, n = 150 individual cells, 50 per experiment at metaphase. Data analysed using one way ANOVA with Tukey post-hoc test.

centrosome number reduces to ~6, the same as under DCB treatment (Figure 5.16 A and B). Analysis of centrosome clustering further showed that under these conditions centrosome clustering reflects the low level of centrosome clustering efficiency observed with DCB treatment at ~40% (Figure 5.16 C). These data support that the increased clustering efficiency in the MCF10A.pInducer.PLK4 observed is due to the high levels of centrosome amplification, but when centrosome number is lower, centrosome clustering is similar to the clustering efficiency observed in DCB treated cells, this is hypothesised to be due to the proximity of the centrosomes, enabling HSET to facilitate centrosome clustering.

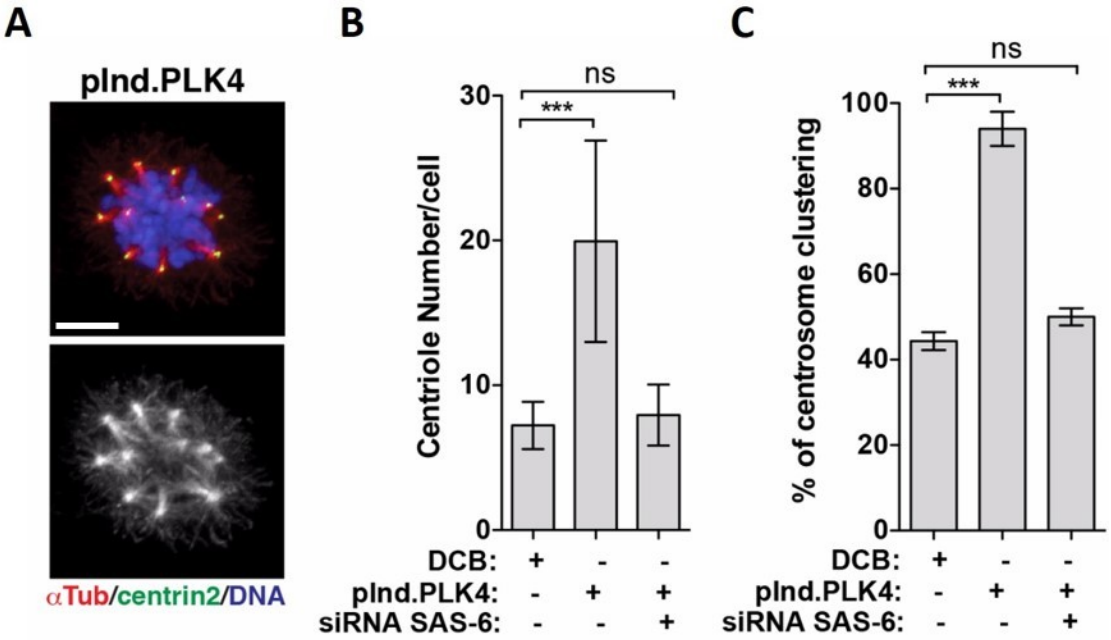

Figure 5.16: Lower levels of centrosome amplification in MCF10A.pInducer.PLK4 leads to lower efficiency of centrosome clustering

A) Immunofluorescence images depicting examples of MCF10A.pInduer.PLK4 after 48h Dox treatment showing high levels of centrosome amplification. Top – merge, Bottom – α-tubulin. Scale bar = 10µM. **B)** Quantification of centriole number in MCF10A with DCB treatment and MCF10A.pInducer.PLK4 with 2µg doxycycline, with and without 72 hours SAS-6 siRNA treatment. SAS-6 siRNA treatment reflects the centrosome number observed with DCB treatment. Data are mean ± SD, n = 150 individual cells, 50 per experiment at metaphase. **C)** Quantification of centrosome clustering in MCF10A with DCB treatment and MCF10A.pInducer.PLK4 with 2µg doxycycline, with and without 72 hours SAS-6 siRNA treatment. SAS-6 siRNA treatment reflects the centrosome clustering efficiency observed with DCB treatment. Data are mean ± SD, n = 150 individual cells, 50 per experiment at cytokinesis. Data analysed using one way ANOVA with Tukey post-hoc test. *** $p<0.001$.

5.8 Discussion

In epithelial cells, downregulation of cortical contractility is achieved via inhibition of the RhoA-ROCK pathway downstream of E-cadherin (Hidalgo-Carcedo *et al.*, 2011). Because E-cadherin cell junctions are maintained during mitosis and play a role in the orientation of the mitotic spindle (Baker and Garrod, 1993; den Elzen *et al.*, 2009), it was hypothesised that decreased cortical contractility impairs efficient clustering in epithelial cells. To test this atomic force microscopy (AFM) was used to measure cortical elasticity, which acts as a proxy for tension and stiffness. *CDH1-/-* cells were shown to have significantly higher cortical contractility than the E-cadherin control cells in a monolayer in both the MCF10A and HaCaT cell lines. Interestingly, this effect is lost when individual cells are quantified, suggesting that the formation of adherens junctions is required to decrease contractility, a process that depends on E-cadherin and DDR1.

Inhibition of cortical contractility through blebbistatin (a MyoII inhibitor) or a ROCK1 inhibitor treatments impaired centrosome clustering, particularly in cells that do not have E-cadherin, supporting a role for cortical contractility in driving efficient centrosome clustering. Similarly use of the broad phosphatase inhibitor Calyculin-A which results in increased p-MLC and therefore increased actomyosin contractility resulted in more efficient centrosome clustering.

The observation that the supernumerary centrosomes are closer in tripolar metaphases in *CDH1-/-* cells suggested that cortical contractility enables centrosomes to move in closer proximity, which then enables more efficient centrosome clustering. It is unclear how contractility promotes centrosome movement. One possibility is by regulating microtubule stability at the cortex. For example, RhoA, ROCK and myosin-dependent contractility were shown to promote microtubule destabilisation in different contexts (Palazzo *et al.*, 2001; Even-Ram *et al.*, 2007; Takesono *et al.*, 2010). Thus, it is possible that in epithelial cells, low contractility leads to increased astral microtubule stability thereby preventing centrosome movement. However, even in the absence of cortical contractility there is still a 30-40% chance that centrosomes can cluster, suggesting that in these cells the centrosomes are then close enough for clustering to occur independently of actoymyosin contractility.

A role for astral microtubules supporting centrosome clustering has previously been described, but the mechanism was not elucidated (Kwon *et al.*, 2008). The depletion of astral microtubules by low doses of nocodazole resulted in impaired centrosome clustering regardless of E-cadherin status, therefore indicating that

astral microtubules are important for translating the actomyosin contractility to the centrosomes enabling them to be within the closer proximity.

Depletion of HSET by siRNA results in a loss of centrosome clustering in both control and *CDH1-/-* cell lines, but does not affect the proximity of centrosomes in tripolar metaphases. These data suggest that HSET is still fundamentally required for centrosome clustering, however cortical contractility is required to bring the centrosomes within close enough proximity for HSET to facilitate the clustering. Therefore, whilst cells have the intrinsic mechanisms for centrosome clustering, adaptation is required to enable those mechanisms to work efficiently.

The data suggest that the role of cortical contractility in bringing centrosomes close enough together for HSET to cluster is the most fundamental part in cellular adaptation to supernumerary centrosomes. In the MCF10A.pInducer.PLK4 cell lines where high levels of centrosome amplification per cell were generated, these cells were able to cluster very efficiently regardless of their E-cadherin status. This would suggest that because there are so many centrosomes within the cell, they are already within proximity for HSET to then cluster them together. This was supported by use of SAS-6 siRNA to deplete centrosome number which confirmed that centrosome clustering can also be correlated to the level of supernumerary centrosomes per cell, with very high numbers, where they are in closer proximity clustering efficiently, whereas those with lower numbers and therefore further apart being less efficient. How the orientation and direction of this clustering occurs when there are so many supernumerary centrosomes is unknown. In these latter cases where centrosome number per cell is not as high it is then expected that cortical contractility is required to bring the centrosomes together for HSET to take over.

Chapter 6

Discussion

Whilst the mechanisms for centrosome clustering have previously been explored, these data show for the first time in human cells that not all cell types are inherently able to cluster. In particular, cells from an epithelial origin have inefficient clustering mechanisms and need to adapt to centrosome amplification in order to survive.

Previous work has shown a role for the spindle assembly checkpoint (SAC) in centrosome clustering, in allowing a longer time in metaphase, giving sufficient time for the centrosome clustering to occur before anaphase onset (Weaver and Cleveland, 2005; Nezi and Musacchio, 2009; Maresca and Salmon, 2010). Therefore, it was hypothesised that the MCF10A, HaCaT and J3B1A might have been able to cluster their supernumerary centrosomes more efficiently if given more time in metaphase. The proteasome inhibitor MG132 was used to prolong metaphase, and cells were quantified after MG132 washout. No improvement on centrosome clustering occurred, suggesting that the differences between the two groups of cells could not be attributed to time in mitosis, but must be due to another independent mechanism.

The kinesin HSET has previously been identified as being essential for centrosome clustering, by binding to microtubules and bringing the centrosomes together (discussed in more detail later) (Endow and Komma 1998; Basto *et al.* 2008; Kwon *et al.* 2008). To determine if varying levels of HSET may account for differences in centrosome clustering efficiency HSET levels were analysed by western blot analysis in the panel of cell lines. HSET was ubiquitously expressed between all six cell lines, therefore the level of HSET was not a limiting factor for centrosome clustering efficiency. Similarly, later work in the panel of 16 breast cancer cell lines showed that HSET was comparatively expressed, however, centrosome clustering efficiency varied between the cell lines. Therefore, whilst all cell lines expressed this essential component for centrosome clustering, there is still a further process of adaptation which must occur for a cell to efficiently cluster.

It was observed that the epithelial cell lines, expressing E-cadherin had impaired centrosome clustering compared to the fibroblast cell lines and RPE-1 which whilst

of an epithelial origin no longer expresses E-cadherin. Differences in the ability of cells with extra centrosomes to divide in a bipolar fashion have been previously observed in *Drosophila*, where epithelial cells in the developing wing disks have increased multipolar divisions when compared with neuroblasts upon SAK/PLK4 overexpression (Basto *et al.*, 2008; Sabino *et al.*, 2015). However, these differences are not due to centrosome clustering but rather centrosome inactivation, characterised by low centrosomal levels of pericentrin and γ-tubulin, which has been observed in flies with extra centrosomes (Basto *et al.*, 2008; Sabino *et al.*, 2015). Overexpression of moesin, the sole member of the conserved ezrin-radixin-moesin (ERM) family of proteins, in *Drosophila* wing disks with extra centrosomes impairs centrosome inactivation, leading to increased multipolar divisions in these cells (Sabino *et al.*, 2015). Nonetheless, no evidence of centrosome inactivation was observed in any of the cell lines upon centrosome amplification, and all extra centrosomes in multipolar or clustered spindles show similar levels of both pericentrin and γ-tubulin. In addition, the levels of ERM proteins were unchanged in epithelial cells with or without E-cadherin and did not correlate with the presence of centrosome amplification in a panel of breast cancer cell lines. It is possible that the prevalence of mechanisms that allow the formation of pseudobipolar spindles and survival of cells with supernumerary centrosomes varies between cell types and organisms. Indeed, while *Drosophila* neuroblasts cluster efficiently, induction of extra centrosomes in the mouse brain showed that not all neuronal stem cells can cluster extra centrosomes, leading to multipolar divisions and microcephaly (Basto *et al.*, 2008; Marthiens *et al.*, 2013). To test the role of E-cadherin in centrosome clustering siRNA, shRNA and CRISPR-Cas9 were used to deplete E-cadherin, resulting in increased centrosome clustering. Therefore, showing that expression of E-cadherin impairs centrosome clustering. This was supported in the RPE-1 cells where full-length E-cadherin was expressed resulting in impaired centrosome clustering.

Changes in centrosome clustering upon loss of E-cadherin were not due to epithelial to mesenchymal transition (EMT) as observed by no change in expression of EMT markers. Similarly, no effect on cell rounding was observed upon loss of E-cadherin.

Cortical contractility has previously been identified as being important in centrosome clustering, although the mechanism was not explored (Kwon *et al.*, 2008). Interestingly a link between E-cadherin and decreased cortical contractility has been previously described (Hidalgo-Carcedo *et al.*, 2011), therefore suggesting that E-cadherin may impair centrosome clustering through decreased cortical contractility. Hidalgo-Carcedo *et al.* reported that E-cadherin localises DDR1 to the cell-cell contacts where through a signalling cascade it impairs phosphorylation of MLC,

resulting in decreased contractility at the adherens junctions. They suggested that this was important in collective cell migration, where the impairment of cortical contractility as the adherens junctions was important for the maintenance of the cell-cell adhesion, allowing for cells to move together rather than apart (Hidalgo-Carcedo *et al.*, 2011). Interestingly, when comparing DDR1 levels in the panel of six cell lines, there was also a correlation of loss of DDR1 with increased centrosome clustering, which correlates with E-cadherin levels. This hypothesis was then supported using siRNA to deplete DDR1 which resulted in increased centrosome clustering in the epithelial cell lines.

The previous work by Hidalgo-Carcedo *et al.* reported that E-cadherin is involved in recruiting DDR1 to the cell membrane. Using calcium washout to deplete E-cadherin they observed a loss of DDR1 at the membrane, which was restored upon the re-addition of calcium and the return of E-cadherin to the membrane, from this they stated that E-cadherin therefore recruits DDR1 to the membrane (Hidalgo-Carcedo *et al.*, 2011). However, the observation in the E-cadherin knockout (*CDH1-/-*) cell lines, that DDR1 protein level is lost, draws this conclusion into question. It would appear that E-cadherin does not just play a role in recruitment of DDR1 to the membrane, but in its stabilisation, or indeed both its stabilisation and localisation. There was no difference in DDR1 mRNA, suggesting that E-cadherin does not control DDR1 transcription, but somehow regulates and stabilises the protein itself. Whether this is through E-cadherin directly stabilising DDR1 or through a signalling mechanism is still to be determined. One study has suggested that E-cadherin and DDR1 can directly bind in their extracellular domains, however this work was done with E-cadherin overexpression, and it is unknown if this binding may occur with endogenous proteins (Wang, Yeh and Tang, 2009). The hypothesis that E-cadherin leads to stabilisation and not just localisation of DDR1 is supported in the RPE-1 cell line, where expression of E-cadherin is sufficient to drive DDR1 protein expression. Conversely, DDR1 levels do not affect E-cadherin protein levels or its localisation as previously shown in the MDCK epithelial cell line (Hidalgo-Carcedo *et al.*, 2011). Thus, it is likely that regulation of contractility by DDR1, and not adherens junctions per se, is playing a role in centrosome clustering (Eswaramoorthy *et al.*, 2010).

The hypothesis linking E-cadherin and DDR1 to impaired centrosome clustering relied on decreased cortical contractility at the adherens junctions. To test this atomic force microscopy was done showing that there was increased cortical stiffness/tension in the *CDH1-/-* cell lines. This quantification works on the Sneddon model of elasticity, which is based on the observations of objects of a different shape being lowered into materials of known elasticity and then calculating the flex to establish

a model. However, this model has limitations as it assumes that the cantilever is being lowered onto an object (cell) with the same elasticity throughout. Therefore, whilst the Sneddon model is currently the standard used for quantifying elasticity within the field, further work is being undertaken to generate models which more accurately reflect the lipid bilayer with different elasticity at the cortex compared to the cytoplasm. Similarly, the Sneddon model would not take into account different parts of the cortex having different stiffness/tension such as junctions.

Whilst the pathway linking E-cadherin and DDR1 to the downregulation of pMLC is not fully understood, previous work suggests that DDR1 through Par3/Par6 may inactivate RhoA via the recruitment of the RhoA negative regulator p190RhoGAP, which in turn antagonise ROCK. Therefore, to test the role of this pathway on centrosome clustering siRNA was used to deplete p190RhoGAP in epithelial cells. No increase in centrosome clustering was observed, suggesting that p190RhoGAP is not involved in the regulation of centrosome clustering by E-cadherin and DDR1. DLC3 is another RhoA negative regulator, which localises to focal adhesions to regulate cell shape, however, similarly upon depletion by siRNA no effect on centrosome clustering was observed (Hendrick *et al.*, 2016). These observations would suggest that RhoA GAPs that control cortical contractility are not involved in centrosome clustering. RhoE, which can directly inhibit ROCK through direct binding, was shown to control cortical contractility downstream of DDR1. RhoE may then directly impair ROCK preventing actomyosin contractility (Riento *et al.*, 2003) (Figure 6.1). It is therefore suggested that DDR1 may potentially directly regulate RhoE, rather than through a RhoA regulator. Nevertheless, it is possible that RhoA may play a role, and this could be tested using siRNA or a RhoA inhibitor.

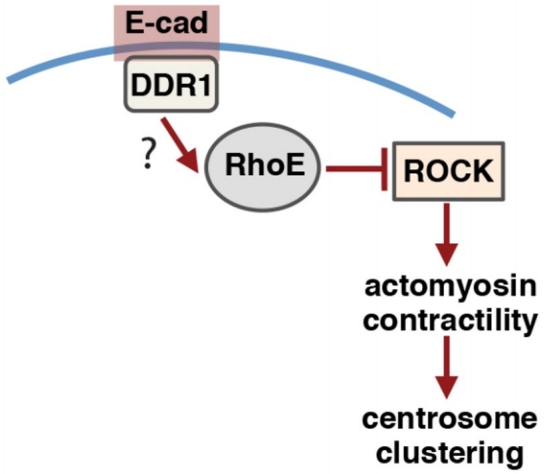

Figure 6.1: Regulation of cortical contractility through RhoE
Schematic representation of RhoE mediated regulation of cortical contractility downstream of E-cadherin. RhoE may directly impair ROCK leading to increased actomyosin contractility leading to increased centrosome clustering efficiency.

Based on the observations of E-cadherin and DDR1's regulation of cortical contractility impairing centrosome clustering, and the required role of HSET and astral microtubules for this process, a two-stage model for centrosome clustering is proposed. The first stage involves cortical contractility bringing the centrosomes into close proximity, this is facilitated by the astral microtubules translating the actomyosin contractility into centrosome movement. This could be through two potential mechanisms. The first is that the increased cortical contractility restricts centrosome movement, possibly through the regulation of microtubule pulling forces that are generated at the cortex. This restricted movement then allows HSET to bind and cluster the centrosomes. Another hypothesis is that the increased contractility destabilises the astral microtubules allowing them to be more free-moving across the cortex bringing the centrosomes into closer proximity. Further work would need to be done to elucidate this mechanism (discussed in more detail later). The second stage where the centrosomes are close enough is facilitated by the kinesin HSET bringing the centrosomes together (Figure 6.2). As HSET is a microtubule motor, that can bind microtubules, it will require centrosomes to be in close enough proximity where it can then bind to microtubules emanating from both centrosomes. Once bound to these microtubules from multiple centrosomes HSET can then move along the microtubules bringing the centrosomes together. If the centrosomes are too far apart, then the microtubules will not be close enough for HSET to bind and therefore be unable to cluster the supernumerary centrosomes.

The role of contractility at adherens junctions is complex. As described previously it

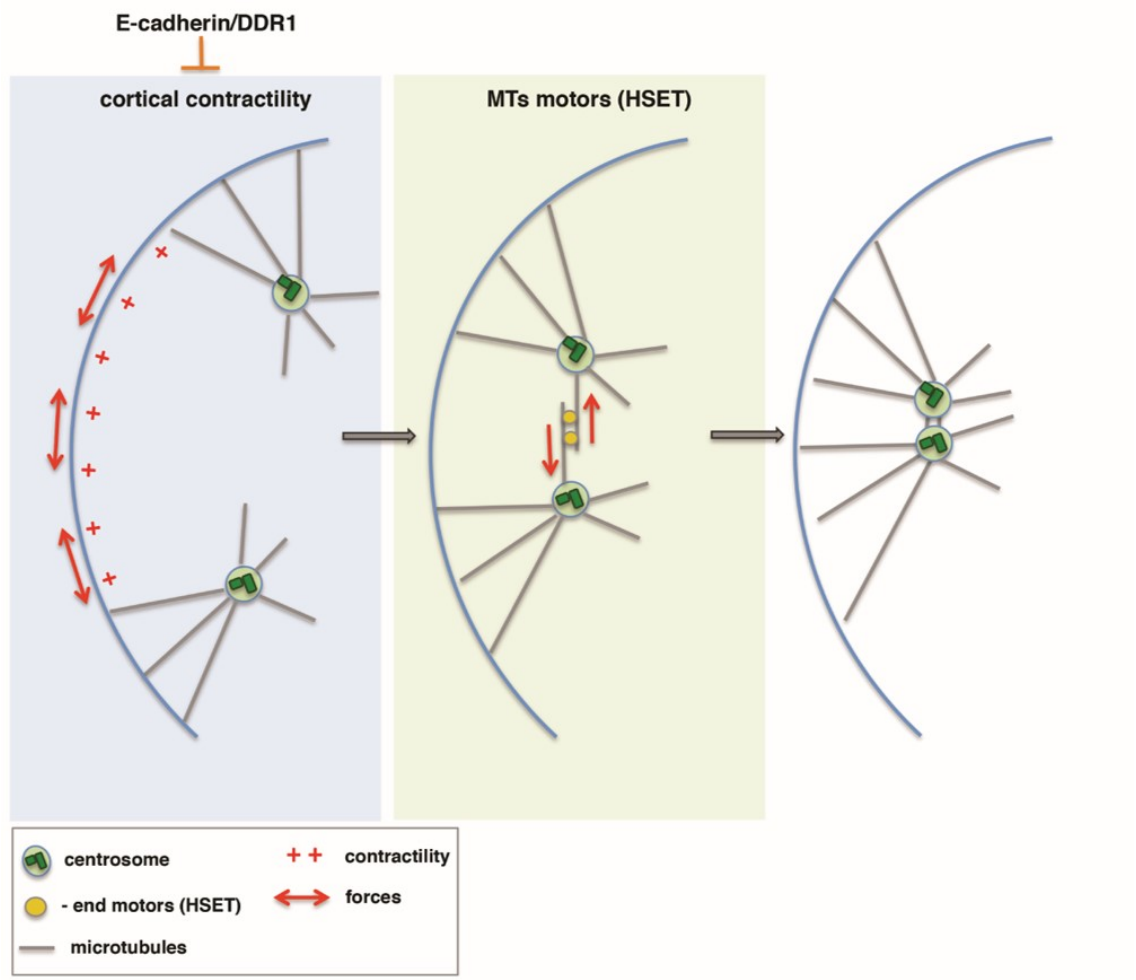

Figure 6.2: Step-wise model for centrosome clustering
Schematic representation of the centrosome clustering model. It is proposed that centrosome clustering occurs in a stepwise fashion. The first step depends on cortical contractility and brings centrosomes together at a distance where anti-parallel microtubules can interact. Following this, the second step requires the minus end microtubule motor HSET, that bind to microtubules emanating from different centrosomes and through their motor activity clusters extra centrosomes together.

has been reported that E-cadherin at adherens junctions impairs cortical contractility (Hidalgo-Carcedo *et al.*, 2011). However, other studies have shown that adherens junctions display contractile tension (Lecuit and Yap, 2015). This tension is best understood to play a role during morphogenesis (Martin and Goldstein, 2014; Mason *et al.*, 2016), however it has also been reported in stable monolayers independently of morphogenesis, but the role that this contractility plays in an epithelial monolayer is not understood. This contractile tension is generated through the actomyosin complex which is coupled to E-cadherin, where they form actomyosin bundles which form a ring, further stabilising the E-cadherin (Smutny and Yap, 2010; Priya, Yap and Gomez, 2013; Wu *et al.*, 2014). These actoymosin bundles are maintained by a number of molecular processes, many relying on E-cadherin for their recruitment,

such as RhoA (Ratheesh *et al.*, 2012; Priya *et al.*, 2015).

Previous work identified a role for certain formins, a diverse class of actin regulators that influence filament dynamics and organisation, in controlling contractility at adherens junctions (Kobielak, Pasolli and Fuchs, 2004; Carramusa *et al.*, 2007; Homem and Peifer, 2008; Mason, Tworoger and Martin, 2013; Grikscheit *et al.*, 2015; Rao and Zaidel-Bar, 2016). Whilst formins had been identified as localising to adherens junctions, their role had been uncharacterised. Acharya *et al.* reported that the formin mDia1 (Diaphanous 1) facilitated control of contractility at the adherens junctions (Acharya *et al.*, 2017). They showed that mDia1 was important for reorganising F-actin into stable bundles that could then resist myosin-induced stress. They also observed a role for mDia1 in stabilising tight junctions. Therefore, loss of E-cadherin could also perturb control of cortical contractility, not only through DDR1, but potentially through loss of mDia1 localisation as well. Therefore, further understanding of the contrasting dynamics of E-cadherin and its control of cortical contractility at adherens junctions is needed to fully understand how this then facilitates centrosome clustering. The role of formins, and the actin bundles would be particularly interesting to explore.

Recent work by Afshar *et al.* in *Caenorhabditis elegans* identified that the protein phosphatase PPH-6 and one of its associated subunits SAPS-1 forms a complex which is required for the contractility of the actomyosin network and proper spindle positioning(Afshar *et al.*, 2016). They showed that PPH-6/SAPS-1 regulated the organisation of cortical myosin II, and contributes to cytokinesis by stimulating actomyosin contractility. Similarly, the PPH-6/SAPS-1 is required for the generation of pulling forces on the spindle poles during anaphase. Therefore, investigating these proteins and their role in cortical myosin II in centrosome clustering may help evaluate other mechanisms of cortical contractility independently of adherens junctions in centrosome clustering.

The model proposed here of loss of E-cadherin as a mechanism of adaptation to supernumerary centrosomes is important, particularly in light of the recent mouse models developed to assess the role of centrosome amplification in tumourigenesis. The majority of models showed that the generation of supernumerary centrosomes, resulting from PLK4 overexpression was not sufficient to induce tumourigenesis (Coelho *et al.*, 2015; Serçin *et al.*, 2015; Vitre *et al.*, 2015). This is likely because centrosome amplification induces a p53-mediated cell cycle arrest within normal cells (Holland *et al.*, 2012). However, in the absence of p53, induction of supernumerary centrosomes was able to accelerate tumourigenesis in two different mouse models

(Coelho *et al.*, 2015; Serçin *et al.*, 2015). A more recent study has questioned this view, where Levine *et al.* reported that transient overexpression of PLK4 was able to lead to tumourigenesis in some tissues, even in the presence of p53. Therefore, the role of centrosome amplification in tumourigenesis is still disputed. Centrosome amplification was shown to cause lymphomas and sarcomas in mice, which are of mesenchymal origin, whereas epithelial tumours were not observed. Both the lymphomas and sarcomas maintained high levels of supernumerary centrosomes (Coelho *et al.*, 2015). The induction of centrosome amplification in the developing skin of p53 deficient mice was also reported to lead to accelerated tumour formation and penetrance when compared to p53 deficiency alone. In contrast however, these tumours did not display evidence of centrosome amplification, suggesting that supernumerary centrosomes are not maintained within the epithelial compartment (Serçin *et al.*, 2015).

Taken together these results suggest that some tissues are more prone to maintenance of centrosome amplification, whereas others require adaptation to maintain proliferating populations of cells with extra centrosomes. The data demonstrate that loss of E-cadherin might be one mechanism that allows epithelial cells to maintain extra centrosomes by facilitating clustering. It would be interesting to assess if loss of E-cadherin or DDR1 enables skin tumours to maintain their extra centrosomes.

Interestingly, more recent work showed squamous cell carcinoma (SCC) cells derived from epithelial cells with supernumerary centrosomes, potentially conflicting with the view that epithelial cells need to adapt to survive in the presence of centrosome amplification, however, E-cadherin expression in these cells was not assessed (Levine *et al.*, 2017). It would be interesting to explore if E-cadherin may have been lost prior to SCC development, where centrosome amplification may have driven loss of E-cadherin in order to survive. There is already evidence suggesting that SCC cell lines lose E-cadherin in their tumour development, suggesting that this could be a process for maintaining their extra centrosomes (Hashimoto *et al.*, 2012; Stewart and Crook, 2017). However, no study looking at a correlation between supernumerary centrosomes and E-cadherin expression has been carried out.

Whilst the large majority of tumours come from an epithelial background, centrosome amplification is a common occurrence in cancer. This work would suggest that a loss of E-cadherin could be a mechanism of adaptation, and indeed E-cadherin loss is often observed in cancer. Cancer evolution results in changes in tumours overtime with progressive mutations taking place. Therefore, it is unclear if centrosome amplification may drive E-cadherin loss in order to survive, or if the loss of E-

cadherin may lead to the accumulation of supernumerary centrosomes. Further work would need to be done to explore which process drives the other.

E-cadherin loss is commonly associated with increased metastatic potential. This could therefore help explain why centrosome amplification is correlated with later stages and poor prognosis where not only are cells with centrosome amplification already more invasive, but that a mechanism for adaptation to centrosome clustering (loss of E-cadherin) also makes cells more metastatic.

6.1 Future directions

As strategies to inhibit centrosome clustering emerge from basic biology to allow the development of specific inhibitors, approaches to identify patients that would respond to such drugs will become essential (Rebacz *et al.*, 2007; Kwon *et al.*, 2008; Ganem, Godinho and Pellman, 2009; Karna *et al.*, 2011; Watts *et al.*, 2013; Wu *et al.*, 2013). At present the only method for analysing if a patient has centrosome amplification, and therefore might benefit from a centrosome amplification targeting therapy, is to take a biopsy and then stain for centriole markers, this is therefore too impractical based on invasiveness, time, expertise and cost to be done systematically. Identifying features that permit cells to efficiently divide and proliferate in the presence of extra centrosomes could be used as biomarkers to identify tumours containing extra centrosomes. This work suggests that loss of E-cadherin, which is routinely assessed in the clinic by immunohistochemistry, could potentially be used to stratify which breast cancer patients would respond to drugs that target centrosome clustering. Further exploring the use of E-cadherin and DDR1 loss as a biomarker for treatment targeting centrosome amplification would be an interesting approach towards personalised medicine. There are two different members of the DDR family, DDR1 and DDR2. Interestingly, DDR switching is often described within solid tumours where DDR expression goes from DDR1 to DDR2 expression (Maeyama *et al.*, 2008; Toy *et al.*, 2015). It is possible that as tumours progress and lose E-cadherin, and therefore lose DDR1 this may then allow for an increase in DDR2 expression. However, bioinformatic and protein analysis would be required to test this hypothesis. Therefore, it would be interesting to also explore if DDR1 switching to DDR2 is correlated with centrosome amplification and could be used as a biomarker.

Whilst astral microtubules have previously been reported as having a role in facilitating centrosome clustering, and here the data supports that role by translating the

cortical forces to the centrosomes, it is unclear how this mechanism functions. The data show that centrosomes are closer in tripolar metaphases in *CDH1-/-* cell lines, suggesting that the movement of the centrosomes is restricted. How contractility might restrict centrosome movement during mitosis remains unclear. One possibility is by regulating microtubule-pulling forces that are generated by motors at the cortex, such as dynein. It has been previously proposed that efficient pulling forces important for spindle positioning require the microtubule plus ends to be anchored to a relatively stiff cortex (Carreno *et al.*, 2008; Kunda *et al.*, 2008). Indeed, actomyosin contractility was shown to be important for dynein-mediated pulling forces on the microtubules and to prevent membrane invaginations at the sites of microtubule pulling forces in *C. elegans* embryos (Redemann *et al.*, 2010; De Simone, Nédélec and Gönczy, 2016). Thus, it is possible that in epithelial cells, low contractility could lead to inefficient microtubule pulling forces at the cortex leading to increased random centrosome movement that prevents efficient centrosome clustering. Another hypothesis is that the additional contractility destabilises the centrosomes at the cortex making them more free-moving. Understanding the astral microtubule dynamics in detail would help to fully elucidate this model. This could be identified by doing live cell imaging of the centrosomes, such as through GFP labelled centrin, to actively track centrosome movement during mitosis. Whilst this will not elucidate microtubule dynamics it will enable to distinguish if centrosomes are fixed or motile and therefore distinguish between the two hypotheses. This would help to further illuminate the clustering process. It would be predicted from the proposed 2-stage model that in the initial stage centrosomes would move closer together, where HSET in the second stage would then bring the centrosomes together more rapidly. However, this could only be explored more fully through live-cell tracking.

Interestingly, upon mitotic entry, NuMA is released from the nucleus and displaced LGN from E-cadherin forming the LGN/NuMA complex (Gloerich *et al.*, 2017). This complex can then facilitate the stabilisation of astral microtubule interactions at the cell cortex, which in turn orientates the mitotic spindle. Therefore, in the absence of E-cadherin this complex may already be stabilised, as the process of displacement is not required, allowing for more stable astral microtubule associations at the cortex. Exploring this mechanism more fully may help elucidate the process for astral microtubules in translating the cortical forces to facilitate centrosome clustering.

E-cadherin was initially shown to lead to the recruitment of DDR1 to the adherens junctions. However, these experiments were based on the observations when E-cadherin was removed by calcium wash-out coinciding with a loss of DDR1, which was

rescued by re-addition of calcium. The data here suggest an alternative mechanism, whereby DDR1 is not just localised due to E-cadherin, but that it is actually stabilised by E-cadherin. Both localisation and stabilisation of DDR1 are not necessarily exclusive, so E-cadherin may be important for both, and further understanding this relationship would be an interesting area to explore. Whilst it has been proposed that E-cadherin and DDR1 can directly bind in their extracellular domains, this was done by overexpression of E-cadherin and it is yet to be reported if this happens with endogenous proteins. It would therefore be interesting to explore if E-cadherin and DDR1 bind in normal cellular conditions.

Similarly, whilst it is hypothesised that DDR1 may be able to directly regulate RhoE and the signalling cascade reducing actomyosin contractility, this needs validation. Indeed, depletion of RhoA and its effect on centrosome clustering was not explored, and could still act as a potential link between DDR1 and RhoE through a yet to be explored RhoA regulator.

This proposed two stage model fundamentally relies on increased cortical contractility to facilitate the first stage of centrosome clustering. Control of cortical contractility independently of E-cadherin may then lead to increased centrosome clustering. Exploring other mechanisms of cortical contractility regulation in centrosome clustering would be an interesting future approach, such as depleting phosphatases which may lead to accumulation of pMLC, and identifying if there is an increase in centrosome clustering.

This thesis would suggest that adaptation to centrosome amplification, by centrosome clustering, is required for the survival of epithelial cells as shown by the cell viability experiments. However, it would be exciting to see if this could then be recapitulated *in vivo* such as with the skin tumour model using PLK4 overexpression to induce centrosome amplification. It would be expected that the loss of E-cadherin would then allow for continued cell proliferation and survival, whereas the E-cadherin positive cells would not survive due to the multipolar cell divisions. To test this an *in vivo* model could be used where epithelial cells with supernumerary centrosomes are injected sub-cutaneously compared to *CDH1-/-* cells with supernumerary centrosomes. Based on the hypothesis it would be expected that the epithelial cells would not form a tumour, whereas the *CDH1-/-* should form a tumour due to increased cell survival. This would then confirm that E-cadherin loss is an adaptation mechanism *in vivo* to centrosome amplification in epithelial cells. It would therefore be interesting to examine how loss of E-cadherin and centrosome amplification synergise during tumour development to understand this inter-relationship.

Chapter 7

Supplementary

Table 7.1: Centrosome amplification and centrosome clustering (part I)

Quantification of centrosome amplifcation and centrosome clustering at metaphase and cytokinesis (n= 300 cells, 100 per experiment at metaphase and 150 cells, 50 per experiment at cytokinesis)

Cell Line	Treatment	Figure	Centrosome amplification (%)		Centrosome clustering Metaphase (%)		Centrosome clustering Cytokinesis (%)	
			Mean	± SD	Mean	± SD	Mean	± SD
MCF10A	Untreated	3.4	18.0	2.0	-	-	-	-
	DCB	3.4	58.0	2.0	42.7	2.3	44.0	2.0
	Blebbistatin	3.4	45.3	3.1	30.7	3.1	40.0	2.0
	CDK1i	3.4	90.7	1.2	24.3	0.6	39.3	1.2
HaCaT	Untreated	3.4	18.7	3.1	-	-	-	-
	DCB	3.4	40.0	2.0	30.0	4.0	48.0	4.0
	Blebbistatin	3.4	52.0	2.0	31.3	5.0	31.3	4.2
	CDK1i	3.4	77.3	4.2	25.3	4.2	38.0	2.0
J3B1A	Untreated	3.4	16.7	3.1	-	-	-	-
	DCB	3.4	73.3	3.1	8.0	2.0	8.0	2.0
	Blebbistatin	3.4	49.3	1.2	5.3	3.1	10.0	2.0
	CDK1i	3.4	68.3	3.5	28.7	6.1	30.0	4.0
NIH-3T3	Untreated	3.4	25.3	1.2	-	-	-	-
	DCB	3.4	62.0	2.0	23.3	2.3	82.0	2.0
	Blebbistatin	3.4	53.3	3.1	27.0	2.6	95.3	1.2
	CDK1i	3.4	64.7	3.1	48.0	2.0	84.7	4.2
BJ	Untreated	3.4	6.7	4.2	-	-	-	-
	DCB	3.4	50.0	2.0	79.3	3.1	86.7	5.0
	Blebbistatin	3.4	44.0	3.5	79.3	3.1	95.3	1.2
	CDK1i	3.4	70.7	3.1	47.3	5.0	96.0	3.5
RPE-1	Untreated	3.4	10.0	2.0	-	-	-	-
	DCB	3.4	36.0	2.0	52.7	3.1	94.0	2.0
	Blebbistatin	3.4	46.7	3.1	50.7	5.0	82.7	3.1
MCF10A	DCB + p38i	3.5	59.0	3.6	42.0	2.0	46.0	2.0
	DCB - p38i	3.5	60.0	2.0	42.7	3.1	46.0	2.0

Table 7.1: Centrosome amplification and centrosome clustering (part II)

Cell Line	Treatment	Figure	Centrosome amplification (%)		Centrosome clustering Metaphase (%)		Centrosome clustering Cytokinesis (%)	
			Mean	± SD	Mean	± SD	Mean	± SD
MCF10A.TetR.PLK4	Untreated	3.7 and 3.8	23.3	1.2	-	-	-	-
	Dox	3.7 and 3.8	78.3	1.5	34.0	2.0	60.0	4.0
HaCaT.TetR.PLK4	Untreated	3.7 and 3.8	20.0	4.0	-	-	-	-
	Dox	3.7 and 3.8	79.3	6.4	32.7	11.0	61.3	1.2
NIH-3T3.TetR.PLK4	Untreated	3.7 and 3.8	28.0	2.0	-	-	-	-
	Dox	3.7 and 3.8	38.0	2.0	59.3	2.3	59.3	2.3
BJ.TetR.PLK4	Untreated	3.7 and 3.8	9.3	3.1	-	-	-	-
	Dox	3.7 and 3.8	76.7	1.2	28.0	4.0	78.7	4.2
RPE-1.TetR.PLK4	Untreated	3.7 and 3.8	14.0	2.0	-	-	-	-
	Dox	3.7 and 3.8	76.0	2.0	14.7	1.2	62.0	2.0
MCF10A	Untreated	3.9	20.0	2.0	-	-	-	-
	Dox	3.9	20.0	4.0	-	-	-	-
	DCB	3.9	58.7	2.1	42.0	2.0	46.0	2.0
	DCB + Dox	3.9	61.3	3.1	42.7	2.3	64.7	3.1
MCF10A	DCB	3.10	58.0	2.0	42.0	2.0	44.0	2.0
MCF10A.TetR	DCB	3.10	60.0	2.0	52.7	3.1	64.7	3.1
MCF10A.TetR.PLK4	DCB	3.10	59.3	3.8	46.0	2.0	65.3	5.0
MCF10A	DCB	4.1	58.0	4.0	42.0	2.0	44.7	3.1
	DCB + MG132	4.1	58.7	4.2	42.0	4.0	44.0	4.0
HaCaT	DCB	4.1	46.0	2.0	30.7	3.1	44.0	4.0
	DCB + MG132	4.1	40.7	4.2	32.0	2.0	44.0	2.0
MCF10A	Non-targeting siRNA + DCB	4.4	60.0	2.0	-	-	42.7	4.2
	E-cadherin siRNA + DCB	4.4	58.7	4.2	-	-	70.7	3.1

Table 7.1: Centrosome amplification and centrosome clustering (part V)

Cell Line	Treatment	Figure	Centrosome amplification (%)		Centrosome clustering Metaphase (%)		Centrosome clustering Cytokinesis (%)	
			Mean	± SD	Mean	± SD	Mean	± SD
HaCaT.TetR.PLK4.H2B-GFP	Untreated	4.14	20.8	1.6	-	-	-	-
	Dox	4.14	82.2	0.9	32.1	1.2	59.2	1.6
HaCaT.*CDH1-/-*.TetR.PLK4.H2B-GFP	Untreated	4.14	22.1	2.8	-	-	-	-
	Dox	4.14	75.6	4.1	60.1	3.2	76.5	1.2
MCF10A	Non-targeting siRNA + DCB	4.20	57.0	1.8	-	-	46.0	3.5
	DDR1 siRNA + DCB	4.20	58.3	2.5	-	-	81.7	3.5
HaCaT	Non-targeting siRNA + DCB	4.20	42.1	3.6	-	-	46.7	3.1
	DDR1 siRNA + DCB	4.20	40.6	1.2	-	-	82.3	3.8
RPE-1.Ecad	DCB	4.23	38.0	1.5	-	-	30.7	6.1
	Non-targeting siRNA + DCB	4.23	36.4	2.6	-	-	34.0	6.0
	DDR1 siRNA + DCB	4.23	38.0	6.0	-	-	73.3	4.2
MCF10A	DCB	4.24	56.9	1.9	42.1	1.2	48.2	2.3
	DCB + DDR1 inhibitor	4.24	57.4	2.5	43.2	1.6	47.0	2.1
MCF10A	Non-targeting siRNA + DCB	4.25	58.6	1.8	-	-	42.3	0.8
	p190RhoGAP siRNA + DCB	4.25	54.9	1.8	-	-	40.5	2.5
HaCaT	Non-targeting siRNA + DCB	4.25	45.2	2.9	-	-	44.2	1.0
	p190RhoGAP siRNA + DCB	4.25	43.2	1.0	-	-	48.6	4.2
MCF10A	Non-targeting siRNA + DCB	4.26	56.8	2.9	-	-	44.7	4.2
	DLC3 siRNA + DCB	4.26	57.4	1.8	-	-	42.7	3.1
HaCaT	Non-targeting siRNA + DCB	4.26	43.8	1.8	-	-	44.0	4.0
	DLC3 siRNA + DCB	4.26	46.2	4.0	-	-	50.7	5.0

Table 7.1: Centrosome amplification and centrosome clustering (part VI)

Cell Line	Treatment	Figure	Centrosome amplification (%)		Centrosome clustering Metaphase (%)		Centrosome clustering Cytokinesis (%)	
			Mean	± SD	Mean	± SD	Mean	± SD
HaCaT	Non-targeting siRNA + DCB	4.27	45.1	2.9	-	-	42.6	2.1
	RhoE siRNA pool + DCB	4.27	44.6	2.9	-	-	28.2	1.5
HaCaT	Non-targeting siRNA + DCB	4.30	47.3	1.0	-	-	44.0	2.0
	Non-targeting siRNA + DCB + MG132	4.30	46.2	3.3	-	-	48.7	1.2
	RhoE siRNA pool + DCB	4.30	43.9	1.0	-	-	27.7	2.5
	RhoE siRNA pool + DCB + MG132	4.30	44.5	1.8	-	-	68.3	3.5
HaCaT	Non-targeting siRNA + DCB	4.31	43.7	2.9	-	-	44.2	1.6
	single RhoE siRNA + DCB	4.31	44.0	2.9	-	-	72.8	2.5
MCF10A	DCB	5.5	58.2	4.0	-	-	45.0	3.0
	DCB + 4h Blebbistatin	5.5	59.1	1.8	-	-	30.7	3.1
MCF10A.*CDH1-/-*	DCB	5.5	60.1	3.3	-	-	77.0	6.6
	DCB + 4h Blebbistatin	5.5	57.2	2.9	-	-	32.3	3.5
HaCaT	DCB	5.5	45.6	1.8	-	-	47.7	2.5
	DCB + 4h Blebbistatin	5.5	45.0	1.8	-	-	31.7	3.8
HaCaT.*CDH1-/-*	DCB	5.5	44.2	2.9	-	-	73.3	3.8
	DCB + 4h Blebbistatin	5.5	44.1	3.4	-	-	29.7	2.1
RPE-1	DCB	5.5	34.2	1.8	-	-	94.3	2.1
	DCB + 4h Blebbistatin	5.5	36.8	1.0	-	-	31.0	2.6
BJ	DCB	5.5	50.1	1.3	-	-	86.7	5.0
	DCB + 4h Blebbistatin	5.5	52.3	3.8	-	-	40.3	1.5

Table 7.1: Centrosome amplification and centrosome clustering (part VII)

Cell Line	Treatment	Figure	Centrosome amplification (%)		Centrosome clustering Metaphase (%)		Centrosome clustering Cytokinesis (%)	
			Mean	± SD	Mean	± SD	Mean	± SD
MCF10A	DCB	5.6	53.9	6.2	-	-	45.3	5.0
	DCB + ROCKinhib	5.6	58.2	1.8	-	-	28.7	4.2
MCF10A.*CDH1-/-*	DCB	5.6	59.2	1.8	-	-	74.0	5.3
	DCB + ROCKinhib	5.6	57.4	2.9	-	-	33.3	4.2
HaCaT	DCB	5.6	46.2	1.0	-	-	47.7	2.5
	DCB + ROCKinhib	5.6	45.2	1.8	-	-	31.7	3.8
HaCaT.*CDH1-/-*	DCB	5.6	47.0	1.8	-	-	73.3	4.2
	DCB + ROCKinhib	5.6	46.1	1.8	-	-	30.7	3.1
MCF10A	DCB	5.7	57.4	3.8	-	-	47.3	2.1
	DCB + Calyculin A	5.7	56.2	1.9	-	-	64.7	2.5
HaCaT	DCB	5.7	43.8	2.9	-	-	46.7	3.1
	DCB + Calyculin A	5.7	43.1	1.8	-	-	55.0	3.0
MCF10A	DCB	5.10	57.6	1.8	-	-	44.3	2.1
	DCB + Nocodazole	5.10	58.2	3.6	-	-	32.7	2.5
MCF10A.*CDH1-/-*	DCB	5.10	59.0	3.8	-	-	78.0	4.4
	DCB + Nocodazole	5.10	56.5	4.0	-	-	27.3	6.8
HaCaT	DCB	5.10	45.8	1.8	-	-	46.7	3.1
	DCB + Nocodazole	5.10	44.2	4.0	-	-	33.0	4.4
HaCaT.*CDH1-/-*	DCB	5.10	43.0	1.8	-	-	75.3	4.0
	DCB + Nocodazole	5.10	46.3	4.0	-	-	28.3	6.5

Table 7.1: Centrosome amplification and centrosome clustering (part VIII)

Cell Line	Treatment	Figure	Centrosome amplification (%)		Centrosome clustering Metaphase (%)		Centrosome clustering Cytokinesis (%)	
			Mean	± SD	Mean	± SD	Mean	± SD
MCF10A	Non-targeting siRNA + DCB	5.11	58.8	4.0	-	-	44.3	2.1
	HSET siRNA + DCB	5.11	59.3	2.1	-	-	7.3	1.2
MCF10A.*CDH1-/-*	Non-targeting siRNA + DCB	5.11	57.6	4.8	-	-	78.7	4.2
	HSET siRNA + DCB	5.11	57.3	1.8	-	-	9.3	1.2
HaCaT	Non-targeting siRNA + DCB	5.11	43.2	4.0	-	-	46.7	3.1
	HSET siRNA + DCB	5.11	44.5	4.0	-	-	4.7	1.2
HaCaT.*CDH1-/-*	Non-targeting siRNA + DCB	5.11	42.1	1.8	-	-	75.3	3.1
	HSET siRNA + DCB	5.11	44.3	1.0	-	-	10.0	2.0
MCF10A	DCB	5.13	58.1	4.8	-	-	46.0	1.0
MCF10A.TetR.PLK4	DCB	5.13	57.6	2.1	-	-	64.0	2.0
MCF10A.pInducer.PLK4	DCB	5.13	59.2	7.9	-	-	44.7	3.1
MCF10A	DCB	5.14	57.1	2.9	-	-	44.3	2.1
MCF10A.TetR.PLK4	Dox	5.14	62.0	1.0	-	-	60.0	4.0
MCF10A.pInducer.PLK4	Dox	5.14	97.0	1.0	-	-	94.0	4.0
MCF10A.pInducer.PLK4	DCB	5.16	46.0	4.0	-	-	46.0	2.0
	Dox	5.16	98.0	2.9	-	-	95.3	3.1
	Sas-6 siRNA + Dox	5.16	52.0	1.0	-	-	50.0	2.0

Bibliography

Acharya, B. R., Wu, S. K., Lieu, Z. Z., Parton, R. G., Grill, S. W., Bershadsky, A. D., Gomez, G. A., and Yap, A. S. (2017). "Mammalian Diaphanous 1 Mediates a Pathway for E-cadherin to Stabilize Epithelial Barriers through Junctional Contractility." In: *Cell reports* 18.12, pp. 2854–2867.

Afshar, K., Werner, M. E., Tse, Y. C., Glotzer, M., and Gönczy, P. (2016). "Regulation of cortical contractility and spindle positioning by the protein phosphatase 6 PPH-6 in one-cell stage C. elegans embryos". In: *Development* 143.14, pp. 2689–2689.

Akao, J., Matsuyama, H., Yamamoto, Y., Sasaki, K., and Naito, K. (2006). "Chromosome 20q13.2 gain may predict intravesical recurrence after nephroureterectomy in upper urinary tract urothelial tumors". In: *Clinical Cancer Research* 12.23, pp. 7004–7008.

Allen, R. D. (1969). "The morphogenesis of basal bodies and accessory structures of the cortex of the ciliated protozoan Tetrahymena pyriformis." In: *Journal of Cell Biology* 40.3, pp. 716–733.

Alves, F., Saupe, S., Ledwon, M., Schaub, F., Hiddemann, W., and Vogel, W. F. (2001). "Identification of two novel, kinase-deficient variants of discoidin domain receptor 1: differential expression in human colon cancer cell lines." In: *FASEB journal : official publication of the Federation of American Societies for Experimental Biology* 15.7, pp. 1321–3.

Alves, F., Vogel, W., Mossie, K., Millauer, B., Höfler, H., and Ullrich, A. (1995). "Distinct structural characteristics of discoidin I subfamily receptor tyrosine kinases and complementary expression in human cancer." In: *Oncogene* 10.3, pp. 609–18.

Andersen, J., Wilkinson, C., and Mayor, T. (2003). "Proteomic characterization of the human centrosome by protein correlation profiling". In: *Nature* 426.6966, pp. 570–574.

Andreassen, P. R., Lohez, O. D., Lacroix, F. B., and Margolis, R. L. (2001). "Tetraploid state induces p53-dependent arrest of nontransformed mammalian cells in G1." In: *Molecular biology of the cell* 12.5, pp. 1315–28.

Arquint, C., Sonnen, K. F., Stierhof, Y. D., and Nigg, E. A. (2012). "Cell-cycle-regulated expression of STIL controls centriole number in human cells". In: *J Cell Sci* 125.Pt 5, pp. 1342–1352.

Arquint, C., Gabryjonczyk, A.-M., and Nigg, E. a. (2014). "Centrosomes as signalling centres." In: *Philosophical transactions of the Royal Society of London. Series B, Biological sciences* 369.1650, pp. 20130464–.

Assent, D., Bourgot, I., Hennuy, B., Geurts, P., Noël, A., Foidart, J.-M., and Maquoi, E. (2015). "A membrane-type-1 matrix metalloproteinase (MT1-MMP)-discoidin domain receptor 1 axis regulates collagen-induced apoptosis in breast cancer cells." In: *PloS one* 10.3. Ed. by J. Cao, e0116006.

Azimzadeh, J., Wong, M. L., Downhour, D. M., Alvarado, A. S., and Marshall, W. F. (2012). "Centrosome Loss in the Evolution of Planarians". In: *Science* 335.6067, pp. 461–463.

Bagheri-Yarmand, R., Biernacka, A., Hunt, K. K., and Keyomarsi, K. (2010). "Low molecular weight cyclin E overexpression shortens mitosis, leading to chromosome missegregation and centrosome amplification". In: *Cancer Research* 70.12, pp. 5074–5084.

Bagheri-Yarmand, R., Nanos-Webb, A., Biernacka, A., Bui, T., and Keyomarsi, K. (2010). "Cyclin E deregulation impairs mitotic progression through premature activation of Cdc25C". In: *Cancer Research* 70.12, pp. 5085–5095.

Bahe, S., Stierhof, Y. D., Wilkinson, C. J., Leiss, F., and Nigg, E. A. (2005). "Rootletin forms centriole-associated filaments and functions in centrosome cohesion". In: *Journal of Cell Biology* 171.1, pp. 27–33.

Baker, J. and Garrod, D. (1993). "Epithelial cells retain junctions during mitosis." In: *Journal of cell science* 104 (Pt 2), pp. 415–25.

Bardin, a. J. and Amon, A. (2001). "Men and sin: what's the difference?" In: *Nature Reviews. Molecular Cell Biology* 2.11, pp. 815–826.

Basto, R., Brunk, K., Vinadogrova, T., Peel, N., Franz, A., Khodjakov, A., and Raff, J. W. (2008). "Centrosome amplification can initiate tumorigenesis in flies." In: *Cell* 133.6, pp. 1032–42.

Basto, R., Lau, J., Vinogradova, T., Gardiol, A., Woods, C. G., Khodjakov, A., and Raff, J. W. (2006). "Flies without Centrioles". In: *Cell* 125.7, pp. 1375–1386.

Becker, K. F., Atkinson, M. J., Reich, U., Huang, H. H., Nekarda, H., Siewert, J. R., and Höfler, H. (1993). "Exon skipping in the E-cadherin gene transcript in metastatic human gastric carcinomas." In: *Human molecular genetics* 2.6, pp. 803–4.

Bergmann, S., Royer-Pokora, B., Fietze, E., Jürchott, K., Hildebrandt, B., Trost, D., Leenders, F., Claude, J.-C., Theuring, F., Bargou, R., Dietel, M., and Royer, H.-D. (2005). "YB-1 provokes breast cancer through the induction of chromosomal instability that emerges from mitotic failure and centrosome amplification." In: *Cancer research* 65.10, pp. 4078–87.

Beronja, S., Livshits, G., Williams, S., and Fuchs, E. (2010). "Rapid functional dissection of genetic networks via tissue-specific transduction and RNAi in mouse embryos." In: *Nature medicine* 16.7, pp. 821–827.

Bertran, M. T., Sdelci, S., Regué, L., Avruch, J., Caelles, C., and Roig, J. (2011). "Nek9 is a Plk1-activated kinase that controls early centrosome separation through Nek6/7 and Eg5." In: *The EMBO journal* 30.13, pp. 2634–47.

Berx, G., Cleton-Jansen, A. M., Strumane, K., Leeuw, W. J. de, Nollet, F., Roy, F. van, and Cornelisse, C. (1996). "E-cadherin is inactivated in a majority of invasive human lobular breast cancers by truncation mutations throughout its extracellular domain." In: *Oncogene* 13.9, pp. 1919–25.

Berx, G., Becker, K. F., Höfler, H., and Van Roy, F. (1998). "Mutations of the human E-cadherin (CDH1) gene". In: *Human Mutation* 12.4, pp. 226–237.

Berx, G., Staes, K., Hengel, J. van, Molemans, F., Bussemakers, M. J. G., Bokhoven, A. van, and Roy, F. van (1995). "Cloning and characterization of the human invasion suppressor gene E-cadherin (CDH1)". In: *Genomics* 26.2, pp. 281–289.

Betschinger, J. and Knoblich, J. A. (2004). "Dare to be different: asymmetric cell division in Drosophila, C. elegans and vertebrates." In: *Current biology : CB* 14.16, R674–85.

Bettencourt-Dias, M., Rodrigues-Martins, A., Carpenter, L., Riparbelli, M., Lehmann, L., Gatt, M. K., Carmo, N., Balloux, F., Callaini, G., and Glover, D. M. (2005). "SAK/PLK4 is required for centriole duplication and flagella development." In: *Current biology : CB* 15.24, pp. 2199–207.

Bettencourt-Dias, M. and Glover, D. M. (2007). "Centrosome biogenesis and function: centrosomics brings new understanding." In: *Nature reviews. Molecular cell biology* 8.6, pp. 451–63.

Bhakta-Guha, D., Saeed, M. E. M., Greten, H. J., and Efferth, T. (2015). "Disorganizing centrosomal clusters: specific cancer therapy for a generic spread?" In: *Current medicinal chemistry* 22.6, pp. 685–94.

Bignold, L. P., Coghlan, B. L. D., and Jersmann, H. P. A. (2006). "Hansemann, Boveri, chromosomes and the gametogenesis-related theories of tumours." In: *Cell biology international* 30.7, pp. 640–4.

Biswas, K. H. and Zaidel-Bar, R. (2017). "Early events in the assembly of E-cadherin adhesions". In: *Experimental Cell Research*.

Blanco, M. J., Moreno-Bueno, G., Sarrio, D., Locascio, a., Cano, a., Palacios, J., and Nieto, M. a. (2002). "Correlation of Snail expression with histological grade and lymph node status in breast carcinomas". In: *Oncogene* 21.20, pp. 3241–3246.

Boveri, T. (1887). "Uber die Befunchtung der Eier von Ascaris megalocephala". In: *SitzBer. Ges. Morph. Phys. Munchen* 3, pp. 71–80.

Boveri, T. (1888). "Zellen-Studien 2: Die Befrunchtung und Telung des Eies von Ascaris megalocephala". In: *Jenaische Zeitschr. Med. Naturw* 22, pp. 685–882.

Boveri, T. (1902). "Uber mehrpolige mitosen als mittel zur analyse des zellkerns." In: *Verhandl. Phys. Med. Ges. Wurzburg* 35, 67–90 (in German).

Boveri, T. (2008). "Concerning the origin of malignant tumours by Theodor Boveri. Translated and annotated by Henry Harris." In: *Journal of cell science* 121 Suppl, pp. 1–84.

Brasch, J., Harrison, O. J., Honig, B., and Shapiro, L. (2012). "Thinking outside the cell: How cadherins drive adhesion". In: *Trends in Cell Biology* 22.6, pp. 299–310.

Breuer, W. and Siu, C. H. (1981). "Identification of endogenous binding proteins for the lectin discoidin-I in Dictyostelium discoideum." In: *Proceedings of the National Academy of Sciences* 78.4, pp. 2115–2119.

Breugel, M. van, Hirono, M., Andreeva, A., Yanagisawa, H., Yamaguchi, S., Nakazawa, Y., Morgner, N., Petrovich, M., Ebong, I., Robinson, C., Johnson, C., Veprintsev, D., and Zuber, B. (2011). "Structures of SAS-6 suggest its organization in centrioles". In: *Science* 331.6021, pp. 1196–1199.

Brinkley, B. R., Cox, S. M., Pepper, D. A., Wible, L., Brenner, S. L., and Pardue, R. L. (1981). "Tubulin assembly sites and the organization of cytoplasmic microtubules in cultured mammalian cells." In: *The Journal of cell biology* 90.3, pp. 554–62.

Brito, D. A., Gouveia, S. M., and Bettencourt-Dias, M. (2012). "Deconstructing the centriole: Structure and number control". In: *Current Opinion in Cell Biology* 24.1, pp. 4–13.

Brooks-Wilson, A. R., Kaurah, P., Suriano, G., Leach, S., Senz, J., Grehan, N., Butterfield, Y. S. N., Jeyes, J., Schinas, J., Bacani, J., Kelsey, M., Ferreira, P., MacGillivray, B., MacLeod, P., Micek, M., Ford, J., Foulkes, W., Australie, K., Greenberg, C., LaPointe, M., Gilpin, C., Nikkel, S., Gilchrist, D., Hughes, R., Jackson, C. E., Monaghan, K. G., Oliveira, M. J., Seruca, R., Gallinger, S., Caldas, C., and Huntsman, D. (2004). "Germline E-cadherin mutations in hereditary diffuse gastric cancer: assessment of 42 new families and review of genetic screening criteria." In: *Journal of medical genetics* 41.7, pp. 508–17.

Brownlee, C. W., Klebba, J. E., Buster, D. W., and Rogers, G. C. (2011). "The protein phosphatase 2A regulatory subunit Twins stabilizes Plk4 to induce centriole amplification". In: *Journal of Cell Biology* 195.2, pp. 231–243.

Cader, F. Z., Vockerodt, M., Bose, S., Nagy, E., Brundler, M.-A., Kearns, P., and Murray, P. G. (2013). "The EBV oncogene LMP1 protects lymphoma cells from cell death through the collagen-mediated activation of DDR1". In: *Blood* 122.26, pp. 4237–4245.

Caldas, C., Carneiro, F., Lynch, H. T., Yokota, J., Wiesner, G. L., Powell, S. M., Lewis, F. R., Huntsman, D. G., Pharoah, P. D., Jankowski, J. a., MacLeod, P., Vogelsang, H., Keller, G., Park, K. G., Richards, F. M., Maher, E. R., Gayther, S. a., Oliveira, C., Grehan, N., Wight, D., Seruca, R., Roviello, F., Ponder, B. a., and Jackson, C. E. (1999). "Familial gastric cancer: overview and guidelines for management." In: *Journal of medical genetics* 36.12, pp. 873–80.

Cao, Y. and Prescott, S. M. (2002). "Many actions of cyclooxygenase-2 in cellular dynamics and in cancer." In: *Journal of cellular physiology* 190.3, pp. 279–86.

Caracciolo, V., D'Agostino, L., Dráberová, E., Sládková, V., Crozier-Fitzgerald, C., Agamanolis, D. P., Chadarévian, J.-P. de, Legido, A., Giordano, A., Dráber, P., and Katsetos, C. D. (2010). "Differential expression and cellular distribution of gamma-tubulin and betaIII-tubulin in medulloblastomas and human medulloblastoma cell lines." In: *Journal of cellular physiology* 223.2, pp. 519–529.

Carafoli, F. and Hohenester, E. (2013). "Collagen recognition and transmembrane signalling by discoidin domain receptors". In: *Biochimica et Biophysica Acta - Proteins and Proteomics* 1834.10, pp. 2187–2197.

Carneiro, F., Oliveira, C., Suriano, G., and Seruca, R. (2008). "Molecular pathology of familial gastric cancer, with an emphasis on hereditary diffuse gastric cancer". In: *Journal of clinical pathology* 61, pp. 25–30.

Carramusa, L., Ballestrem, C., Zilberman, Y., and Bershadsky, A. D. (2007). "Mammalian diaphanous-related formin Dia1 controls the organization of E-cadherin-mediated cell-cell junctions". In: *Journal of Cell Science* 120.21, pp. 3870–3882.

Carreno, S., Kouranti, I., Glusman, E. S., Fuller, M. T., Echard, A., and Payre, F. (2008). "Moesin and its activating kinase Slik are required for cortical stability and microtubule organization in mitotic cells". In: *The Journal of Cell Biology* 180.4, pp. 739–746.

Carroll, P. E., Okuda, M., Horn, H. F., Biddinger, P., Stambrook, P. J., Gleich, L. L., Li, Y. Q., Tarapore, P., and Fukasawa, K. (1999). "Centrosome hyperamplification in human cancer: chromosome instability induced by p53 mutation and/or Mdm2 overexpression." In: *Oncogene* 18.11, pp. 1935–1944.

Carvalho-Santos, Z., Azimzadeh, J., Pereira-Leal, J. B., and Bettencourt-Dias, M. (2011). "Tracing the origins of centrioles, cilia, and flagella". In: *Journal of Cell Biology* 194.2, pp. 165–175.

Castellanos, E., Dominguez, P., and Gonzalez, C. (2008). "Centrosome dysfunction in Drosophila neural stem cells causes tumors that are not due to genome instability." In: *Current biology : CB* 18.16, pp. 1209–14.

Castiel, A., Visochek, L., Mittelman, L., Dantzer, F., Izraeli, S., and Cohen-Armon, M. (2011). "A phenanthrene derived PARP inhibitor is an extra-centrosomes de-clustering agent exclusively eradicating human cancer cells." In: *BMC cancer* 11, p. 412.

Castro-Sanchez, L., Soto-Guzman, A., Navarro-Tito, N., Martinez-Orozco, R., and Salazar, E. P. (2010). "Native type IV collagen induces cell migration through a CD9 and DDR1-dependent pathway in MDA-MB-231 breast cancer cells." In: *European journal of cell biology* 89.11, pp. 843–52.

Caussinus, E. and Gonzalez, C. (2005). "Induction of tumor growth by altered stem-cell asymmetric division in Drosophila melanogaster." In: *Nature genetics* 37.10, pp. 1125–9.

Cavalier-Smith, T. (1974). "Basal body and flagellar development during the vegetative cell cycle and the sexual cycle of Chlamydomonas reinhardii." In: *Journal of cell science* 16.3, pp. 529–56.

Cavazza, T. and Vernos, I. (2015). "The RanGTP Pathway: From Nucleo-Cytoplasmic Transport to Spindle Assembly and Beyond." In: *Frontiers in cell and developmental biology* 3, p. 82.

Chan, J. Y. (2011). "A clinical overview of centrosome amplification in human cancers." In: *International journal of biological sciences* 7.8, pp. 1122–44.

Chang, H. W., Chow, V., Lam, K. Y., Wei, W. I., and WingYuen, A. P. (2002). "Loss of E-cadherin expression resulting from promoter hypermethylation in oral tongue carcinoma and its prognostic significance". In: *Cancer* 94.2, pp. 386–392.

Chang, J., Cizmecioglu, O., Hoffmann, I., and Rhee, K. (2010). "PLK2 phosphorylation is critical for CPAP function in procentriole formation during the centrosome cycle." In: *The EMBO journal* 29.14, pp. 2395–406.

Chang, Y.-C., Nalbant, P., Birkenfeld, J., Chang, Z.-F., and Bokoch, G. M. (2007). "GEF-H1 Couples Nocodazole-induced Microtubule Disassembly to Cell Contractility via RhoA". In: *Molecular biology of the cell* 19.1, pp. 308–317.

Chen, A., Beetham, H., Black, M. a., Priya, R., Telford, B. J., Guest, J., Wiggins, G. a. R., Godwin, T. D., Yap, A. S., and Guilford, P. J. (2014). "E-cadherin loss alters cytoskeletal organization and adhesion in non-malignant breast cells but is insufficient to induce an epithelial-mesenchymal transition." In: *BMC cancer* 14.1, p. 552.

Chen, D., Wilkinson, C. R. M., Watt, S., Penkett, C. J., Toone, W. M., Jones, N., and Bähler, J. (2008). "CDK5RAP2 Is a Pericentriolar Protein That Functions in Centrosomal Attachment of the γ-Tubulin Ring Complex". In: *Molecular biology of the cell* 19.1, pp. 308–317.

Chen, Z., Indjeian, V. B., McManus, M., Wang, L., and Dynlacht, B. D. (2002). "CP110, a cell cycle-dependent CDK substrate, regulates centrosome duplication in human cells". In: *Developmental Cell* 3.3, pp. 339–350.

Cheng, C. W., Wu, P. E., Yu, J. C., Huang, C. S., Yue, C. T., Wu, C. W., and Shen, C. Y. (2001). "Mechanisms of inactivation of E-cadherin in breast carcinoma: modification of the two-hit hypothesis of tumor suppressor gene." In: *Oncogene* 20.29, pp. 3814–3823.

Chiba, S., Okuda, M., Mussman, J. G., and Fukasawa, K. (2000). "Genomic convergence and suppression of centrosome hyperamplification in primary p53-/- cells in prolonged culture." In: *Experimental cell research* 258.2, pp. 310–21.

Chng, W. J., Ahmann, G. J., Henderson, K., Santana-Davila, R., Greipp, P. R., Gertz, M. A., Lacy, M. Q., Dispenzieri, A., Kumar, S., Rajkumar, S. V., Lust, J. A., Kyle, R. A., Zeldenrust, S. R., Hayman, S. R., and Fonseca, R. (2006). "Clinical implication of centrosome amplification in plasma cell neoplasm". In: *Blood* 107.9, pp. 3669–3675.

Ciferri, C., Musacchio, A., and Petrovic, A. (2007). "The Ndc80 complex: hub of kinetochore activity." In: *FEBS letters* 581.15, pp. 2862–9.

Cimini, D. (2008). "Merotelic kinetochore orientation, aneuploidy, and cancer." In: *Biochimica et biophysica acta* 1786.1, pp. 32–40.

Cleton-Jansen, A. M., Callen, D. F., Seshadri, R., Goldup, S., McCallum, B., Crawford, J., Powell, J. A., Settasatian, C., Van Beerendonk, H., Moerland, E. W., Smit, V. T. B. H. M., Harris, W. H., Millis, R., Morgan, N. V., Barnes, D., Mathew, C. G., and Cornelisse, C. J. (2001). "Loss of heterozygosity mapping at chromosome arm 16q in 712 breast tumors reveals factors that influence delineation of candidate regions". In: *Cancer Research* 61.3, pp. 1171–1177.

Coelho, P. A., Bury, L., Shahbazi, M. N., Liakath-Ali, K., Tate, P. H., Wormald, S., Hindley, C. J., Huch, M., Archer, J., Skarnes, W. C., Zernicka-Goetz, M., and Glover, D. M. (2015). "Over-expression of Plk4 induces centrosome amplification, loss of primary cilia and associated tissue hyperplasia in the mouse." In: *Open biology* 5.12.

Comartin, D., Gupta, G. D., Fussner, E., Coyaud, É., Hasegan, M., Archinti, M., Cheung, S. W. T., Pinchev, D., Lawo, S., Raught, B., Bazett-Jones, D. P., Lüders, J., and Pelletier, L. (2013). "CEP120 and SPICE1 cooperate with CPAP in centriole elongation". In: *Current Biology* 23.14, pp. 1360–1366.

Cong, L., Ran, F. A., Cox, D., Lin, S., Barretto, R., Habib, N., Hsu, P. D., Wu, X., Jiang, W., Marraffini, L. A., and Zhang, F. (2013). "Multiplex Genome Engineering Using CRISPR/Cas System". In: *Science* 339.2, pp. 819–824.

Coon, B. G., Baeyens, N., Han, J., Budatha, M., Ross, T. D., Fang, J. S., Yun, S., Thomas, J. L., and Schwartz, M. A. (2015). "Intramembrane binding of VE-cadherin to VEGFR2 and VEGFR3 assembles the endothelial mechanosensory complex". In: *Journal of Cell Biology* 208.7, pp. 975–986.

Crasta, K., Ganem, N. J., Dagher, R., Lantermann, A. B., Ivanova, E. V., Pan, Y., Nezi, L., Protopopov, A., Chowdhury, D., and Pellman, D. (2012). "DNA

breaks and chromosome pulverization from errors in mitosis." In: *Nature* 482.7383, pp. 53–8.

Crick, S. L. and Yin, F. C. P. (2007). "Assessing micromechanical properties of cells with atomic force microscopy: Importance of the contact point". In: *Biomechanics and Modeling in Mechanobiology* 6.3, pp. 199–210.

Cunha-Ferreira, I., Rodrigues-Martins, A., Bento, I., Riparbelli, M., Zhang, W., Laue, E., Callaini, G., Glover, D. M., and Bettencourt-Dias, M. (2009). "The SCF/Slimb Ubiquitin Ligase Limits Centrosome Amplification through Degradation of SAK/PLK4". In: *Current Biology* 19.1, pp. 43–49.

Dammermann, A., Müller-Reichert, T., Pelletier, L., Habermann, B., Desai, A., and Oegema, K. (2004). "Centriole assembly requires both centriolar and pericentriolar material proteins". In: *Developmental Cell* 7.6, pp. 815–829.

Das, S., Ongusaha, P. P., Yang, Y. S., Park, J.-M., Aaronson, S. A., and Lee, S. W. (2006). "Discoidin domain receptor 1 receptor tyrosine kinase induces cyclooxygenase-2 and promotes chemoresistance through nuclear factor-kappaB pathway activation." In: *Cancer research* 66.16, pp. 8123–30.

D'Assoro, A. B., Barrett, S. L., Folk, C., Negron, V. C., Boeneman, K., Busby, R., Whitehead, C., Stivala, F., Lingle, W. L., and Salisbury, J. L. (2002). "Amplified centrosomes in breast cancer: a potential indicator of tumor aggressiveness." In: *Breast cancer research and treatment* 75.1, pp. 25–34.

Davies, A. H., Barrett, I., Pambid, M. R., Hu, K., Stratford, A. L., Freeman, S., Berquin, I. M., Pelech, S., Hieter, P., Maxwell, C., and Dunn, S. E. (2011). "YB-1 evokes susceptibility to cancer through cytokinesis failure, mitotic dysfunction and HER2 amplification." In: *Oncogene* 30.34, pp. 3649–60.

Davoli, T. and Lange, T. de (2012). "Telomere-Driven Tetraploidization Occurs in Human Cells Undergoing Crisis and Promotes Transformation of Mouse Cells". In: *Cancer Cell* 21.6, pp. 765–776.

De Simone, A., Nédélec, F., and Gönczy, P. (2016). "Dynein Transmits Polarized Actomyosin Cortical Flows to Promote Centrosome Separation." In: *Cell reports* 14.9, pp. 2250–62.

De Wever, O., Derycke, L., Hendrix, A., De Meerleer, G., Godeau, F., Depypere, H., and Bracke, M. (2007). "Soluble cadherins as cancer biomarkers". In: *Clinical and Experimental Metastasis* 24.8, pp. 685–697.

Debec, A. (1978). “Haploid cell cultures of Drosophila melanogaster.” In: *Nature* 274.5668, pp. 255–6.

Delattre, M., Leidel, S., Wani, K., Baumer, K., Bamat, J., Schnabel, H., Feichtinger, R., Schnabel, R., and Gönczy, P. (2004). “Centriolar SAS-5 is required for centrosome duplication in C. elegans”. In: *Nat Cell Biol* 6.7, pp. 656–664.

Dementyeva, E., Nemec, P., Kryukov, F., Muthu Raja, K. R., Smetana, J., Zaoralova, R., Greslikova, H., Kupska, R., Kuglik, P., and Hajek, R. (2010). “Centrosome amplification as a possible marker of mitotic disruptions and cellular carcinogenesis in multiple myeloma.” In: *Leukemia research* 34.8, pp. 1007–11.

Deng, C. X. (2001). “Tumorigenesis as a consequence of genetic instability in Brca1 mutant mice.” In: *Mutation research* 477.1-2, pp. 183–9.

Denu, R. A., Zasadil, L. M., Kanugh, C., Laffin, J., Weaver, B. A., and Burkard, M. E. (2016). “Centrosome amplification induces high grade features and is prognostic of worse outcomes in breast cancer.” In: *BMC cancer* 16.1, p. 47.

Dietz, R. (1966). “The dispensability of the centrioles in the spermatocyte division of Pales ferruginea (Nematocera)”. In: *Darlington CD, Lewis KR (eds) Chromosomes today*. Ed. by O. and Boyd. London, pp. 161–166.

Drosopoulos, K., Tang, C., Chao, W. C. H., and Linardopoulos, S. (2014). “APC/C is an essential regulator of centrosome clustering.” en. In: *Nature communications* 5, p. 3686.

Duelli, D. M., Padilla-Nash, H. M., Berman, D., Murphy, K. M., Ried, T., and Lazebnik, Y. (2007). “A Virus Causes Cancer by Inducing Massive Chromosomal Instability through Cell Fusion”. In: *Current Biology* 17.5, pp. 431–437.

Duensing, A., Chin, A., Wang, L., Kuan, S. F., and Duensing, S. (2008). “Analysis of centrosome overduplication in correlation to cell division errors in high-risk human papillomavirus (HPV)-associated anal neoplasms”. In: *Virology* 372.1, pp. 157–164.

Duensing, A., Spardy, N., Chatterjee, P., Zheng, L., Parry, J., Cuevas, R., Korzeniewski, N., and Duensing, S. (2009). “Centrosome overduplication, chromosomal instability, and human papillomavirus oncoproteins”. In: *Environmental and Molecular Mutagenesis* 50.8, pp. 741–747.

Duensing, S., Lee, B. H., Dal Cin, P., and Münger, K. (2003). “Excessive centrosome abnormalities without ongoing numerical chromosome instability in a Burkitt’s lymphoma.” In: *Molecular cancer* 2.1, p. 30.

Dupin, I., Camand, E., and Etienne-Manneville, S. (2009). "Classical cadherins control nucleus and centrosome position and cell polarity". In: *Journal of Cell Biology* 185.5, pp. 779–786.

Eger, A., Aigner, K., Sonderegger, S., Dampier, B., Oehler, S., Schreiber, M., Berx, G., Cano, A., Beug, H., and Foisner, R. (2005). "DeltaEF1 is a transcriptional repressor of E-cadherin and regulates epithelial plasticity in breast cancer cells." In: *Oncogene* 24.14, pp. 2375–85.

Elzen, N. den, Buttery, C. V., Maddugoda, M. P., Ren, G., and Yap, A. S. (2009). "Cadherin adhesion receptors orient the mitotic spindle during symmetric cell division in mammalian epithelia." In: *Molecular biology of the cell* 20.16, pp. 3740–50.

Erickson, H. P. (2000). "Gamma-tubulin nucleation: template or protofilament?" In: *Nature cell biology* 2.6, E93–E96.

Eswaramoorthy, R., Wang, C.-K., Chen, W.-C., Tang, M.-J., Ho, M.-L., Hwang, C.-C., Wang, H.-M., and Wang, C.-Z. (2010). "DDR1 regulates the stabilization of cell surface E-cadherin and E-cadherin-mediated cell aggregation." In: *Journal of cellular physiology* 224.2, pp. 387–97.

Even-Ram, S., Doyle, A. D., Conti, M. A., Matsumoto, K., Adelstein, R. S., and Yamada, K. M. (2007). "Myosin IIA regulates cell motility and actomyosin-microtubule crosstalk." In: *Nature cell biology* 9.3, pp. 299–309.

Fabarius, A., Giehl, M., Rebacz, B., Kramer, A., Frank, O., Haferlach, C., Duesberg, P., Hehlmann, R., Seifarth, W., and Hochhaus, A. (2008). "Centrosome aberrations and G1 phase arrest after in vitro and in vivo treatment with the SRC/ABL inhibitor dasatinib". In: *Haematologica* 93.8, pp. 1145–1154.

Fava, L. L., Schuler, F., Sladky, V., Haschka, M. D., Soratroi, C., Eiterer, L., Demetz, E., Weiss, G., Geley, S., Nigg, E. A., and Villunger, A. (2017). "The PIDDosome activates p53 in response to supernumerary centrosomes". In: *Genes & Development* 31.1, pp. 34–45.

Fielding, A. B., Dobreva, I., McDonald, P. C., Foster, L. J., and Dedhar, S. (2008). "Integrin-linked kinase localizes to the centrosome and regulates mitotic spindle organization." In: *The Journal of cell biology* 180.4, pp. 681–9.

Fink, J., Carpi, N., Betz, T., Bétard, A., Chebah, M., Azioune, A., Bornens, M., Sykes, C., Fetler, L., Cuvelier, D., and Piel, M. (2011). "External forces control mitotic spindle positioning." In: *Nature cell biology* 13.7, pp. 771–8.

Fisk, H. A. and Winey, M. (2001). "The mouse Mps1p-like kinase regulates centrosome duplication". In: *Cell* 106.1, pp. 95–104.

Fırat-karalar, E. N. and Stearns, T. (2014). "The centriole duplication cycle." In: *Philosophical transactions of the Royal Society of London. Series B, Biological sciences* 369.July, pp. 1–10.

Fong, C. S., Kim, M., Yang, T. T., Liao, J. C., and Tsou, M. F. B. (2014). "SAS-6 Assembly Templated by the Lumen of Cartwheel-less Centrioles Precedes Centriole Duplication". In: *Developmental Cell* 30.2, pp. 238–245.

Ford, C. E., Lau, S. K., Zhu, C. Q., Andersson, T., Tsao, M. S., and Vogel, W. F. (2007). "Expression and mutation analysis of the discoidin domain receptors 1 and 2 in non-small cell lung carcinoma." In: *British journal of cancer* 96.5, pp. 808–14.

Fritz-Laylin, L. K., Assaf, Z. J., Chen, S., and Cande, W. Z. (2010). "Naegleria gruberi de novo basal body assembly occurs via stepwise incorporation of conserved proteins". In: *Eukaryotic Cell* 9.6, pp. 860–865.

Frixen, U. H., Behrens, J., Sachs, M., Eberle, G., Voss, B., Warda, A., Lochner, D., and Birchmeier, W. (1991). "E-cadherin-mediated cell-cell adhesion prevents invasiveness of human carcinoma cells". In: *Journal of Cell Biology* 113.1, pp. 173–185.

Fry, A. M., Mayor, T., Meraldi, P., Stierhof, Y. D., Tanaka, K., and Nigg, E. A. (1998). "C-Nap1, a novel centrosomal coiled-coil protein and candidate substrate of the cell cycle-regulated protein kinase Nek2". In: *Journal of Cell Biology* 141.7, pp. 1563–1574.

Fu, J. and Glover, D. M. (2012). "Structured illumination of the interface between centriole and peri-centriolar material." In: *Open biology* 2.8, p. 120104.

Fu, J., Hagan, I. M., and Glover, D. M. (2015). "The centrosome and its duplication cycle." In: *Cold Spring Harbor perspectives in biology* 7.2, a015800.

Fuentealba, L. C., Eivers, E., Ikeda, A., Hurtado, C., Kuroda, H., Pera, E. M., and De Robertis, E. M. (2007). "Integrating Patterning Signals: Wnt/GSK3 Regulates the Duration of the BMP/Smad1 Signal". In: *Cell* 131.5, pp. 980–993.

Fujita, H., Yoshino, Y., and Chiba, N. (2016). "Regulation of the centrosome cycle." In: *Molecular & cellular oncology* 3.2, e1075643.

Fujita, Y., Krause, G., Scheffner, M., Zechner, D., Leddy, H. E. M., Behrens, J., Sommer, T., and Birchmeier, W. (2002). "Hakai, a c-Cbl-like protein, ubiquitinates and induces endocytosis of the E-cadherin complex." In: *Nature cell biology* 4.3, pp. 222–231.

Fujiwara, T., Bandi, M., Nitta, M., Ivanova, E. V., Bronson, R. T., and Pellman, D. (2005). "Cytokinesis failure generating tetraploids promotes tumorigenesis in p53-null cells." In: *Nature* 437.7061, pp. 1043–7.

Fukasawa, K., Choi, T., Kuriyama, R., Rulong, S., and Vande Woude, G. F. (1996). "Abnormal centrosome amplification in the absence of p53." In: *Science (New York, N.Y.)* 271.5256, pp. 1744–1747.

Fukushi, D., Watanabe, N., Kasai, F., Haruta, M., Kikuchi, A., Kikuta, A., Kato, K., Nakadate, H., Tsunematsu, Y., and Kaneko, Y. (2009). "Centrosome amplification is correlated with ploidy divergence, but not with MYCN amplification, in neuroblastoma tumors". In: *Cancer Genetics and Cytogenetics* 188.1, pp. 32–41.

Galeotti (1893). "Beitrag zum Studium des Chromatins in den Epithelzellen der Carcinome". In: *Beitr. Pathol. Anal. Allg. Pathol* 14, pp. 249–271.

Ganem, N. J., Cornils, H., Chiu, S.-Y. Y., O'Rourke, K. P., Arnaud, J., Yimlamai, D., Théry, M., Camargo, F. D., and Pellman, D. (2014). "Cytokinesis failure triggers hippo tumor suppressor pathway activation". In: *Cell* 158.4, pp. 833–848.

Ganem, N. J., Godinho, S. A., and Pellman, D. (2009). "A mechanism linking extra centrosomes to chromosomal instability." In: *Nature* 460.7252, pp. 278–82.

Ganem, N. J., Storchova, Z., and Pellman, D. (2007). "Tetraploidy, aneuploidy and cancer". In: *Current Opinion in Genetics and Development* 17.2, pp. 157–162.

Gao, Y. and Zhang, B. (2009). "[Expression of TEIF protein in colorectal tumors and its correlation with centrosome abnormality]." In: *Ai zheng = Aizheng = Chinese journal of cancer* 28.12, pp. 1277–1282.

Giehl, M., Fabarius, A., Frank, O., Hochhaus, A., Hafner, M., Hehlmann, R., and Seifarth, W. (2005). "Centrosome aberrations in chronic myeloid leukemia correlate with stage of disease and chromosomal instability." In: *Leukemia* 19.7, pp. 1192–7.

Gisselsson, D., Gorunova, L., Hoglund, M., Mandahl, N., and Elfving, P. (2004). "Telomere shortening and mitotic dysfunction generate cytogenetic heterogeneity in a subgroup of renal cell carcinomas". In: *Br J Cancer* 91.2, pp. 327–332.

Gisselsson, D., Jonson, T., Yu, C., Martins, C., Mandahl, N., Wiegant, J., Jin, Y., Mertens, F., and Jin, C. (2002). "Centrosomal abnormalities, multipolar mitoses, and chromosomal instability in head and neck tumours with dysfunctional telomeres." In: *British journal of cancer* 87.2, pp. 202–7.

Gloerich, M., Bianchini, J. M., Siemers, K. A., Cohen, D. J., and Nelson, W. J. (2017). "Cell division orientation is coupled to cell-cell adhesion by the E-cadherin/LGN complex." In: *Nature communications* 8, p. 13996.

Godinho, S. A. and Pellman, D. (2014). "Causes and consequences of centrosome abnormalities in cancer." In: *Philosophical transactions of the Royal Society of London. Series B, Biological sciences* 369.1650.

Godinho, S. A., Kwon, M., and Pellman, D. (2009). "Centrosomes and cancer: how cancer cells divide with too many centrosomes." In: *Cancer metastasis reviews* 28.1-2, pp. 85–98.

Godinho, S. A., Picone, R., Burute, M., Dagher, R., Su, Y., Leung, C. T., Polyak, K., Brugge, J. S., Théry, M., and Pellman, D. (2014). "Oncogene-like induction of cellular invasion from centrosome amplification." In: *Nature* 510.7503, pp. 167–71.

Gönczy, P. (2012). "Towards a molecular architecture of centriole assembly". In: *Nature Reviews Molecular Cell Biology* 13.7, pp. 425–435.

Gönczy, P. (2015). "Centrosomes and cancer: revisiting a long-standing relationship". In: *Nat Rev Cancer* 15.11, pp. 639–652.

Gong, Y., Sun, Y., McNutt, M. a., Sun, Q., Hou, L., Liu, H., Shen, Q., Ling, Y., Chi, Y., and Zhang, B. (2009). "Localization of TEIF in the centrosome and its functional association with centrosome amplification in DNA damage, telomere dysfunction and human cancers". In: *Oncogene* 28.November 2008, pp. 1549–1560.

Gopalakrishnan, J., Mennella, V., Blachon, S., Zhai, B., Smith, A. H., Megraw, T. L., Nicastro, D., Gygi, S. P., Agard, D. A., and Avidor-Reiss, T. (2011). "Sas-4 provides a scaffold for cytoplasmic complexes and tethers them in a centrosome." In: *Nature communications* 2.May, p. 359.

Gräf, R., Euteneuer, U., Ho, T.-H., and Rehberg, M. (2003). "Regulated expression of the centrosomal protein DdCP224 affects microtubule dynamics and reveals mechanisms for the control of supernumerary centrosome number." In: *Molecular biology of the cell* 14.10, pp. 4067–74.

Graff, J. R., Herman, J. G., Lapidus, R. G., Chopra, H., Xu, R., Pitha, P. M., Davidson, N. E., Baylin, S. B., Jarrard, D. F., and Isaacs, W. B. (1995). "E-Cadherin Expression Is Silenced by DNA Hypermethylation in Human Breast and Prostate Carcinomas". In: *Cancer Research* 55.22, pp. 5195–5199.

Grallert, A., Chan, K. Y., Alonso-Nuñez, M. L., Madrid, M., Biswas, A., Alvarez-Tabarés, I., Connolly, Y., Tanaka, K., Robertson, A., Ortiz, J. M., Smith, D. L., and Hagan, I. M. (2013). "Removal of centrosomal PP1 by NIMA kinase unlocks the MPF feedback loop to promote mitotic commitment in S. pombe". In: *Current Biology* 23.3, pp. 213–222.

Graser, S., Stierhof, Y.-D., and Nigg, E. A. (2007). "Cep68 and Cep215 (Cdk5rap2) are required for centrosome cohesion." In: *Journal of cell science* 120.Pt 24, pp. 4321–4331.

Grikscheit, K., Frank, T., Wang, Y., and Grosse, R. (2015). "Junctional actin assembly is mediated by Formin-like 2 downstream of Rac1". In: *The Journal of Cell Biology* 209.3, pp. 367–376.

Guaita, S., Puig, I., Francí, C., Garrido, M., Domínguez, D., Batlle, E., Sancho, E., Dedhar, S., De Herreros, A. G., and Baulida, J. (2002). "Snail induction of epithelial to mesenchymal transition in tumor cells is accompanied by MUC1 repression and ZEB1 expression". In: *Journal of Biological Chemistry* 277.42, pp. 39209–39216.

Guardavaccaro, D., Kudo, Y., Boulaire, J., Barchi, M., Busino, L., Donzelli, M., Margottin-Goguet, F., Jackson, P. K., Yamasaki, L., and Pagano, M. (2003). "Control of meiotic and mitotic progression by the F box protein β-Trcp1 in vivo". In: *Developmental Cell* 4.6, pp. 799–812.

Guderian, G., Westendorf, J., Uldschmid, A., and Nigg, E. A. (2010). "Plk4 trans-autophosphorylation regulates centriole number by controlling betaTrCP-mediated degradation." In: *Journal of cell science* 123.Pt 13, pp. 2163–9.

Gudi, R., Haycraft, C. J., Bell, P. D., Li, Z., and Vasu, C. (2015). "Centrobin-mediated regulation of the centrosomal protein 4.1-associated protein (CPAP) level limits centriole length during elongation stage". In: *Journal of Biological Chemistry* 290.11, pp. 6890–6902.

Gudi, R., Zou, C., Dhar, J., Gao, Q., and Vasu, C. (2014). "Centrobin-centrosomal protein 4.1-associated protein (CPAP) interaction promotes CPAP localization to

the centrioles during centriole duplication". In: *Journal of Biological Chemistry* 289.22, pp. 15166–15178.

Gudi, R., Zou, C., Li, J., and Gao, Q. (2011). "Centrobin-tubulin interaction is required for centriole elongation and stability". In: *Journal of Cell Biology* 193.4, pp. 711–725.

Guichard, P., Chretien, D., Marco, S., and Tassin, A. M. (2010). "Procentriole assembly revealed by cryo-electron tomography". In: *EMBO J* 29.9, pp. 1565–1572.

Gumbiner, B. M. (2005). "Regulation of cadherin-mediated adhesion in morphogenesis." In: *Nature reviews. Molecular cell biology* 6.8, pp. 622–34.

Guo, H.-q., Gao, M., Ma, J., Xiao, T., Zhao, L.-l., Gao, Y., and Pan, Q.-j. (2007). "Analysis of the cellular centrosome in fine-needle aspirations of the breast." In: *Breast cancer research : BCR* 9.4, R48.

Guo, Z., Neilson, L. J., Zhong, H., Murray, P. S., Zanivan, S., and Zaidel-Bar, R. (2014). "E-cadherin interactome complexity and robustness resolved by quantitative proteomics." In: *Science signaling* 7.354, rs7.

Gustafson, L. M., Gleich, L. L., Fukasawa, K., Chadwell, J., Miller, M. A., Stambrook, P. J., and Gluckman, J. L. (2000). "Centrosome hyperamplification in head and neck squamous cell carcinoma: a potential phenotypic marker of tumor aggressiveness." In: *The Laryngoscope* 110.11, pp. 1798–801.

Habedanck, R., Stierhof, Y.-D., Wilkinson, C. J., and Nigg, E. A. (2005). "The Polo kinase Plk4 functions in centriole duplication." In: *Nature cell biology* 7.11, pp. 1140–6.

Hachet, V., Canard, C., and Gönczy, P. (2007). "Centrosomes Promote Timely Mitotic Entry in C. elegans Embryos". In: *Developmental Cell* 12.4, pp. 531–541.

Hagan, I. M. (2008). "The spindle pole body plays a key role in controlling mitotic commitment in the fission yeast Schizosaccharomyces pombe." In: *Biochemical Society transactions* 36, pp. 1097–1101.

Hagan, I. M. and Grallert, A. (2013). "Spatial control of mitotic commitment in fission yeast." In: *Biochemical Society transactions* 41.6, pp. 1766–71.

Halbleib, J. M. and Nelson, W. J. (2006). "Cadherins in development: Cell adhesion, sorting, and tissue morphogenesis". In: *Genes and Development* 20.23, pp. 3199–3214.

Hama, S., Matsuura, S., Tauchi, H., Yamasaki, F., Kajiwara, Y., Arita, K., Yoshioka, H., Heike, Y., Mandai, K., and Kurisu, K. (2003). "p16 Gene transfer increases cell killing with abnormal nucleation after ionising radiation in glioma cells." In: *British journal of cancer* 89.9, pp. 1802–11.

Hansemann, D. (1890). "Ueber asymmetrische Zelltheilung in Epithelkrebsen und deren biologische Bedeutung". In: *Archiv für Pathologische Anatomie und Physiologie und für Klinische Medicin* 119.2, pp. 299–326.

Hansen, C., Greengard, P., Nairn, A. C., Andersson, T., and Vogel, W. F. (2006). "Phosphorylation of DARPP-32 regulates breast cancer cell migration downstream of the receptor tyrosine kinase DDR1." In: *Experimental cell research* 312.20, pp. 4011–8.

Hansford, S., Kaurah, P., Li-Chang, H., Woo, M., Senz, J., Pinheiro, H., Schrader, K. A., Schaeffer, D. F., Shumansky, K., Zogopoulos, G., Santos, T. A., Claro, I., Carvalho, J., Nielsen, C., Padilla, S., Lum, A., Talhouk, A., Baker-Lange, K., Richardson, S., Lewis, I., Lindor, N. M., Pennell, E., MacMillan, A., Fernandez, B., Keller, G., Lynch, H., Shah, S. P., Guilford, P., Gallinger, S., Corso, G., Roviello, F., Caldas, C., Oliveira, C., Pharoah, P. D. P., and Huntsman, D. G. (2015). "Hereditary Diffuse Gastric Cancer Syndrome: CDH1 Mutations and Beyond." In: *JAMA oncology* 1.1, pp. 23–32.

Harris, A. R., Daeden, A., and Charras, G. T. (2014). "Formation of adherens junctions leads to the emergence of a tissue-level tension in epithelial monolayers." In: *Journal of cell science* 127.Pt 11, pp. 2507–17.

Hashimoto, T., Soeno, Y., Maeda, G., Taya, Y., Aoba, T., Nasu, M., Kawashiri, S., and Imai, K. (2012). "Progression of Oral Squamous Cell Carcinoma Accompanied with Reduced E-Cadherin Expression but Not Cadherin Switch". In: *PLoS ONE* 7.10. Ed. by K. M. R, e47899.

Hatch, E. M., Fischer, A. H., Deerinck, T. J., and Hetzer, M. W. (2013). "Catastrophic nuclear envelope collapse in cancer cell micronuclei." English. In: *Cell* 154.1, pp. 47–60.

Hayward, D. G., Clarke, R. B., Faragher, A. J., Pillai, M. R., Hagan, I. M., and Fry, A. M. (2004). "The centrosomal kinase Nek2 displays elevated levels of protein expression in human breast cancer." In: *Cancer research* 64.20, pp. 7370–6.

Hazan, R. B., Qiao, R., Keren, R., Badano, I., and Suyama, K. (2004). "Cadherin switch in tumor progression". In: *Annals of the New York Academy of Sciences* 1014, pp. 155–163.

He, R., Huang, N., Bao, Y., Zhou, H., Teng, J., and Chen, J. (2013). "LRRC45 Is a Centrosome Linker Component Required for Centrosome Cohesion". In: *Cell Reports* 4.6, pp. 1100–1107.

Heald, R., Tournebize, R., Blank, T., Sandaltzopoulos, R., Becker, P., Hyman, A., and Karsenti, E. (1996). "Self-organization of microtubules into bipolar spindles around artificial chromosomes in Xenopus egg extracts." In: *Nature* 382.6590, pp. 420–5.

Hendrick, J., Franz-Wachtel, M., Moeller, Y., Schmid, S., Macek, B., and Olayioye, M. A. (2016). "The polarity protein Scribble positions DLC3 at adherens junctions to regulate Rho signaling." In: *Journal of cell science* 129.19, jcs.190074.

Hensel, M., Zoz, M., Giesecke, C., Benner, A., Neben, K., Jauch, A., Stilgenbauer, S., Ho, A. D., and Krämer, A. (2007). "High rate of centrosome aberrations and correlation with proliferative activity in patients with untreated B-cell chronic lymphocytic leukemia." In: *International journal of cancer. Journal international du cancer* 121.5, pp. 978–83.

Hidalgo-Carcedo, C., Hooper, S., Chaudhry, S. I., Williamson, P., Harrington, K., Leitinger, B., and Sahai, E. (2011). "Collective cell migration requires suppression of actomyosin at cell-cell contacts mediated by DDR1 and the cell polarity regulators Par3 and Par6." In: *Nature cell biology* 13.1, pp. 49–58.

Hinchcliffe, E. H., Li, C., Thompson, E. a., Maller, J. L., and Sluder, G. (1999). "Requirement of Cdk2-cyclin E activity for repeated centrosome reproduction in Xenopus egg extracts." In: *Science (New York, N.Y.)* 283.5403, pp. 851–854.

Hodges, M. E., Scheumann, N., Wickstead, B., Langdale, J. A., and Gull, K. (2010). "Reconstructing the evolutionary history of the centriole from protein components". In: *J Cell Sci* 123.Pt 9, pp. 1407–1413.

Hoh, R. A., Stowe, T. R., Turk, E., and Stearns, T. (2012). "Transcriptional Program of Ciliated Epithelial Cells Reveals New Cilium and Centrosome Components and Links to Human Disease". In: *PLoS ONE* 7.12.

Holland, A. J. and Cleveland, D. W. (2012). "Losing balance: the origin and impact of aneuploidy in cancer." In: *EMBO reports* 13.6, pp. 501–14.

Holland, A. J., Fachinetti, D., Zhu, Q., Bauer, M., Verma, I. M., Nigg, E. A., and Cleveland, D. W. (2012). "The autoregulated instability of Polo-like kinase 4 limits centrosome duplication to once per cell cycle." In: *Genes & development* 26.24, pp. 2684–9.

Holland, A. J., Lan, W., and Cleveland, D. W. (2010). "Centriole duplication: A lesson in self-control". In: *Cell Cycle* 9.14, pp. 2731–2736.

Holland, A. J., Lan, W., Niessen, S., Hoover, H., and Cleveland, D. W. (2010). "Polo-like kinase 4 kinase activity limits centrosome overduplication by autoregulating its own stability". In: *Journal of Cell Biology* 188.2, pp. 191–198.

Homem, C. C. F. and Peifer, M. (2008). "Diaphanous regulates myosin and adherens junctions to control cell contractility and protrusive behavior during morphogenesis". In: *Development* 135.6, pp. 1005–1018.

Hoque, A., Carter, J., Xia, W., Hung, M.-C. C., Sahin, A. A., Sen, S., and Lippman, S. M. (2003). "Loss of Aurora A/STK15/BTAK A/STK]5/BTAK Overexpression Correlates with Transition of in Situ to Invasive Ductal Carcinoma of the Breast". In: *Cancer Epidemiology Biomarkers and Prevention* 12.12, pp. 1518–1522.

Hsu, L.-C., Kapali, M., DeLoia, J. A., and Gallion, H. H. (2005). "Centrosome abnormalities in ovarian cancer." In: *International journal of cancer. Journal international du cancer* 113.5, pp. 746–51.

Hu, Y., Liu, J., Jiang, B., Chen, J., Fu, Z., Bai, F., Jiang, J., and Tang, Z. (2014). "MiR-199a-5p Loss Up-Regulated DDR1 Aggravated Colorectal Cancer by Activating Epithelial-to-Mesenchymal Transition Related Signaling". In: *Digestive Diseases and Sciences* 59.9, pp. 2163–2172.

Huang, Y., Arora, P., McCulloch, C. A., and Vogel, W. F. (2009). "The collagen receptor DDR1 regulates cell spreading and motility by associating with myosin IIA." In: *Journal of cell science* 122.Pt 10, pp. 1637–46.

Hwang, W. Y., Fu, Y., Reyon, D., Maeder, M. L., Tsai, S. Q., Sander, J. D., Peterson, R. T., Yeh, J. R., and Joung, J. K. (2013). "Efficient genome editing in zebrafish using a CRISPR-Cas system". In: *Nat Biotechnol* 31.3, pp. 227–229.

Ikeda, K., Wang, L.-H., Torres, R., Zhao, H., Olaso, E., Eng, F. J., Labrador, P., Klein, R., Lovett, D., Yancopoulos, G. D., Friedman, S. L., and Lin, H. C. (2002).

"Discoidin Domain Receptor 2 Interacts with Src and Shc following Its Activation by Type I Collagen". In: *Journal of Biological Chemistry* 277.21, pp. 19206–19212.

Inaba, M., Yuan, H., Salzmann, V., Fuller, M. T., and Yamashita, Y. M. (2010). "E-Cadherin is required for centrosome and spindle orientation in Drosophila male germline stem cells". In: *PLoS ONE* 5.8.

Ishihara, H., Martin, B. L., Brautigan, D. L., Karaki, H., Ozaki, H., Kato, Y., Fusetani, N., Watabe, S., Hashimoto, K., Uemura, D., and Hartshorne, D. J. (1989). "Calyculin A and okadaic acid: Inhibitors of protein phosphatase activity". In: *Biochemical and Biophysical Research Communications* 159.3, pp. 871–877.

Itoh, K., Jenny, A., Mlodzik, M., and Sokol, S. Y. (2009). "Centrosomal localization of Diversin and its relevance to Wnt signaling." In: *Journal of cell science* 122, pp. 3791–3798.

Iwao, Y., Murakawa, T., Yamaguchi, J., and Yamashita, M. (2002). "Localization of gamma-tubulin and cyclin B during early cleavage in physiologically polyspermic newt eggs." In: *Development, growth & differentiation* 44.6, pp. 489–99.

Izumi, H. and Kaneko, Y. (2012). "Evidence of asymmetric cell division and centrosome inheritance in human neuroblastoma cells". In: *Proceedings of the National Academy of Sciences* 109.44, pp. 18048–18053.

Jackman, M., Lindon, C., Nigg, E. a., and Pines, J. (2003). "Active cyclin B1-Cdk1 first appears on centrosomes in prophase." In: *Nature cell biology* 5.2, pp. 143–148.

Jakobsen, L., Vanselow, K., Skogs, M., Toyoda, Y., Lundberg, E., Poser, I., Falkenby, L. G., Bennetzen, M., Westendorf, J., Nigg, E. A., Uhlen, M., Hyman, A. A., and Andersen, J. S. (2011). "Novel asymmetrically localizing components of human centrosomes identified by complementary proteomics methods." In: *The EMBO journal* 30.8, pp. 1520–35.

Janssen, A., Burg, M. van der, Szuhai, K., Kops, G. J. P. L., and Medema, R. H. (2011). "Chromosome segregation errors as a cause of DNA damage and structural chromosome aberrations." In: *Science (New York, N.Y.)* 333.6051, pp. 1895–8.

Jaspersen, S. L. and Winey, M. (2004). "The budding yeast spindle pole body: structure, duplication, and function." In: *Annual review of cell and developmental biology* 20, pp. 1–28.

Jiang, F., Caraway, N. P., Sabichi, A. L., Zhang, H. Z., Ruitrok, A., Grossman, H. B., Gu, J., Lerner, S. P., Lippman, S., and Katz, R. L. (2003). "Centrosomal

abnormality is common in and a potential biomarker for bladder cancer". In: *International Journal of Cancer* 106.5, pp. 661–665.

Jinek, M., Chylinski, K., Fonfara, I., Hauer, M., Doudna, J. A., and Charpentier, E. (2012). "A Programmable Dual-RNA – Guided DNA Endonuclease in Adaptice Bacterial Immunity". In: *Science (New York, N.Y.)* 337.August, pp. 816–822.

Juin, A., Di Martino, J., Leitinger, B., Henriet, E., Gary, A.-S., Paysan, L., Bomo, J., Baffet, G., Gauthier-Rouvière, C., Rosenbaum, J., Moreau, V., and Saltel, F. (2014). "Discoidin domain receptor 1 controls linear invadosome formation via a Cdc42-Tuba pathway." In: *The Journal of cell biology* 207.4, pp. 517–33.

Jung, C. K., Jung, J. H., Lee, K. Y., Kang, C. S., Kim, M., Ko, Y. H., and Oh, C. S. (2007). "Centrosome abnormalities in non-small cell lung cancer: Correlations with DNA aneuploidy and expression of cell cycle regulatory proteins". In: *Pathology Research and Practice* 203.12, pp. 839–847.

Kanai, Y., Ushijima, S., Tsuda, H., Sakamoto, M., and Hirohashi, S. (2000). "Aberrant DNA methylation precedes loss of heterozygosity on chromosome 16 in chronic hepatitis and liver cirrhosis." In: *Cancer letters* 148.1, pp. 73–80.

Kanazawa, T., Watanabe, T., Kazama, S., Tada, T., Koketsu, S., and Nagawa, H. (2002). "Poorly differentiated adenocarcinoma and mucinous carcinoma of the colon and rectum show higher rates of loss of heterozygosity and loss of E-cadherin expression due to methylation of promoter region". In: *International Journal of Cancer* 102.3, pp. 225–229.

Kaneko, H., Ishikawa, S., Sumida, T., Sekiya, M., Toshima, M., Kobayashi, H., and Naka, Y. (1980). "Ultrastructural studies of a thymic carcinoid tumor". In: *Acta Pathol Jpn* 30.4, pp. 651–658.

Karna, P., Rida, P. C. G., Pannu, V., Gupta, K. K., Dalton, W. B., Joshi, H., Yang, V. W., Zhou, J., and Aneja, R. (2011). "A novel microtubule-modulating noscapinoid triggers apoptosis by inducing spindle multipolarity via centrosome amplification and declustering." In: *Cell death and differentiation* 18.4, pp. 632–44.

Karsenti, E., Newport, J., and Kirschner, M. (1984). "Respective roles of centrosomes and chromatin in the conversion of microtubule arrays from interphase to metaphase." In: *The Journal of cell biology* 99.1 Pt 2, 47s–54s.

Katayama, H., Sasai, K., Kawai, H., Yuan, Z.-M., Bondaruk, J., Suzuki, F., Fujii, S., Arlinghaus, R. B., Czerniak, B. A., and Sen, S. (2004). "Phosphorylation by

aurora kinase A induces Mdm2-mediated destabilization and inhibition of p53." In: *Nature genetics* 36.1, pp. 55–62.

Katsetos, C. D., Reddy, G., Dráberová, E., Smejkalová, B., Del Valle, L., Ashraf, Q., Tadevosyan, A., Yelin, K., Maraziotis, T., Mishra, O. P., Mörk, S., Legido, A., Nissanov, J., Baas, P. W., Chadarévian, J.-P. de, and Dráber, P. (2006). "Altered cellular distribution and subcellular sorting of gamma-tubulin in diffuse astrocytic gliomas and human glioblastoma cell lines." In: *Journal of neuropathology and experimental neurology* 65.5, pp. 465–477.

Kawamura, K., Fujikawa-Yamamoto, K., Ozaki, M., Iwabuchi, K., Nakashima, H., Domiki, C., Morita, N., Inoue, M., Tokunaga, K., Shiba, N., Ikeda, R., and Suzuki, K. (2004). "Centrosome hyperamplification and chromosomal damage after exposure to radiation." In: *Oncology* 67.5-6, pp. 460–70.

Kawamura, K., Izumi, H., Ma, Z., Ikeda, R., Moriyama, M., Tanaka, T., Nojima, T., Levin, L. S., Fujikawa-Yamamoto, K., Suzuki, K., and Fukasawa, K. (2004). "Induction of centrosome amplification and chromosome instability in human bladder cancer cells by p53 mutation and cyclin E overexpression". In: *Cancer Research* 64.14, pp. 4800–4809.

Kayser, G., Gerlach, U., Walch, A., Nitschke, R., Haxelmans, S., Kayser, K., Hopt, U., Werner, M., and Lassmann, S. (2005). "Numerical and structural centrosome aberrations are an early and stable event in the adenoma-carcinoma sequence of colorectal carcinomas". In: *Virchows Archiv* 447.1, pp. 61–65.

Kearns, W. G., Yamaguchi, H., Young, N. S., and Liu, J. M. (2004). "Centrosome amplification and aneuploidy in bone marrow failure patients." In: *Genes, chromosomes & cancer* 40.4, pp. 329–33.

Keating, T. J. and Borisy, G. G. (2000). "Immunostructural evidence for the template mechanism of microtubule nucleation." In: *Nature cell biology* 2.6, pp. 352–357.

Keller, L. C., Romijn, E. P., Zamora, I., Yates, J. R., and Marshall, W. F. (2005). "Proteomic analysis of isolated Chlamydomonas centrioles reveals orthologs of ciliary-disease genes". In: *Current Biology* 15.12, pp. 1090–1098.

Kfoury, Y., Nasr, R., Favre-Bonvin, a., El-Sabban, M., Renault, N., Giron, M.-L., Setterblad, N., Hajj, H. E., Chiari, E., Mikati, a. G., Hermine, O., Saib, a., Thé, H. de, Pique, C., and Bazarbachi, a. (2008). "Ubiquitylated Tax targets and binds the IKK signalosome at the centrosome." In: *Oncogene* 27.12, pp. 1665–1676.

Kim, D. Y. and Roy, R. (2006). "Cell cycle regulators control centrosome elimination during oogenesis in Caenorhabditis elegans." In: *The Journal of cell biology* 174.6, pp. 751–7.

Kim, H.-G., Hwang, S.-Y., Aaronson, S. A., Mandinova, A., and Lee, S. W. (2011). "DDR1 receptor tyrosine kinase promotes prosurvival pathway through Notch1 activation." In: *The Journal of biological chemistry* 286.20, pp. 17672–81.

Kim, S. and Dynlacht, B. D. (2013). "Assembling a primary cilium." In: *Current opinion in cell biology* 25.4, pp. 506–11.

Kim, T.-S., Park, J.-E., Shukla, A., Choi, S., Murugan, R. N., Lee, J. H., Ahn, M., Rhee, K., Bang, J. K., Kim, B. Y., Loncarek, J., Erikson, R. L., and Lee, K. S. (2013). "Hierarchical recruitment of Plk4 and regulation of centriole biogenesis by two centrosomal scaffolds, Cep192 and Cep152." In: *Proceedings of the National Academy of Sciences of the United States of America* 110.50, E4849–57.

Kirkham, M., Müller-Reichert, T., Oegema, K., Grill, S., and Hyman, A. A. (2003). "SAS-4 is a C. elegans centriolar protein that controls centrosome size". In: *Cell* 112.4, pp. 575–587.

Kitagawa, D., Busso, C., Flückiger, I., and Gönczy, P. (2009). "Phosphorylation of SAS-6 by ZYG-1 Is Critical for Centriole Formation in C. elegans Embryos". In: *Developmental Cell* 17.6, pp. 900–907.

Kitagawa, D., Vakonakis, I., Olieric, N., Hilbert, M., Keller, D., Olieric, V., Bortfeld, M., Erat, M. C., Flückiger, I., Gönczy, P., and Steinmetz, M. O. (2011). "Structural basis of the 9-fold symmetry of centrioles". In: *Cell* 144.3, pp. 364–375.

Kleylein-Sohn, J., Westendorf, J., Le Clech, M., Habedanck, R., Stierhof, Y.-D., and Nigg, E. A. (2007). "Plk4-induced centriole biogenesis in human cells." In: *Developmental cell* 13.2, pp. 190–202.

Ko, M. J., Murata, K., Hwang, D.-S., and Parvin, J. D. (2006). "Inhibition of BRCA1 in breast cell lines causes the centrosome duplication cycle to be disconnected from the cell cycle." In: *Oncogene* 25.2, pp. 298–303.

Kobielak, A., Pasolli, H. A., and Fuchs, E. (2004). "Mammalian formin-1 participates in adherens junctions and polymerization of linear actin cables". In: *Nature Cell Biology* 6.1, pp. 21–30.

Koh, M., Woo, Y., Valiathan, R. R., Jung, H. Y., Park, S. Y., Kim, Y. N., Kim, H.-R. C., Fridman, R., and Moon, A. (2015). "Discoidin domain receptor 1 is a

novel transcriptional target of ZEB1 in breast epithelial cells undergoing H-Ras-induced epithelial to mesenchymal transition." In: *International journal of cancer* 136.6, E508–20.

Kohlmaier, G., Lončarek, J., Meng, X., McEwen, B. F., Mogensen, M. M., Spektor, A., Dynlacht, B. D., Khodjakov, A., and Gönczy, P. (2009). "Overly Long Centrioles and Defective Cell Division upon Excess of the SAS-4-Related Protein CPAP". In: *Current Biology* 19.12, pp. 1012–1018.

Korzeniewski, N., Treat, B., and Duensing, S. (2011). "The HPV-16 E7 oncoprotein induces centriole multiplication through deregulation of Polo-like kinase 4 expression." In: *Molecular cancer* 10, p. 61.

Korzeniewski, N., Wheeler, S., Chatterjee, P., Duensing, A., and Duensing, S. (2010). "A novel role of the aryl hydrocarbon receptor (AhR) in centrosome amplification - implications for chemoprevention." In: *Molecular cancer* 9, p. 153.

Koutsami, M. K., Tsantoulis, P. K., Kouloukoussa, M., Apostolopoulou, K., Pateras, I. S., Spartinou, Z., Drougou, A., Evangelou, K., Kittas, C., Bartkova, J., Bartek, J., and Gorgoulis, V. G. (2006). "Centrosome abnormalities are frequently observed in non-small-cell lung cancer and are associated with aneuploidy and cyclin E overexpression". In: *Journal of Pathology* 209.4, pp. 512–521.

Krämer, a., Schweizer, S., Neben, K., Giesecke, C., Kalla, J., Katzenberger, T., Benner, A., Müller-Hermelink, H. K., Ho, a. D., and Ott, G. (2003). "Centrosome aberrations as a possible mechanism for chromosomal instability in non-Hodgkin's lymphoma". In: *Leukemia : official journal of the Leukemia Society of America, Leukemia Research Fund, U.K* 17.11, pp. 2207–13.

Krämer, A., Maier, B., and Bartek, J. (2011). "Centrosome clustering and chromosomal (in)stability: a matter of life and death." In: *Molecular oncology* 5.4, pp. 324–35.

Krämer, A., Neben, K., and Ho, A. D. (2005). "Centrosome aberrations in hematological malignancies." In: *Cell biology international* 29.5, pp. 375–83.

Kronenwett, U., Huwendiek, S., Castro, J., Ried, T., and Auer, G. (2005). "Characterisation of breast fine-needle aspiration biopsies by centrosome aberrations and genomic instability." In: *British journal of cancer* 92.2, pp. 389–95.

Kronenwett, U., Hawendiek, S., Östring, C., Portwood, N., Roblick, U. J., Pawitan, Y., Alaiya, A., Sennerstam, R., Zetterberg, A., and Auer, G. (2004). "Improved

Grading of Breast Adenocarcinomas Based on Genomic Instability". In: *Cancer Research* 64.3, pp. 904–909.

Krzywicka-Racka, A. and Sluder, G. (2011). "Repeated cleavage failure does not establish centrosome amplification in untransformed human cells." In: *Journal of Cell Biology* 194.2, pp. 199–207.

Kuhn, E., Wang, T.-L., Doberstein, K., Bahadirli-Talbott, A., Ayhan, A., Sehdev, A. S., Drapkin, R., Kurman, R. J., and Shih, I.-M. (2016). "CCNE1 amplification and centrosome number abnormality in serous tubal intraepithelial carcinoma: further evidence supporting its role as a precursor of ovarian high-grade serous carcinoma". In: *Modern Pathology* 29.10, pp. 1254–1261.

Kulukian, A., Holland, A. J., Vitre, B., Naik, S., Cleveland, D. W., and Fuchs, E. (2015). "Epidermal development, growth control, and homeostasis in the face of centrosome amplification." In: *Proceedings of the National Academy of Sciences of the United States of America* 112.46, E6311–20.

Kunda, P., Pelling, A. E., Liu, T., and Baum, B. (2008). "Moesin controls cortical rigidity, cell rounding, and spindle morphogenesis during mitosis." In: *Current biology : CB* 18.2, pp. 91–101.

Kwon, M., Bagonis, M., Danuser, G., and Pellman, D. (2015). "Direct Microtubule-Binding by Myosin-10 Orients Centrosomes toward Retraction Fibers and Subcortical Actin Clouds". In: *Developmental Cell* 34.3, pp. 323–37.

Kwon, M., Godinho, S. A., Chandhok, N. S., Ganem, N. J., Azioune, A., Thery, M., and Pellman, D. (2008). "Mechanisms to suppress multipolar divisions in cancer cells with extra centrosomes." In: *Genes & development* 22.16, pp. 2189–203.

Lacey, K. R., Jackson, P. K., and Stearns, T. (1999). "Cyclin-dependent kinase control of centrosome duplication." In: *Proceedings of the National Academy of Sciences of the United States of America* 96.6, pp. 2817–22.

Lambert, R. A. (1913). "Comparative studies upon cancer cells and normal cells: II. The character of growth in vitro with special reference to cell division." In: *The Journal of experimental medicine* 17.5, pp. 499–510.

Landen, C. N., Lin, Y. G., Immaneni, A., Deavers, M. T., Merritt, W. M., Spannuth, W. A., Bodurka, D. C., Gershenson, D. M., Brinkley, W. R., and Sood, A. K. (2007). "Overexpression of the centrosomal protein Aurora-A kinase is associated with poor prognosis in epithelial ovarian cancer patients". In: *Clinical Cancer Research* 13.14, pp. 4098–4104.

Lara-Gonzalez, P., Westhorpe, F. G., and Taylor, S. S. (2012). "The Spindle Assembly Checkpoint". In: *Current Biology* 22.22, R966–R980.

Lawo, S., Hasegan, M., Gupta, G. D., and Pelletier, L. (2012). "Subdiffraction imaging of centrosomes reveals higher-order organizational features of pericentriolar material". In: *Nature Cell Biology* 12.1, pp. 308–317.

Leber, B., Maier, B., Fuchs, F., Chi, J., Riffel, P., Anderhub, S., Wagner, L., Ho, A. D., Salisbury, J. L., Boutros, M., and Krämer, A. (2010). "Proteins required for centrosome clustering in cancer cells." In: *Science translational medicine* 2.33, 33ra38.

Lecuit, T. and Yap, A. S. (2015). "E-cadherin junctions as active mechanical integrators in tissue dynamics". In: *Nature Cell Biology* 17.5, pp. 533–539.

Lee, K. and Rhee, K. (2011). "PLK1 phosphorylation of pericentrin initiates centrosome maturation at the onset of mitosis". In: *Journal of Cell Biology* 195.7, pp. 1093–1101.

Lee, K. and Rhee, K. (2012). "Separase-dependent cleavage of pericentrin B is necessary and sufficient for centriole disengagement during mitosis". In: *Cell Cycle* 11.13, pp. 2476–2485.

Leidel, S., Delattre, M., Cerutti, L., Baumer, K., and Gönczy, P. (2005). "SAS-6 defines a protein family required for centrosome duplication in C. elegans and in human cells". In: *Nat Cell Biol* 7.2, pp. 115–125.

Leitinger, B. (2011). "Transmembrane collagen receptors". In: *Annu Rev Cell Dev Biol* 27, pp. 265–290.

Leitinger, B. and Kwan, A. P. (2006). "The discoidin domain receptor DDR2 is a receptor for type X collagen". In: *Matrix Biology* 25.6, pp. 355–364.

Lens, S. M., Voest, E. E., and Medema, R. H. (2010). "Shared and separate functions of polo-like kinases and aurora kinases in cancer". In: *Nature Reviews Cancer* 10.12, pp. 825–841.

Lettman, M., Wong, Y., Viscardi, V., Niessen, S., Chen, S. hong, Shiau, A., Zhou, H., Desai, A., and Oegema, K. (2013). "Direct Binding of SAS-6 to ZYG-1 Recruits SAS-6 to the Mother Centriole for Cartwheel Assembly". In: *Developmental Cell* 25.3, pp. 284–298.

Levine, D. S., Sanchez, C. A., Rabinovitch, P. S., and Reid, B. J. (1991). "Formation of the tetraploid intermediate is associated with the development of cells with more than four centrioles in the elastase-simian virus 40 tumor antigen transgenic mouse model of pancreatic cancer." In: *Proceedings of the National Academy of Sciences of the United States of America* 88.15, pp. 6427–31.

Levine, M. S., Bakker, B., Boeckx, B., Moyett, J., Lu, J., Vitre, B., Spierings, D. C., Lansdorp, P. M., Cleveland, D. W., Lambrechts, D., Foijer, F., and Holland, A. J. (2017). "Centrosome Amplification Is Sufficient to Promote Spontaneous Tumorigenesis in Mammals". In: *Developmental Cell* 40.3, 313–322.e5.

Li, J., D'Angiolella, V., Seeley, E. S., Kim, S., Kobayashi, T., Fu, W., Campos, E. I., Pagano, M., and Dynlacht, B. D. (2013). "USP33 regulates centrosome biogenesis via deubiquitination of the centriolar protein CP110." In: *Nature* 495.7440, pp. 255–9.

Li, J., Xuan, J. W., Khatamianfar, V., Valiyeva, F., Moussa, M., Sadek, A., Yang, B. B., Dong, B. J., Huang, Y. R., and Gao, W. Q. (2014). "SKA1 over-expression promotes centriole over-duplication, centrosome amplification and prostate tumourigenesis". In: *Journal of Pathology* 234.2, pp. 178–189.

Li, J. J., Weroha, S. J., Lingle, W. L., Papa, D., Salisbury, J. L., and Li, S. A. (2004). "Estrogen mediates Aurora-A overexpression, centrosome amplification, chromosomal instability, and breast cancer in female ACI rats." In: *Proceedings of the National Academy of Sciences of the United States of America* 101.52, pp. 18123–8.

Li, J., Tan, M., Li, L., Pamarthy, D., Lawrence, T. S., and Sun, Y. (2005). "{SAK,} a new polo-like kinase, is transcriptionally repressed by p53 and induces apoptosis upon {RNAi} silencing." In: *Neoplasia* 7.4, pp. 312–323.

Li, Y., Lu, W., Chen, D., Boohaker, R. J., Zhai, L., Padmalayam, I., Wennerberg, K., Xu, B., and Zhang, W. (2015). "KIFC1 is a novel potential therapeutic target for breast cancer." In: *Cancer biology & therapy* 16.9, pp. 1316–22.

Lien, W. H., Klezovitch, O., and Vasioukhin, V. (2006). "Cadherin-catenin proteins in vertebrate development". In: *Current Opinion in Cell Biology* 18.5, pp. 499–506.

Lin, Y.-N. Y.-C. Y.-N. Y.-C., Chang, C.-W., Hsu, W.-B., Tang, C.-J. C., Lin, Y.-N. Y.-C. Y.-N. Y.-C., Chou, E.-J., Wu, C.-T., and Tang, T. K. (2013). "Human microcephaly protein CEP135 binds to hSAS-6 and CPAP, and is required for centriole assembly." In: *The EMBO journal* 32.8, pp. 1141–54.

Lin, Y. N., Wu, C. T., Lin, Y. C., Hsu, W. B., Tang, C. J. C., Chang, C. W., and Tang, T. K. (2013). "CEP120 interacts with CPAP and positively regulates centriole elongation". In: *Journal of Cell Biology* 202.2, pp. 211–219.

Lingle, W. L., Lutz, W. H., Ingle, J. N., Maihle, N. J., and Salisbury, J. L. (1998). "Centrosome hypertrophy in human breast tumors: implications for genomic stability and cell polarity." In: *Proceedings of the National Academy of Sciences of the United States of America* 95.6, pp. 2950–5.

Lingle, W. L., Barrett, S. L., Negron, V. C., D'Assoro, A. B., Boeneman, K., Liu, W., Whitehead, C. M., Reynolds, C., and Salisbury, J. L. (2002). "Centrosome amplification drives chromosomal instability in breast tumor development." In: *Proceedings of the National Academy of Sciences of the United States of America* 99.4, pp. 1978–83.

Lingle, W. L. and Salisbury, J. L. (1999). "Altered Centrosome Structure Is Associated with Abnormal Mitoses in Human Breast Tumors". In: *The American Journal of Pathology* 155.6, pp. 1941–1951.

Loh, J.-K., Lieu, A.-S., Chou, C.-H., Lin, F.-Y., Wu, C.-H., Howng, S.-L., Chio, C.-C., and Hong, Y.-R. (2010). "Differential expression of centrosomal proteins at different stages of human glioma." In: *BMC cancer* 10, p. 268.

Lončarek, J., Hergert, P., and Khodjakov, A. (2010). "Centriole reduplication during prolonged interphase requires procentriole maturation governed by plk1". In: *Current Biology* 20.14, pp. 1277–1282.

Loncarek, J., Hergert, P., Magidson, V., and Khodjakov, A. (2008). "Control of daughter centriole formation by the pericentriolar material." In: *Nature cell biology* 10.3, pp. 322–8.

Lozano, E., Betson, M., and Braga, V. M. M. (2003). "Tumor progression: Small GTpases and loss of cell-cell adhesion". In: *BioEssays* 25.5, pp. 452–463.

Lüders, J. (2012). "The amorphous pericentriolar cloud takes shape." In: *Nature cell biology* 14.11, pp. 1126–8.

Machado, J. C., Oliveira, C., Carvalho, R., Soares, P., Berx, G., Caldas, C., Seruca, R., Carneiro, F., and Sobrinho-Simöes, M. (2001). "E-cadherin gene (CDH1) promoter methylation as the second hit in sporadic diffuse gastric carcinoma." In: *Oncogene* 20, pp. 1525–1528.

Maeyama, M., Koga, H., Selvendiran, K., Yanagimoto, C., Hanada, S., Taniguchi, E., Kawaguchi, T., Harada, M., Ueno, T., and Sata, M. (2008). "Switching in discoid domain receptor expressions in SLUG-induced epithelial-mesenchymal transition." In: *Cancer* 113.10, pp. 2823–31.

Mahen, R., Jeyasekharan, A. D., Barry, N. P., and Venkitaraman, A. R. (2011). "Continuous polo-like kinase 1 activity regulates diffusion to maintain centrosome self-organization during mitosis." In: *Proceedings of the National Academy of Sciences of the United States of America* 108.22, pp. 9310–9315.

Mahjoub, M. R. and Stearns, T. (2012). "Supernumerary centrosomes nucleate extra cilia and compromise primary cilium signaling." In: *Current biology : CB* 22.17, pp. 1628–34.

Mali, P., Yang, L., Esvelt, K. M., Aach, J., Guell, M., DiCarlo, J. E., Norville, J. E., Church, G. M., Wiedenheft, B., Sternberg, S. H., Doudna, J. A., Bhaya, D., Davison, M., Barrangou, R., Terns, M. P., Terns, R. M., Jinek, M., Gasiunas, G., Barrangou, R., Horvath, P., Siksnys, V., Sapranauskas, R., Brummelkamp, T. R., Bernards, R., Agami, R., Miyagishi, M., Taira, K., Deltcheva, E., Zou, J., Mali, P., Huang, X., Dowey, S. N., Cheng, L., Sanjana, N. E., Lee, J. H., Hockemeyer, D., Kosuri, S., Pattanayak, V., Ramirez, C. L., Joung, J. K., Liu, D. R., King, N. M., Cohen-Haguenauer, O., Kim, Y. G., Cha, J., Chandrasegaran, S., Rebar, E. J., Pabo, C. O., Boch, J., Moscou, M. J., Bogdanove, A. J., Khalil, A. S., Collins, J. J., Purnick, P. E., Weiss, R., Zou, J., Holt, N., Urnov, F. D., Lombardo, A., Li, H., Makarova, K. S., Horvath, P., Barrangou, R., Deveau, H., Ploeg, J. R. van der, Rho, M., Wu, Y. W., Tang, H., Doak, T. G., Ye, Y., Pride, D. T., Garneau, J. E., Esvelt, K. M., Carlson, J. C., Liu, D. R., Barrangou, R., Horvath, P., Kent, W. J., Dreszer, T. R., Karolchik, D., Quinlan, A. R., Hall, I. M., Langmead, B., Trapnell, C., Pop, M., Salzberg, S. L., Lorenz, R., Mathews, D. H., Sabina, J., Zuker, M., Turner, D. H., Thurman, R. E., Xu, Q., Schlabach, M. R., Hannon, G. J., and Elledge, S. J. (2013). "RNA-guided human genome engineering via Cas9." In: *Science (New York, N.Y.)* 339.6121, pp. 823–6.

Manandhar, G., Schatten, H., and Sutovsky, P. (2005). "Centrosome reduction during gametogenesis and its significance." In: *Biology of reproduction* 72.1, pp. 2–13.

Maquoi, E., Assent, D., Detilleux, J., Pequeux, C., Foidart, J.-M., and Noël, A. (2012). "MT1-MMP protects breast carcinoma cells against type I collagen-induced apoptosis". In: *Oncogene* 31.4, pp. 480–493.

Mardin, B. R., Lange, C., Baxter, J. E., Hardy, T., Scholz, S. R., Fry, A. M., and Schiebel, E. (2010). "Components of the Hippo pathway cooperate with Nek2 kinase to regulate centrosome disjunction". In: *Nat Cell Biol* 12.12, pp. 1166–1176.

Mardin, B. R., Agircan, F. G., Lange, C., and Schiebel, E. (2011). "Plk1 controls the Nek2A-PP1γ Antagonism in centrosome disjunction". In: *Current Biology* 21.13, pp. 1145–1151.

Mardin, B. R. and Schiebel, E. (2012). "Breaking the ties that bind: new advances in centrosome biology." In: *The Journal of cell biology* 197.1, pp. 11–8.

Maresca, T. J. and Salmon, E. D. (2010). "Welcome to a new kind of tension: translating kinetochore mechanics into a wait-anaphase signal." In: *Journal of cell science* 123.Pt 6, pp. 825–35.

Marthiens, V., Piel, M., and Basto, R. (2012). "Never tear us apart–the importance of centrosome clustering." In: *Journal of cell science* 125.Pt 14, pp. 3281–92.

Marthiens, V., Rujano, M. A., Pennetier, C., Tessier, S., Paul-Gilloteaux, P., and Basto, R. (2013). "Centrosome amplification causes microcephaly." In: *Nature cell biology* 15.7, pp. 731–40.

Martin, A. C. and Goldstein, B. (2014). "Apical constriction: themes and variations on a cellular mechanism driving morphogenesis." In: *Development (Cambridge, England)* 141.10, pp. 1987–98.

Martin, T. a., Goyal, A., Watkins, G., and Jiang, W. G. (2005). "Expression of the transcription factors snail, slug, and twist and their clinical significance in human breast cancer." In: *Annals of surgical oncology* 12.6, pp. 488–96.

Martin-Subero, J. I., Knippschild, U., Harder, L., Barth, T. F., Riemke, J., Grohmann, S., Gesk, S., Hoppner, J., Moller, P., Parwaresch, R. M., and Siebert, R. (2003). "Segmental chromosomal aberrations and centrosome amplifications: pathogenetic mechanisms in Hodgkin and Reed-Sternberg cells of classical Hodgkin's lymphoma?" In: *Leukemia* 17.11, pp. 2214–2219.

Mason, F. M., Tworoger, M., and Martin, A. C. (2013). "Apical domain polarization localizes actin-myosin activity to drive ratchet-like apical constriction." In: *Nature cell biology* 15.8, pp. 926–36.

Mason, F. M., Xie, S., Vasquez, C. G., Tworoger, M., and Martin, A. C. (2016). "RhoA GTPase inhibition organizes contraction during epithelial morphogenesis". In: *The Journal of Cell Biology* 214.5, pp. 603–617.

Matsumoto, Y., Hayashi, K., and Nishida, E. (1999). "Cyclin-dependent kinase 2 (Cdk2) is required for centrosome duplication in mammalian cells". In: *Current Biology* 9.8, pp. 429–432.

Matsuo, K., Ohsumi, K., Iwabuchi, M., Kawamata, T., Ono, Y., and Takahashi, M. (2012). "Kendrin is a novel substrate for separase involved in the licensing of centriole duplication". In: *Current Biology* 22.10, pp. 915–921.

Maxwell, C. A., Keats, J. J., Belch, A. R., Pilarski, L. M., and Reiman, T. (2005). "Receptor for hyaluronan-mediated motility correlates with centrosome abnormalities in multiple myeloma and maintains mitotic integrity." In: *Cancer research* 65.3, pp. 850–60.

Mayer, F., Stoop, H., Sen, S., Bokemeyer, C., Oosterhuis, J. W., and Looijenga, L. H. J. (2003). "Aneuploidy of human testicular germ cell tumors is associated with amplification of centrosomes". In: *Oncogene* 22.25, pp. 3859–3866.

McEwen, A. E., Escobar, D. E., and Gottardi, C. J. (2012). "Signaling from the adherens junction." In: *Sub-cellular biochemistry* 60, pp. 171–196.

Meerbrey, K. L., Hu, G., Kessler, J. D., Roarty, K., Li, M. Z., Fang, J. E., Herschkowitz, J. I., Burrows, A. E., Ciccia, A., Sun, T., Schmitt, E. M., Bernardi, R. J., Fu, X., Bland, C. S., Cooper, T. A., Schiff, R., Rosen, J. M., Westbrook, T. F., and Elledge, S. J. (2011). "The pINDUCER lentiviral toolkit for inducible RNA interference in vitro and in vivo." In: *Proceedings of the National Academy of Sciences of the United States of America* 108.9, pp. 3665–70.

Meng, W. and Takeichi, M. (2009). "Adherens junction: molecular architecture and regulation." In: *Cold Spring Harbor perspectives in biology* 1.6.

Mennella, V., Keszthelyi, B., McDonald, K. L., Chhun, B., Kan, F., Rogers, G. C., Huang, B., and Agard, D. A. (2012). "Subdiffraction-resolution fluorescence microscopy reveals a domain of the centrosome critical for pericentriolar material organization." In: *Nature cell biology* 14.11, pp. 1159–68.

Meraldi, P., Lukas, J., Fry, A. M., Bartek, J., and Nigg, E. A. (1999). "Centrosome duplication in mammalian somatic cells requires E2F and Cdk2-cyclin A." In: *Nature cell biology* 1.2, pp. 88–93.

Miao, L., Zhu, S., Wang, Y., Li, Y., Ding, J., Dai, J., Cai, H., Zhang, D., and Song, Y. (2013). "Discoidin domain receptor 1 is associated with poor prognosis of non-small cell lung cancer and promotes cell invasion via epithelial-to-mesenchymal transition." In: *Medical oncology (Northwood, London, England)* 30.3, p. 626.

Mikeladze-Dvali, T., Tobel, L. von, Strnad, P., Knott, G., Leonhardt, H., Schermelleh, L., and Gönczy, P. (2012). "Analysis of centriole elimination during C. elegans oogenesis." In: *Development (Cambridge, England)* 139.9, pp. 1670–9.

Mikulenkova, E., Neradil, J., Zitterbart, K., Sterba, J., and Veselska, R. (2015). "Overexpression of the ΔNp73 isoform is associated with centrosome amplification in brain tumor cell lines." In: *Tumour biology : the journal of the International Society for Oncodevelopmental Biology and Medicine* 36.10, pp. 7483–91.

Mitchison, T. J. (1992). "Actin based motility on retraction fibers in mitotic PtK2 cells." In: *Cell motility and the cytoskeleton* 22.2, pp. 135–51.

Miyachika, Y., Yamamoto, Y., Matsumoto, H., Nishijima, J., Kawai, Y., Nagao, K., Hara, T., Sakano, S., and Matsuyama, H. (2013). "Centrosome amplification in bladder washing cytology specimens is a useful prognostic biomarker for non-muscle invasive bladder cancer". In: *Cancer Genetics* 206.1-2, pp. 12–18.

Montagna, C., Andrechek, E. R., Padilla-Nash, H., Muller, W. J., and Ried, T. (2002). "Centrosome abnormalities, recurring deletions of chromosome 4, and genomic amplification of HER2/neu define mouse mammary gland adenocarcinomas induced by mutant HER2/neu". In: *Oncogene* 21.6, pp. 890–898.

Morrison, S. J. and Kimble, J. (2006). "Asymmetric and symmetric stem-cell divisions in development and cancer." In: *Nature* 441.7097, pp. 1068–74.

Moskovszky, L., Dezsö, K., Athanasou, N., Szendröi, M., Kopper, L., Kliskey, K., Picci, P., and Sápi, Z. (2010). "Centrosome abnormalities in giant cell tumour of bone: possible association with chromosomal instability." In: *Modern pathology : an official journal of the United States and Canadian Academy of Pathology, Inc* 23.3, pp. 359–66.

Nagar, B., Overduin, M., Ikura, M., and Rini, J. M. (1996). "Structural basis of calcium-induced E-cadherin rigidification and dimerization". In: *Nature* 380.6572, pp. 360–364.

Nakada, C., Tsukamoto, Y., Matsuura, K., Nguyen, T. L., Hijiya, N., Uchida, T., Sato, F., Mimata, H., Seto, M., and Moriyama, M. (2011). "Overexpression of miR-210, a downstream target of HIF1α, causes centrosome amplification in renal carcinoma cells". In: *The Journal of Pathology* 224.2, pp. 280–288.

Nass, S. J., Herman, J. G., Gabrielson, E., Iversen, P. W., Parl, F. F., Davidson, N. E., and Graff, J. R. (2000). "Aberrant methylation of the estrogen receptor

and E-cadherin 5' CpG islands increases with malignant progression in human breast cancer". In: *Cancer Research* 60.16, pp. 4346–4348.

Neben, K., Giesecke, C., Schweizer, S., Ho, A. D., and Krämer, A. (2003). "Centrosome aberrations in acute myeloid leukemia are correlated with cytogenetic risk profile." In: *Blood* 101.1, pp. 289–91.

Neben, K., Ott, G., Schweizer, S., Kalla, J., Tews, B., Katzenberger, T., Hahn, M., Rosenwald, A., Ho, A. D., Müller-Hermelink, H. K., Lichter, P., and Krämer, A. (2007). "Expression of centrosome-associated gene products is linked to tetraploidization in mantle cell lymphoma". In: *International Journal of Cancer* 120.8, pp. 1669–1677.

Neuhaus, B., Bühren, S., Böck, B., Alves, F., Vogel, W. F., and Kiefer, F. (2011). "Migration inhibition of mammary epithelial cells by Syk is blocked in the presence of DDR1 receptors." In: *Cellular and molecular life sciences : CMLS* 68.22, pp. 3757–70.

Nezi, L. and Musacchio, A. (2009). "Sister chromatid tension and the spindle assembly checkpoint." In: *Current opinion in cell biology* 21.6, pp. 785–95.

Nigg, E. A. (2002). "Centrosome aberrations: cause or consequence of cancer progression?" In: *Nature reviews. Cancer* 2.11, pp. 815–25.

Nigg, E. A. and Stearns, T. (2011). "The centrosome cycle: Centriole biogenesis, duplication and inherent asymmetries." In: *Nature cell biology* 13.10, pp. 1154–60.

Nitta, T., Kanai, M., Sugihara, E., Tanaka, M., Sun, B., Nagasawa, T., Sonoda, S., Saya, H., and Miwa, M. (2006). "Centrosome amplification in adult T-cell leukemia and human T-cell leukemia virus type 1 Tax-induced human T cells." In: *Cancer science* 97.9, pp. 836–41.

Noordeen, N. A., Carafoli, F., Hohenester, E., Horton, M. A., and Leitinger, B. (2006). "A transmembrane leucine zipper is required for activation of the dimeric receptor tyrosine kinase DDR1." In: *The Journal of biological chemistry* 281.32, pp. 22744–51.

O'Connell, K. F., Caron, C., Kopish, K. R., Hurd, D. D., Kemphues, K. J., Li, Y., and White, J. G. (2001). "The C. elegans zyg-1 gene encodes a regulator of centrosome duplication with distinct maternal and paternal roles in the embryo". In: *Cell* 105.4, pp. 547–558.

Okuda, M., Horn, H. F., Tarapore, P., Tokuyama, Y., Smulian, A., Chan, P.-K., Knudsen, E. S., Hofmann, I. A., Snyder, J. D., Bove, K. E., and Fukasawa, K. (2000). "Nucleophosmin/B23 Is a Target of CDK2/Cyclin E in Centrosome Duplication". In: *Cell* 103.1, pp. 127–140.

Oliveira, R. A. and Nasmyth, K. (2013). "Cohesin cleavage is insufficient for centriole disengagement in Drosophila". In: *Current Biology* 23.14.

Onder, T. T., Gupta, P. B., Mani, S. A., Yang, J., Lander, E. S., and Weinberg, R. A. (2008). "Loss of E-cadherin promotes metastasis via multiple downstream transcriptional pathways". In: *Cancer Research* 68.10, pp. 3645–3654.

Ongusaha, P. P., Kim, J.-i., Fang, L., Wong, T. W., Yancopoulos, G. D., Aaronson, S. A., and Lee, S. W. (2003). "p53 induction and activation of DDR1 kinase counteract p53-mediated apoptosis and influence p53 regulation through a positive feedback loop". In: *The EMBO Journal* 22.6, pp. 1289–1301.

Ottaggio, L., Zunino, A., Maric, I., Grozio, A., Rossi, E., Spriano, M., and Viaggi, S. (2008). "The presence of high-risk chromosome aberrations in chronic lymphocytic leukaemia does not correlate with centrosome aberrations." In: *Hematological oncology* 26.1, pp. 39–42.

Palazzo, A. F., Cook, T. A., Alberts, A. S., and Gundersen, G. G. (2001). "mDia mediates Rho-regulated formation and orientation of stable microtubules." In: *Nature cell biology* 3.8, pp. 723–9.

Pannu, V., Rida, P. C. G., Celik, B., Turaga, R. C., Ogden, A., Cantuaria, G., Gopalakrishnan, J., and Aneja, R. (2014). "Centrosome-declustering drugs mediate a two-pronged attack on interphase and mitosis in supercentrosomal cancer cells." In: *Cell death & disease* 5, e1538.

Park, H. S., Kim, K. R., Lee, H. J., Choi, H. N., Kim, D. K., Kim, B. T., and Moon, W. S. (2007). "Overexpression of discoidin domain receptor 1 increases the migration and invasion of hepatocellular carcinoma cells in association with matrix metalloproteinase." In: *Oncology reports* 18.6, pp. 1435–41.

Park, S. Y., Park, J. E., Kim, T. S., Kim, J. H., Kwak, M. J., Ku, B., Tian, L., Murugan, R. N., Ahn, M., Komiya, S., Hojo, H., Kim, N. H., Kim, B. Y., Bang, J. K., Erikson, R. L., Lee, K. W. S., Kim, S. J., Oh, B. H., Yang, W., and Lee, K. W. S. (2014). "Molecular basis for unidirectional scaffold switching of human Plk4 in centriole biogenesis". In: *Nat Struct Mol Biol* 21.8, pp. 696–703.

Patel, H. and Gordon, M. Y. (2009). "Abnormal centrosome-centriole cycle in chronic myeloid leukaemia?" In: *British Journal of Haematology* 146.4, pp. 408–417.

Perez-Mongiovi, D., Beckhelling, C., Chang, P., Ford, C. C., and Houliston, E. (2000). "Nuclei and microtubule asters stimulate maturation/M phase promoting factor (MPF) activation in Xenopus eggs and egg cytoplasmic extracts". In: *Journal of Cell Biology* 150.5, pp. 963–974.

Perl, A.-K., Wilgenbus, P., Dahl, U., Semb, H., and Christofori, G. (1998). "A causal role for E-cadherin in the transition from adenoma to carcinoma". In: *Nature* 392.6672, pp. 190–193.

Pertz, O., Bozic, D., Koch, a. W., Fauser, C., Brancaccio, a., and Engel, J. (1999). "A new crystal structure, Ca2+ dependence and mutational analysis reveal molecular details of E-cadherin homoassociation." In: *Embo J* 18.7, pp. 1738–1747.

Perucca-Lostanlen, D., Rostagno, P., Grosgeorge, J., Marcié, S., Gaudray, P., and Turc-Carel, C. (2004). "Distinct MDM2 and P14ARF Expression and Centrosome Amplification in Well-Differentiated Liposarcomas". In: *Genes Chromosomes and Cancer* 39.2, pp. 99–109.

Peters, J. M. (2006). "The anaphase promoting complex/cyclosome: a machine designed to destroy". In: *Nat Rev Mol Cell Biol* 7.9, pp. 644–656.

Peters, J. M. (2002). "The anaphase-promoting complex: Proteolysis in mitosis and beyond". In: *Molecular Cell* 9.5, pp. 931–943.

Pharoah, P. D., Guilford, P., and Caldas, C. (2001). "Incidence of gastric cancer and breast cancer in CDH1 (E-cadherin) mutation carriers from hereditary diffuse gastric cancer families." In: *Gastroenterology* 121.6, pp. 1348–1353.

Pickett-Heaps, J. (1971). "The autonomy of the centriole: fact or fallacy?" In: *Cytobios* 3, pp. 205–214.

Pihan, G. A., Purohit, A., Wallace, J., Knecht, H., Woda, B., Quesenberry, P., and Doxsey, S. J. (1998). "Centrosome defects and genetic instability in malignant tumors." In: *Cancer research* 58.17, pp. 3974–85.

Pihan, G. A., Purohit, A., Wallace, J., Malhotra, R., Liotta, L., and Doxsey, S. J. (2001). "Centrosome defects can account for cellular and genetic changes that characterize prostate cancer progression". In: *Cancer Research* 61.5, pp. 2212–2219.

Pihan, G. A., Wallace, J., Zhou, Y., and Doxsey, S. J. (2003). "Centrosome abnormalities and chromosome instability occur together in pre-invasive carcinomas." In: *Cancer research* 63.6, pp. 1398–404.

Pinho, S. S., Seruca, R., Gärtner, F., Yamaguchi, Y., Gu, J., Taniguchi, N., and Reis, C. A. (2011). "Modulation of E-cadherin function and dysfunction by N-glycosylation". In: *Cellular and Molecular Life Sciences* 68.6, pp. 1011–1020.

Pokutta, S., Herrenknecht, K., Kemler, R., and Engel, J. (1994). "Conformational changes of the recombinant extracellular domain of E-cadherin upon calcium binding." In: *European journal of biochemistry* 223.3, pp. 1019–26.

Portier, N., Audhya, A., Maddox, P. S., Green, R. A., Dammermann, A., Desai, A., and Oegema, K. (2007). "A Microtubule-Independent Role for Centrosomes and Aurora A in Nuclear Envelope Breakdown". In: *Developmental Cell* 12.4, pp. 515–529.

Priya, R., Gomez, G. A., Budnar, S., Verma, S., Cox, H. L., Hamilton, N. A., and Yap, A. S. (2015). "Feedback regulation through myosin II confers robustness on RhoA signalling at E-cadherin junctions." In: *Nature cell biology* 17.10, pp. 1282–93.

Priya, R., Yap, A. S., and Gomez, G. A. (2013). "E-cadherin supports steady-state Rho signaling at the epithelial zonula adherens." In: *Differentiation; research in biological diversity* 86.3, pp. 133–40.

Quintyne, N. J., Reing, J. E., Hoffelder, D. R., Gollin, S. M., and Saunders, W. S. (2005). "Spindle multipolarity is prevented by centrosomal clustering." In: *Science (New York, N.Y.)* 307.5706, pp. 127–9.

R Development Core Team (2016). "R: A Language and Environment for Statistical Computing". In: *R Foundation for Statistical Computing Vienna Austria*, {ISBN} 3–900051–07–.

Raab, M. S., Breitkreutz, I., Anderhub, S., Rønnest, M. H., Leber, B., Larsen, T. O., Weiz, L., Konotop, G., Hayden, P. J., Podar, K., Fruehauf, J., Nissen, F., Mier, W., Haberkorn, U., Ho, A. D., Goldschmidt, H., Anderson, K. C., Clausen, M. H., and Krämer, A. (2012). "GF-15, a novel inhibitor of centrosomal clustering, suppresses tumor cell growth in vitro and in vivo." In: *Cancer research* 72.20, pp. 5374–85.

Raaijmakers, J. A. and Medema, R. H. (2014). "Function and regulation of dynein in mitotic chromosome segregation". In: *Chromosoma* 123.5, pp. 407–422.

Raaijmakers, J. a., Heesbeen, R. G. H. P. van, Meaders, J. L., Geers, E. F., Fernandez-Garcia, B., Medema, R. H., and Tanenbaum, M. E. (2012). "Nuclear envelope-associated dynein drives prophase centrosome separation and enables Eg5-independent bipolar spindle formation." In: *Embo J.* 31.21, pp. 4179–4190.

Rai, R., Phadnis, A., Haralkar, S., Badwe, R. A., Dai, H., Li, K., and Lin, S.-Y. (2008). "Differential regulation of centrosome integrity by DNA damage response proteins". In: *Cell Cycle* 7.14, pp. 2225–2233.

Ram, R., Lorente, G., Nikolich, K., Urfer, R., Foehr, E., and Nagavarapu, U. (2006). "Discoidin domain receptor-1a (DDR1a) promotes glioma cell invasion and adhesion in association with matrix metalloproteinase-2." In: *Journal of neuro-oncology* 76.3, pp. 239–48.

Rammal, H., Saby, C., Magnien, K., Van-Gulick, L., Garnotel, R., Buache, E., El Btaouri, H., Jeannesson, P., and Morjani, H. (2016). "Discoidin domain receptors: Potential actors and targets in cancer". In: *Frontiers in Pharmacology* 7.MAR.

Rao, M. V. and Zaidel-Bar, R. (2016). "Formin-mediated actin polymerization at cell-cell junctions stabilizes E-cadherin and maintains monolayer integrity during wound repair." In: *Molecular biology of the cell* 27.18, pp. 2844–56.

Ratheesh, A., Gomez, G. A., Priya, R., Verma, S., Kovacs, E. M., Jiang, K., Brown, N. H., Akhmanova, A., Stehbens, S. J., and Yap, A. S. (2012). "Centralspindlin and β-catenin regulate Rho signalling at the epithelial zonula adherens". In: *Nature Cell Biology* 14.8, pp. 818–828.

Rebacz, B., Larsen, T. O., Clausen, M. H., Rønnest, M. H., Löffler, H., Ho, A. D., and Krämer, A. (2007). "Identification of griseofulvin as an inhibitor of centrosomal clustering in a phenotype-based screen." In: *Cancer research* 67.13, pp. 6342–50.

Redemann, S., Pecreaux, J., Goehring, N. W., Khairy, K., Stelzer, E. H. K., Hyman, A. A., and Howard, J. (2010). "Membrane invaginations reveal cortical sites that pull on mitotic spindles in one-cell C. elegans embryos." In: *PloS one* 5.8. Ed. by D. Cimini, e12301.

Reina, J. and Gonzalez, C. (2014). "When fate follows age: unequal centrosomes in asymmetric cell division." In: *Philosophical transactions of the Royal Society of London. Series B, Biological sciences* 369.1650, pp. 20130466–.

Reiter, R., Gais, P., Jutting, U., Steuer-Vogt, M. K., Pickhard, A., Bink, K., Rauser, S., Lassmann, S., Höfler, H., Werner, M., and Walch, A. (2006). "Aurora kinase A messenger RNA overexpression is correlated with tumor progression and shortened

survival in head and neck squamous cell carcinoma". In: *Clinical Cancer Research* 12.17, pp. 5136–5141.

Reiter, R., Gais, P., Steuer-Vogt, M. K., Boulesteix, A.-L., Deutschle, T., Hampel, R., Wagenpfeil, S., Rauser, S., Walch, A., Bink, K., Jutting, U., Neff, F., Arnold, W., Hofler, H., and Pickhard, A. (2009). "Centrosome abnormalities in head and neck squamous cell carcinoma (HNSCC)." In: *Acta oto-laryngologica* 129.2, pp. 205–13.

Reynolds, A. B. and Carnahan, R. H. (2004). "Regulation of cadherin stability and turnover by p120ctn: Implications in disease and cancer". In: *Seminars in Cell and Developmental Biology* 15.6 SPEC. ISS. Pp. 657–663.

Riento, K., Guasch, R. M., Garg, R., Jin, B., and Ridley, A. J. (2003). "RhoE binds to ROCK I and inhibits downstream signaling." In: *Molecular and cellular biology* 23.12, pp. 4219–4229.

Ring, D., Hubble, R., and Kirschner, M. (1982). "Mitosis in a cell with multiple centrioles." In: *The Journal of cell biology* 94.3, pp. 549–56.

Rios-Doria, J., Day, K. C., Kuefer, R., Rashid, M. G., Chinnaiyan, A. M., Rubin, M. A., and Day, M. L. (2003). "The role of calpain in the proteolytic cleavage of E-cadherin in prostate and mammary epithelial cells". In: *Journal of Biological Chemistry* 278.2, pp. 1372–1379.

Robbins, E., Jentzsch, G., and Micali, A. (1968). "The centriole cycle in synchronized HeLa cells." In: *Journal of Cell Biology* 36.2, pp. 329–339.

Rogers, G. C., Rusan, N. M., Roberts, D. M., Peifer, M., and Rogers, S. L. (2009). "The SCF Slimb ubiquitin ligase regulates Plk4/Sak levels to block centriole reduplication". In: *Journal of Cell Biology* 184.2, pp. 225–229.

Al-Romaih, K., Bayani, J., Vorobyova, J., Karaskova, J., Park, P. C., Zielenska, M., and Squire, J. A. (2003). "Chromosomal instability in osteosarcoma and its association with centrosome abnormalities". In: *Cancer Genetics and Cytogenetics* 144.2, pp. 91–99.

Rosenblatt, J., Cramer, L. P., Baum, B., and McGee, K. M. (2004). "Myosin II-dependent cortical movement is required for centrosome separation and positioning during mitotic spindle assembly." In: *Cell* 117.3, pp. 361–72.

Roshani, L., Fujioka, K., Auer, G., Kjellman, M., Lagercrantz, S., and Larsson, C. (2002). "Aberrations of centrosomes in adrenocortical tumors." In: *International journal of oncology* 20.6, pp. 1161–1165.

Rudra-Ganguly, N., Lowe, C., Mattie, M., Chang, M. S., Satpayev, D., Verlinsky, A., An, Z., Hu, L., Yang, P., Challita-Eid, P., Stover, D. R., and Pereira, D. S. (2014). "Discoidin domain receptor 1 contributes to tumorigenesis through modulation of TGFBI expression." In: *PloS one* 9.11. Ed. by T. S. Acott, e111515.

Sabino, D., Gogendeau, D., Gambarotto, D., Nano, M., Pennetier, C., Dingli, F., Arras, G., Loew, D., and Basto, R. (2015). "Moesin is a major regulator of centrosome behavior in epithelial cells with extra centrosomes". In: *Current Biology* 25.7, pp. 879–889.

Salisbury, J. L., D'Assoro, A. B., and Lingle, W. L. (2004). "Centrosome amplification and the origin of chromosomal instability in breast cancer". In: *Journal of Mammary Gland Biology and Neoplasia* 9.3, pp. 275–283.

Sánchez-Aguilera, A., Montalbán, C., De La Cueva, P., Sánchez-Verde, L., Morente, M. M., García-Cosío, M., García-Laraña, J., Bellas, C., Provencio, M., Romagosa, V., Fernández De Sevilla, A., Menárguez, J., Sabín, P., Mestre, M. J., Méndez, M., Fresno, M. F., Nicolás, C., Piris, M. A., and García, J. F. (2006). "Tumor microenvironment and mitotic checkpoint are key factors in the outcome of classic Hodgkin lymphoma". In: *Blood* 108.2, pp. 662–668.

Sander, E. E., Klooster, J. P. ten, Delft, S. van, Kammen, R. A. van der, and Collard, J. G. (1999). "Rac downregulates Rho activity: reciprocal balance between both GTPases determines cellular morphology and migratory behavior." In: *The Journal of cell biology* 147.5, pp. 1009–22.

Sankaran, S., Crone, D. E., Palazzo, R. E., and Parvin, J. D. (2007). "Aurora-A kinase regulates breast cancer associated gene 1 inhibition of centrosome-dependent microtubule nucleation." In: *Cancer research* 67.23, pp. 11186–94.

Sankaran, S., Starita, L. M., Groen, A. C., Ko, M. J., and Parvin, J. D. (2005). "Centrosomal microtubule nucleation activity is inhibited by BRCA1-dependent ubiquitination." In: *Molecular and cellular biology* 25.19, pp. 8656–68.

Santamaria, A., Wang, B., Elowe, S., Malik, R., Zhang, F., Bauer, M., Schmidt, A., Silljé, H. H. W., Körner, R., and Nigg, E. a. (2011). "The Plk1-dependent phosphoproteome of the early mitotic spindle." In: *Molecular & cellular proteomics : MCP* 10.1, p. M110.004457.

Sato, N., Mizumoto, K., Nakamura, M., Nakamura, K., Kusumoto, M., Niiyama, H., Ogawa, T., and Tanaka, M. (1999). "Centrosome abnormalities in pancreatic

ductal carcinoma." In: *Clinical cancer research : an official journal of the American Association for Cancer Research* 5.5, pp. 963–70.

Sato, N., Mizumoto, K., Nakamura, M., Maehara, N., Minamishima, Y. A., Nishio, S., Nagai, E., and Tanaka, M. (2001). "Correlation between centrosome abnormalities and chromosomal instability in human pancreatic cancer cells". In: *Cancer Genetics and Cytogenetics* 126.1, pp. 13–19.

Schlegel, B. P., Starita, L. M., and Parvin, J. D. (2003). "Overexpression of a protein fragment of RNA helicase A causes inhibition of endogenous BRCA1 function and defects in ploidy and cytokinesis in mammary epithelial cells". In: *Oncogene* 22.7, pp. 983–991.

Schmidt, T. I., Kleylein-Sohn, J., Westendorf, J., Le Clech, M., Lavoie, S. B., Stierhof, Y. D., and Nigg, E. A. (2009). "Control of Centriole Length by CPAP and CP110". In: *Current Biology* 19.12, pp. 1005–1011.

Schneeweiss, A., Sinn, H. P., Ehemann, V., Khbeis, T., Neben, K., Krause, U., Ho, A. D., Bastert, G., and Krämer, A. (2003). "Centrosomal aberrations in primary invasive breast cancer are associated with nodal status and hormone receptor expression". In: *International Journal of Cancer* 107.3, pp. 346–352.

Schockel, L., Mockel, M., Mayer, B., Boos, D., and Stemmann, O. (2011). "Cleavage of cohesin rings coordinates the separation of centrioles and chromatids". In: *Nat Cell Biol* 13.8, pp. 966–972.

Segat, D., Cassaro, M., Dazzo, E., Cavallini, L., Romualdi, C., Salvador, R., Vitale, M. P., Vitiello, L., Fassan, M., Rugge, M., Zaninotto, G., Ancona, E., and Baroni, M. D. (2010). "Pericentriolar material analyses in normal esophageal mucosa, Barrett's metaplasia and adenocarcinoma." In: *Histology and histopathology* 25.5, pp. 551–60.

Seifert, H. W. (1978). "[Electron microscopic investigation on cutaneous leiomyosarcoma (author's transl)]." In: *Archives of dermatological research* 263.2, pp. 159–69.

Serçin, Ö., Larsimont, J.-C., Karambelas, A. E., Marthiens, V., Moers, V., Boeckx, B., Le Mercier, M., Lambrechts, D., Basto, R., and Blanpain, C. (2015). "Transient PLK4 overexpression accelerates tumorigenesis in p53-deficient epidermis." In: *Nature cell biology*.

Shalem, O., Sanjana, N. E., Hartenian, E., Shi, X., Scott, D. a., Mikkelsen, T. S., Heckl, D., Ebert, B. L., Root, D. E., Doench, J. G., and Zhang, F. (2014).

"LentiCRISPRv2 and lentiGuide-Puro: lentiviral CRISPR/Cas9 and single guide RNA CRISPR Genome-scale CRISPR-Cas9 knockout screening in human cells." In: *Science (New York, N.Y.)* 343, pp. 84–7.

Shao, S., Liu, R., Wang, Y., Song, Y., Zuo, L., Xue, L., Lu, N., Hou, N., Wang, M., Yang, X., and Zhan, Q. (2010). "Centrosomal Nlp is an oncogenic protein that is gene-amplified in human tumors and causes spontaneous tumorigenesis in transgenic mice". In: *Journal of Clinical Investigation* 120.2, pp. 498–507.

Shapiro, L. and Weis, W. I. (2009). "Structure and biochemistry of cadherins and catenins." In: *Cold Spring Harbor perspectives in biology* 1.3.

Shen, Y., Hirsch, D. S., Sasiela, C. A., and Wen, J. W. (2008). "Cdc42 regulates E-cadherin ubiquitination and degradation through an epidermal growth factor receptor to Src-mediated pathway". In: *Journal of Biological Chemistry* 283.8, pp. 5127–5137.

Shimada, K., Nakamura, M., Ishida, E., Higuchi, T., Yamamoto, H., Tsujikawa, K., and Konishi, N. (2008). "Prostate cancer antigen-1 contributes to cell survival and invasion though discoidin receptor 1 in human prostate cancer." In: *Cancer science* 99.1, pp. 39–45.

Shimomura, A., Miyoshi, Y., Taguchi, T., Tamaki, Y., and Noguchi, S. (2009). "Association of loss of BRCA1 expression with centrosome aberration in human breast cancer". In: *Journal of Cancer Research and Clinical Oncology* 135.3, pp. 421–430.

Shinmura, K., Kato, H., Kawanishi, Y., Nagura, K., Kamo, T., Okubo, Y., Inoue, Y., Kurabe, N., Du, C., Iwaizumi, M., Kurachi, K., Nakamura, T., and Sugimura, H. (2015). "SASS6 overexpression is associated with mitotic chromosomal abnormalities and a poor prognosis in patients with colorectal cancer". In: *Oncology Reports* 34.2, pp. 727–38.

Shintani, Y., Fukumoto, Y., Chaika, N., Svoboda, R., Wheelock, M. J., and Johnson, K. R. (2008). "Collagen I-mediated up-regulation of N-cadherin requires cooperative signals from integrins and discoidin domain receptor 1." In: *The Journal of cell biology* 180.6, pp. 1277–89.

Shono, M., Sato, N., Mizumoto, K., Maehara, N., Nakamura, M., Nagai, E., and Tanaka, M. (2001). "Stepwise progression of centrosome defects associated with local tumor growth and metastatic process of human pancreatic carcinoma cells transplanted orthotopically into nude mice". In: *Lab Invest* 81.7, pp. 945–952.

Shrivastava, A., Radziejewski, C., Campbell, E., Kovac, L., McGlynn, M., Ryan, T. E., Davis, S., Goldfarb, M. P., Glass, D. J., Lemke, G., and Yancopoulos, G. D. (1997). "An Orphan Receptor Tyrosine Kinase Family Whose Members Serve as Nonintegrin Collagen Receptors". In: *Molecular Cell* 1.1, pp. 25–34.

Sigoillot, F. D., Lyman, S., Huckins, J. F., Adamson, B., Chung, E., Quattrochi, B., and King, R. W. (2012). "A bioinformatics method identifies prominent off-targeted transcripts in RNAi screens." In: *Nature methods* 9.4, pp. 363–6.

Silkworth, W. T., Nardi, I. K., Scholl, L. M., and Cimini, D. (2009). "Multipolar spindle pole coalescence is a major source of kinetochore mis-attachment and chromosome mis-segregation in cancer cells." In: *PloS one* 4.8, e6564.

Siller, K. H. and Doe, C. Q. (2009). "Spindle orientation during asymmetric cell division." In: *Nature cell biology* 11.4, pp. 365–74.

Sillibourne, J. E., Tack, F., Vloemans, N., Boeckx, A., Thambirajah, S., Bonnet, P., Ramaekers, F. C. S., Bornens, M., and Grand-Perret, T. (2010). "Autophosphorylation of polo-like kinase 4 and its role in centriole duplication." In: *Molecular biology of the cell* 21.4, pp. 547–61.

Silljé, H. H. W., Nagel, S., Körner, R., and Nigg, E. A. (2006). "HURP is a Ran-importin beta-regulated protein that stabilizes kinetochore microtubules in the vicinity of chromosomes." In: *Current biology : CB* 16.8, pp. 731–42.

Sir, J.-H., Pütz, M., Daly, O., Morrison, C. G., Dunning, M., Kilmartin, J. V., and Gergely, F. (2013). "Loss of centrioles causes chromosomal instability in vertebrate somatic cells." In: *The Journal of cell biology* 203.5, pp. 747–56.

Skyldberg, B., Fujioka, K., Hellström, a. C., Sylvén, L., Moberger, B., and Auer, G. (2001). "Human papillomavirus infection, centrosome aberration, and genetic stability in cervical lesions." In: *Modern pathology : an official journal of the United States and Canadian Academy of Pathology, Inc* 14.4, pp. 279–84.

Sluder, G., Thompson, E. A., Miller, F. J., Hayes, J., and Rieder, C. L. (1997). "The checkpoint control for anaphase onset does not monitor excess numbers of spindle poles or bipolar spindle symmetry." In: *Journal of cell science* 110 (Pt 4, pp. 421–9.

Smith, E., Hégarat, N., Vesely, C., Roseboom, I., Larch, C., Streicher, H., Straatman, K., Flynn, H., Skehel, M., Hirota, T., Kuriyama, R., and Hochegger, H. (2011). "Differential control of Eg5-dependent centrosome separation by Plk1 and Cdk1". In: *Embo J* 30.11, pp. 2233–2245.

Smutny, M. and Yap, A. S. (2010). "Neighborly relations: cadherins and mechanotransduction." In: *The Journal of cell biology* 189.7, pp. 1075–7.

Sneddon, I. N. (1965). "The relation between load and penetration in the axisymmetric boussinesq problem for a punch of arbitrary profile". In: *International Journal of Engineering Science* 3.1, pp. 47–57.

Sonnen, K. F., Gabryjonczyk, A.-M., Anselm, E., Stierhof, Y.-D., and Nigg, E. a. (2013). "Human Cep192 and Cep152 cooperate in Plk4 recruitment and centriole duplication." In: *J Cell Sci.* 126.Pt 14, pp. 3223–33.

Sonnen, K. F., Schermelleh, L., Leonhardt, H., and Nigg, E. A. (2012). "3D-structured illumination microscopy provides novel insight into architecture of human centrosomes." In: *Biology open* 1.10, pp. 965–76.

Spaderna, S., Schmalhofer, O., Wahlbuhl, M., Dimmler, A., Bauer, K., Sultan, A., Hlubek, F., Jung, A., Strand, D., Eger, A., Kirchner, T., Behrens, J., and Brabletz, T. (2008). "The transcriptional repressor ZEB1 promotes metastasis and loss of cell polarity in cancer". In: *Cancer Research* 68.2, pp. 537–544.

Springer, W. R., Cooper, D. N. W., and Barondes, S. H. (1984). "Discoidin I is implicated in cell-substratum attachment and ordered cell migration of dictyostelium discoideum and resembles fibronectin". In: *Cell* 39.3 PART 2, pp. 557–564.

Starita, L. M., Machida, Y., Sankaran, S., Elias, J. E., Griffin, K., Schlegel, B. P., Gygi, S. P., and Parvin, J. D. (2004). "BRCA1-dependent ubiquitination of gamma-tubulin regulates centrosome number." In: *Molecular and cellular biology* 24.19, pp. 8457–66.

Steere, N., Wagner, M., Beishir, S., Smith, E., Breslin, L., Morrison, C. G., Hochegger, H., and Kuriyama, R. (2011). "Centrosome amplification in CHO and DT40 cells by inactivation of cyclin-dependent kinases". In: *Cytoskeleton* 68.8, pp. 446–458.

Stehbens, S. and Wittmann, T. (2012). "Targeting and transport: How microtubules control focal adhesion dynamics". In: *Journal of Cell Biology* 198.4, pp. 481–489.

Steinhusen, U., Weiske, J., Badock, V., Tauber, R., Bommert, K., and Huber, O. (2001). "Cleavage and Shedding of E-cadherin after Induction of Apoptosis". In: *Journal of Biological Chemistry* 276.7, pp. 4972–4980.

Stephens, P. J., Greenman, C. D., Fu, B., Yang, F., Bignell, G. R., Mudie, L. J., Pleasance, E. D., Lau, K. W., Beare, D., Stebbings, L. A., McLaren, S., Lin, M.-L., McBride, D. J., Varela, I., Nik-Zainal, S., Leroy, C., Jia, M., Menzies, A.,

Butler, A. P., Teague, J. W., Quail, M. A., Burton, J., Swerdlow, H., Carter, N. P., Morsberger, L. A., Iacobuzio-Donahue, C., Follows, G. A., Green, A. R., Flanagan, A. M., Stratton, M. R., Futreal, P. A., and Campbell, P. J. (2011). "Massive genomic rearrangement acquired in a single catastrophic event during cancer development." In: *Cell* 144.1, pp. 27–40.

Stewart, C. J. R. and Crook, M. L. (2017). "Cervical intraepithelial neoplasia (CIN) 3-like squamous cell carcinoma of the cervix: a review of 14 cases with comparison of E-cadherin and cyclin D1 expression in the CIN 3-like and infiltrative tumour elements". In: *Histopathology* 70.3, pp. 367–374.

Strnad, P., Leidel, S., Vinogradova, T., Euteneuer, U., Khodjakov, A., and Gönczy, P. (2007). "Regulated HsSAS-6 Levels Ensure Formation of a Single Procentriole per Centriole during the Centrosome Duplication Cycle". In: *Developmental Cell* 13.2, pp. 203–213.

Strumane, K., Berx, G., and Van Roy, F. (2004). "Cadherins in cancer." In: *Handbook of experimental pharmacology* 165, pp. 69–103.

Suizu, F., Ryo, A., Wulf, G., Lim, J., and Lu, K. P. (2006). "Pin1 regulates centrosome duplication, and its overexpression induces centrosome amplification, chromosome instability, and oncogenesis." In: *Molecular and cellular biology* 26.4, pp. 1463–1479.

Sumara, I., Vorlaufer, E., Stukenberg, P. T., Kelm, O., Redemann, N., Nigg, E. A., and Peters, J. M. (2002). "The dissociation of cohesin from chromosomes in prophase is regulated by polo-like kinase". In: *Molecular Cell* 9.3, pp. 515–525.

Suriano, G., Yew, S., Ferreira, P., Senz, J., Kaurah, P., Ford, J. M., Longacre, T. A., Norton, J. A., Chun, N., Young, S., Oliveira, M. J., MacGillivray, B., Rao, A., Sears, D., Jackson, C. E., Boyd, J., Yee, C., Deters, C., Pai, G. S., Hammond, L. S., McGivern, B. J., Medgyesy, D., Sartz, D., Arun, B., Oelschlager, B. K., Upton, M. P., Neufeld-Kaiser, W., Silva, O. E., Donenberg, T. R., Kooby, D. A., Sharma, S., Jonsson, B. A., Gronberg, H., Gallinger, S., Seruca, R., Lynch, H., and Huntsman, D. G. (2005). "Characterization of a recurrent germ line mutation of the E-cadherin gene: Implications for genetic testing and clinical management". In: *Clinical Cancer Research* 11.15, pp. 5401–5409.

Syed, M. I., Syed, S., Minty, F., Harrower, S., Singh, J., Chin, A., McLellan, D. R., Parkinson, E. K., and Clark, L. J. (2009). "Gamma tubulin: A promising indicator of recurrence in squamous cell carcinoma of the larynx". In: *Otolaryngology - Head and Neck Surgery* 140.4, pp. 498–504.

Takesono, A., Heasman, S. J., Wojciak-Stothard, B., Garg, R., and Ridley, A. J. (2010). "Microtubules regulate migratory polarity through Rho/ROCK signaling in T cells." In: *PloS one* 5.1. Ed. by J. Z. Rappoport, e8774.

Tame, M. A., Raaijmakers, J. A., Van Den Broek, B., Lindqvist, A., Jalink, K., and Medema, R. H. (2014). "Astral microtubules control redistribution of dynein at the cell cortex to facilitate spindle positioning". In: *Cell Cycle* 13.7, pp. 1162–1170.

Tang, C. J., Fu, R. H., Wu, K. S., Hsu, W. B., and Tang, T. K. (2009). "CPAP is a cell-cycle regulated protein that controls centriole length". In: *Nat Cell Biol* 11.7, pp. 825–831.

Tang, C.-J. C., Hu, H.-M., and Tang, T. K. (2004). "NuMA Expression and Function in Mouse Oocytes and Early Embryos". In: *Journal of Biomedical Science* 11.3, pp. 370–376.

Tang, N. and Marshall, W. F. (2012). "Centrosome positioning in vertebrate development". In: *Journal of Cell Science* 125.21, pp. 4951–4961.

Telentschak, S., Soliwoda, M., Nohroudi, K., Addicks, K., and Klinz, F.-J. (2015). "Cytokinesis failure and successful multipolar mitoses drive aneuploidy in glioblastoma cells". In: *Oncology Reports* 33.4, pp. 2001–8.

Théry, M., Racine, V., Pépin, A., Piel, M., Chen, Y., Sibarita, J.-B., and Bornens, M. (2005). "The extracellular matrix guides the orientation of the cell division axis." In: *Nature cell biology* 7.10, pp. 947–53.

Thiery, J. P., Acloque, H., Huang, R. Y., and Nieto, M. A. (2009). "Epithelial-Mesenchymal Transitions in Development and Disease". In: *Cell* 139.5, pp. 871–890.

Thirthagiri, E., Robinson, C. M., Huntley, S., Davies, M., Yap, L. F., Prime, S. S., and Paterson, I. C. (2007). "Spindle assembly checkpoint and centrosome abnormalities in oral cancer". In: *Cancer Letters* 258.2, pp. 276–285.

Thompson, S. L. and Compton, D. A. (2010). "Proliferation of aneuploid human cells is limited by a p53-dependent mechanism." In: *The Journal of cell biology* 188.3, pp. 369–81.

Thompson, S. L. and Compton, D. A. (2011). "Chromosomes and cancer cells." In: *Chromosome research : an international journal on the molecular, supramolecular and evolutionary aspects of chromosome biology* 19.3, pp. 433–44.

Toma, M. I., Friedrich, K., Meyer, W., Fröhner, M., Schneider, S., Wirth, M., and Baretton, G. B. (2010). "Correlation of centrosomal aberrations with cell differentiation and DNA ploidy in prostate cancer". In: *Analytical and Quantitative Cytology and Histology* 32.1, pp. 1–10.

Tong, W. M., Yang, Y. G., Cao, W. H., Galendo, D., Frappart, L., Shen, Y., and Wang, Z. Q. (2007). "Poly(ADP-ribose) polymerase-1 plays a role in suppressing mammary tumourigenesis in mice." In: *Oncogene* 26.26, pp. 3857–67.

Toy, K. A., Valiathan, R. R., Núñez, F., Kidwell, K. M., Gonzalez, M. E., Fridman, R., and Kleer, C. G. (2015). "Tyrosine kinase discoidin domain receptors DDR1 and DDR2 are coordinately deregulated in triple-negative breast cancer." In: *Breast cancer research and treatment* 150.1, pp. 9–18.

Tsou, M. F. B., Wang, W. J., George, K. A., Uryu, K., Stearns, T., and Jallepalli, P. V. (2009). "Polo Kinase and Separase Regulate the Mitotic Licensing of Centriole Duplication in Human Cells". In: *Developmental Cell* 17.3, pp. 344–354.

Tsou, M.-F. B. and Stearns, T. (2006). "Mechanism limiting centrosome duplication to once per cell cycle." In: *Nature* 442.7105, pp. 947–51.

Uccella, S., Tibiletti, M. G., Bernasconi, B., Finzi, G., Oldrini, R., and Capella, C. (2005). "Aneuploidy, centrosome alteration and securin overexpression as features of pituitary somatotroph and lactotroph adenomas". In: *Analytical and Quantitative Cytology and Histology* 27.5, pp. 241–252.

Valiathan, R. R., Marco, M., Leitinger, B., Kleer, C. G., and Fridman, R. (2012). "Discoidin domain receptor tyrosine kinases: new players in cancer progression". In: *Cancer and Metastasis Reviews* 31.1-2, pp. 295–321.

Van Horck, F. P. G., Ahmadian, M. R., Haeusler, L. C., Moolenaar, W. H., and Kranenburg, O. (2001). "Characterization of p190RhoGEF, A RhoA-specific Guanine Nucleotide Exchange Factor That Interacts with Microtubules". In: *Journal of Biological Chemistry* 276.7, pp. 4948–4956.

Van Roy, F. and Berx, G. (2008). "The cell-cell adhesion molecule E-cadherin". In: *Cellular and Molecular Life Sciences* 65.23, pp. 3756–3788.

Ventura, R. A., Martin-Subero, J. I., Knippschild, U., Gascoyne, R. D., Delsol, G., Mason, D. Y., and Siebert, R. (2004). "Centrosome abnormalities in ALK-positive anaplastic large-cell lymphoma." In: *Leukemia* 18.11, pp. 1910–1.

Vitre, B., Holland, A. J., Kulukian, A., Shoshani, O., Hirai, M., Wang, Y., Maldonado, M., Cho, T., Boubaker, J., Swing, D. A., Tessarollo, L., Evans, S. M., Fuchs, E., and Cleveland, D. W. (2015). "Chronic centrosome amplification without tumorigenesis." In: *Proceedings of the National Academy of Sciences of the United States of America* 112.46, E6321–E6330.

Vleminckx, K., Vakaet, L., Mareel, M., Fiers, W., and Van Roy, F. (1991). "Genetic manipulation of E-cadherin expression by epithelial tumor cells reveals an invasion suppressor role". In: *Cell* 66.1, pp. 107–119.

Vogel, W. (1999). "Discoidin domain receptors: structural relations and functional implications." In: *The FASEB journal : official publication of the Federation of American Societies for Experimental Biology* 13 Suppl.9001, S77–S82.

Vogel, W., Gish, G. D., Alves, F., and Pawson, T. (1997). "The discoidin domain receptor tyrosine kinases are activated by collagen." In: *Molecular cell* 1.1, pp. 13–23.

Vorobjev, I. A. and Chentsov Yu., S. (1982). "Centrioles in the cell cycle. I. Epithelial cells". In: *Journal of Cell Biology* 93.3, pp. 938–949.

Walsh, L. A., Nawshad, A., and Medici, D. (2011). "Discoidin domain receptor 2 is a critical regulator of epithelial-mesenchymal transition." In: *Matrix biology : journal of the International Society for Matrix Biology* 30.4, pp. 243–7.

Wang, C.-Z., Yeh, Y.-C., and Tang, M.-J. (2009). "DDR1/E-cadherin complex regulates the activation of DDR1 and cell spreading". In: *AJP: Cell Physiology* 297.2, pp. C419–C429.

Wang, X., Zhou, Y.-X., Qiao, W., Tominaga, Y., Ouchi, M., Ouchi, T., and Deng, C.-X. (2006). "Overexpression of aurora kinase A in mouse mammary epithelium induces genetic instability preceding mammary tumor formation". In: *Oncogene* 25.54, pp. 7148–7158.

Wang, Y., Jin, F., Higgins, R., and McKnight, K. (2014). "The current view for the silencing of the spindle assembly checkpoint." In: *Cell cycle (Georgetown, Tex.)* 13.11, pp. 1694–701.

Waterman-Storer, C. M., Worthylake, R. a., Liu, B. P., Burridge, K., and Salmon, E. D. (1999). "Microtubule growth activates Rac1 to promote lamellipodial protrusion in fibroblasts." In: *Nature cell biology* 1.1, pp. 45–50.

Watts, C. A. A., Richards, F. M. M., Bender, A., Bond, P. J. J., Korb, O., Kern, O., Riddick, M., Owen, P., Myers, R. M. M., Raff, J., Gergely, F., Jodrell, D. I. I., and Ley, S. V. V. (2013). "Design, synthesis, and biological evaluation of an allosteric inhibitor of HSET that targets cancer cells with supernumerary centrosomes." In: *Chemistry & biology* 20.11, pp. 1399–410.

Weaver, B. A. A. and Cleveland, D. W. (2005). "Decoding the links between mitosis, cancer, and chemotherapy: The mitotic checkpoint, adaptation, and cell death." In: *Cancer cell* 8.1, pp. 7–12.

Weaver, B. A. A., Silk, A. D., Montagna, C., Verdier-Pinard, P., and Cleveland, D. W. (2007). "Aneuploidy acts both oncogenically and as a tumor suppressor." In: *Cancer cell* 11.1, pp. 25–36.

Weber, R. G., Bridger, J. M., Benner, a., Weisenberger, D., Ehemann, V., Reifenberger, G., and Lichter, P. (1998). "Centrosome amplification as a possible mechanism for numerical chromosome aberrations in cerebral primitive neuroectodermal tumors with TP53 mutations." In: *Cytogenetics and cell genetics* 83.3-4, pp. 266–9.

Wheelock, M. J., Shintani, Y., Maeda, M., Fukumoto, Y., and Johnson, K. R. (2008). "Cadherin switching." In: *Journal of cell science* 121.Pt 6, pp. 727–735.

Wickham, H. (2009). *Ggplot2*. Vol. 35. July, p. 211. ISBN: 978-0-387-98140-6.

Wickham, H. and Francois, R. (2015). "dplyr: A Grammar of Data Manipulation". In: *R package version 0.4.2*. P. 3.

Wigley, C. W., Fabunmi, R. P., Lee, M. G., Marino, C. R., Muallem, S., DeMartino, G. N., and Thomas, P. J. (1999). "Dynamic association of proteasomal machinery with the centrosome". In: *Journal of Cell Biology* 145.3, pp. 481–490.

Wojcik, E. J., Glover, D. M., and Hays, T. S. (2000). "The SCF ubiquitin ligase protein Slimb regulates centrosome dulplication in Drosophila". In: *Current Biology* 10.18, pp. 1131–1134.

Wong, J. and Fang, G. (2006). "HURP controls spindle dynamics to promote proper interkinetochore tension and efficient kinetochore capture." In: *The Journal of cell biology* 173.6, pp. 879–91.

Wu, J., Mikule, K., Wang, W., Su, N., Petteruti, P., Gharahdaghi, F., Code, E., Zhu, X., Jacques, K., Lai, Z., Yang, B., Lamb, M. L., Chuaqui, C., Keen, N., and Chen, H. (2013). "Discovery and mechanistic study of a small molecule inhibitor for motor protein KIFC1." In: *ACS chemical biology* 8.10, pp. 2201–8.

Wu, S. K., Budnar, S., Yap, A. S., and Gomez, G. A. (2014). "Pulsatile contractility of actomyosin networks organizes the cellular cortex at lateral cadherin junctions". In: *European Journal of Cell Biology* 93.10-12, pp. 396–404.

Xu, X., Weaver, Z., Linke, S. P., Li, C., Gotay, J., Wang, X. W., Harris, C. C., Ried, T., and Deng, C. X. (1999). "Centrosome amplification and a defective G2-M cell cycle checkpoint induce genetic instability in BRCA1 exon 11 isoform-deficient cells." In: *Molecular cell* 3.3, pp. 389–95.

Yamamoto, Y., Matsuyama, H., Chochi, Y., Okuda, M., Kawauchi, S., Inoue, R., Furuya, T., Oga, A., Naito, K., and Sasaki, K. (2007). "Overexpression of BUBR1 is associated with chromosomal instability in bladder cancer". In: *Cancer Genetics and Cytogenetics* 174.1, pp. 42–47.

Yamamoto, Y., Matsuyama, H., Furuya, T., Oga, A., Yoshihiro, S., Okuda, M., Kawauchi, S., Sasaki, K., and Naito, K. (2004). "Centrosome hyperamplification predicts progression and tumor recurrence in bladder cancer." In: *Clinical cancer research : an official journal of the American Association for Cancer Research* 10.19, pp. 6449–55.

Yamamoto, Y., Matsuyama, H., Kawauchi, S., Furuya, T., Liu, X. P., Ikemoto, K., Oga, A., Naito, K., and Sasaki, K. (2006). "Biological characteristics in bladder cancer depend on the type of genetic instability". In: *Clinical Cancer Research* 12.9, pp. 2752–2758.

Yamamoto, Y., Misumi, T., Eguchi, S., Chochi, Y., Kitahara, S., Nakao, M., Nagao, K., Hara, T., Sakano, S., Furuya, T., Oga, A., Kawauchi, S., Sasaki, K., and Matsuyama, H. (2011). "Centrosome amplification as a putative prognostic biomarker for the classification of urothelial carcinomas". In: *Human Pathology* 42.12, pp. 1923–1930.

Yamanaka, R., Arao, T., Yajima, N., Tsuchiya, N., Homma, J., Tanaka, R., Sano, M., Oide, A., Sekijima, M., and Nishio, K. (2006). "Identification of expressed genes characterizing long-term survival in malignant glioma patients." In: *Oncogene* 25.44, pp. 5994–6002.

Yang, J.-Y., Zong, C. S., Xia, W., Wei, Y., Ali-Seyed, M., Li, Z., Broglio, K., Berry, D. A., and Hung, M.-C. (2006). "MDM2 promotes cell motility and invasiveness by regulating E-cadherin degradation." In: *Molecular and cellular biology* 26.19, pp. 7269–82.

Yang, J., Mani, S. A., Donaher, J. L., Ramaswamy, S., Itzykson, R. A., Come, C., Savagner, P., Gitelman, I., Richardson, A., and Weinberg, R. A. (2004). "Twist, a master regulator of morphogenesis, plays an essential role in tumor metastasis". In: *Cell* 117.7, pp. 927–939.

Yang, S. H., Baek, H. A., Lee, H. J., Park, H. S., Jang, K. Y., Kang, M. J., Lee, D. G., Lee, Y. C., Moon, W. S., and Chung, M. J. (2010). "Discoidin domain receptor 1 is associated with poor prognosis of non-small cell lung carcinomas." In: *Oncology reports* 24.2, pp. 311–9.

Yang, Z., Loncarek, J., Khodjakov, A., and Rieder, C. L. (2008). "Extra centrosomes and/or chromosomes prolong mitosis in human cells." In: *Nature cell biology* 10.6, pp. 748–51.

Yonemura, S. (2011). "Cadherin-actin interactions at adherens junctions". In: *Current Opinion in Cell Biology* 23.5, pp. 515–522.

Yoshida, D. and Teramoto, A. (2007). "Enhancement of pituitary adenoma cell invasion and adhesion is mediated by discoidin domain receptor-1". In: *Journal of Neuro-Oncology* 82.1, pp. 29–40.

Yoshiura, K., Kanai, Y., Ochiai, a., Shimoyama, Y., Sugimura, T., and Hirohashi, S. (1995). "Silencing of the E-cadherin invasion-suppressor gene by CpG methylation in human carcinomas." In: *Proceedings of the National Academy of Sciences of the United States of America* 92.16, pp. 7416–7419.

Yu, Q., Zhang, K., Wang, X., Liu, X., and Zhang, Z. (2010). "Expression of transcription factors snail, slug, and twist in human bladder carcinoma". In: *Journal of Experimental & Clinical Cancer Research* 29, p. 119.

Zaidel-Bar, R. (2013). "Cadherin adhesome at a glance". In: *Journal of Cell Science* 126.2, pp. 373–378.

Zarubin, T. and Han, J. (2005). "Activation and signaling of the p38 MAP kinase pathway." In: *Cell research* 15.1, pp. 11–18.

Zeng, X., Shaikh, F. Y., Harrison, M. K., Adon, A. M., Trimboli, A. J., Carroll, K. A., Sharma, N., Timmers, C., Chodosh, L. A., Leone, G., and Saavedra, H. I. (2010). "The Ras oncogene signals centrosome amplification in mammary epithelial cells through cyclin D1/Cdk4 and Nek2." In: *Oncogene* 29.36, pp. 5103–12.

Zhang, C.-Z., Spektor, A., Cornils, H., Francis, J. M., Jackson, E. K., Liu, S., Meyerson, M., and Pellman, D. (2015). "Chromothripsis from DNA damage in micronuclei". In: *Nature* 522.7555, pp. 179–84.

Zhang, Y., Tian, Y., Yu, J.-J., He, J., Luo, J., Zhang, S., Tang, C.-E., and Tao, Y.-m. (2013). "Overexpression of WDR62 is associated with centrosome amplification in human ovarian cancer". In: *Journal of Ovarian Research* 6.1, p. 55.

Zheng, X., Gooi, L. M., Wason, A., Gabriel, E., Mehrjardi, N. Z., Yang, Q., Zhang, X., Debec, A., Basiri, M. L., Avidor-Reiss, T., Pozniakovsky, A., Poser, I., Saric, T., Hyman, A. a., Li, H., and Gopalakrishnan, J. (2014). "Conserved TCP domain of Sas-4/CPAP is essential for pericentriolar material tethering during centrosome biogenesis." In: *Proceedings of the National Academy of Sciences of the United States of America* 111.3, E354–63.

Zhou, H., Kuang, J., Zhong, L., Kuo, W. L., Gray, J. W., Sahin, A., Brinkley, B. R., and Sen, S. (1998). "Tumour amplified kinase STK15/BTAK induces centrosome amplification, aneuploidy and transformation." In: *Nature genetics* 20.2, pp. 189–93.

Zhu, F., Lawo, S., Bird, A., Pinchev, D., Ralph, A., Richter, C., Müller-Reichert, T., Kittler, R., Hyman, A. A., and Pelletier, L. (2008). "The Mammalian SPD-2 Ortholog Cep192 Regulates Centrosome Biogenesis". In: *Current Biology* 18.2, pp. 136–141.

Zhu, J., Abbruzzese, J. L., Izzo, J., Hittelman, W. N., and Li, D. (2005). "AURKA amplification, chromosome instability, and centrosome abnormality in human pancreatic carcinoma cells". In: *Cancer Genetics and Cytogenetics* 159.1, pp. 10–17.

Zyss, D. and Gergely, F. (2009). "Centrosome function in cancer: guilty or innocent?" In: *Trends in cell biology* 19.7, pp. 334–46.